POST-TRAUMATIC NEUROPATHIC PAIN: THE ROLE OF THE SKIN

Liron S. Duraku

Liron S. Duraku
Post-Traumatic Neuropathic Pain: The Role Of The Skin

ISBN: 978-94-6182-311-3
Printed by Offpage, Amsterdam

Cover: Jorien de Wandeler, Lukas Jorissen en Pim van Dijk
Layout: Pim van Dijk, info@dijkvanpim.com

Mede gerealiseerd door: J.E. Juriaanse Stichting en Esser Stichting

Post-Traumatic Neuropathic Pain: The Role Of The Skin
Post-Traumatische neuropathische pijn: De rol van de huid

PROEFSCHRIFT

ter verkrijging van de graad van doctor aan de Erasmus Universiteit Rotterdam
op gezag van de rector magnificus

Prof.dr. H.G. Schmidt

en volgens besluit van het College voor Promoties.

De openbare verdediging zal plaatsvinden op:

woensdag 18 september 2013
om 09.30 uur

door

Ljiron Duraku
geboren te Bar, Montenegro

PROMOTIECOMMISSIE:

Promotor:
Prof.dr. S.E.R. Hovius

Overige leden:
Prof.dr. F.J.P.M. Huygen
Prof.dr. E.P. Prens
Prof.dr. P.A. van Doorn

Copromotoren:
Dr. E.T. Walbeehm
Dr. T.J.H. Ruigrok

Paranimfen:
Drs. T.A. van Essen
Drs. M.R.W. Guijt

Për babain dhe nënën,
njerëzit më të bukur në rruzullin e dheut.

Sabahet Duraku dhe Aldiana Rexha-Duraku

TABLE OF CONTENTS

1

INTRODUCTION

'Imagine boiling drops of water dribbling on your arm,
riddling your skin with pain
Imagine the excruciating pain that crawls down your body
every time your clothes rub over your skin,
Imagine bursts of 'pins and needles' perforating your skin
every time a cold wind strokes your arm,
Imagine a continuous crushing pain in your amputated limb,
a realistic pain in a phantom limb that imprisons your mind!'

(Costigan, Scholz and Woolf, 2009) [1]

These are only a few examples of the devastating symptoms that patients with post-traumatic neuropathic pain may experience. Post-traumatic neuropathic pain patients suffer from spontaneous pain in the absence of noxious stimuli and/or allodynia (the experience of pain evoked by normally non-painful mechanical and/or thermal stimuli) and/or hyperalgesia (exaggerated pain experience induced by noxious stimuli) after peripheral nerve- trauma or surgery [2]. These debilitating symptoms usually have profound negative effects on the quality of life, with no curative therapies at hand [1, 3, 4]. Neuropathic pain has been associated with a poorer quality of life than other chronic conditions including cancer, heart failure, type 2 diabetes, Parkinson's disease and stroke [5]. Unfortunately, there are only a few reports on the incidence and prevalence of post-traumatic neuropathic pain and their specific symptoms [6, 7]. Information illustrating the overall impact of post-traumatic neuropathic pain in health care is lacking. Since post-traumatic neuropathic pain symptoms are diverse and their underlying pathologic mechanisms differ from each other, it is necessary to differentiate between the different neuropathic symptoms in order to develop efficient therapeutic strategies.

The quantification of epidermal nerve fibers in skin biopsies of patients with neuropathic pain has proven to be a powerful diagnostic tool for small fiber neuropathies in patients with diabetes, AIDS and post herpetic neuralgia [8]. Such diagnostic tools are, however, lacking for assessing post-traumatic neuropathic pain. In this PhD project, we have investigated the nerve innervation pattern of the epidermis and dermis in the foot sole of rats with post-traumatic neuropathic pain and rats with a nerve reconstruction after nerve injury. Additionally, the possible role of skin peripheral thermoregulation in the hind paw of nerve injury induced neuropathic pain rats has been examined. Furthermore, we developed a novel device to objectively measure thermal allodynia and hyperalgesia in freely behaving post-traumatic neuropathic pain rats. The current thesis discusses these results and the value of implementing skin biopsies as a diagnostic tool for assessing and classifying post-traumatic neuropathic pain.

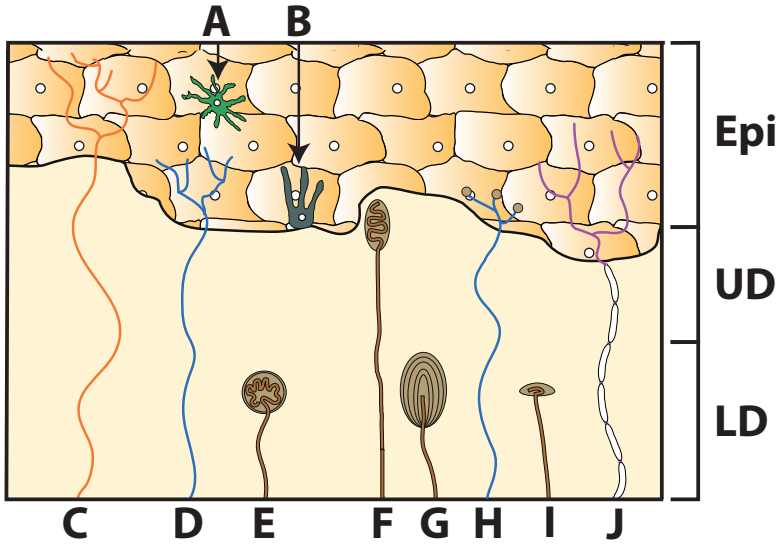

	Type	Location	Function
A	Langerhans cell	Stratum spinosum (epi)	Presents antigens
B	Melanocyte	Stratum basale (epi)	Produces melanine
C	Non-peptidergic C fiber	Mainly stratum granulosum (epi)	Transmits nociception and itch
D	Peptidergic C fiber	Mainly stratum spinosum (epi)	Transmits nociception and itch
E	Krause bulb	Lower Dermis	Detects low-frequency vibrations
F	Meissner corpuscule	Upper Dermis	Transmits light touch (rapidly adapting)
G	Pacini corpuscule	Lower Dermis	Detects vibrations and pressure
H	Merkel cell	Stratum basale (epi)	Transmits light touch (slowly adapting)
I	Ruffini corpuscule	Lower Dermis	Sensitive to skin stretch
J	Aδ fiber	Epidermis	Transmits nociception

FIGURE 1

Figure 1 displays the architectural epidermal and dermal organization of the plantar side rat's hind limb foot sole.

EPIDERMIS: A SENSORY ORGAN

In the past decades, a body of evidence has shown that the uppermost layer of the skin, the epidermis, not only serves as a protective layer but also plays a pivotal role in the transmission of painful and non-painful stimuli to the central nervous system [9]. The epidermis consists of five layers (Fig. 1): stratum basale, stratum spinosum, stratum granulosum, stratum lucidum (only in palmar and plantar skin) and stratum corneum, from the inner-most to the outer-most layer, respectively. The epidermis contains keratinocytes, which undergo gradual differentiation as they progress from the basal layer to the stratum corneum, with a turnover time of about 27 days. Keratinocytes relay sensory information as they are activated by mechanical, thermal and noxious stimuli and they transmit their information indirectly to the spinal cord by activating nearby located peripheral nerve fibers [10]. For example, upon activation, keratinocytes secrete adenosine triphosphate (ATP), which binds to and activates P2X purinoceptor 3 (P2X3), receptors expressed on adjacent epidermal nerve fibers [11]. In addition to keratinocytes, the epidermis contains Merkel cells, melanocytes and Langerhans cells, all of which serve different sensory purposes (Fig. 1). Merkel cells are believed to play a prominent role in the transduction of light touch [9]. Melanocytes are UV sensitive cells that produce melanin, a pigment that has photo protectant properties. Langerhans cells are antigen-presenting cells, but are also sensitive to thermal stimulation, such as the increasing skin temperature occurring during local inflammation [1, 6].

For transmission of signals to the central nervous system, several populations of nerve fibers terminate in the epidermis. Sensory nerve fibers in the skin have different conduction properties according to their degree of myelination and the layer of skin in which they terminate. Thick myelinated nerve fibers, Aβ fibers, are the faster conducting fibers as compared with the thinly and non-myelinated fibers, Aδ and C fibers, respectively. Aβ fibers respond to signals originating from Pacinian and Ruffini corpuscles, which are the mechanoreceptors of the skin and mainly transmit information about touch and skin vibration [12]. Aβ fibers innervate the lower dermis of the skin. Nerve fibers that respond to noxious stimuli are termed nociceptors, and include Aδ and C fibers [13]; the latter are believed to be also involved in itch transmission [14]. Both Aδ and C fibers innervate the epidermis and upper dermis. Since Aδ fibers are myelinated, they are the fast conducting nociceptors. They are responsible for the sharp and short lasting pain, also termed ‘first’ pain. C-fibers are the unmyelinated slow conducting nociceptors that produce the ‘second’ pain, which is delayed, diffuse in location and often outlasts the duration of the stimulus [15]. In addition, Transient Receptor Potential (TRP) channels, expressed in Aδ and C nerve fibers, as well as by keratinocytes, detect thermal stimuli [16]. Six TRP channels are identified in humans, of which the vanilloid receptors TRPV2 and TRPV1 are responsible for detecting noxious heat, whereas the TRPV4 and TRPV3 receptors detect innocuous

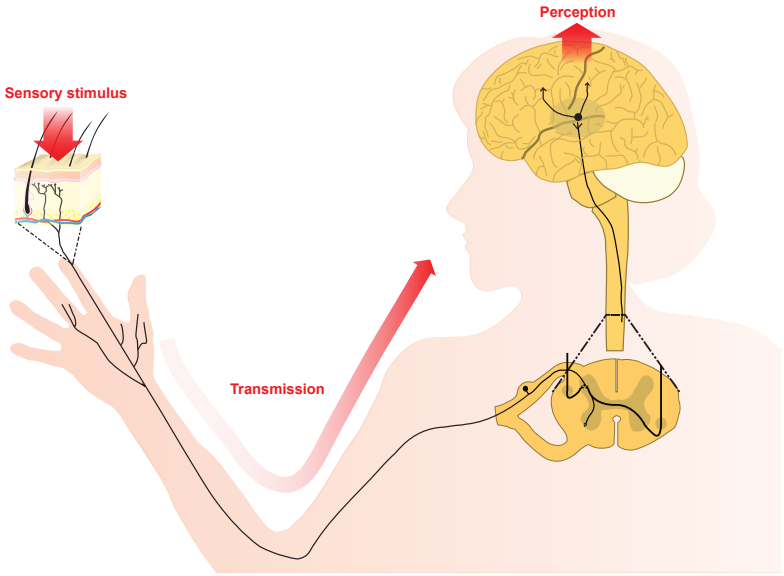

FIGURE 2

The epidermis is capable of detecting noxious and non-noxious stimuli and transmitting this information to the spinal cord by specialized nerve fibers. In the spinal cord, sensory information is conveyed to higher structures in the central nervous system, eventually leading to perception of sensory stimuli.

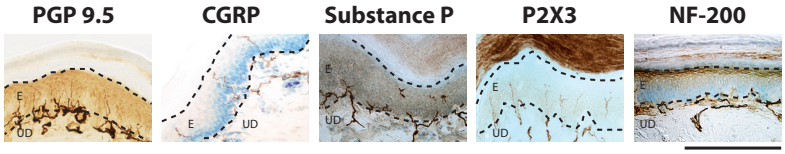

FIGURE 3

Light microscopic micrographs showing nerve fibers for the immunomarkers that have been used in the current thesis to label the specific subclasses of sensory skin fibers. Epidermal nerve fibers are divided in slow conducting unmyelinated C-fibers and fast conducting, thinly myelinated A-δ, mainly for detecting noxious stimuli. PGP 9.5 is a pan-neuronal marker, which labels all the sensory skin fibers. Unmyelinated C-fibers are either peptidergic and contain the neuropeptides calcitonin gene-related peptide (CGRP) and/ or Substance P or are non-peptidergic and are identified by their expression of purinergic receptor P2X3. A-δ fibers are exclusively peptidergic and contain CGRP but can be distinguished from unmyelinated CGRP fibers by their co-expression of the marker neurofilament 200 (NF-200). E: Epidermis, UD: Upper dermis. Scale bar: 250 um.

heat. The melastatin receptor TRPM8 can detect innocuous cold while the ankyrin TRPA1 receptor is involved in detecting noxious cold [17].
In conclusion, the epidermis is capable of detecting noxious and non-noxious stimuli and transmits this information to the spinal cord by specialized nerve fibers. In the spinal cord, sensory information is conveyed to higher structures in the central nervous system, eventually leading to perception of sensory stimuli (Fig. 2).

PEPTIDERGIC AND NON-PEPTIDERGIC FIBERS

Epidermal Aδ and C-fiber nociceptors are subdivided into peptidergic and non-peptidergic fibers by their expression of different neurotrophic receptors; they show different peripheral and central terminations [18]. Peptidergic nociceptors, in addition to the classical neurotransmitter glutamate, contain one or more neuropeptides, such as Substance P (SubP) (C-fibers), Calcitonin Gene-Related Peptide (CGRP) (Aδ and C- fibers), galanin, somatostatin and others (Fig. 3). They also express TrkA, the receptor for Nerve Growth Factor (NGF) [19], and use Brain-Derived Neurotrophic Factor (BDNF) as a transmitter [20]. Non-peptidergic epidermal fibers (C-fiber) only use glutamate as a transmitter. They are further characterized by expression of the plant lectin isolectin B4 (IB4) and P2X3 and by containing the receptor components for Glial cell line-Derived Neurotrophic Factor (GDNF), i.e. RET [21, 22] (Fig.3).
Peptidergic fibers terminate in the skin, muscles and joints alike, while non-peptidergic fibers terminate mainly in the skin [23-25]. Furthermore, peptidergic fibers terminate in the stratum spinosum layer of the epidermis while non-peptidergic fibers terminate more superficially in the stratum granulosum layer [26]. In the epidermis, in approximately 15%, there is an intertwining between the peptidergic and non-peptidergic fibers [26]. This suggests that intertwined peptidergic and non-peptidergic nociceptive fibers may have the capacity to cross-activate, sensitize, or desensitize one another under different conditions. Thus, although there is a topographic distinction in the epidermal innervation pattern by peptidergic and non-peptidergic fibers, they may still show interactions. Remarkably, a distinct topographic innervation pattern has been shown in the central termination pattern of these fibers in the spinal cord. Here, peptidergic nociceptors terminate in the superficial spinal lamina I and the outer layer of lamina II [27] while non-peptidergic nociceptors terminate preferentially in the inner region of laminae II [28]. This topographic distinction continues in the pathways transmitting nociceptive stimuli to higher located target nuclei in the CNS.
It has been suggested that there may be two systems that are responsible for the perception of pain: one consisting of the peptidergic nociceptors that subserve the sensory-discriminative aspects of pain (e.g. where is the pain stimulus located, is the stimulus thermal or mechanical?) and the other of the non-peptidergic nociceptors that operate the affective-motivational aspects of pain (e.g. how unpleasant is the pain?) [29]. However, several decades after their discovery, the reason for the exis-

tence of both peptidergic and non-peptidergic fibers in mammals and their specific role in nociception is still unclear.

SKIN BIOPSY USED AS A DIAGNOSTIC TOOL

Determining the epidermal innervation pattern is an accepted tool for diagnosing small fiber neuropathy, such as in patients with diabetes, HIV and post-herpetic induced neuralgia [30, 31]. Small fiber peripheral neuropathy is a type of peripheral neuropathy that occurs from damage to the small unmyelinated peripheral nerve fibers. Small fiber neuropathies are diagnosed by determining the epidermal innervation pattern using three mm wide skin punch biopsies taken from the skin area with behavioral signs of neuropathic pain. Small fiber neuropathies are fiber length-dependent neuropathies as longer nerve fibers are affected first, resulting in the early involvement of the distal extremities - the most common locations for performing skin biopsies [8, 30]. These skin samples are then processed for PGP 9.5 staining, a pan-neuronal marker, and the number of PGP-9.5 immunoreactive (IF) fibers crossing the dermal-epidermal border is examined according to the internationally accepted protocol issued by the European Federation of Neurological Societies [32, 33]. The severity of small fiber neuropathic symptoms is proportionally related to the density of epidermal nerve fibers, in which a lower density of epidermal fibers is associated with a more severe neuropathy [8]. Using this correlation, disease progression and the efficacy of a treatment is assessed by performing a second skin biopsy near the site of the first biopsy and comparing these outcomes. However, with the implementation of antibodies raised against peptidergic (i.e. CGRP and Substance-P) and non-peptidergic (P2X3) fibers it is possible to make a more thorough analysis of the skin fibers in neuropathic pain patients compared to the current method. In addition, distinguishing between myelinated (Aδ-and Aβ-fibers) and unmyelinated C-fibers, for example by using the NF-200 marker, which stains myelinated fibers, could be of great value for diagnostic purposes of neuropathic pain.

The skin biopsy diagnostic tool has been standardized for small fiber neuropathies, but for post-traumatic neuropathic pain standardized diagnostic tools are lacking. In contrast to small fiber neuropathy, in post-traumatic neuropathic pain (in humans and animal models) there have been reports of both significant increases and decreases in epidermal fiber densities as compared to naïve epidermis [34-37]. In addition, post-traumatic neuropathic pain is restricted to a specific skin area after traumatic nerve injury, while small fiber neuropathy is more diffusely located and is secondary to a systemic disease. Hence, in order to gain more insight into the pathophysiology of peripheral nerve fibers in post-traumatic neuropathic pain, a quantitative diagnostic tool for assessing the innervation pattern of the epidermis and dermis is required.

POST-TRAUMATIC NEUROPATHIC PAIN AND SKIN NERVE FIBERS

In the last two decades, different animal models have been developed for the investigation of mechanisms that are important for the induction and/or maintenance of post-traumatic neuropathic pain. The chronic constructive injury (CCI) model, one of the earliest models developed by Bennet et. al. (1988) uses four loosely tied ligations around the sciatic nerve, resulting in intraneural edema and constriction of the sciatic nerve [38]. This leads to the development of thermal and mechanical allodynia and hyperalgesia in the affected hind paw. Using the CCI model, several studies have investigated the reinnervation pattern of nerve fibers in the affected skin area, however, with contradicting results. In short, there is evidence for a decrease in epidermal fibers, associated with post-traumatic neuropathic pain in rodents [34, 35], in similar fashion to small fiber neuropathy in humans [15]. In contrast, other reports showed that there is a significantly higher density of epidermal nerve fibers in a CCI rat model [36], [39]. Furthermore, in humans, only one study has investigated the hypersensitive skin areas of patients that suffer from post-traumatic neuropathic pain [37]. They found an increase in the number of epidermal nerve fibers that expressed the TRPV1 receptor, a receptor which is (fully) co-localized with the peptidergic CGRP fibers. In summary there is a general lack of unifying data on the nerve injury-induced changes in the epidermal and dermal innervation pattern and its correlation with behavioral signs of neuropathic pain.

UNINJURED NERVE FIBERS IN POST-TRAUMATIC NEUROPATHIC PAIN

In the past decades, many investigations have focused on the changes that occur in the reactions and reinnervation patterns of injured nerve fibers following post-traumatic neuropathic pain. With the development of the spinal nerve ligation (SNL) [40] and the spared nerve injury (SNI) [41] models, it was evident that uninjured fibers (adjacent to injured fibers) also may play a pivotal role in the development and maintenance of neuropathic pain. In the SNL model, one or more spinal nerves innervating the hind limb are ligated and cut, whereas in the SNI model, the common peroneal and tibial branches of the sciatic nerve are ligated and cut while sparing the sural nerve. Both models result in denervation of specific skin areas in the foot sole of the affected hind paw, allowing investigations of both injured and uninjured nerve fibers and the innervation pattern of their respective territories. In rodent models with post-traumatic neuropathic pain, it has been shown that after nerve injury the uninjured nerve fibers of unmyelinated subtypes, which are located in the innervation area of the injured nerve, are spontaneously active [42, 43]. These spontaneous activities explain, in part, the spontaneous pain that occurs in neuropathic pain. Further, it has been suggested that the increased sensitivity to innocuous heat and cold stimuli is partly caused by the increase in expression of TRPV1 and TRPA1 channels, respectively, in the dorsal root ganglion (DRG) of uninjured afferent nerve fibers [44, 45].

In conclusion, uninjured nerve fibers seem to play a substantial role in the development of neuropathic pain behavior. Nevertheless, despite the findings mentioned earlier, there is limited knowledge on the changes in the epidermal and dermal innervation pattern of uninjured fibers and their possible role in post-traumatic neuropathic pain. The importance of these fibers in diagnostic skin biopsies is yet to be determined.

MIRROR IMAGE PAIN

In some patients with post-traumatic neuropathic pain in a body part, the same but uninjured body part on the contralateral side also develops symptoms of neuropathic pain, a condition known as 'mirror image pain' [46]. This phenomenon has been described in different neuropathic pain states, particularly those after peripheral nerve damage by trauma [47]. However, previous studies have shown contradictory results concerning the morphological changes of nerve fibers in the contralateral body part after an ipsilateral nerve injury. Several reports have revealed that on the side contralateral to the nerve lesion there was sprouting of peripheral motor [48, 49], autonomic [50, 51] and sensory fibers [52, 53], while others reported a decrease in sensory fibers on that side [54, 55]. Therefore, it still remains unclear what kind of changes take place in the contralateral side after ipsilateral nerve lesion. In addition, it is unknown which types of sensory skin nerve fibers are involved in the development of mirror image pain.

SKIN BIOPSIES AFTER NERVE RECONSTRUCTION

The purpose of nerve reconstruction is to allow reinnervation of the target organs by guiding the regenerating sensory, motor and autonomic axons into the environment of the distal nerve without losing a significant number of axons at the site of injury. Despite the development and improvement of techniques and different repair methods in the last century, the rate of successful recovery from peripheral nerve lesions is far from optimal [56-58]. As explained earlier, the skin itself is one of the most important and complex organs for detection of external sensory stimuli. Previous reports showed that, after a nerve crush, the number of intra-epidermal PGP 9.5 stained fibers was close to normal, but the axon profiles tended to be abnormally short [59, 60]. Despite this defect, nociceptive responses to painful stimuli can easily recover due to detection by the free nerve endings reaching deep layers of the epidermis. On the other hand, fine mechanoreceptive sensitivity is usually deficient, as the number of reinnervated corpuscular receptors is reduced after nerve crush [61, 62] and show an abnormal configuration [59] that may affect stimulus transduction. However, it remains elusive how sensory nerve fibers reinnervate the skin after an indirect (i.e. placement of graft or conduit) nerve repair. There are no reports of human or animal studies that show development of post-traumatic neuropathic pain after nerve repair. Investigating the reinnervation pattern of different subtypes of epidermal and upper dermal

sensory fibers after a nerve reconstruction in the rat will provide more insight into the pathogenesis of sensory recovery after nerve reconstruction and post-traumatic neuropathic pain.

MEASURING THERMAL HYPERSENSITIVITY IN RODENTS WITH NEUROPATHIC PAIN

The golden standard to examine heat and cold allodynia and hyperalgesia is the so-called 'paw lift' latency, which refers to the time between the first contact of a hind paw with a hot or cold plate and the lifting of the hind paw from the plate [63-66]. The parameters that are used in this procedure are the total number of 'paw lifts', the cumulative number of 'paw lifts' and the latency to the first 'paw lift'. However, since rodents with neuropathic pain also develop spontaneous pain [67, 68], it is uncertain if the 'paw lift' is the direct effect of the cold or hot plate or due to spontaneous pain-induced 'paw lift' unrelated to the temperature of the plate. Furthermore, a 'paw lift' reaction elicited by a flexion reflex cannot be excluded. In addition, experimental paradigms that measure 'paw lift' latency are usually conducted in see-through Plexiglas boxes with an open roof in a room with light. This may lead to increased stress levels of these animals because rodents may differ in behavior in different environments and, rodents being nocturnal animals, light may interfere with the outcomes of the experiment. In other research areas that examine behavioral responses of higher integrated systems of the central nervous system, for example learning, it is of vital importance to create a completely controlled environment and to exclude as many variables as possible. Perception of pain in rodents is like learning, a higher integrated mechanism, and the numerous factors that might interfere during the 'paw lift test' can lead to misinterpretation of the data. Therefore, a universal experimental setup that would circumvent all the above-mentioned problems would be of great value for determining objectively thermal hypersensitivity in neuropathic pain rodent models.

AIM OF THIS PHD PROJECT

The aim of this PhD project was to investigate the innervation pattern of nerve fibers in the epidermis and upper dermis in rats with post-traumatic neuropathic pain and rats with nerve reconstruction after peripheral nerve injury. For this purpose, we employed immunohistochemistry for labeling epidermal and upper dermal nerve fibers and used the SNI model for induction of post-traumatic neuropathic pain in rats. A nerve autograft and a vein-muscle graft with additional BMSCs were applied to reconstruct a nerve and subsequently examine the skin reinnervation. Furthermore, the possible role of skin peripheral thermoregulation in the hind paw of post-traumatic neuropathic pain rats has been examined. In addition, a novel device was made that measured allodynia and hyperalgesia to (non-) noxious cold and hot stimuli. The experiments and their results will be described in the following chapters of this thesis:

CHAPTER 2 AND 3: Up to 80% of patients with post-traumatic neuropathic pain, due to upper extremity nerve injury, suffer from cold intolerance, i.e. the experience of pain to cold non-painful temperatures, a subtype of post-traumatic neuropathic pain [6, 7, 69, 70]. It has been proposed that in humans a correlation exists between disturbed peripheral thermoregulation and cold intolerance [71, 72]. However, other factors, such as vascular damage, were never excluded in these studies, which in turn might be an issue in disturbing the peripheral thermoregulation in these post-traumatic cold intolerant patients. Therefore, in chapter 2, we examined cold-induced vasodilation (cyclic response of vasoconstriction and dilatation upon cold exposure) during cold exposure and the subsequent rewarming pattern (chapter 3) in hind paws of post-traumatic neuropathic pain (SNI) rats. In this experiment, we used a control rat model (sham), in which we conducted the same surgery as in the SNI-treated group without damaging the nerves, thus excluding the confounding factor of vascular damage.

CHAPTER 4: In this chapter, the innervation pattern of CGRP fibers in the rat foot sole is presented using a novel 2D reconstruction method. In addition, we have investigated the reinnervation pattern of uninjured CGRP fibers adjacent to injured nerve fibers in the foot sole of rats with SNI-induced neuropathic pain.

CHAPTER 5: Together, with chapter 4, this chapter provides an overview of the changes in innervation (Substance-P, P2X3, P2X3 and PGP 9.5) of the denervated and adjacent non-denervated skin and allows conclusions, which changes may correlate best with the developing neuropathic pain.

CHAPTER 6: It is known that rats with SNI-induced neuropathic pain develop mirror image pain to mechanical stimuli. In chapter 6, the changes in the innervation pattern of peptidergic (CGRP, Substance-P and NF-200) and non-peptidergic (P2X3) skin nerve fibers on the contralateral side of the affected hind limb have been determined.

CHAPTER 7: A novel device is used, in this chapter, the Rotterdam Advanced Multiple Plate (RAMP), for investigating cold and hot allodynia and hyperalgesia objectively in the SNI model.

CHAPTER 8: In this chapter, we determined the regeneration pattern of the peptidergic and non-peptidergic sensory skin fibers (CGRP, Substance P, NF-200, P2X3 and PGP 9.5) 12 weeks after reconstruction of a 15mm nerve defect using a nerve autograft

CHAPTER 9: As in chapter 8 the same evaluation technique is used to allow us to visualize the reinnervation of the sensory skin fibers (CGRP, Substance P, NF-200, P2X3 and PGP 9.5) 12 weeks after reconstructing the nerve using a vein-muscle graft with or without additional BMSCs as a luminal additive.

CHAPTER 10: Finally, the last chapter of the thesis will provide and overview of the main results and discusses their relevance for future containment and treatment of nerve trauma induced neuropathic pain.

REFERENCES

1.
Costigan, M., Scholz, J., and Woolf, C.J., Neuropathic pain: a maladaptive response of the nervous system to damage. Annu Rev Neurosci 2009; 32: 1-32.

2.
Baron, R., Mechanisms of disease: neuropathic pain--a clinical perspective. Nat Clin Pract Neurol 2006; 2(2): 95-106.

3.
O'Connor, A.B. and Dworkin, R.H., Treatment of neuropathic pain: an overview of recent guidelines. Am J Med 2009; 122(10 Suppl): S22-32.

4.
Galvez, R., Marsal, C., Vidal, J., Ruiz, M., and Rejas, J., Cross-sectional evaluation of patient functioning and health-related quality of life in patients with neuropathic pain under standard care conditions. Eur J Pain 2007; 11(3): 244-55.

5.
Doth, A.H., Hansson, P.T., Jensen, M.P., and Taylor, R.S., The burden of neuropathic pain: a systematic review and meta-analysis of health utilities. Pain 2010; 149(2): 338-44.

6.
Lenoble, E., Dumontier, C., Meriaux, J.L., et al., [Cold sensitivity after median or ulnar nerve injury based on a series of 82 cases]. Ann Chir Main Memb Super 1990; 9(1): 9-14.

7.
Collins, E.D., Novak, C.B., Mackinnon, S.E., and Weisenborn, S.A., Long-term follow-up evaluation of cold sensitivity following nerve injury. J Hand Surg Am 1996; 21(6): 1078-85.

8.
Lauria, G. and Devigili, G., Skin biopsy as a diagnostic tool in peripheral neuropathy. Nat Clin Pract Neurol 2007; 3(10): 546-57.

9.
Boulais, N. and Misery, L., The epidermis: a sensory tissue. Eur J Dermatol 2008; 18(2): 119-27.

10.
Denda, M., Nakatani, M., Ikeyama, K., Tsutsumi, M., and Denda, S., Epidermal keratinocytes as the forefront of the sensory system. Exp Dermatol 2007; 16(3): 157-61.

11.
Lumpkin, E.A. and Caterina, M.J., Mechanisms of sensory transduction in the skin. Nature 2007; 445(7130): 858-65.

12.
McGlone, F. and Reilly, D., The cutaneous sensory system. Neurosci Biobehav Rev 2010; 34(2): 148-59.

13.
Schaible, H.G. and Richter, F., Pathophysiology of pain. Langenbecks Arch Surg 2004; 389(4): 237-43.

14.
Ikoma, A., Cevikbas, F., Kempkes, C., and Steinhoff, M., Anatomy and neurophysiology of pruritus. Semin Cutan Med Surg 2011; 30(2): 64-70.

15.
Oaklander, A.L. and Siegel, S.M., Cutaneous innervation: form and function. J Am Acad Dermatol 2005; 53(6): 1027-37.

16.
Reaves, B.J. and Wolstenholme, A.J., The TRP channel superfamily: insights into how structure, protein-lipid interactions and localization influence function. Biochem Soc Trans 2007; 35(Pt 1): 77-80

17.
Tominaga, M. and Caterina, M.J., Thermosensation and pain. J Neurobiol 2004; 61(1): 3-12.

18.
Snider, W.D. and McMahon, S.B., Tackling pain at the source: new ideas about nociceptors. Neuron 1998; 20(4): 629-32.

19.
Anand, P., Neurotrophic factors and their receptors in human sensory neuropathies. Prog Brain Res 2004; 146: 477-92.

20.
Pezet, S. and McMahon, S.B., Neurotrophins: mediators and modulators of pain. Annu Rev Neurosci 2006; 29: 507-38.

21.
Molliver, D.C., Wright, D.E., Leitner, M.L., et al., IB4-binding DRG neurons switch from NGF to GDNF dependence in early postnatal life. Neuron 1997; 19(4): 849-61.

22.
Burnstock, G., P2X receptors in sensory neurones. Br J Anaesth 2000; 84(4): 476-88.

23.
Plenderleith, M.B. and Snow, P.J., The plant lectin Bandeiraea simplicifolia I-B4 identifies a subpopulation of small diameter primary sensory neurones which innervate the skin in the rat. Neurosci Lett 1993; 159(1-2): 17-20.

24.
Perry, M.J. and Lawson, S.N., Differences in expression of oligosaccharides, neuropeptides, carbonic anhydrase and neurofilament in rat primary afferent neurons retrogradely labelled via skin, muscle or visceral nerves. Neuroscience 1998; 85(1): 293-310.

25.
Bennett, D.L., Dmietrieva, N., Priestley, J.V., Clary, D., and McMahon, S.B., trkA, CGRP and IB4 expression in retrogradely labelled cutaneous and visceral primary sensory neurones in the rat. Neurosci Lett 1996; 206(1): 33-6.

26.
Zylka, M.J., Rice, F.L., and Anderson, D.J., Topographically distinct epidermal nociceptive circuits revealed by axonal tracers targeted to Mrgprd. Neuron 2005; 45(1): 17-25.

27.
Rexed, B., The cytoarchitectonic organization of the spinal cord in the cat. J Comp Neurol 1952; 96(3): 414-95.

28.
Julius, D. and Basbaum, A.I., Molecular mechanisms of nociception. Nature 2001; 413(6852): 203-10.

29.
Braz, J.M., Nassar, M.A., Wood, J.N., and Basbaum, A.I., Parallel "pain" pathways arise from subpopulations of primary afferent nociceptor. Neuron 2005; 47(6): 787-93.

30.
Lauria, G., Lombardi, R., Camozzi, F., and Devigili, G., Skin biopsy for the diagnosis of peripheral neuropathy. Histopathology 2009; 54(3): 273-85.

31.
Lauria, G., Cazzato, D., Porretta-Serapiglia, C., et al., Morphometry of dermal nerve fibers in human skin. Neurology 2011; 77(3): 242-9.

32.
Lauria, G., Hsieh, S.T., Johansson, O., et al., European Federation of Neurological Societies/ Peripheral Nerve Society Guideline on the use of skin biopsy in the diagnosis of small fiber neuropathy. Report of a joint task force of the European Federation of Neurological Societies and the Peripheral Nerve Society. Eur J Neurol 2010; 17(7): 903-12, e44-9.

33.
European Federation of Neurological Societies/ Peripheral Nerve Society Guideline on the use of skin biopsy in the diagnosis of small fiber neuropathy. Report of a joint task force of the European Federation of Neurological Societies and the Peripheral Nerve Society. J Peripher Nerv Syst 2010; 15(2): 79-92.

34.
Lindenlaub, T. and Sommer, C., Epidermal innervation density after partial sciatic nerve lesion and pain-related behavior in the rat. Acta Neuropathol 2002; 104(2): 137-43.

35.
Ma, W. and Bisby, M.A., Calcitonin gene-related peptide, substance P and protein gene product 9.5 immunoreactive axonal fibers in the rat footpad skin following partial sciatic nerve injuries. J Neurocytol 2000; 29(4): 249-62.

36.
Yen, L.D., Bennett, G.J., and Ribeiro-da-Silva, A., Sympathetic sprouting and changes in nociceptive sensory innervation in the glabrous skin of the rat hind paw following partial peripheral nerve injury. J Comp Neurol 2006; 495(6): 679-90.

37.
Facer, P., Casula, M.A., Smith, G.D., et al., Differential expression of the capsaicin receptor TRPV1 and related novel receptors TRPV3, TRPV4 and TRPM8 in normal human tissues and changes in traumatic and diabetic neuropathy. BMC Neurol 2007; 7: 11.

38.
Bennett, G.J. and Xie, Y.K., A peripheral mononeuropathy in rat that produces disorders of pain sensation like those seen in man. Pain 1988; 33(1): 87-107.

39.
Peleshok, J.C. and Ribeiro-da-Silva, A., Delayed reinnervation by nonpeptidergic nociceptive afferents of the glabrous skin of the rat hindpaw in a neuropathic pain model. J Comp Neurol 2011; 519(1): 49-63.

40.
Kim, S.H. and Chung, J.M., An experimental model for peripheral neuropathy produced by segmental spinal nerve ligation in the rat. Pain 1992; 50(3): 355-63.

41.
Decosterd, I. and Woolf, C.J., Spared nerve injury: an animal model of persistent peripheral neuropathic pain. Pain 2000; 87(2): 149-58.

42.
Wu, G., Ringkamp, M., Hartke, T.V., et al., Early onset of spontaneous activity in uninjured C-fiber nociceptors after injury to neighboring nerve fibers. J Neurosci 2001; 21(8): RC140.

43.
Wu, G., Ringkamp, M., Murinson, B.B., et al., Degeneration of myelinated efferent fibers induces spontaneous activity in uninjured C-fiber afferents. J Neurosci 2002; 22(17): 7746-53.

44.
Hudson, L.J., Bevan, S., Wotherspoon, G., et al., VR1 protein expression increases in undamaged DRG neurons after partial nerve injury. Eur J Neurosci 2001; 13(11): 2105-14.

45.
Katsura, H., Obata, K., Mizushima, T., et al., Antisense knock down of TRPA1, but not TRPM8, alleviates cold hyperalgesia after spinal nerve ligation in rats. Exp Neurol 2006; 200(1): 112-23.

46.
Huang, D. and Yu, B., The mirror-image pain: an unclered phenomenon and its possible mechanism. Neurosci Biobehav Rev 2010; 34(4): 528-32.

47.
Koltzenburg, M., Wall, P.D., and McMahon, S.B., Does the right side know what the left is doing? Trends Neurosci 1999; 22(3): 122-7.

48.
Pachter, B.R. and Eberstein, A., Nerve sprouting and endplate growth induced in normal muscle by contralateral partial denervation of rat plantaris. Brain Res 1991; 560(1-2): 311-4.

49.
Rotshenker, S., Transneuronal and peripheral mechanisms for the induction of motor neuron sprouting. J Neurosci 1982; 2(10): 1359-68.

50.
Gabella, G., Berggren, T., and Uvelius, B., Hypertrophy and reversal of hypertrophy in rat pelvic ganglion neurons. J Neurocytol 1992; 21(9): 649-62.

51.
McLachlan, E.M., Janig, W., Devor, M., and Michaelis, M., Peripheral nerve injury triggers noradrenergic sprouting within dorsal root ganglia. Nature 1993; 363(6429): 543-6.

52.
Chiaia, N.L., Allen, Z., Carlson, E., MacDonald, G., and Rhoades, R.W., Neonatal infraorbital nerve transection in rat results in peripheral trigeminal sprouting. J Comp Neurol 1988; 274(1): 101-14.

53.
Doubleday, B. and Robinson, P.P., Nerve growth factor depletion reduces collateral sprouting of cutaneous mechanoreceptive and tooth-pulp axons in ferrets. J Physiol 1994; 481 (Pt 3): 709-18.

54.
Kolston, J., Lisney, S.J., Mulholland, M.N., and Passant, C.D., Transneuronal effects triggered by saphenous nerve injury on one side of a rat are restricted to neurones of the contralateral, homologous nerve. Neurosci Lett 1991; 130(2): 187-9.

55.
Oaklander, A.L. and Brown, J.M., Unilateral nerve injury produces bilateral loss of distal innervation. Ann Neurol 2004; 55(5): 639-44.

56.
Johnson, E.O. and Soucacos, P.N., Nerve repair: experimental and clinical evaluation of biodegradable artificial nerve guides. Injury 2008; 39 Suppl 3: S30-6.

57.
Lundborg, G. and Rosen, B., Hand function after nerve repair. Acta Physiol (Oxf) 2007; 189(2): 207-17.

58.
Wolford, L.M. and Stevao, E.L., Considerations in nerve repair. Proc (Bayl Univ Med Cent) 2003; 16(2): 152-6.

59.
Navarro, X., Verdu, E., Wendelschafer-Crabb, G., and Kennedy, W.R., Immunohistochemical study of skin reinnervation by regenerative axons. J Comp Neurol 1997; 380(2): 164-74.

60.
Stankovic, N., Johansson, O., and Hildebrand, C., Occurrence of epidermal nerve endings in glabrous and hairy skin of the rat foot after sciatic nerve regeneration. Cell Tissue Res 1996; 284(1): 161-6.

61.
Nurse, C.A., Macintyre, L., and Diamond, J., Reinnervation of the rat touch dome restores the Merkel cell population reduced after denervation. Neuroscience 1984; 13(2): 563-71.

62.
Wong, W.C. and Kanagasuntheram, R., Early and late effects of median nerve injury on Meissner's and Pacinian corpuscles of the hand of the macaque (M. fascicularis). J Anat 1971; 109(Pt 1): 135-42.

63.
Jasmin, L., Kohan, L., Franssen, M., Janni, G., and Goff, J.R., The cold plate as a test of nociceptive behaviors: description and application to the study of chronic neuropathic and inflammatory pain models. Pain 1998; 75(2-3): 367-82.

64.
Allchorne, A.J., Broom, D.C., and Woolf, C.J., Detection of cold pain, cold allodynia and cold hyperalgesia in freely behaving rats. Mol Pain 2005; 1: 36.

65.
Yalcin, I., Charlet, A., Freund-Mercier, M.J., Barrot, M., and Poisbeau, P., Differentiating thermal allodynia and hyperalgesia using dynamic hot and cold plate in rodents. J Pain 2009; 10(7): 767-73.

66.
Tanimoto-Mori, S., Nakazato-Imasato, E., Toide, K., and Kita, Y., Pharmacologic investigation of the mechanism underlying cold allodynia using a new cold plate procedure in rats with chronic constriction injuries. Behav Pharmacol 2008; 19(1): 85-90.

67. Wang, L.X. and Wang, Z.J., Animal and cellular models of chronic pain. Adv Drug Deliv Rev 2003; 55(8): 949-65.

68.
Mogil, J.S., Animal models of pain: progress and challenges. Nat Rev Neurosci 2009; 10(4): 283-94.

69.
Irwin, M.S., Gilbert, S.E., Terenghi, G., Smith, R.W., and Green, C.J., Cold intolerance following peripheral nerve injury. Natural history and factors predicting severity of symptoms. J Hand Surg Br 1997; 22(3): 308-16.

70.
Ruijs, A.C., Jaquet, J.B., van Riel, W.G., Daanen, H.A., and Hovius, S.E., Cold intolerance following median and ulnar nerve injuries: prognosis and predictors. J Hand Surg Eur Vol 2007; 32(4): 434-9.

71.
Ruijs, A.C., Niehof, S.P., Selles, R.W., et al., Digital rewarming patterns after median and ulnar nerve injury. J Hand Surg Am 2009; 34(1): 54-64.

72.
Ruijs, A.C., Niehof, S.P., Hovius, S.E., and Selles, R.W., Cold-induced vasodilatation following traumatic median or ulnar nerve injury. J Hand Surg Am 2011; 36(6): 986-93.

2

COLD INDUCED VASODILATATION IN COLD INTOLERANT RATS AFTER NERVE INJURY

L.S. Duraku [1*]
E.S. Smits [1*]
S.P. Niehof [2]
H.A.M. Daanen [3,4]
S.E.R. Hovius [1]
R.W. Selles [1,5]
E.T. Walbeehm [1]

*Both authors contributed equally

1. Department of Plastic, Reconstructive and Hand Surgery, Erasmus MC, University Medical Center, Rotterdam, The Netherlands

2. Pain Treatment Center, Erasmus MC, University Medical Center, Rotterdam, The Netherlands

3. Research Institute MOVE, Faculty of Human Movement Sciences, VU University, Amsterdam, The Netherlands

4. TNO Behavioral and Societal Sciences, Soesterberg, The Netherlands

5. Department of Rehabilitation Medicine, Erasmus MC, University Medical Center, Rotterdam, The Netherlands

ABSTRACT

Cold Induced Vasodilatation (CIVD) is a cyclic regulation of blood flow during prolonged cooling of protruding body parts. It is generally considered to be a protective mechanism against local cold injuries and cold intolerance after peripheral nerve injury. The aim of this study was to determine the role of the sympathetic system in initiating a CIVD response. Eight rats were operated according to the Spared Nerve Injury (SNI) model, eight underwent a Complete Sciatic Lesion (CSL) and six underwent a sham operation. Prior to operation, three, six and nine weeks postoperatively, both hind limbs were cooled and skin temperature was recorded to evaluate the presence of CIVD reactions. Cold intolerance was determined using the cold plate test and mechanical hypersensitivity was measured using the Von Frey test. No significant difference in CIVD was found comparing the lateral operated hind limb for time (preoperatively and three, six and nine weeks postoperatively; $p=0.397$) and for group (SNI, CSL and Sham; $p=0.695$). SNI and CSL rats developed cold intolerance and mechanical hypersensitivity. Our data show that the underlying mechanisms that initiate a CIVD reaction are not affected by damage to a peripheral nerve that includes the sympathetic fibers. We conclude that the sympathetic system does not play a major role in the initiation of CIVD in the hind limb of a rat. No substantial changes in the CIVD reaction after peripheral nerve injury imply that the origin of cold intolerance after a traumatic nerve injury is initiated by local factors and has a more neurological cause. This is an important finding for future developing treatments for this common problem, since treatment focusing on vaso-regulation may not help diminish symptoms of cold intolerant patients.

INTRODUCTION

Abnormal pain after exposure to cold is one of the most common long-term complaints of patients after a nerve injury. The incidence of cold intolerance in humans with a nerve injury is estimated to be 56 % to 83% [1-4]. Unfortunately, the only remedy described for cold intolerance is to instruct this patient group to avoid cold stimulations [5]. An important reason why treatment is unavailable may be that the pathophysiology of cold intolerance is still unclear, in particular the mechanism of Cold Induced Vasodilatation (CIVD).

CIVD is a cyclic regulation of blood flow during prolonged cooling of protruding body parts, such as the hands, feet, chin and nose[6, 7]. Lewis et al. first described CIVD in 1930 [8], and it is generally seen as a protective mechanism for local cold injuries [9, 10]. In healthy humans, CIVD generally occurs after a minimum cooling time of 5 minutes in an environment of maximally 15°C [11]. However, changes in CIVD response in individuals who live in cold environments appear to be neither guaranteed nor predictable [12]. The presence and nature of a CIVD reaction depends on a large number of variables. For example, a higher body core temperature as well as the intake of food leads to a stronger and faster CIVD reaction [6, 13-15]. Changes in the CIVD reaction have been described in patients with cold intolerance after a traumatic peripheral nerve injury [16-19]. It has been suggested that there is a relation between CIVD and the treatment of posttraumatic cold intolerance [19].

It is undisputed that the sympathetic nervous system plays a role in the magnitude of CIVD, since the magnitude of CIVD is strongly dependent on central body temperature [14, 20]. However, it is still debated if the sympathetic system is initiating the CIVD response or if peripheral triggers are responsible. Flouris et al. (2008) exposed ten appropriately dressed adults to -20°C and observed oscillatory changes in finger blood flow that were related to body core temperature [21]. They concluded that these changes, which they called CIVD, appeared to be the 'eventuality of the thermoregulatory function based on the suppression and activation of the sympathetic vasoconstrictor system'. Daanen (2009), however, argued that these changes should not be named CIVD, since the finger skin temperatures ranged from 7.2 to 33.5°C and the observed fluctuations during the experiment did not resemble the typical cyclic CIVD reaction [22]. Later, Flouris and Cheung (2009) concluded from changes in heat balance during exposure of hands to cold air that "CIVD is a centrally originating phenomenon caused by sympathetic vasoconstrictor withdrawal" [23]. It was challenged that these observations showed that finger blood flow and body heat content were unrelated [24]. Since eliminating the sympathetic drive is hard to accomplish in humans without side effects, we decided to investigate the role of the sympathetic system in rat paws in a systematic way. Although the locations

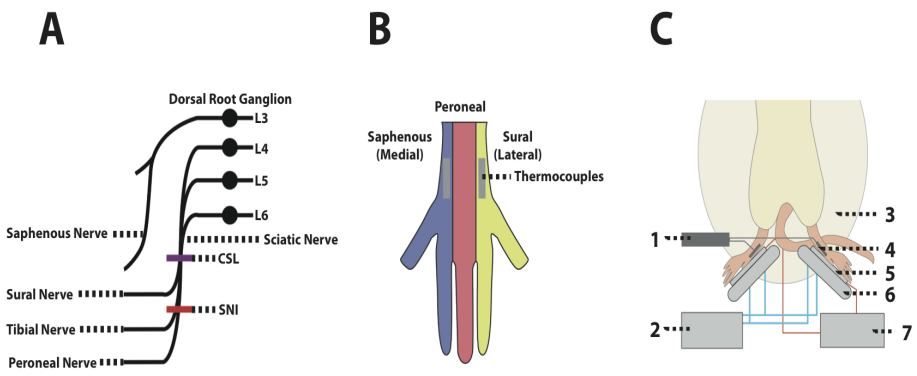

FIGURE 1

1A: Operation methods of the Spared Nerve Injury (SNI) and the Complete Sciatic Lesion (CSL). The SNI procedure a ligation of the tibial and common peroneal nerves leaving the sural nerve intact. CSL compromised a ligation of the sciatic nerve, 1 cm above the three main branches of the sciatic nerve. Sham controls involved exposure of the sciatic nerve and its branches without any lesion. 1B: Positioning of the thermocouples on the hind limbs of the rat. Innervated areas of the nerves are colored on the hind limbs. 1C: Illustration of the cooling setup and positioning of the rat. 1: USB-based 8-channel thermocouple input module, 2: Thermostatic bath, 3: Heating mattress. 4: Thermocouples, 5: Peltier elements, 6: Water coolers, 7: Power supply.

Location	Time	Mean Temperature °C (SD)
Operated paw	Pre-operative	27.4 (3.1)
	3 weeks	26.7 (3.2)
	6 weeks	27.2 (0.6)
	9 weeks	25.9 (2.3)
Rectal	Pre-operative	36.5 (1.1)
	3 weeks	36.0 (1.2)
	6 weeks	34.8 (1.9)
	9 weeks	35.9 (1.1)

TABLE 1

Displayed are the mean operated paw and rectal temperatures during cooling in °C at the different time points.

where CIVD is observed differ between rats (mainly tail and paws) and humans (mainly fingers and toes), the mechanism and control seems to be comparable, the Arterio-Venous Anastomoses (AVA's) that are under sympathetic control are the anatomical structures where CIVD is observed [24-27]. In this study, we evaluated the CIVD reaction in rats with different types of nerve injury because this allows us to standardize the nerve lesion and to exclude additional factors caused by the trauma such as vascular damage. To do so, a spared nerve injury model (SNI), and complete sciatic lesion (CSL) model [28, 29] was used. The SNI and CSL models are well-documented nerve injury models that are known to be cold intolerant [29, 30]. As in cold stress testing, evaluation of the CIVD reaction may be a tool to assess the quality of the thermoregulatory system in rats after peripheral nerve injuries. It is presently unknown if the timing and amplitude of the CIVD reaction during cold stress is modified in rats with peripheral nerve injuries and whether the presence or absence of a CIVD reaction is related to cold intolerance.

The aim of this study was to determine the role of the sympathetic system in initiating a CIVD response. To do so, prior to operation as well as three, six and nine weeks postoperatively, both hind limbs were cooled and skin temperature was recorded to evaluate the presence and absence of CIVD reactions. The rats were measured if they experienced presence of cold intolerance and mechanical hypersensitivity.

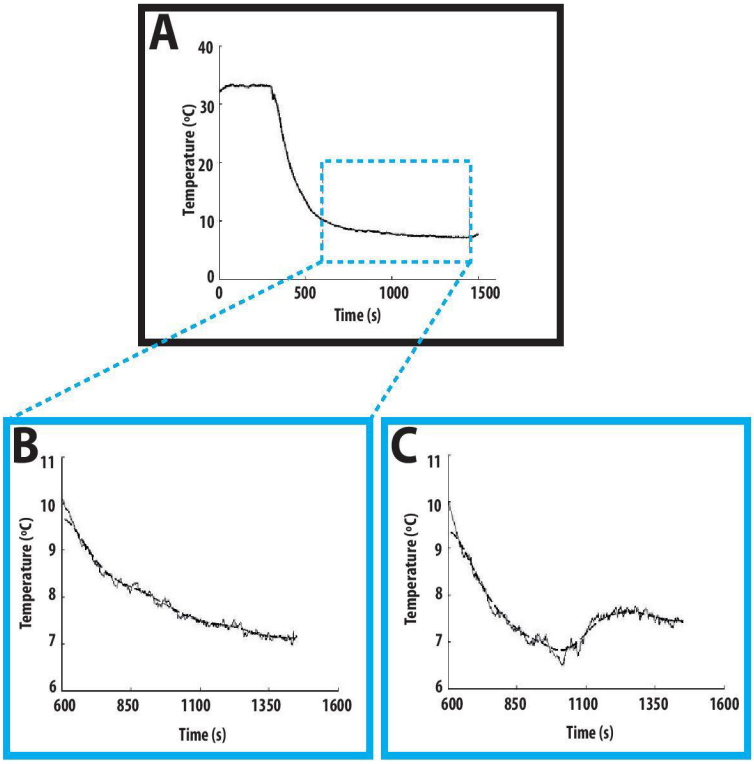

FIGURE 2

Typical example of temperature during the cooling phase, illustration of the Cold Induced Vasodilatation, the so-called Hunting reaction, in one of the rats. A) Illustration of the total pre- and cooling phase. The analysis period started 375 seconds after the start of cooling and lasted for 850 seconds. The selected cooling phase in Figure 1B and 1C are raw and filtered data. B) A typical example of a cooling phase without CIVD reaction. C) A typical example of a CIVD reaction during the cooling phase. A CIVD was identified when the temperature of the filtered signal increased at least 0.4 °C during the cooling phase.

MATERIAL AND METHODS

A recently developed and validated set-up [31] was used to measure the CIVD response bilaterally. All animal experimental procedures were approved by the Animal Experiment Commission of the Erasmus MC and were performed in accordance with the National Institutes of Health guidelines on animal care.
Twenty-two male Wistar rats, (weights 350-500g) were randomly divided into three groups. In one group (n=8) the left hind limb was operated according to the SNI model of Decosterd and Woolf [29], in the second group (n=8) the left hind limb of the rats underwent a Complete Sciatic Lesion (CSL) [30] and in the third group (n=6) the left hind limb was operated according to the sham model [29] to compare and verify these models. All Wistar rats underwent the same general treatment and were not significantly different for gender, weight, habitat and nutrition.

SURGERY

Under isoflurane (2%) anesthesia, the skin on the left lateral surface of the thigh was incised and a deviation was made through the septum of the biceps femoris muscle exposing the sciatic nerve and its three main branches: the sural, common peroneal and tibial nerves. The SNI procedure comprised an axotomy and ligation of the tibial and common peroneal nerves leaving the sural nerve intact. The common peroneal and the tibial nerves were tightly ligated with 8.0 ethilon and sectioned distal to the ligation, removing 1.0 mm of the distal nerve stump. Great care was taken to avoid any contact with, or stretching of the intact sural nerve. Septum and skin were closed in two layers. CSL compromised a ligation of the sciatic nerve, 1 cm above the three main branches of the sciatic nerve (Figure 1 A). Sham controls involved exposure of the sciatic nerve and its branches without any lesion.

COLD PLATE TEST

To measure the presence of cold intolerance we evaluated the limb withdrawal time. The rats were placed in a clear covered chamber black-blinded Plexiglas cage (50 cm × 50 cm × 50 cm) on an aluminum plate with a surface temperature of 5°C. We measured the limb withdrawal latency, which defines the latency of the rat first limb lift after the rat has been placed on the cold plate [32]. An experimenter who was blinded for the test groups manually measured the latency. Measurement of the limb withdrawal latency was performed preoperatively and three, six and nine weeks postoperatively.

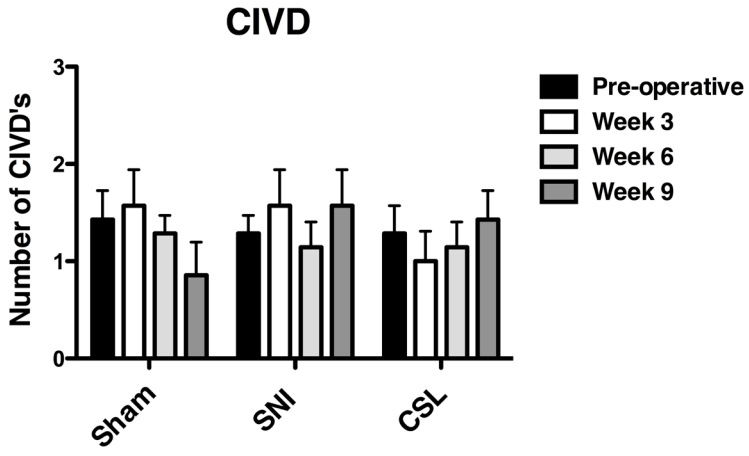

FIGURE 3

The amount of CIVD reactions displayed. No significant differences were found between the groups. The X-axis shows the three operated groups: A sham operated group, a spared nerve injury model (SNI) operated group and a complete sciatic lesion (CSL) operated group. The Y-axis shows the number of CIVD reactions during the cooling phase.

Cold Plate Test (s)	3 weeks	6 weeks	9 weeks
CSL	160.3 (28.5)	35.4 (24.3)	43.6 (29.9)
SNI	10.2 (7.8)	8.9 (9.0)	9.0 (8.3)
Sham	163.5 (33.9)	152.4 (37.8)	159.2 (35.5)

TABLE 2

Cold plate test for cold hypersensitivity. The paw lift latency is shown in seconds with standard deviation between parenthesis during the different measurement times in all three groups. After 3 weeks SNI rats developed a significant cold hypersensitivity as compared to the sham group and the CSL rats. The latter group also developed these symptoms after 6 weeks.

VON FREY TEST

To measure the presence of mechanical hypersensitivity we used the Von Frey test. Withdrawal threshold to touch was measured with a set of Von Frey hairs ranging from 0.25 to 60.0g. The rat was placed in a chamber with a mesh metal floor, covered by a Plexiglas dome of 20 x 30cm and 10cm high. The dome enabled the rat to walk freely but not to rear up on its hind limbs. Hence, the experimenter was able to reach the plantar surface of the limbs from beneath, unobserved by the rat. Each Von Frey hair was applied for 2s at 5s intervals. When at least 3 of the 5 applied applications evoked responses, the Von Frey test was considered positive. At threshold, rats responded by a quick limb flick. An experimenter who was blind for the different test groups measured this manually. Measurement of the Von Frey test was performed preoperatively and three, six and nine weeks postoperatively.

EVOKING CIVD REACTIONS

The rats were placed in a supine position (Figure 1 C). We measured temperature on seven different points on the lower extremities as well as rectally. The ventral sides of the hind limbs were placed onto two vertically positioned Peltier cooling elements (Figure 1 C) using surgical tape. A Peltier cooler is a solid-state active heat pump that transfers heat from one side of the device to the other to generate cooling. The dorsal sides of the limbs were left exposed for thermocouple attachment and to allow thermographic recording.

The thermocouple probes were placed on the marked areas on both limbs (Figure 1 B). One thermocouple was attached to a rectal probe to monitor the core temperature and one thermocouple measured the ambient temperature. Thermocouple registration with a sample rate of 2 measurements every second was done by an USB-based 8-channel thermocouple input module (Measurement Computing). Calibration of the device and the thermocouples was performed using Instacal (v5.82, Measurement Computing). The data storage was provided using an in house developed program in Labview (v7.1, National Instruments) and data were exported to Matlab (version 7.8 R2009a). Peltier elements were controlled at a temperature of 3°C, resulting in the cooling of both limbs of the rat. In order to prevent a drop in rectal temperature in an anesthetized rat due to hind limb cooling, a heating mattress (39.5°C) was used to maintain body core temperature during the pre phase and the cooling phase. Respiratory rate was monitored as indicator of depth of anesthesia throughout the experiment.

The measurement was divided into two phases. We started with a pre-phase of five minutes to measure the temperature of the anesthetized rat at rest without cooling. Thereafter we cooled the rats for twenty minutes to evoke a CIVD reaction. Based on the literature of work in rat tails by Thomas et al. and Gardner et al. and in humans by Daanen [6, 25, 28] we chose a cooling period of 20 minutes to investigate the role of

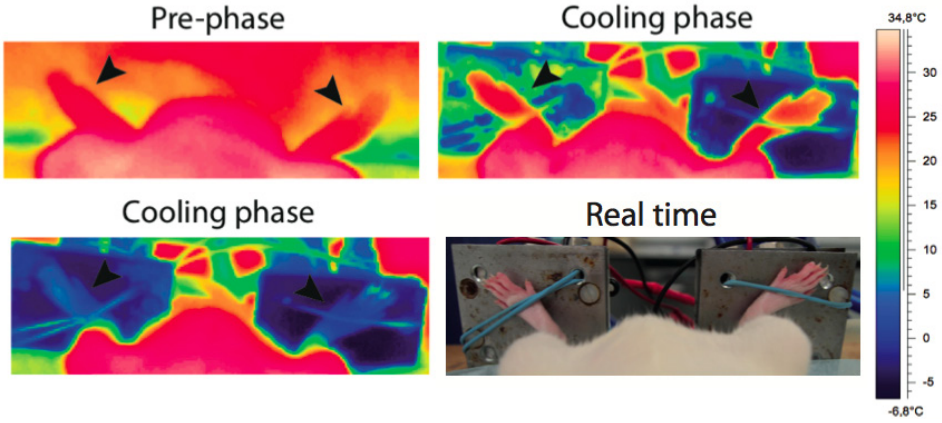

FIGURE 4

Thermographic imaging and a real time photo of the body of the rat during the experiment, both hind limbs and the Peltier element. Pre-phase: Rat is dorsally positioned under anesthesia to measure baseline temperatures of the hind limbs. Cooling phase (20 min.): Both hind limbs are attached to the Peltier elements. The color indicates that both Peltier elements and hind limbs get equally cooled.

Von Frey Test (g)	3 weeks	6 weeks	9 weeks
CSL	43.6 (20.7)	8.4 (3.5)	8.6 (4.7)
SNI	3.0 (1.7)	2.4 (1.9)	3.6 (1.5)
Sham	31.9 (20.2)	39.0 (20.0)	30.3 (21.1)

TABLE 3

Von Frey Test for mechanical hypersensitivity. The amount of force (g) is shown of the Von Frey filaments needed to obtain a mechanical reflex withdrawal response with standard deviation between parentheses. After 3 weeks SNI rats developed a significant mechanical hypersensitivity as compared to the sham group and the CSL rats. The latter group also developed these symptoms after 6 weeks.

the sympathetic system in initiating a CIVD response.
Temperature measurements (CIVD reactions) were performed pre-operatively and on three, six and nine week's post-operative. All measurements took place at the same location under similar conditions. All rats were cared for each day for the duration of the entire experiment. Rats stayed in the experiment room until the anesthesia had worn out. The rats were provided with water and food ad libitum. All rats were habituated for at least seven days before any measurements were executed. The weight of the rat was recorded on every day of the measurement.The measurement period started 375 seconds after the start of cooling and lasted for 850 seconds. As a first step, we fitted the data using a low-pass Gaussian filter with a standard deviation of 44 seconds to model the overall change in temperature and to remove higher frequency noise (see Figure 2). CIVD was defined as an increase in temperature of the filtered signal of at least 0.4 °C. When CIVD was present, we scored the number of CIVD reactions in each rat as well as the increase in temperature of each CIVD. The amount of CIVD waves was counted; the height of the CIVD reaction was scored from 1 to 4. The height was scored from 1-4 based on temperature increase in tenths of °C. We plotted the raw and the filtered data and cut and enlarged the CIVD reaction. Three investigators scored the blinded plots. When the investigators disagreed in scoring they discussed the situation and together they defined the score. When all CIVD's were identified, we scored the number of CIVD reactions in each rat and calculated the time of onset of the CIVD after cooling was initiated.

STATISTICAL ANALYSIS
Values are means ± SEM. The software package SPSS was used for all statistical analysis. Effects were considered significant if $P \leq 0.05$. We used a two way ANOVA with one repeated-measures factor for time (pre operative and three, six and nine weeks post-operative) and one between-subject factor for group (SNI, CSL and Sham) to evaluate changes of time and differences between groups. To test the normality of the data of each week we used a Shapiro-Wilk test.

RESULTS

Ambient temperature during the experiment averaged 25.1°C. The minimum ambient temperature was 22.8ºC (SD 0.73ºC). The core temperature of the rats was stabile at 35.9ºC (SD 1.4ºC). Mean temperatures of the operated paw and rectal temperatures in °C are displayed in Table 1, showing the variation in temperature during cooling. One rat passed away after the measurements of the third week. The rat was part of the SNI group, reducing the number of rats in this group to 7.

COLD PLATE TEST

For the reference test for cold intolerance, we found that the sham group showed no paw withdrawal response when exposed to the cold plate surface of 5 ºC for 140 seconds. In contrast, the SNI-group showed a significant reduced paw-withdrawal latency at all postoperative time points ($p<0.001$). The CSL-group had a significant reduced paw-withdrawal latency only at 6 and 9 weeks as compared to the sham group ($p<0.001$). There was no significant difference between the SNI and CSL rats at 6 and 9 weeks in paw withdrawal response due to exposure to a 5 ºC cold plate (Table 2). These results show that the SNI and CSL rats developed cold hypersensitivity due to nerve injury.

VON FREY TEST

The results of the Von Frey test display that the SNI group has a significant mechanical hypersensitivity due to nerve injury (Table 3). For the reference for mechanical hypersensitivity, we found that the amount of force of the Von Frey filaments needed to obtain a mechanical withdrawal reflex was lower in the SNI group at all postoperatively (3,6 and 9 weeks) time-points as compared to the Sham group. The CSL displayed a lower mechanical withdrawal threshold as compared to the Sham group at 6 and 9 weeks postoperatively; however, this difference was not statistically significant. No significant differences were found between the mechanical withdrawal thresholds of the SNI and CSL rats.

CIVD REACTIONS

The investigators differed in 5.9% of the manual CIVD scores of the temperature curves but rapidly came to consensus. No significant effect of time (preoperatively and three, six and nine weeks postoperatively; $p=0.397$) and group (SNI, CSL and Sham; $p=0.695$) were found for the number of CIVD's in the lateral operated hind limb (Fig. 3).

DISCUSSION

The aim of this study was to determine the role of the sympathetic system of initiating a CIVD response. The results of the cold plate test and the von Frey test clearly demonstrated that the SNI and CSL rats developed cold intolerance and mechanical hypersensitivity. The nerve lesions of the tibial nerve resulted in cold and mechanical hypersensitivity at 3, 6 and 9 weeks after the lesion. The sciatic nerve lesion resulted in cold and mechanical hypersensitivity at 6 and 9 weeks after the operation, but not after 3 weeks.

In this study no significant differences in CIVD reactions were observed between CSL, SNI and the sham operated rats. The sympathetic nerves are part of the nerves that were cut during the operation. Therefore, we can conclude that the sympathetic system initiating the CIVD response has no effect on the CIVD reaction and that peripheral triggers are more likely responsible for initiating a CIVD reaction.

A possible explanation for the absence of changes in patterns of the CIVD reactions could be that vascular control can function without peripheral nerve innervation and that the smooth muscles in the vessel wall have no effect on any type of denervation of the peripheral nerve. It could be possible that more local factors such as norepinephrine have more influence [33] than denervation of the hind paw by a nerve lesion. Active cutaneous vasodilatation occurs via cholinergic nerve co-transmission and has been shown to include potential roles for nitric oxide, vasoactive intestinal peptide, prostaglandins, and substance P. It has been proven both interesting and challenging that not one substance has been identified as the sole mediator of active cutaneous vasodilatation [34]. It could be that noradrenaline plays an important role, as Stephens et al. (2001) identified in young men. Stephens et al. (2001) also showed that complete postsynaptic blockade of norepinephrine-mediated vasoconstriction did not completely inhibit the reflex vasoconstrictor response to 15 min of progressive decrease in skin temperature, although presynaptic inhibition with bretylium abolished response [34, 35].

In the study of Eide (1976) tail temperature increased after an initial temperature decrease produced by immersion in ice water, followed by several CIVD cycles after varying time periods [36]. In contrast, the CIVD response was completely absent in the study of Thomas et al. (1994) in cold injured rat-tails. CIVD remained absent at least several weeks after exposure to the injury condition, implicating the loss of CIVD [25, 37]. For future studies on the onset of a CIVD, we suggest cooling the rat's paw for at least 20 minutes between 0-5 °C, and measure with a time interval of maximally 1 second. When the experimental setting would allow this, cooling for longer periods (e.g, 40 minutes) would yield multiple CIVD reactions in a single recording.

Our findings may seem in contrast with a recently published study of Wen Hu et al. 2012 [38] that showed a significant difference in CIVD reaction of the hindpaw following an autograft repair after a sciatic nerve injury when compared to a control group. However, the differences may be explained by the fact that we measured during cooling and Wen Hu et al. measured after cooling. Wen Hu et al. initially cooled the hind paws in smashed ice for 5 minutes, immediately dried the hind paws with a towel and then measured the blood perfusion by means of a laser Doppler when the cooling has already stopped. This approach is not in line with the common definition of a CIVD reaction as a cyclic vasodilatation response during cooling [39]. Wen Hu et al. shows that after the cooling phase, a vasodilatory response occurs in the first minutes which disappears after about 10 minutes; after this period no cyclic vasodilatation or vasoconstriction occurs. Therefore we believe that the measured blood perfusion changes are not CIVD's but are active rewarming patterns, which, due to vasodilatation [40], occur after a period of cold exposure and have been shown to be disturbed in patients with peripheral nerve injury [41]. Other explanations between the discrepancies between our and their study may be the usage of different strains of rats (Wistar vs Sprague-Dawley) and/or different models of nerve manipulation. In the current study the nerve injury leads to distinct neuropathic pain behavior, whereas in the study conducted by Wen Hu et al. the nerve injury and reconstruction does not result in any pain behavior. This implies that peripheral nerves are altered differently in the two models, which in turn may alter peripheral thermoregulation and can lead in different results.

Generating cold intolerance using the operation models for SNI and CSL has proven to be successful, as demonstrated with the cold plate test (cold intolerance) and the Von Frey test (mechanical hypersensitivity). In addition, the sham operation apparently has no consequences for the sensitivity to temperature or mechanical pain, and SNI and CSL are therefore appropriate models to evoke cold intolerance. It has been described that the innervation differs between the different operation models. In the SNI model, the medial and lateral sides of the foot sole are still innervated, these are stimulated during the behavioral tests [29, 42, 43]. In the CSL model the foot sole is de-innervated after a sciatic nerve lesion. It is known that after approximately 3 weeks after nerve injury sprouting of non-injured fibers starts [27, 44]. Therefore in the CSL model the foot sole probably starts to re-innervate after 3 weeks, therefore the hypersensitivity to mechanical and cold stimuli is evident only after 6 weeks.

We continued to monitor the rat when it was removed from the Peltier elements and occasionally the rectal probe shifted and was exposed to surrounding temperature, this explains why the minimum rectal temperatures sometimes dropped below the 35 °C. Re-evaluating the data, we found that when the probe was placed back into the rectum, core temperature had not decreased lower than 35 °C. Core and surrounding temperature were monitored very strictly during the entire experiment

as previous work described the importance of a stable environment and core temperature [6].

The observed cyclic changes after cooling the rat hind limbs are strongly indicative of the phenomenon of CIVD, and appear qualitatively similar to CIVD reactions reported in rats' tail and in human's, and display considerable pattern variability as also observed in humans and in rat tails [6, 8, 25]. Moreover, these cyclic patterns appear comparable to patterns of CIVD reported in an in vitro preparation of isolated segments of rat tail arteries exposed to cold [28]. The currently employed study design [31] may add to the existing methods. CIVD research is hampered by the absence of a uniform quantification of CIVD responses. Therefore, we would like to stress that studies should try to develop a schematic algorithm to define a CIVD reaction which takes different variables such as core temperature, cooling temperature, subject and surrounding temperature into account.

Greenfield et al. demonstrated in 1951 that intact peripheral nerves are not essential to the vasodilatation phase of the CIVD in humans [45]. Daanen and Ducharme et al. demonstrated in humans that the axon reflexes do not occur in a cold-exposed hand and thus are unlikely to explain the CIVD phenomenon [46]. Based on previous work and the results of our study we conclude that rats and possibly humans that underwent a peripheral nerve injury still experience the so-called hunting reaction. Humans and rats will still experience an aching in the hands and paws respectively which corresponds to cutaneous vasoconstriction, and periods of warmness and tingling may follow corresponding to vasodilatation and renewed blood flow [8, 28]. We suggest that the underlying mechanisms that initiate a CIVD reaction are not affected by damage to a peripheral nerve. We conclude that the sympathetic system, which initiates the CIVD response, has no effect on the CIVD reaction and local triggers are more likely responsible for the CIVD reaction. No substantial changes in the CIVD reaction after peripheral nerve injury imply that the origin of cold intolerance after a traumatic nerve injury is initiated by local factors. Further research on the pathophysiology of cold intolerance should concentrate on local biochemical changes and their effects on small nerve fiber endings and micorovascularisation.

REFERENCES

1.
Collins, E.D., Novak, C.B., Mackinnon, S.E., and Weisenborn, S.A., Long-term follow-up evaluation of cold sensitivity following nerve injury. J Hand Surg Am 1996; 21(6): 1078-85.

2.
Irwin, M.S., Gilbert, S.E., Terenghi, G., Smith, R.W., and Green, C.J., Cold intolerance following peripheral nerve injury. Natural history and factors predicting severity of symptoms. J Hand Surg Br 1997; 22(3): 308-16. Table1.jpg

3.
Lenoble, E., Dumontier, C., Meriaux, J.L., et al., [Cold sensitivity after median or ulnar nerve injury based on a series of 82 cases]. Ann Chir Main Memb Super 1990; 9(1): 9-14.

4.
Ruijs, A.C., Jaquet, J.B., van Riel, W.G., Daanen, H.A., and Hovius, S.E., Cold intolerance following median and ulnar nerve injuries: prognosis and predictors. J Hand Surg Eur Vol 2007; 32(4):
434-9.

5.
Lithell, M., Backman, C., and Nystrom, A., Pattern recognition in post-traumatic cold intolerance. J Hand Surg Br 1997; 22(6): 783-7.

6.
Daanen, H.A., Finger cold-induced vasodilation: a review. Eur J Appl Physiol 2003; 89(5): 411-26.

7.
LeBlanc, J., Dulac, S., Cote, J., and Girard, B., Autonomic nervous system and adaptation to cold in man. J Appl Physiol 1975; 39(2): 181-6.

8.
Lewis, T., Observation upon the reactions of the vessels of the human skin to cold. Heart 1930; (15): p. 177-208.

9.
Daanen, H.A. and van der Struijs, N.R., Resistance Index of Frostbite as a predictor of cold injury in arctic operations. Aviat Space Environ Med 2005; 76(12):
1119-22.

10.
Wilson, O. and Goldman, R.F., Role of air temperature and wind in the time necessary for a finger to freeze. J Appl in the treatment of posttraumatic digital cold intolerance. J Hand Surg Am 1986; 11(3): 382-7.

11.
Van der Struijs, N.R., Van Es, E.M., Raymann, R.J., and Daanen, H.A., Finger and toe temperatures on exposure to cold water and cold air. Aviat Space Environ Med 2008; 79(10): 941-6.

12.
Cheung, S.S. and Daanen, H.A., Dynamic adaptation of the peripheral circulation to cold exposure. Microcirculation 2012; 19(1): 65-77.

13.
Cheung, S.S. and Mekjavic, I.B., Cold-induced vasodilatation is not homogenous or generalizable across the hand and feet. Eur J Appl Physiol 2007; 99(6): 701-5.

14.
Daanen, H.A., Van de Linde, F.J., Romet, T.T., and Ducharme, M.B., The effect of body temperature on the hunting response of the middle finger skin temperature. Eur J Appl Physiol Occup Physiol 1997; 76(6): 538-43.

15.
Takano, N. and Kotani, M., Influence of food intake on cold-induced vasodilatation of finger. Jpn J Physiol 1989; 39(5): 755-65.

16.
Backman, C.O., Nystrom, A., Backman, C., and Bjerle, P., Cold induced vasospasm in replanted digits: a comparison between different methods of arterial reconstruction. Scand J Plast Reconstr Surg Hand Surg 1995; 29(4): 343-8.

17.
Ruijs, A.C., Niehof, S.P., Hovius, S.E., and Selles, R.W., Cold-induced vasodilatation following traumatic median or ulnar nerve injury. J Hand Surg Am 2011; 36(6): 986-93.

18.
Isogai, N., Fukunishi, K., and Kamiishi, H., Patterns of thermoregulation associated with cold intolerance after digital replantation. Microsurgery 1995; 16(8): 556-65.

19.
Brown, F.E., Jobe, J.B., Hamlet, M., and Rubright, A., Induced vasodilation in the treatment of posttraumatic digital cold intolerance. J Hand Surg Am 1986; 11(3): 382-7.

20.
Daanen, H.A. and Ducharme, M.B., Finger cold-induced vasodilation during mild hypothermia, hyperthermia and at thermoneutrality. Aviat Space Environ Med 1999; 70(12): 1206-10.

21.
Flouris, A.D., Westwood, D.A., Mekjavic, I.B., and Cheung, S.S., Effect of body temperature on cold induced vasodilation. Eur J Appl Physiol 2008; 104(3): 491-9.

22.
Daanen, H.A. and Layden, J.D., Reply to A. D. Flouris and S. S. Cheung reply letter regarding "cold-induced vasodilation". Eur J Appl Physiol 2010; 108(1): 215-6.

23.
Flouris, A.D. and Cheung, S.S., Influence of thermal balance on cold-induced vasodilation. J Appl Physiol 2009; 106(4): 1264-71.

24.
Daanen, H., Cold-induced vasodilation. Eur J Appl Physiol 2009; 105(4): 663-4.

25.
Thomas, J.R., Shurtleff, D., Schrot, J., and Ahlers, S.T., Cold-induced perturbation of cutaneous blood flow in the rat tail: a model of nonfreezing cold injury. Microvasc Res 1994; 47(2): 166-76.

26.
O'Brien, C. and Montain, S.J., Hypohydration effect on finger skin temperature and blood flow during cold-water finger immersion. J Appl Physiol 2003; 94(2): 598-603.

27.
Daanen, H.A., van de Vliert, E., and Huang, X., Driving performance in cold, warm, and thermoneutral environments. Appl Ergon 2003; 34(6): 597-602.

28.
Gardner, C.A. and Webb, R.C., Cold-induced vasodilatation in isolated, perfused rat tail artery. Am J Physiol 1986; 251(1 Pt 2): H176-81.

29.
Decosterd, I. and Woolf, C.J., Spared nerve injury: an animal model of persistent peripheral neuropathic pain. Pain 2000; 87(2): 149-58.

3

THERMOREGULATION IN PERIPHERAL NERVE INJURY INDUCED COLD INTOLERANT RATS

L.S. Duraku [1*]
E.S. Smits [1*]
S.P. Niehof [2]
S.E.R. Hovius [1]
R.W. Selles [1,3]
E.T. Walbeehm [1]

*Both authors contributed equally

1. Department of Plastic, Reconstructive and Hand Surgery, Erasmus MC, University Medical Center, Rotterdam, The Netherlands

2. Pain Treatment Center, Erasmus MC, University Medical Center, Rotterdam, The Netherlands

3. Department of Rehabilitation Medicine, Erasmus MC, University Medical Center, Rotterdam, The Netherlands

ABSTRACT

Cold intolerance is defined as pain after exposure to non-painful cold. It is suggested that cold intolerance may be related to dysfunctional thermoregulation in upper extremity nerve injury patients. Purpose of this study was to examine if the rewarming of a rat hind paw is altered in different peripheral nerve injury models and if these patterns are related to severity of cold intolerance. In the Spared Nerve Injury (SNI) and Complete Sciatic Lesion (CSL) model the rewarming patterns after cold stress exposure were investigated preoperatively and at 3, 6 and 9 weeks post-operatively with a device to induce cooling of the hind paws. Thermocouples were attached on the dorsal side of the hind paw to monitor rewarming patterns. The Von Frey test and cold plate test indicated a significantly lower paw-withdrawal threshold and latency in the SNI compared to the Sham model. The CSL group, however, had only significantly lower paw-withdrawal latency on the cold plate test compared to the Sham group. While we found no significantly different rewarming patterns in the SNI and CSL group compared to Sham group, we did find a tendency in temperature increase in the CSL group 3 weeks post-operatively. Overall, our findings indicate that rewarming patterns are not altered after peripheral nerve injury in these rat models despite the fact that these animals did develop cold intolerance. This suggests that disturbed thermoregulation may not be the prime mechanism for cold intolerance and that other, most likely, neurological mechanisms may play a more important role. There is no direct correlation between cold intolerance and rewarming patterns in different peripheral nerve injury rat models. This is an important finding for future developing treatments for this common problem, since treatment focusing on vaso-regulation may not help diminish symptoms of cold intolerant patients.

INTRODUCTION

Cold intolerance (CI) is defined as abnormal pain after exposure to mild to severe cold, with or without discoloration or stiffness of the hand and fingers [1-5]. CI is a frequent sequel of upper extremity injury, especially when neurovascular structures are involved [5-9]. Its reported incidence varies, probably due to variability in testing method, between 56% and 83% in humans [1, 4, 10]. CI has been found to be the most disabling symptom following peripheral nerve injury, and it does not diminish over time [1, 3, 5, 10, 11]. CI has been reported in a wide range of pathologies, such as patients with Raynaud's disease [12-15,] upper extremity fractures [15], digital replantation [6, 7, 16-19], and after raising radial forearm flaps. Unfortunately, because the pathophysiology of CI is still unclear, there is no treatment available, other than symptomatic relief.

CI may be related to dysfunctional thermoregulation in peripheral nerve injury patients [16, 20]. In healthy people, after cooling of an extremity, the thermoregulatory system increases blood-flow to counteract decrease in temperature and to prevent pain and frostbite [21]. After a peripheral nerve injury, thermoregulation may be impaired, as was shown by Ruijs et al [20]. However, other studies do not support this theory, because low blood flow does not correlate with subjective symptoms of CI [7, 16, 18]. This was both found in patients with digital replantation or revascularization and in patients followed by raising a radial forearm flap for reconstruction purposes [7, 22-25]. The diversity and complexity of the pathogenesis of CI could be a reason for the inconsistent results. Co-morbidity, such as vascular damage, could be a major factor. Gender, age and different definitions of CI could also be attributed for different outcomes.

An unresolved issue remains how different types of nerve injury influence thermoregulation. In clinical studies, because of the complexity of upper extremity traumas, regeneration and re-innervation of damaged and undamaged nerves is difficult to determine. An animal study with a nerve injury model that systematically inflicts CI would be a suitable set-up to answer these questions. Well-documented nerve injury rat models that are known to be cold hypersensitive are the Spared Nerve Injury [26] (SNI) and the Complete Sciatic Lesion (CSL) [27] models. Advantages of these models are the reproducibility and circumscriptive nerve injury application and the subsequent well-characterized CI behaviour. However, there are no studies that investigate the relation between peripheral nerve injuries causing CI in a rat model and thermoregulation. To determine the function of thermoregulation, the re-warming pattern after cold stress exposure was used as a measure, a frequently performed and validated method to evaluate thermoregulation [20, 28]. Our hypothesis was that thermoregulation of rat hind paw is altered in peripheral nerve injury and that these patterns are related to the severity of CI.

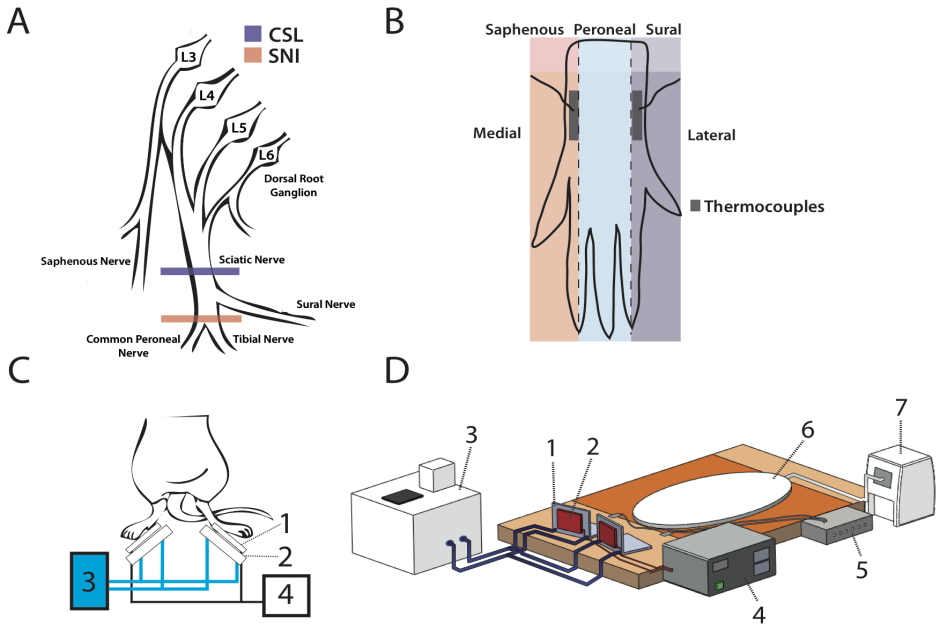

FIGURE 1:

Illustration of the experiment. A: The complete Sciatic Lesion model (CSL) comprises a lesion of the sciatic nerve while the Spared Nerve Injury model (SNI) comprises a lesion of the tibial and common peroneal nerve. B: Dorsal sides of a rat hind paw with its nerve innervations areas. Thermocouples are attached on the medial (saphenous) and lateral (sural) part of the paw. C: Illustration of the cooling set-up. 1: Peltier elements, 2: Water coolers, 3: Thermostatic bath, 4: Power supply. Under anesthesia the rat is positioned on the dorsal side with the hind paws placed on the Peltier elements for cooling. D: Illustration of the complete cooling set-up. 1: Peltier elements, 2: Water coolers, 3: Thermostatic bath, 4: Power supply, 5: USB-based 8-channel thermocouple input module, 6: Heating mattress, 7: Heating mattress regulator.

	MEAN	STD. DEVIATION
Mean rectal	35.87	1.43
Minimal rectal	35.07	1.95
Maximum rectal	36.88	0.90
Mean surrounding	25.10	0.83
Minimal surrounding	24.63	0.73
Maximal surrounding	25.74	0.89

TABLE 1

Ambient and rectal temperatures during the experiments.

METHODS

The Animal Ethic Experiment Commission approved all experimental procedures. Twenty-four male Wistar rats, weight 300-350g, were divided into three groups. The first group (n=8) was operated on the left hind limb using the SNI model 26. The second group (n=8) received the sham model [26], while the third group (n=8) had the CSL operation. Two of the eight SNI rats, however, were excluded from further analysis because of auto mutilation. All measurements were at the same location under similar conditions.

SURGERY

Under isoflurane (2%) anaesthesia the skin on the left lateral surface of the thigh was incised and a division was made through the biceps femoris muscle exposing the sciatic nerve and its three main branches: the sural, common peroneal, and tibial nerves. A transection and ligation with 5.0 silk of the tibial and common peroneal nerves was performed leaving the sural nerve intact in the SNI model (Fig.1A). Great care was taken to prevent contacting or stretching the intact sural nerve. CSL involved a ligation of the sciatic nerve, 1 cm above the three main branches of the sciatic nerve (Fig1A). Sham controls involved exposure of the sciatic nerve and its branches without nerve damage.

MEASUREMENTS

Measurements were performed one day preoperatively and at three, six and nine weeks postoperatively. Von Frey test and Cold plate test were taken prior to the measurements. Before each experiment the rats were habituated to the experimenter, the experiment room and the cages where the behavioural tests were performed for 5 days. Thereafter, the rats where habituated for 30 minutes prior to each experiment to reduce stress.

COLD PLATE TEST

During the cold plate test, rats were placed in a clear covered chamber black-blinded Plexiglas cage (50 cm × 50 cm × 50 cm) on an aluminium plate with a surface temperature of 5°C. We measured the paw withdrawal latency, defined as the latency of the first operated paw lift after rat placement on the cold plate. An experimenter who was blinded for the test groups manually measured the latency of the operated hind paw.

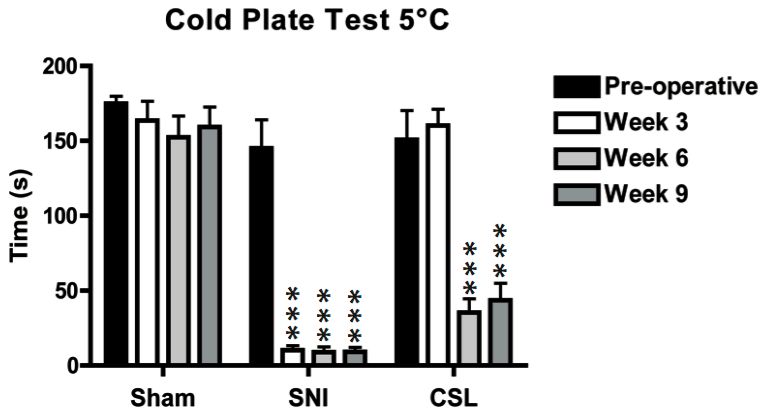

FIGURE 2A:

Cold Plate Test and Von Frey Test. A: The paw lift latency in seconds during the different measurement times in all three groups. Paw lift was significantly faster in the SNI group at all postoperative times (3W: 10.2 ± 3. 6W: 8.9 ± 3.0 9W: 9.0 ± 3.4) as compared to the sham group (175.0 ± 4.9). For the CSL group there was no significant difference at 3 weeks postoperatively as compared to the sham group in paw withdrawal latency. Only at 6 (35.4 ± 10.8) and 9 weeks (43.6 ± 9.1) postoperatively there was a significantly lower paw lift withdrawal latency in the CSL group as compared to the sham group. p<0,05=, p<0,01=**,p<0,001=***.*

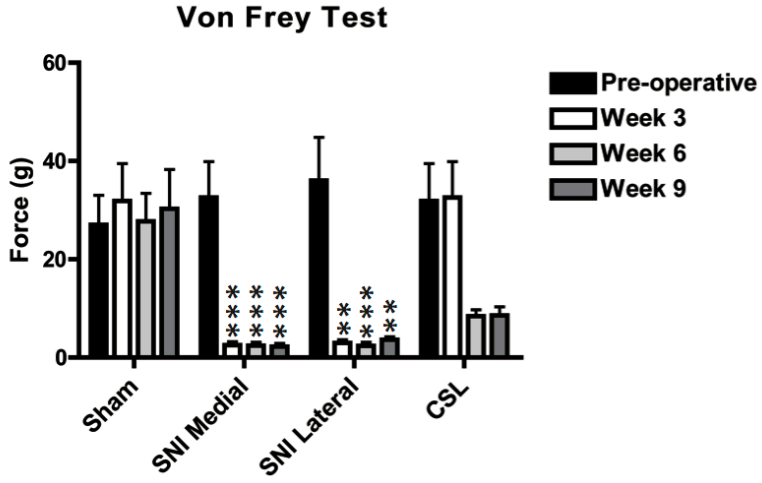

FIGURE 2B:

Amount of force of the Von Frey filaments needed to obtain a mechanical reflex withdrawal response. Force was reduced for the SNI group at 3 (3.0 ± 0.7), 6 (2.4 ± 0.7) and 9 (3.6 ± 0.6) weeks postoperatively compared to the Sham group (27.0 ± 6.0) while the CSL group had no significant lower withdrawal (3W; 32.6 ± 7.3, 6W; 8.4 ± 1.3, 9W; 7.6 ± 1.4) response compared to the Sham group. However there is no significant difference between the CSL and SNI group at 6 and 9 weeks postoperatively. p<0,05=, p<0,01=**,p<0,001=***.*

VON FREY TEST

During the Von Frey test, withdrawal threshold to touch was measured with a set of Von Frey hairs ranging from 0.6 to 300 g in a set of 14 filaments steps. The rat was placed in a chamber with a mesh metal floor, covered by a Plexiglas dome of 20 x 30cm and 10cm high. The dome enabled the rat to walk freely but not to rear up on its hind limbs. Hence, the experimenter was able to reach the plantar surfaces of the operated paw from below, unobserved by the rat. Each Von Frey hair was applied for 2 s at 5 s intervals. The Von Frey test was considered positive when at least 3 of 5 applications evoked responses.

REWARMING AFTER COLD EXPOSURE

Our department developed a set-up to induce cold stress exposure bilaterally in the hind paws of a rat and to measure skin surface temperature at the same time [29].

The anaesthetized rats were placed in a dorsal position, with the hind paws in prone position. The ventral sides of the hind paws were placed onto two vertically positioned Peltier cooling elements using surgical tape (Fig 1C). A Peltier cooler is a solid-state active heat pump that transfers heat from one side of the device to the other to generate cooling. The dorsal side of the paws was left exposed for thermocouple attachment to measure the temperature.

The thermocouple probes were placed on lateral and medial side of both limbs (Fig 1B). A rectal probe was used to monitor the core temperature and one thermocouple measured the ambient temperature. A sample rate of 2 measurements every second was used by an USB-based 8-channel thermocouple input module (Measurement Computing); Calibration of the device and the thermocouples was performed using Instacal (v5.82, Measurement Computing). The data storage was provided using a custom developed program in Labview (v7.1, National Instruments). Because both hind limbs were cooled, body core temperatures had a tendency to decrease, therefore a heating mattress (39.5°C) was used to maintain body core temperature. Both Peltier elements were set at a temperature of three degrees Celsius. Respiratory rate was monitored as an indicator of depth of anaesthesia throughout the experiment.

The measurement had three phases. A pre-phase (five minutes) to measure the temperature without cooling and also to measure the standardized baseline temperature of an anesthetized rat. Secondly, we cooled the rats for 20 minutes. In the third phase (also 20 minutes) we measured the rewarming pattern of the rat, after the hind limbs were detached from the Peltier elements. The total measurement took 45 minutes for each rat.

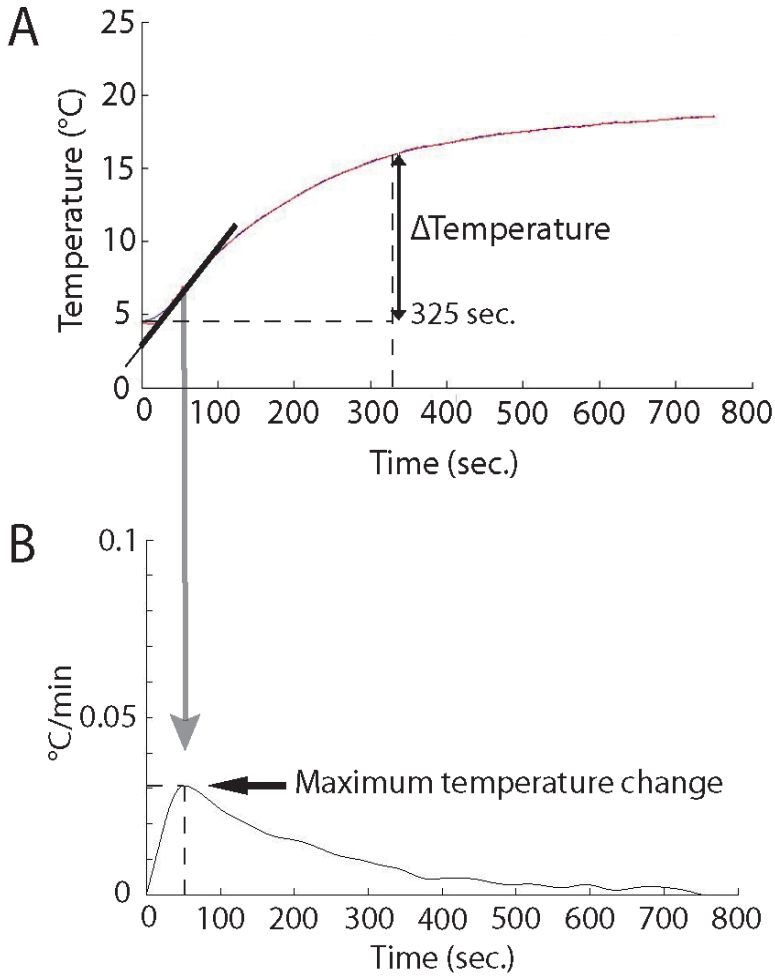

FIGURE 3:

Typical example of the temperature during the rewarming phase and illustration of the outcome measures. A: Increase in temperature is determined by calculating the difference between the lowest and highest temperature of the rewarming curve (Δ Temperature) during the first 325 seconds in the rewarming phase. B: Maximum rate of temperature increase was calculated by taking the first derivative of the time temperature curve. The highest point in the first derivative graph (°C/min.) is the maximum change in temperature during the rewarming phase.

QUANTIFICATION OF THE REWARMING PATTERN

Measured temperatures were stored in an in-house developed Labview program; the raw data were exported to Matlab. We used two methods to quantify the warming patterns. First, the increase in temperature of the rewarming curve was determined by calculating the difference between the start of the rewarming curve and the highest temperature during the first 325 seconds of the rewarming phase (Fig. 3 A). In addition, the first derivative of the time–temperature curve was calculated. From this first derivative, we determine the maximum rate of temperature change (°C/min) (Fig. 3B) during the first 325 seconds.

STATISTICAL ANALYSIS

Values are means ± SE. The software package SPSS was used for all statistical analysis. Effects were considered significant if $P \leq 0.05$. We used a two way ANOVA with one repeated-measures factor time (preoperatively and three, six and nine weeks postoperatively), and one between-subject factor group (SNI, CSL and Sham). To test differences between medial and lateral side of the hind paw we also used the Two-way ANOVA. To test the normality of the data of each week we used a Shapiro-Wilk test. In case of a significant main effect, a Bonferroni-corrected post-hoc test was performed. For the Von Frey test we used a non-parametric Kruskal-Wallis test with the same factors (time and group) and a Dunn's post-hoc test.

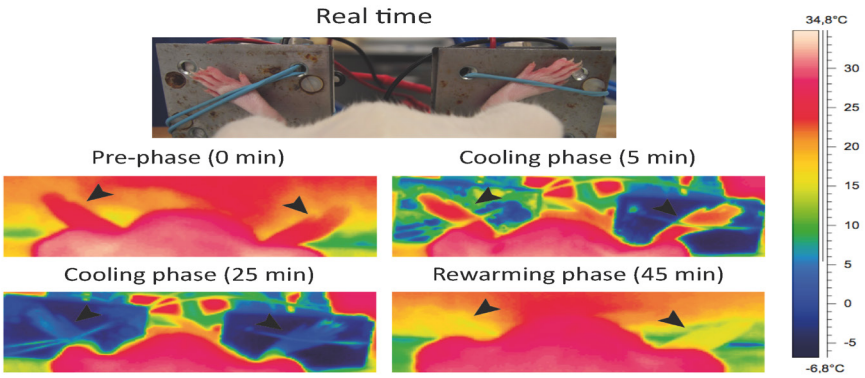

FIGURE 4:

Thermographic imaging of the experiment illustration the body of the rat, both hind paws and the Peltier element. Pre-phase (5 min.): Rat is dorsally positioned under anesthesia to measure baseline temperatures of the hind paws. Cooling phase (20 min.): Both hind paws are attached to the Peltier elements. The color indicates that both Peltier elements and hind paws get equally cooled. Rewarming phase (20 min.): Hind paws are detached from the Peltier elements and the elements are displaced, therefore not being able to affect the environmental temperature.

RESULTS

COLD PLATE AND VON FREY TEST

The sham rats displayed no paw withdrawal responses (PWL) when placed on a temperature controlled surface of 5°C up until 140 seconds. Paw withdrawal latency in SNI rats was significantly reduced as compared to the sham operated rats at all postoperatively time-points ($p < 0,001$). CSL rats showed a significant reduced PWL only at 6 and 9 weeks compared to Sham rats ($p < 0,001$). There was no significant difference between the CSL and SNI group at 6 and 9 weeks postoperatively (Fig. 2A). The SNI group had a significantly lower withdrawal response of the paw during the Von Frey test at all investigated postoperatively times as compared to Sham ($p < 0,01$). The CSL group did not have a significantly lower withdrawal response compared to the Sham group. However there was no significant difference between the CSL and SNI group at 6 and 9 weeks (Fig. 2B).

AMBIENT TEMPERATURE AND CORE TEMPERATURE

Mean ambient temperature during the cold exposure experiment was 25.1°C, and minimum surrounding temperature did not drop below 22.8ºC. The core temperature of the rat was stable; 35.9ºC, SD 1.4ºC. Minimum temperature dropped below 35ºC in 24 measurements. All surrounding and rectal temperatures are displayed in Table 1.

REWARMING PATTERN

Figure 3 shows video thermographic images of the cold stress exposure during cooling with the 3°C Peltier plates and during rewarming of the hind paws. Figure 4 shows a typical example of the rewarming pattern of the lateral side after 20 minutes cold stress exposure measured preoperatively in a Sham rat.

We found no significant difference in increase in temperature for the SNI group compared to the Sham group at 3, 6 and 9 weeks post-operatively ($p=0.337$) (Fig. 5). For the CSL group there is a higher tendency in increase in temperature 3 weeks postoperatively compared to the Sham group. At week 6 and 9 this stabilizes to pre-operative levels. There was no difference between the medial and lateral side in Δ temperature in all groups.

Between the different groups, post-surgery, we found no significant difference in rate of rewarming ($p=0.780$) (Fig. 6). In addition, there was also no significant difference between the medial and lateral side of the operated hind paws in the different groups postoperatively.

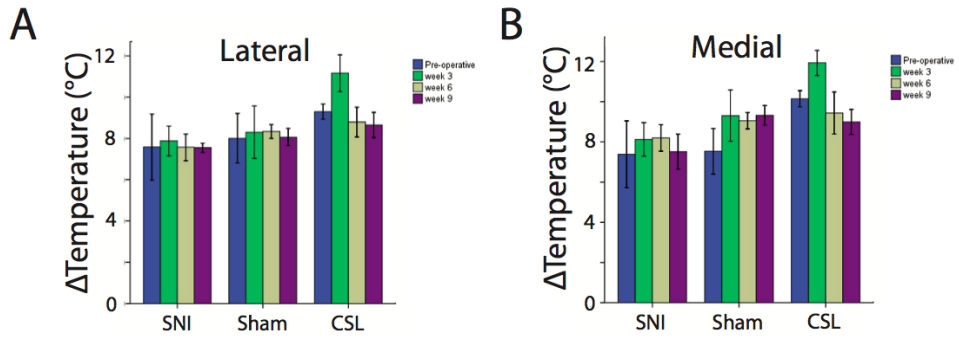

FIGURE 5:

Increase in Temperature: Graphs show the increase in temperature in the rewarming phase. There is no significant difference in the SNI group post-operatively compared to the Sham group. In the CSL group there is a tendency in higher increase in temperature on week 3, compared to the Sham and SNI group. There is no difference in increase of temperature between the measured medial and lateral side. On week 3 with the ANOVA test there was no significant difference between the CSL and Sham group on week 3.

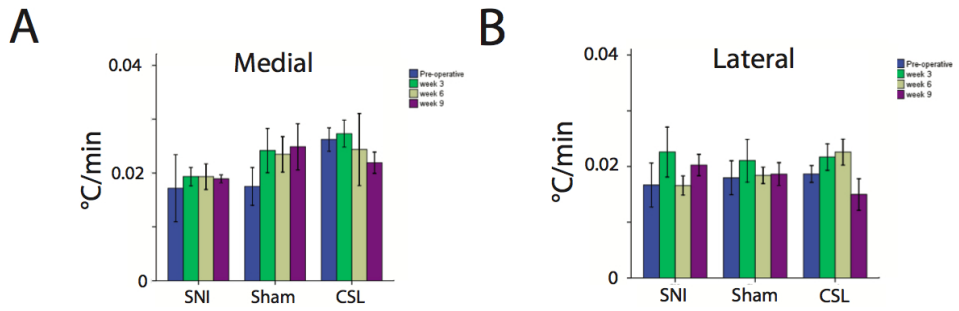

FIGURE 6:

Maximum Change in Temperature. We found no significant difference in maximum change in temperature between the different groups post-operatively and no difference in acceleration speed between the medial and lateral side.

DISCUSSION

The purpose of this study was to examine if the rewarming pattern of a rat hind paw is altered in peripheral nerve injury models and if these patterns are related to severity of CI. We used the SNI and the CSL models, which, based on the Cold Plate Test, both developed cold hypersensitivity. However, only the SNI group displayed a significantly lower PWL. While no significantly different rewarming was found in the SNI and CSL group compared to the Sham group, we did find a tendency in temperature increase in the CSL group 3 weeks postoperatively. However, overall our findings indicate that rewarming patterns are not altered after peripheral nerve injury in these rat models despite the fact that these animals did develop CI.

Our findings seem in contrast with Ruijs et al., [20] who reported abnormal rewarming in peripheral nerve injury patients with cold intolerance. However, an important difference between both studies was that Ruijs et al. studied nerve injury patients after trauma, where possible vascular damage cannot be excluded. This study used a Sham model as a negative control and to exclude vascular damage. Our findings of an absent relation between rewarming pattern after cold stress exposure in CI rats is in line with other clinical studies, although in these studies the extent of nerve and vascular damage is not known [7, 16, 18, 23-25, 30]. Nevertheless, Smits et al. showed that in patients with finger fractures there was no relation between CI complaints and abnormal rewarming pattern after cold stress exposure [31].

It is known that Transient Receptor Potential channels (TRP) register ambient temperature, and that alteration of the properties of these channels could possibly contribute to CI in patients with peripheral nerve injury [32-34]. Despite this, our study indicates that peripheral thermoregulation can still be intact after a peripheral nerve injury in a rat model, possibly suggesting that other receptors could interact with blood vessels and react with different ambient temperatures.

Another explanation for the discrepancy between Ruijs et al. and this study could be the different ratio between extremity size and body size in humans compared to paw size and body size in rats. Extremities of humans are relatively large and distant from the body. Therefore, disruption of thermoregulation could be more difficult for the body to cope with than in rats, where the paws are relatively small and close to the body.

The finding of intact thermoregulation after denervation of the sympathetic system has been reported in a previous study. Kalincik et. al. showed that rats with a complete T11 spinal cord transection did not have a change in tail surface temperature and arterial flow during 20 minutes of cold exposure of 6 - 9°C [35]. In addition, they found a full tail vasoconstriction in the spinal cord transection group during cold exposure.

Although the above-mentioned study did not find substantial alterations in thermoregulation after nerve transection, Laird et al. showed in a T4 spinal cord transection rat model an increase in tail temperature at room temperature (23 °C) [36]. In our study, the CSL model had a higher temperature increase in week 3, but this stabilizes at 6 and 9 weeks postoperatively. The temperature increase in week 3 and stabilization in week 6 and 9 could be explained by a combination of two mechanisms. First, absent of sympathetic activity that leads to a loss of vasoconstrictor tone in cutaneous blood vessels and thus increased skin blood flow may cause a higher temperature increase of the hind paw during the rewarming phase. However, there was no significant difference between the medial and lateral side of the CSL model. Higher temperature increase in the larger denervated lateral and centre area could lead to a higher temperature increase in the smaller innervated medial area. There could be still strong direct vasoconstrictive response by the peripheral vasculature to cold; an in vivo study showed that cutaneous circulation is locally regulated by directly cooling the skin [37].

An alternative explanation for the normal thermoregulation could be the hyperactivity of adrenoceptores of blood vessels to circulating catecholamines. It is known that cold exposure results in an increase in levels of plasma catecholamines, thereby still controlling the denervated vasculature in cold environment [38-40]. A possible explanation for the normal rewarming pattern in the SNI model is that undamaged nerves innervated the measured areas. Sprouting of nerve fibres from the medial area to the centre and lateral area in the CSL group starts at 4 weeks, whereby at 3 weeks the fibres are to far from the denervated blood vessels in the centre and lateral area to exert action on, therefore stabilizing the rewarming pattern at week 6 and 9 [41].

Skin temperature correlates highly with skin blood flow and skin sympathetic nerve activity. Therefore, changes in central or peripheral mechanisms of blood flow regulation are, in part, represented by changes in skin temperature, measured by the thermocouples [20, 42].

Ruch et al. [43] described that skin blood flow can be divided into nutritional flow and thermoregulatory flow. Thermoregulatory blood flow, which is regulated by arteriovenous anastomoses (AVA), accounts for 90% of skin blood flow in humans and therefore skin temperature has a good correlation with skin blood flow [44]. The percentage of thermoregulatory blood flow in rats is unknown. However, because rats are living in homeostasis with their environment, the amount of thermoregulatory blood flow is likely to be similar as in humans. Therefore, we believe that also in rats, AVA's determine the thermoregulatory flow and are related to the hind paw temperature. However, due to shunting of the AVA's, the relation between thermoregulatory flow and skin temperature could be altered. Therefore, future studies may focus on directly measuring blood flow in these CI induced rat models.

A limitation of our study was the utilization of anesthetized rats instead of awake

rats, which may affect our results. However it is not possible to measure these CI rats while awake, since they are cold hypersensitive and will avoid contact with cold surfaces. Another limitation was that the sham-treated animals showed differences in withdrawal response over time during the Von Frey test, although not significant. Presently, the Von Frey test is the only test to measure mechanical sensitivity in rodents. Variability in the sham-treated test could be explained by the non-continues values, which the last three hairs of the test are 15, 26 and 60 grams. In summary, this study revealed that rewarming patterns are not altered after a peripheral nerve injury in these rat models and that these patterns do not relate to CI. This indicates that CI is not influenced by disturbed thermoregulatory vascular responses. Our study suggests that other aetiologies such as changes in properties of the sensory system or abnormal shunting with nutritional deprivation may play an important role in development and maintaining of CI.

REFERENCES

1.
Irwin, M.S., Gilbert, S.E., Terenghi, G., Smith, R.W., and Green, C.J., Cold intolerance following peripheral nerve injury. Natural history and factors predicting severity of symptoms. J Hand Surg Br 1997; 22(3): 308-16.

2.
Koman, L.A., Slone, S.A., Smith, B.P., Ruch, D.S., and Poehling, G.G., Significance of cold intolerance in upper extremity disorders. J South Orthop Assoc 1998; 7(3): 192-7.

3.
Nancarrow, J.D., Rai, S.A., Sterne, G.D., and Thomas, A.K., The natural history of cold intolerance of the hand. Injury 1996; 27(9): 607-11.

4.
Lenoble, E., Dumontier, C., Meriaux, J.L., et al., [Cold sensitivity after median or ulnar nerve injury based on a series of 82 cases]. Ann Chir Main Memb Super 1990; 9(1): 9-14.

5.
McCabe, S.J., Mizgala, C., and Glickman, L., The measurement of cold sensitivity of the hand. J Hand Surg Am 1991; 16(6): 1037-40.

6.
Backman, C., Nystrom, A., and Bjerle, P., Arterial spasticity and cold intolerance in relation to time after digital replantation. J Hand Surg Br 1993; 18(5): 551-5.

7.
Gelberman, R.H., Urbaniak, J.R., Bright, D.S., and Levin, L.S., Digital sensibility following replantation. J Hand Surg Am 1978; 3(4): 313-9.

8. Lithell, M., Backman, C., and Nystrom, A., Pattern recognition in post-traumatic cold intolerance. J Hand Surg Br 1997; 22(6): 783-7.
Am 1986; 11(3): 382-7.

9.
Brown, F.E., Jobe, J.B., Hamlet, M., and Rubright, A., Induced vasodilation in the treatment of posttraumatic digital cold intolerance. J Hand Surg Am 1986; 11(3): 382-7.

10.
Collins, E.D., Novak, C.B., Mackinnon, S.E., and Weisenborn, S.A., Long-term follow-up evaluation of cold sensitivity following nerve injury. J Hand Surg Am 1996; 21(6): 1078-85.

11.
Craigen, M., Kleinert, J.M., Crain, G.M., and McCabe, S.J., Patient and injury characteristics in the development of cold sensitivity of the hand: a prospective cohort study. J Hand Surg Am 1999; 24(1): 8-15.

12.
Merla, A., Di Donato, L., Di Luzio, S., et al., Infrared functional imaging applied to Raynaud's phenomenon. IEEE Eng Med Biol Mag 2002; 21(6): 73-9.

13.
Naidu, S., Baskerville, P.A., Goss, D.E., and Roberts, V.C., Raynaud's phenomenon and cold stress testing: a new approach. Eur J Vasc Surg 1994; 8(5): 567-73.

14.
Maricq, H.R., Weinrich, M.C., Valter, I., Palesch, Y.Y., and Maricq, J.G., Digital vascular responses to cooling in subjects with cold sensitivity, primary Raynaud's phenomenon, or scleroderma spectrum disorders. J Rheumatol 1996; 23(12): 2068-78.

15.
Koman, L.A., Nunley, J.A., Goldner, J.L., Seaber, A.V., and Urbaniak, J.R., Isolated cold stress testing in the assessment of symptoms in the upper extremity: preliminary communication. J Hand Surg Am 1984; 9(3): 305-13.

16.
Isogai, N., Fukunishi, K., and Kamiishi, H., Patterns of thermoregulation associated with cold intolerance after digital replantation. Microsurgery 1995; 16(8): 556-65.

17.
Schlenker, J.D., Kleinert, H.E., and Tsai, T.M., Methods and results of replantation following traumatic amputation of the thumb in sixty-four patients. J Hand Surg Am 1980; 5(1): 63-70.

18.
Kay, S., Venous occlusion plethysmography in patients with cold related symptoms after digital salvage procedures. J Hand Surg Br 1985; 10(2): 151-4.

19.
Nylander, G., Nylander, E., and Lassvik, C., Cold sensitivity after replantation in relation to arterial circulation and vasoregulation. J Hand Surg Br 1987; 12(1): 78-81.

20.
Ruijs, A.C., Niehof, S.P., Selles, R.W., et al., Digital rewarming patterns after median and ulnar nerve injury. J Hand Surg Am 2009; 34(1): 54-64.

21.
Koman, L.A., Smith, B.P., and Smith, T.L., Stress testing in the evaluation of upper-extremity perfusion. Hand Clin 1993; 9(1): 59-83.

22.
Klein-Weigel, P., Pavelka, M., Dabernig, J., et al., Macro- and microcirculatory assessment of cold sensitivity after traumatic finger amputation and microsurgical replantation. Arch Orthop Trauma Surg 2007; 127(5): 355-60.

23.
Suominen, S. and Asko-Seljavaara, S., Thermography of hands after a radial forearm flap has been raised. Scand J Plast Reconstr Surg Hand Surg 1996; 30(4): 307-14.

24. Koman, L.A. and Nunley, J.A., Thermoregulatory control after upper extremity replantation. J Hand Surg Am 1986; 11(4): 548-52.

25.
Freedlander, E., The relationship between cold intolerance and cutaneous blood flow in digital replantation patients. J Hand Surg Br 1986; 11(1): 15-9.

26.
Decosterd, I. and Woolf, C.J., Spared nerve injury: an animal model of persistent peripheral neuropathic pain. Pain 2000; 87(2): 149-58.

27.
Wang, L.X. and Wang, Z.J., Animal and cellular models of chronic pain. Adv Drug Deliv Rev 2003; 55(8): 949-65.

28.
Ruijs, A.C., Jaquet, J.B., Brandsma, M., Daanen, H.A., and Hovius, S.E., Application of infrared thermography for the analysis of rewarming in patients with cold intolerance. Scand J Plast Reconstr Surg Hand Surg 2008; 42(4): 206-10.

29.
Kusters, F.J., Walbeehm, E.T., and Niehof, S.P., Neural influence on cold induced vasodilatation using a new set-up for bilateral measurement in the rat hind limb. J Neurosci Methods 2010; 193(1): 100-5.

30.
Traynor, R. and MacDermid, J.C., Immersion in Cold-Water Evaluation (ICE) and self-reported cold intolerance are reliable but unrelated measures. Hand (N Y) 2008; 3(3): 212-9.

31.
Smits, E.S., Nijhuis, T.H., Huygen, F.J., et al., Rewarming patterns in hand fracture patients with and without cold intolerance. J Hand Surg Am 2011; 36(4): 670-6.

32.
Obata, K., Katsura, H., Mizushima, T., et al., TRPA1 induced in sensory neurons contributes to cold hyperalgesia after inflammation and nerve injury. J Clin Invest 2005; 115(9): 2393-401.

33.
Frederick, J., Buck, M.E., Matson, D.J., and Cortright, D.N., Increased TRPA1, TRPM8, and TRPV2 expression in dorsal root ganglia by nerve injury. Biochem Biophys Res Commun 2007; 358(4): 1058-64.

34.
Kwan, K.Y., Allchorne, A.J., Vollrath, M.A., et al., TRPA1 Contributes to Cold, Mechanical, and Chemical Nociception but Is Not Essential for Hair-Cell Transduction. Neuron 2006; 50(2): 277-289.

35.
Kalincik, T., Jozefcikova, K., Waite, P.M., and Carrive, P., Local response to cold in rat tail after spinal cord transection. J Appl Physiol 2009; 106(6): 1976-85.

36.
Laird, A.S., Carrive, P., and Waite, P.M., Cardiovascular and temperature changes in spinal cord injured rats at rest and during autonomic dysreflexia. J Physiol 2006; 577(Pt 2): 539-48.

37.
Honda, M., Suzuki, M., Nakayama, K., and Ishikawa, T., Role of alpha2C-adrenoceptors in the reduction of skin blood flow induced by local cooling in mice. Br J Pharmacol 2007; 152(1): 91-100.

38.
Benedict, C.R., Fillenz, M., and Stanford, S.C., Plasma noradrenaline levels during exposure to cold [proceedings]. J Physiol 1977; 269(1): 47P-48P.

39.
Brock, J.A., McLachlan, E.M., and Rayner, S.E., Contribution of alpha-adrenoceptors to depolarization and contraction evoked by continuous asynchronous sympathetic nerve activity in rat tail artery. Br J Pharmacol 1997; 120(8): 1513-21.

40.
McCarty, R., Sympathetic-adrenal medullary and cardiovascular responses to acute cold stress in adult and aged rats. J Auton Nerv Syst 1985; 12(1): 15-22.

41. Ro, L.S., Chen, S.T., Tang, L.M., and Chang, H.S., Local application of anti-NGF blocks the collateral sprouting in rats following chronic constriction injury of the sciatic nerve. Neurosci Lett 1996; 218(2): 87-90.

42.
Niehof, S.P., Huygen, F.J., van der Weerd, R.W., Westra, M., and Zijlstra, F.J., Thermography imaging during static and controlled thermoregulation in complex regional pain syndrome type 1: diagnostic value and involvement of the central sympathetic system. Biomed Eng Online 2006; 5: 30.

43.
uch, D.S., Vallee, J., Li, Z., et al., The acute effect of peripheral nerve transection on digital thermoregulatory function. J Hand Surg Am 2003; 28(3): 481-8.

44.
Fagrell, B., Advances in microcirculation network evaluation: an update. Int J Microcirc Clin Exp 1995; 15 Suppl 1: 34-40.

4

SPATIOTEMPORAL DYNAMICS OF RE-INNERVATION AND HYPERINNERVATION PATTERNS BY UNINJURED CGRP FIBERS IN THE RAT FOOT SOLE EPIDERMIS AFTER NERVE INJURY

L. S. Duraku [1,2]
M. Hossaini [2]
S. Hoendervangers [1]
L. L. Falke [2]
S. Kambiz [1,2]
V. C. Mudera [3]
J. C. Holstege [2]
E. T. Walbeehm [1]
T. J. H. Ruigrok [2]

1. Department of Plastic, Reconstructive and Hand Surgery, Erasmus MC, University Medical Center, Rotterdam, The Netherlands

2. Dept. of Neuroscience, Erasmus MC, University Medical Center, Rotterdam, The Netherlands

3. The Institute of Orthopedics and Musculoskeletal Sciences, Royal National Orthopedic Hospital, University College London, Stanmore, United Kingdom

ABSTRACT

The epidermis is innervated by fine nerve endings that are important in mediating nociceptive stimuli. However, their precise role in neuropathic pain is still controversial. Here, we have studied the role of epidermal peptidergic nociceptive fibers that are located adjacent to injured fibers in a rat model of neuropathic pain. Using the Spared Nerve Injury (SNI) model, which involves complete transections of the tibial and common peroneal nerve while sparing the sural and saphenous branches, mechanical hypersensitivity was induced of the uninjured lateral (sural) and medial (saphenous) area of the foot sole. At different time points, a complete foot sole biopsy was taken from the injured paw and processed for Calcitonin Gene-Related Peptide (CGRP) immunohistochemistry. Subsequently, a novel 2D-reconstruction model depicting the density of CGRP fibers was made to evaluate the course of denervation and re-innervation by uninjured CGRP fibers. The results show an increased density of uninjured CGRP-IR epidermal fibers on the lateral and medial side after a SNI procedure at 5 and 10 weeks. Furthermore, although in control animals the density of epidermal CGRP-IR fibers in the footpads was lower compared to the surrounding skin of the foot, 10 weeks after the SNI procedure, the initially denervated footpads displayed a hyper-innervation. These data support the idea that uninjured fibers may play a considerable role in development and maintenance of neuropathic pain and that it is important to take larger biopsies to test the relationship between innervation of injured and uninjured nerve areas.

INTRODUCTION

Noxious stimuli in the epidermis are detected by free nerve endings of thinly myelinated (Aδ) or unmyelinated (C) fibers, which are termed nociceptors [1, 2]. Damage to nociceptive fibers often leads to neuropathic pain [3], however, its etiology is only poorly understood. Epidermal nociceptive fibers can also be subdivided into peptidergic fibers that contain neuropeptides like calcitonin gene-related peptide (CGRP) and/or substance P [4], and non-peptidergic fibers that are identified by isolectine B4 (IB4) [5]. It is specifically the group of peptidergic fibers that is suspected to play an important role in the induction and maintenance of neuropathic pain.[6].

Several animal models of neuropathic pain have been used to study the anatomical changes of epidermal fibers after peripheral nerve injury [7-9]. After a chronic constructive injury (CCI) of the sciatic nerve, a sustained decrease in CGRP epidermal fibers was found together with the development of neuropathic pain behavior [7, 10]. However, using the same model, neuropathic pain has also been reported in combination with an increase of upper-dermal CGRP fibers [8, 11]. Paradoxical results showing both increased and decreased densities of epidermal fibers were also reported for the affected skin of patients suffering neuropathic pain [12, 13]. As yet, these differences have not been related to specific types of nerve injury. The CCI model, which uses catgut ligatures around the sciatic nerve, often results in a local inflammatory reaction, which commonly leads to a local, but variable, compression injury rather than a transection [14, 15 16]. Therefore, it is unclear to what extent changes in density of fibers are due to re-innervation by injured nerves or by collateral sprouting of uninjured nerves from adjacent areas.

In our present study we have determined the effect of nerve transection on subsequent changes in pain thresholds of the different foot sole areas and co-related this to changes in the density of epidermal CGRP fibers in a rat model. For this purpose we have used the spared nerve injury (SNI) model for neuropathic pain in which the common peroneal and tibial nerves are transected leaving the saphenous and sural nerves intact [17]. This procedure denervates the central area of the glabrous skin of the hind paw, but not its medial- and lateral-most areas, and results in the development of neuropathic pain as indicated by hypersensitivity of the intact areas. This procedure better resembles clinical situations where peripheral nerves are transected by trauma or surgery. Moreover, it results in a well-defined separation between injured (peroneal and tibial nerve) and uninjured (saphenous and sural nerves) nerve fibers.

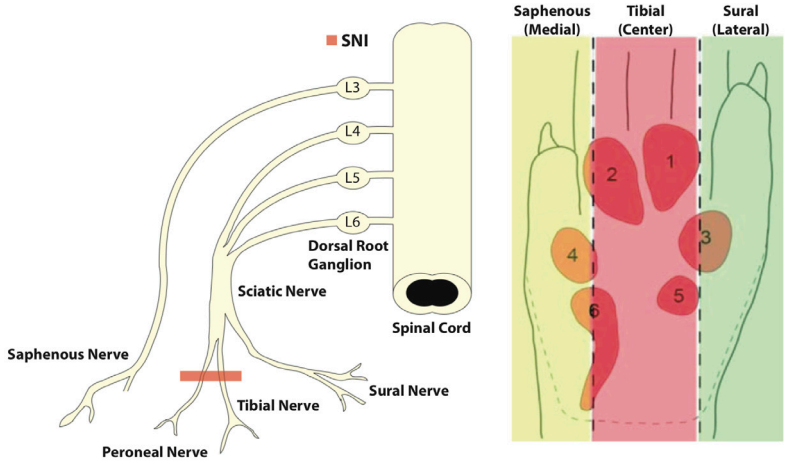

FIGURE 1:

The Spared Nerve Injury (SNI) procedure consists of transection and displacement of the tibial and common peroneal nerves, sparing the adjacent sural and saphenous nerves. This procedure leads to complete denervation of the tibial (central) innervated area (red), but leaves the medial (saphenous: yellow) and lateral (sural: green) sides of the hind paw glabrous skin intact.

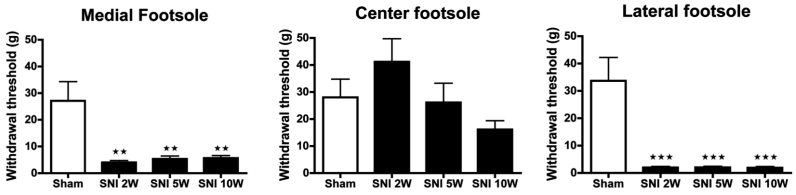

FIGURE 2:

*Histograms showing the mechanical threshold (± SEM) in the lateral, center and medial territories of the affected hind paw glabrous skin as determined with the Von Frey test. The SNI group showed a significantly decreased mechanical withdrawal threshold in the medial and lateral foot sole at 2, 5 and 10 weeks PO compared to the Sham group. Center area of the foot sole of the SNI group showed a somewhat higher mechanical withdrawal threshold, which decreased in week 10 compared to the Sham group, which were not significant. N=6 per group. One-way ANOVA with post-hoc Turkey test, unpaired t-test *: P<0.05, **: P<0.01, ***:P<0.001.*

METHODS

ANIMALS

Experiments were performed on adult male Wistar rats (n=42) (includes 2 rats of 4 months post-surgery SNI treatment). All experiments were approved by the Dutch Ethical Committee on Animal Welfare (DEC) and all procedures adhered to the European guidelines for the care and use of laboratory animals (Council Directive 86/6009/EEC).

THE SPARED NERVE INJURY (SNI) MODEL

For this experiment we used the SNI procedure described by Woolf and Decosterd (2000). Under isoflurane (2%) anesthesia the skin on the left lateral surface of the thigh was incised and the biceps femoris muscle was divided and spread lengthwise to expose the three branches of the sciatic nerve: i.e. the sural, common peroneal and tibial nerves. The tibial and common peroneal nerves were ligated together with 5-0 silk suture and cut approximately 2 mm distal to the ligation (Fig. 1). Great care was taken to avoid any contact with or stretching of the intact sural nerve. This procedure denervates the central part of the footsole while leaving the innervation of both the lateral and medial side of the footsole intact [17]. Sham controls involved only the exposure of the sciatic nerve and its branches without any subsequent handling or lesioning. The skin was sutured and the animals were allowed to recover. In all cases, postoperative analgesia was provided by subcutaneous administration of buprenorphine (0.05-0.1 mg/kg; Temgesic; Schering-Plough BV, Utrecht, the Netherlands). Animals were monitored daily for signs of stress or discomfort but in all cases recovered uneventfully with no autotomy.

BEHAVIORAL EXPERIMENTS

The development and level of neuropathic pain was determined in the affected hind limb 2, 5 and 10 weeks after the SNI procedure. As a control, sham operated animals were tested at the same time points. Two tests were used to examine neuropathic pain development.

VON FREY TEST

At 2, 5 and 10 weeks postoperatively (PO), the mechanical threshold of the hind paws was measured using Von Frey hairs ranging from 0.6 to 300 g in a set of 14 filament steps [44]. In the current experiment we used up-down testing starting with low force followed by gradually increasing forces. Rats were placed in a plastic box with a mesh floor, in which the rats were able to move freely. Each Von Frey hair was applied for 2 s (1 trial) at 5 s intervals; the threshold for a positive test was set at 3

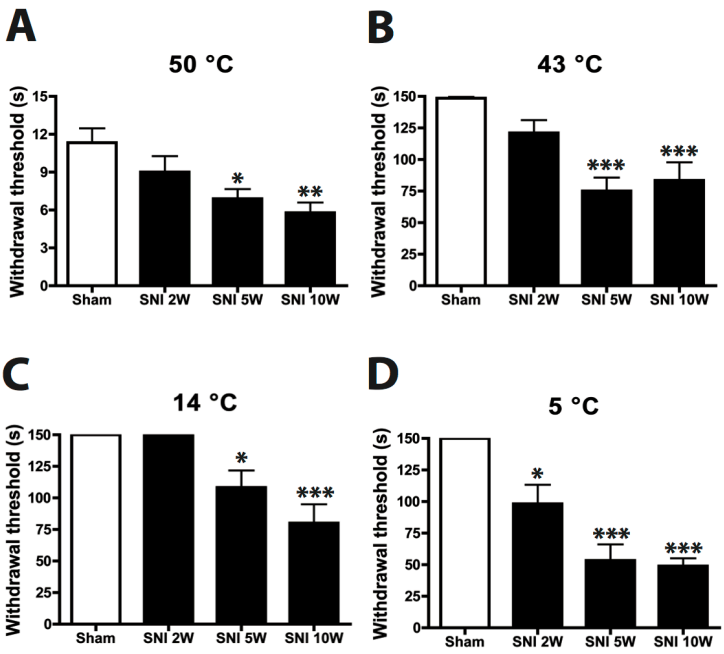

FIGURE 3:

*Histograms showing the temperature withdrawal thresholds of the affected hindpaw glabrous skin as determined by the hot and cold plate test. The SNI group shows a significantly lower paw withdrawal threshold at 50 and 43 ºC after 5 and 10 weeks postoperatively as compared to the sham group. Also at 14 and 5 ºC the SNI group has a significantly lower withdrawal threshold as compared to the Sham group only at 5 and 10 weeks. N=9 per group. One-way ANOVA with post-hoc Turkey test, unpaired t-test *: P<0.05, **: P<0.01, ***:P<0.001.*

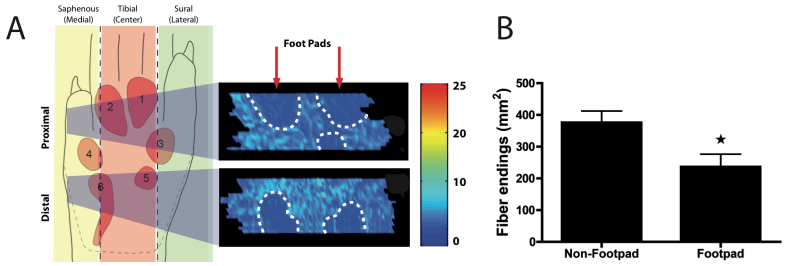

FIGURE 4:

*Epidermal CGRP-IR 2-D density profile of the hind paw glabrous skin. A: Two large skin biopsies (left hand panel, grey shaded areas) are taken from the distal and proximal foot sole and cut transversely. Serial sections were plotted, binned and the density of labeled profiles was visualized in a 2-D density profile that was made using Matlab routines (colorbar reflect number of labeled fibers.) The resulting plots indicate that the footpads are less densely innervated compared to non-footpad areas. B: Quantification shows a significant lower number of epidermal CGRP-IR fibers in the footpads compared to non-footpads. (N=5), student t-test, *P<0.05.*

trials, which evoked responses out of a maximum of 5 trials. A response consists of a flinch or flutter of the tested limb. The medial and lateral sides were stimulated at the transition point from glabrous to hairy skin at either side of footpad 3 and 4 (Fig. 1). The center foot sole was stimulated at its very center between footpad 3 and 4.

HOT/COLD PLATE TEST

The hot/cold plate test [45, 46] consists of one aluminum plate (21 x 21cm) with a see-through Plexiglass cage, in which channels are placed in a spiral form to provide a homogenous adjustment of the plate temperatures. These channels are filled with water that is regulated by a water bath (HAAKE K20), with a temperature range from 0 to 50 °C, a maximum pressure of 300 mbar and a maximum flow rate of 12.5 L/min. The water bath is connected with PVC tubes to the aluminum plates and pumps the water through the plates. We measured the plate temperatures with thermocouples (J-type: Fe/Cu-Ni) at the center of each plate. The plate temperatures corresponded with the water bath temperatures with a maximum discrepancy of ± 0.5 °C. The rats were placed on the hot or cold plate, and the paw withdrawal latency was measured. The measurement started from the first contact of the hind paw with the plate and the time until a positive response was the latency time. Paws lifts are defined as a quick flutter or flinch of the affected hind paw.

TISSUE PREPARATION

Following survival periods of 2, 5 and 10 weeks, all animals received an overdose of pentobarbital (100 mg/kg). Two additional rats were examined after a survival of 4 months. The sham animals were sacrificed at 2 weeks post-surgery and compared to two naïve animals in thermal and mechanical behavior as well as the number of epidermal CGRP fibers in the foot sole (data not shown). There was no significant difference between sham animals post-surgery 2 weeks and naïve rats. Therefore we took 2 weeks post-surgery for the sham animals as a safe time-point to compare to the SNI-treated rats. Under deep anaesthesia the glabrous skin of the affected hind limb was dissected in a distal and proximal strip of tissue, which were immersion-fixed in 2% paraformaldehyde-lysine-periodate for 24 hours at 4˚C. The skins were embedded together with the extracted rat brain in a gel containing 10% gelatin, 4% formaldehyde and 30 % sucrose [47]. Thereafter, transverse sections were cut at 40 µm and collected serially in glycerol in eight numbered vials for long-term storage at –20 °C. Using the brain as an anatomical marker in the gelatin-embedded skin tissue enabled serially mounting of the free floating sections of each vial.

IMMUNOHISTOCHEMISTRY

The sections were pre-incubated (90 min, room temperature (RT)) in a mixture containing bovine serum albumin (BSA 2%) phosphate buffered saline (PBS, pH 7,4).

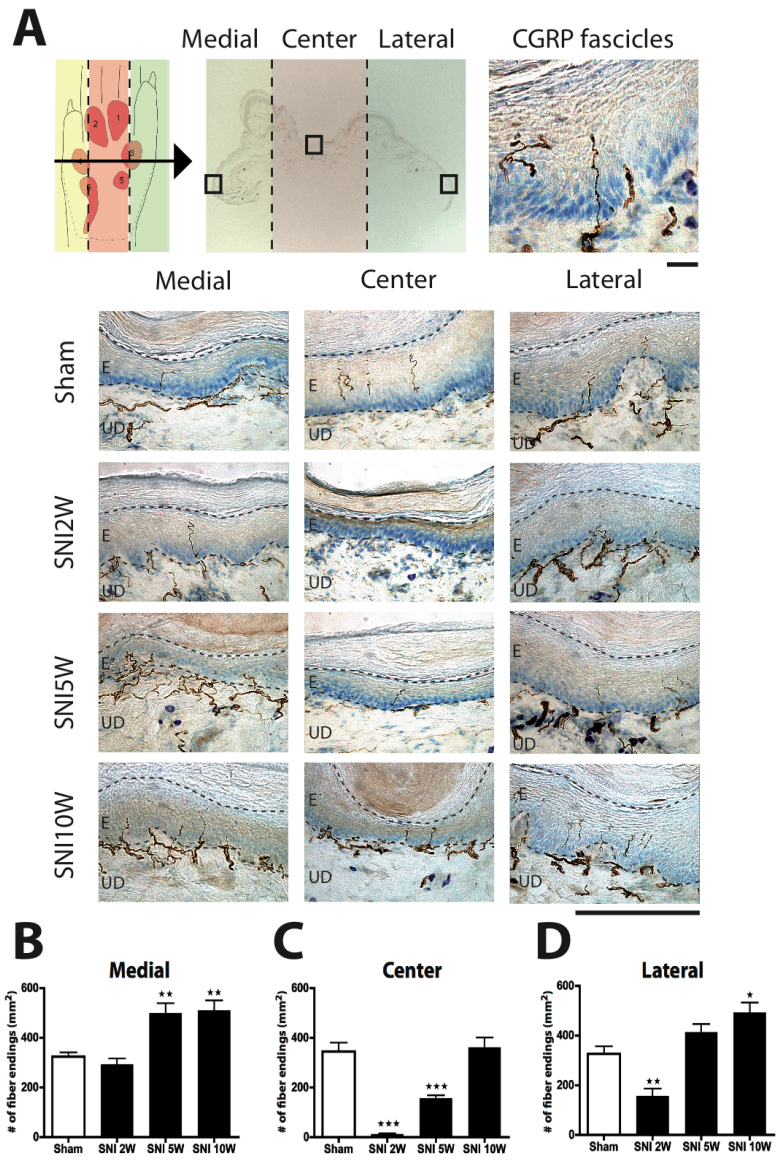

FIGURE 5:

Micrographs showing staining for CGRP-IR fibers in skin biopsies taken from the medial (saphenous), center (tibial) and lateral (sural) part of the foot sole (Fig. 5A). Note that two weeks after SNI a complete loss of CGRP-IR fibers is observed in the central part while preserving CGRP-IR fibers on the medial and lateral side. Five weeks PO, the SNI group shows an increase of CGRP-IR fibers in the medial and lateral part when compared to the sham group. Also, at this time a re-innervation of the center area is noted. Ten weeks PO, the SNI group shows CGRP-IR fibers in all three parts of the foot sole, suggesting complete re-innervation of CGRP-IR fibers in the foot sole. Upper scale bar: 25 µm, and lower scale bar: 250 µm. Diagrams showing

(Fraction V, Roche) and 0.5% Triton X-100. Thereafter, the sections were rinsed in PBS and incubated for 48 hours in a cocktail of 2% BSA containing goat anti-CGRP antibody (Calbiochem, PC205L) (1/30.000). Subsequently, sections where incubated with a secondary antibody rabbit anti-goat for 90 min room temperature. Sections were further processed using a Vectastain Elite ABC kit (Vector, Burlingame, CA) (90 min at RT). Finally, 3,-3δ diaminobenzidine (DAB) enhanced by the glucose oxidase-nickel-DAB method (Kuhlmann and Peschke, 1986) was used to identify antigenic sites. The sections were mounted on gelatinized slides, air dried overnight, counterstained with thionine, dehydrated using absolute ethanol (< 0.01% methanol), transferred to xylene, and coverslip mounted with Permount (Fisher, Hampton, NH). The CGRP antibody used in the present experiments has been extensively characterized earlier [48].

EVANS BLUE EXPERIMENT

The effect of the SNI lesion on the innervation areas of the hind paw skin was also tested by visualizing the extravasation response using Evans Blue (EB) and electrical stimulation of the peroneal and tibial nerves [49]. This extravasation response was determined in four SNI (two tibial and two peroneal nerve stimulations) at 10 weeks PO and in four sham-operated rats (two tibial and two peroneal nerve stimulations). In order to facilitate i.v. injection of EB, the animals were placed on a 38°C surface to induce vasodilatation. Subsequently, the animals were anesthetized with 3% isoflurane and both paws were depilated using depilatory-crème 'Veet' to acquire a clear image of the skin. The sciatic nerve and its tibial and peroneal branches were exposed and carefully inserted in a silicone cuff (diam. 3 mm) that could be opened length-wise and in which anodal and cathodal electrodes were embedded. Proximal to the stimulation site a crush injury was applied to prevent central propagation of the stimulation [50]. This procedure took place under microscopic guidance (Zeiss OP-MI 6-SD; Carl Zeiss, Goettingen, Germany) to minimize damage to the distal part of the nerve. A solution of Evans blue (2% EB solved in 0.9% saline, 4ml/kg body mass) was injected in the tail vein of the rat. Stimulation of the nerve was started 5 minutes after EB injection and lasted for a period of 10 minutes (10Hz, 0.5ms, 12mA: Viking stimulator, Nicolet Biomedical IES405-2). The skin area of the foot innervated by the stimulated nerve exhibited the characteristic deep blue coloration indicating extravasation of Evans blue. Ten minutes after stimulation, the animals were sacrificed by an overdose of pentobarbital (100 mg/kg). Additional extravasation does not occur 10 minutes after stimulation [51]. The animals were not handled during this period to exclude artifactual blue coloration by mechanical stimuli. The affected hind limb was amputated at the level of the ankle and fixed in ethanol. Three-dimensional images (Cys3 fluorescence, 545nm/30nm exciter, 610/75nm emitter) were obtained using a Bioptronics 3D Medical Imaging system.

*CGRP-IR fiber endings (mm²) in the medial, center and lateral area of the hind paw glabrous skin. In the medial area there is a significantly higher density of epidermal CGRP-IR endings at 5 and 10 weeks PO (Fig. 5B-D). The center area shows a decreased number of CGRP-IR fibers at 2 weeks, which normalizes at sham levels at week 10. Lateral area shows an initial decrease of CGRP-IR fibers at 2 weeks that becomes significantly higher at 10 weeks PO. (n=6) One-way ANOVA with post Turkey test *: P<0.05, **:P<0.01, ***:P<0.001.*

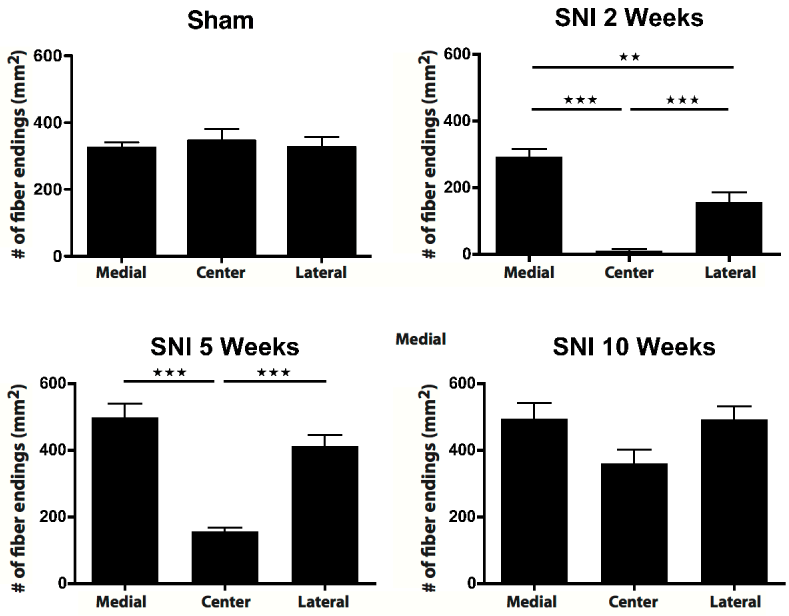

FIGURE 6:

*Diagrams showing the number of epidermal CGRP-IR fibers (mm²) in a group. The lateral area has a significantly lower number of CGRP-IR fibers compared to the medial area at 2 weeks PO, which normalizes at week 5. At 10 weeks PO there is no significant difference between the medial, center and lateral area of the hind paw glabrous skin of the SNI treated animals. (n=6) One-way ANOVA with post Turkey test *: P<0.05, **:P<0.01, ***:P<0.001.*

ANALYSIS OF CGRP TERMINAL FIBERS

Every 8th section of both the distal and proximal strips of the foot sole was used for analysis. These sections were arranged in serial order from proximal to distal using reference brainstem sections that were embedded together with the skin tissue 47. The sections were analyzed by systematically identifying the location of CGRP-IR labeled fibers that crossed the border between the dermis and epidermis (crossing fibers) as well as the number of CGRP-IR fibers terminating in the epidermis using an Olympus BH microscope equipped with a Lucivid™ miniature monitor and Neurolucida™ software (MicroBrightField, Inc., Colchester, VT). Dermal and epidermal contours were drawn using the 2.5x objective and, using systematic scanning of the whole epidermal contour, the CGRP-IR fibers were identified using a 20x objective. Data from 6 rats were subsequently combined at 40 µm intervals and entered in Matlab (The Mathworks, Natick, MA) for the two-dimensional reconstruction of the foot sole. For the remaining rats, the number of crossing and terminal CGRP fibers from the 800 µm of the skin at the most medial and lateral side, starting at the transition point of the hairy to glabrous skin, and the center area (between footpads 3 and 4, see Fig. 1) of the section were counted for statistical analysis of all the 30 sections. This enabled us to quantitate the number of CGRP fiber crossings and endings per mm^2.

EPIDERMAL THICKNESS

The effect of the SNI procedure on the epidermal thickness, defined as the vertical distance between the epidermal-dermal junction and the top of the outermost granular layer [49], was determined using an Olympus BH microscope equipped with a Lucivid miniature monitor and Neurolucida™ software (MicroBrightField, Inc., Colchester, VT) Five sections were randomly chosen from both the proximal and distal areas of the glabrous skin of a foot sole (total 10 sections). Definition of the lateral and medial side was the transition point of the hairy to the glabrous skin area and 375 µm from this point the epidermal thickness was measured. The epidermal thickness of the center area was determined at the center-most point of the transverse skin section but did not involve footpads.

STATISTICAL ANALYSIS

Per group, the results were averaged and compared with the average results of the other groups. Errors in the variations were assessed as the standard error of the mean (SEM). The unpaired t-test or one-way ANOVA with a Tukey post hoc test was performed for statistical comparison between groups, $p < 0.05$ was taken as significant.

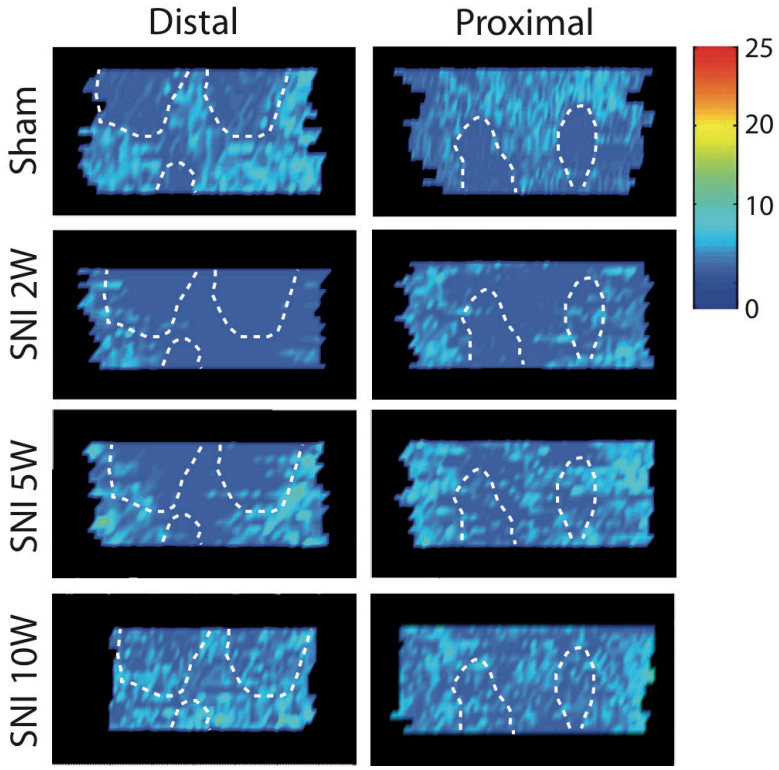

FIGURE 7:

Two-dimensional density profile of epidermal CGRP-IR fibers in the distal and proximal parts of the foot sole. Note patches with lower CGRP-IR density in the sham group, which represent the footpads. After 2 weeks PO there is a complete abolishment of CGRP-IR fibers in the center area (tibial). Five weeks PO an enhanced density of epidermal CGRP-IR fibers within the medial and lateral areas can be observed. Ten weeks PO the epidermal CGRP-IR fiber density profile shows re-innervation of fibers into the previously denervated center area (tibial). Note that the lower density in the footpads that is seen in the sham group is not observed at 10 weeks PO in the SNI group.

RESULTS

MECHANICAL WITHDRAWAL THRESHOLD

Two weeks after the SNI procedure, a severe decrease in the mechanical withdrawal threshold, as determined with the Von Frey test was noted at both the medial and lateral side of the affected foot sole (Fig. 2) This implied a significantly increased sensitivity of these parts, which was seen to persist at 5 and 10 weeks postoperatively (PO). The mechanical withdrawal threshold on the lateral side of the foot sole (sural territory) was somewhat lower than on the medial side (saphenous territory) of the affected hind paw at 2, 5 and 10 weeks post-surgery, however this did not reach statistical significance. Testing the center area of the foot sole showed a higher mechanical threshold (implying reduced sensitivity) 2 weeks PO, however not significant, that reversed after 5 weeks and 10 weeks PO as compared to sham-treated levels. There was no significant change in the mechanical withdrawal threshold of the sham-operated rats.

HOT AND COLD WITHDRAWAL THRESHOLD

Temperature sensitivity was tested by placing the animals on a temperature-controlled surface using a warm and a hot temperature (43ºC and 50ºC) and two graded cold (14ºC and 5ºC) temperatures (Fig. 3). At 2 weeks PO the SNI rats showed a non-significant tendency of having a lower paw withdrawal threshold of the affected hind paw as compared to the sham group for the hot (50ºC) surface. This became significant at 5 and 10 weeks PO for both tested temperatures (Fig. 3A,B) and imply an increased sensitivity for high temperatures of the SNI group as compared to the sham group. Essentially similar but inverse results were obtained for the cold plate test of 14 ºC and 5 ºC (Fig. 3C,D). Note, however that the SNI group already demonstrated a significantly lower withdrawal threshold at 2 weeks PO.

The results of the behavioral tests show that the SNI procedure results in both a prominently increased mechanical and temperature sensitivity reflecting hyperalgesia/allodynia and subsequently suggest that these animals suffer neuropathic pain.

THE DISTRIBUTION OF EPIDERMAL CGRP-IR FIBERS IN FOOT SOLE IN THE CONTROL GROUP

The labeling patterns of CGRP fibers in the skin of the foot sole of the sham-operated (control) group were consistent with results reported in previous studies [4]. In control skin, we found that CGRP-IR fibers form thick fiber fascicles in the superficial and deeper dermis. Most of these CGRP-IR fiber fascicles penetrate the epidermis from which individual fibers leave the fascicle, taking a usually orthogonal course to the surface while displaying several varicosities.

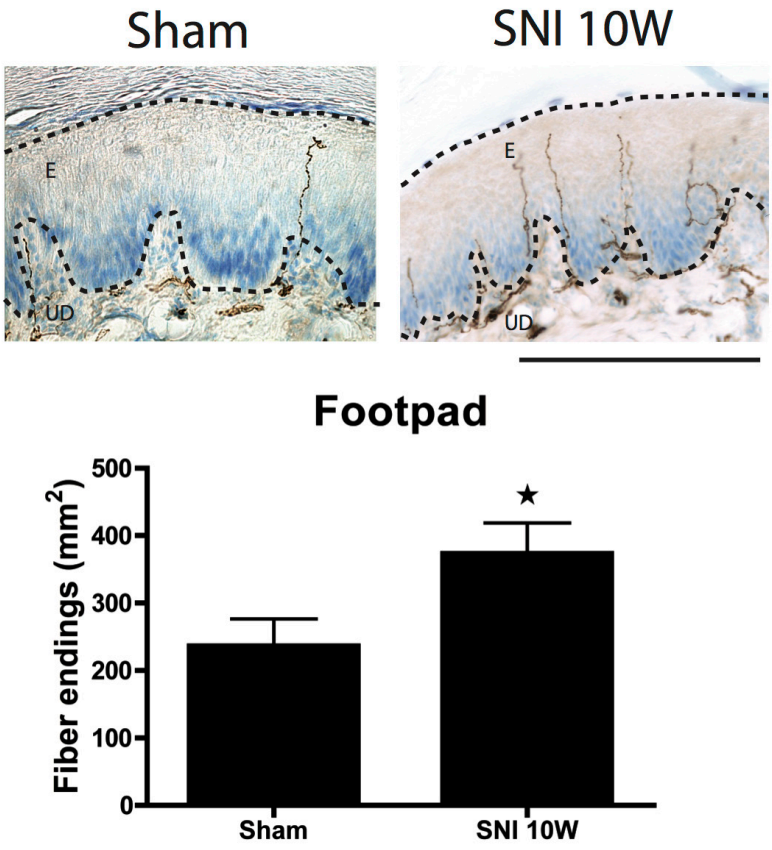

FIGURE 8:

*Micrographs showing footpad epidermal CGRP-IR fibers in the Sham versus SNI 10 week groups. There are a significant higher number of epidermal CGRP-IR fibers in the footpads of the SNI group compared to the Sham group. (n=5), student t-test, * :P<0.05. Scale bar: 250µm.*

Using the serial Neurolucida reconstructions (based on 1 out of every 8 sequential sections) a two-dimensional density profile of terminal CGRP-IR fibers was constructed. This profile showed that the density of epidermal CGRP fiber endings in the foot sole was significantly ($p < 0,001$) lower in the footpads as compared to surrounding non-footpad regions (Fig. 4).

SPATIOTEMPORAL CHANGES IN THE DISTRIBUTION OF EPIDERMAL CGRP-IR FIBERS IN THE SNI MODEL

Figure 5 depicts microphotographs of transverse sections at the level of footpads 3 and 4, showing the appearance of CGRP-IR fibers in the medial, center and lateral areas of the foot sole of sham- and SNI-treated rats after at 2, 5 and 10 weeks PO. From these graphs, it is evident that, two weeks after SNI the center region was completely devoid of CGRP-IR fibers. However, at 5 weeks PO, and especially at 10 weeks PO, a re-innervation of CGRP-IR fibers in this region was noted. From the microphotographs no obvious differences could be discerned of changes in the density in the areas (i.e. medial and lateral) that were not innervated by the transected nerves. Using quantitative data generated on the density of CGRP-IR fibers at the medial, center and lateral region of the foot sole (see Methods), both the density of the number of CGRP-IR fibers that crossed the border between the dermis and epidermis as well as the number of terminal CGRP-IR fibers that seemed to terminated within the epidermis were determined. As analysis of both sets of data revealed similar changes, we have only described the results of the latter quantification (i.e. based on terminal epidermal fibers, however also see Fig. 9 described below).

The overall density of epidermal CGRP fibers in the foot sole (as indicated by the average number of terminal fibers per mm^2) was significantly lower for the SNI group at 2 and 5 weeks PO as compared to the control group, but these returned to control values at 10 weeks PO (data not shown). The density of CGRP-IR fibers of two additional SNI rats with a survival period of 4 months showed no significant difference in epidermal CGRP-IR fibers density with the 10-week SNI group (data not shown). Therefore, 10 weeks was considered to be a stable final state for regeneration of CGRP fibers in this model. Figures 5 and 6 show a temporal and spatial comparison, respectively, of the changes in the density of CGRP-IR epidermal fibers. Indeed, these results demonstrate quite clearly that at two weeks PO, the center region is almost completely devoid of CGRP-IR fibers (Fig. 5C, Fig. 6). At this time point, the innervation of the medial region of the foot sole of SNI-treated rats still resembles that of sham-operated rats (Fig. 5B), whereas the lateral side shows an unexpected but clearly reduced density of CGRP-IR fibers (Fig. 5D, Fig. 6). Five and 10 weeks after SNI, a gradual re-innervation of epidermal CGRP-IR fibers in the center region was found having a density similar to that of sham-operated animals at 10 weeks PO (Fig. 5C). Remarkably, this coincided with an increase (with respect to the sham

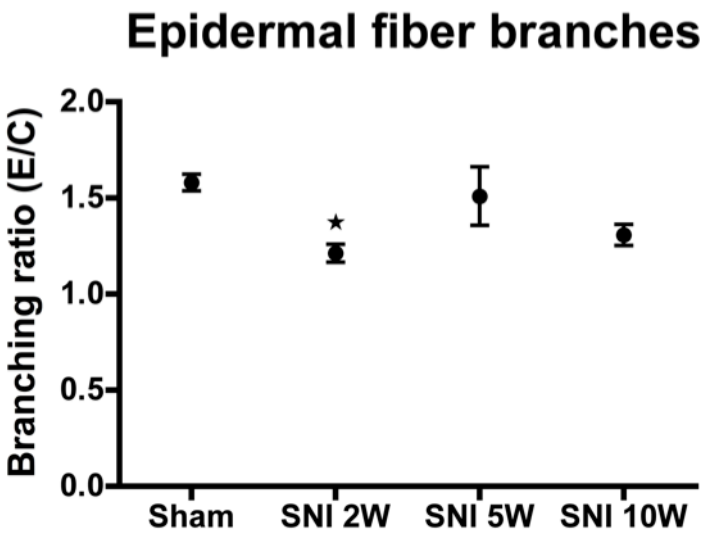

FIGURE 9:

*Histogram showing branching ratio of epidermal CGRP-IR fibers as determined by the number of epidermal endings (E) divided by the number of fibers crossing the dermis/epidermis boundary (C). Note that after an initial decrease of branching ratio these levels are quickly normalized. (n=6), One-way ANOVA with post Turkey test, *: P<0.05*

group) in density of CGRP-IR epidermal fibers of the medial and lateral parts of the foot sole. This was first noted at the medial side (at 5 weeks PO) but later also at the lateral side of the foot sole (Fig. 5 B, D). Note that although the density of CGRP-IR fibers at the lateral side of the foot was not significantly different from that of sham animals at 5 weeks PO, it was considerably increased with respect to the situation at 2 weeks PO (Fig. 5D).

Two-dimensional density profiles of CGRP-IR terminal fibers in the epidermis of the foot sole were prepared of selected specimens at all PO time points and compared to density plots of sham-operated rats. We have already described that normally the footpads display a conspicuously lower density of CGRP-IR epidermal fibers with respect to the non-footpad areas of the foot sole (Fig. 4, Fig. 7). The density profiles also show that two weeks PO a clear decrease of epidermal CGRP-IR fibers in the center area of the foot sole can be seen, which becomes re-innervated from the medial and lateral areas of the glabrous foot sole at week 5. Interestingly, the footpad areas that are normally innervated with relatively low numbers of epidermal CGRP-IR fibers could no longer be distinguished in the SNI rats at 10 weeks PO (Fig. 7). This indicates that the density of the CGRP-IR fibers in the epidermis of the footpad was considerably increased compared to normal. Quantification of the number of CGRP-IR fibers in a pre-determined part of the footpad of Sham and SNI animals at 10 weeks PO further confirmed this finding (Fig. 8).

INTRA-EPIDERMAL SPROUTING

Changes in the density of the epidermal terminal CGRP-IR fibers can also occur due to increased sprouting of re-innervating fibers that enter the epidermis. In order to test this the number of epidermal endings in the medial, center and lateral region of the foot sole were divided by the number of fibers that crossed the dermal-epidermal border. This sprouting ratio at 2 weeks PO was somewhat decreased in all regions (medial, center and lateral), but was not significantly different at the other examined PO time points (Fig. 9). We conclude that increases in the density of epidermal CGRP-IR endings cannot be attributed to changes in the epidermal sprouting ratio.

EPIDERMAL THICKNESS OF THE FOOT SOLE AREAS

Previous reports showed that a crush injury to the sciatic nerve resulted in a significant reduction in epidermal thickness that was accompanied with a substantial decrease in epidermal nerve fibers [18-20]. Because this reduction in epidermal thickness was reversed when fibers re-innervate the denervated epidermis, it was concluded that there is a positive correlation between the epidermal fiber density and epidermal thickness after peripheral nerve injury. In order to see if the observed changes in density of CGRP-IR fibers in the SNI model also correlate with the thickness of the epidermis we have quantified the epidermal thickness of the lateral, center and

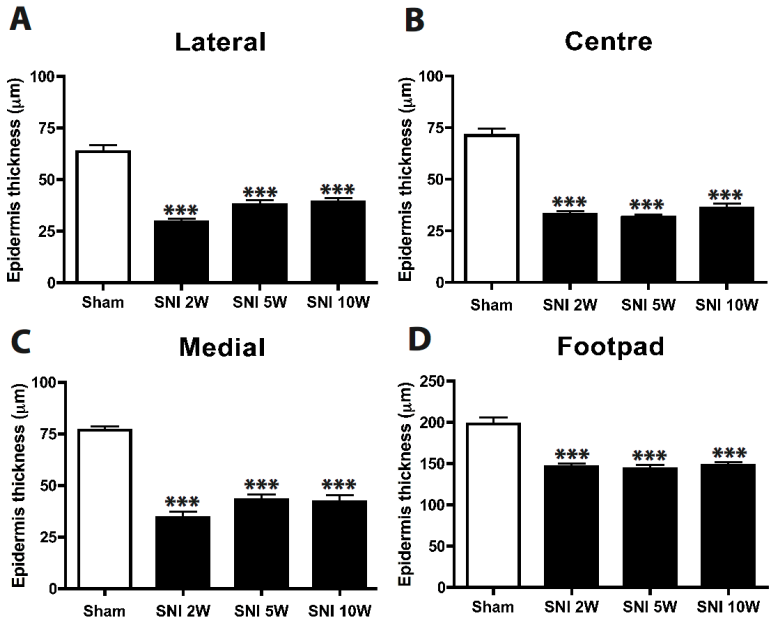

FIGURE 10:

*Figure 10 shows the epidermal thickness of the lateral, centre and medial part of the ipsilateral foot sole. It is evident that all the regions in the ipsilateral side have a significant thinner (p<0,001) epidermis compared to the sham- treated group. (N=6), One-way ANOVA with post Turkey test ***:p<0,001*

medial foot sole. In general, the epidermal thickness in the SNI group (n=6) was significantly reduced with respect to the sham treated animals (n=6, $p<0.001$) at all PO time points (Fig. 10). Hence, a relation between the hyper-innervation of the lateral and medial part of the foot sole and re-innervation of the center part and the thickness of the epidermis could not be established.

EVANS BLUE STAINING

To exclude that there is any re-innervation from the transected tibial and peroneal nerve in the SNI treated animals we performed Evans blue staining of the innervation areas of the tibial and peroneal nerve in the sham (N=4) and SNI-treated group (N=4) at 10 weeks PO. As expected, for sham-operated animals, stimulation of the tibial nerve resulted in blue coloring of the plantar surface of the foot. It is interesting to note that the footpads do not show the same intense blue coloring as the non-foot-pad area, which is in accordance with the decreased epidermal CGRP-IR density of the footpads. Stimulation of the peroneal nerve elicits blue coloring of the dorsal aspect of the foot. Both innervation areas are in accordance with previous reports [17]. In contrast, after stimulating the tibial and peroneal nerve in a SNI-treated rat, there is no Evans blue colouring, implying indirectly that the re-innervation with CGRP fibers in the center area has to come from the uninjured medial (saphenous) and lateral (suralis) areas.

DISCUSSION

In this study the following key observations were made: 1) The distribution of CGRP-IR fibers in the epidermis of the footpads is lower compared to that of the glabrous skin of the foot sole. 2) Denervation of the central foot sole area by the SNI procedure results in a prominent and persistent mechanical hypersensitivity of the lateral and medial sides of the foot sole and in heat and cold hyperalgesia and allodynia. 3) The central area of the foot sole including the footpads re-innervates with CGRP-IR fibers from the lateral and medial sides.

CGRP INNERVATION OF THE NORMAL RAT FOOT SOLE

Most studies on the innervation of the foot sole use relatively small sample areas and do not distinguish between innervation of footpad and non-footpad areas [21-23]. Plantar footpads on the rat foot sole consist of six cushion-like structures [4, 7, 10]. Most of the foot sole area was examined in this study and a lower density of CGRP-IR epidermal fibers in the footpads compared to the surrounding regions was observed. The EB experiment showing poor footpad coloring confirmed this finding. This may have implications on how rodents perceive tactile stimuli and how sensation of the foot should be tested. Von Frey testing for mechanical sensitivity typically uses the center or lateral margins of the foot, usually avoiding the footpads. In thermal tests, however, the footpads are more likely to contact the test surface. Therefore, in experiments assessing mechanical versus thermal response properties in rats, the innervation differences of footpad and non-footpad areas should be taken into account. In the current study we have found that heat (50º and 43ºC) and cold hyperalgesia (5 ºC) and cold allodynia (14 ºC) reach significant levels at 5 and 10 weeks PO. The hyper-innervation of CGRP-IR fibers in the footpads of the SNI-treated animals may account for the thermal hyperalgesia and allodynia, because of the direct contact with the thermal plate.

NEUROPATHIC PAIN AND DENSITY OF CGRP INNERVATION OF THE EPIDERMIS

Our study shows an almost complete loss of CGRP-IR fibers in the center area, following an SNI procedure, whereas the density of the medial part of the foot sole remains unchanged until 5 weeks PO when an increase in density was noted. At the lateral side of the foot, the density of CGRP-IR fibers initially decreased (at 2 weeks PO) but recovered at 5 weeks PO and increased at 10 weeks. Nevertheless, by 2 weeks PO mechanical hypersensitivity at both edges of the foot sole was noted. Because electrophysiological changes accompanying neuropathic pain behavior have also been reported to occur in uninjured fibers as early as one week PO in partial peripheral nerve injury models [24, 25], it seems likely that electrophysiological

and behavioral changes precede detectable changes in morphology. Interestingly, it has also been shown that after a ventral rhizotomy, which results in degeneration of myelinated fibers that in turn leads to neuropathic pain behavior in the rat. The postulated mechanism is that through Wallerian degeneration reacting Schwann cells produces factors that diffuse to nearby uninjured unmyelinated C-fibers and alter their properties [26]. In addition, degeneration of myelinated motor fibers leads to mitogenic changes to nonmyelinating uninjured Schwann cells with intact axons, which in turn may play a significant role in the development of neuropathic pain [27, 28]. However, it is also possible that other subtypes of sensory fibers may show morphological changes that correlate more precisely with the mechanical hypersensitivity. However, preliminary data from our group shows that the peptidergic Substance P, non-peptidergic P2X3 and myelinated NF-200 fibers do not show hyper-innervation of the epidermis in SNI-rats as compared to sham. More specifically the non-peptidergic P2X3 fibers exhibit almost no re-innervation as described in an earlier study [8]. However to discuss this in more detail is out of the scope of the current study.

The sural nerve-innervated lateral aspect of the foot sole has a more severely increased mechanical pain threshold compared to the medial side (innervated by the saphenous nerve). Although agreeing with previous results [17], this seems at odds with the observed initial lateral reduction in density of CGRP-IR fibers. The latter effect indicates that there may be considerable spatial overlap in innervation of the tibial and sural nerves. We suggest that the observed medio-lateral differences in sensitivity at 2 weeks PO could be related to the fact that the saphenous nerve is mostly derived from the L3 dorsal root ganglion where there is less interaction between injured and non-injured neuronal cell bodies (Fig. 1) as compared to the L4-L6 ganglia from which the sural nerve is derived [29]. This may lead to a delayed increase of CGRP-IR epidermal fibers on the sural side compared to the saphenous side, while the sural side has a lower mechanical threshold.

Although the SNI procedure leads to a virtually complete absence of CGRP-IR epidermal fibers in the center area of the foot sole, only a marginally increased mechanical withdrawal threshold nor a complete absence of the withdrawal reflex were noted. This could be due to stimulation of the hypersensitive lateral or medial region of the foot sole, which is inevitable when applying forces exceeding 40 g. At 5 and 10 weeks PO the observed re-innervation of epidermal CGRP-IR in the center area is in accordance with a return of the mechanical withdrawal threshold to control levels. The increase in epidermal CGRP-IR fibers might be an increase in expression levels of CGRP and not an increase of fibers. It is known that after peripheral nerve injury the uninjured DRG neurons, adjacent to injured neurons, increase CGRP expression through the p38 mitogen activated protein kinase (MAPK) pathway [30, 31], consequently leading to increased peripheral transport and filling of nerve terminals in already existing peripheral but undetected in control conditions.

However, the increased density of CGRP-IR fibers in the sural (lateral) and saphenous (medial) territories found at 5 weeks PO, is in accordance with a previous study where, in the SNI model, an increased density was observed in small biopsies of the lateral hind paw area using PGP 9.5, which is a marker for all types of nerve fibers [9]. Therefore the collateral sprouting of CGRP-IR fibers in the SNI model seems more plausible. Other studies, using the CCI neuropathic model, which also leads to thermal and mechanical hypersensitivity [32], have reported both normal as well as inverse correlations between neuropathic pain and density of nociceptive fibers [7, 8, 10, 11]. From these studies it appears that the occurrence and severity of neuropathy in CCI models is highly variable [33-37], which may relate to the varying results in re-innervation patterns in hind paw glabrous skin. The variability in CCI results is likely to be related to inconsistent tightness of the ligatures, which may result in a variable percentage of permanently damaged axons [29]. The CCI procedure also has an inflammatory component, evoking intraneural edema, also resulting in variable constriction [14, 15]. Therefore, it is uncertain if the changes in skin innervation are due to injured, uninjured or a combination of these two groups of fibers.
In the SNI model, the injury consists of a complete transection of nerve fibers, which are subsequently prevented from regrowing by the ligation as was substantiated by the lack of Evans Blue extravasation at 10 weeks PO in SNI rats. Therefore, the re-innervation patterns of epidermal CGRP-IR fibers in the SNI model must originate from uninjured fibers located in adjacent areas. As such, we propose that the SNI model has distinct advantages over the CCI model for studying re-innervation of denervated skin by undamaged axons.

EFFECT OF SNI ON EPIDERMAL THICKNESS

Our results show that, in contrast to previous reports [18, 19, 38], there is an inverse correlation between epidermal thickness and density of intra-epidermal fibers. Peptidergic epidermal fibers have been suggested to promote proliferation of keratinocytes and maintenance of skin tropism [39, 40]. It should be pointed out, however, that the rats in these studies did not suffer chronic neuropathic pain as is the case in the SNI model. Keratinocytes not only produce CGRP-δ (whereas fibers mostly contain CGRP-δ), likely to have an autocrine/paracrine role in epidermal homeostasis [41], but also release δ-endorphin, which, by binding to μ-opioid receptors located on CGRP containing sensory endings, seems to ameliorate heat-pain induced withdrawal [42]. Although CGRP-δ is normally expressed at low levels and rather heterogeneously among epidermal keratinocytes, chronic pain conditions induces an increased and more homogeneous expression [41]. Therefore, we suggest that the combination of chronic pain, increased densities of CGRP-IR fibers and potentially also of increased CGRP-δ release by non-proliferating keratinocytes are instrumental in preventing epidermal thickening.

CONCLUSION

The mechanism of sprouting of intact fibers is still poorly understood. Sprouting of epidermal CGRP-IR fibers is likely to be triggered by enhanced levels of Nerve Growth Factor (NGF), which is secreted by Schwann cells and other non-neuronal cells (e.g. epidermal cells) after nerve lesion [8]. In the CCI model, intact nerve fibers are surrounded by high quantities of NGF binding on the high affinity receptor tyrosine kinase A receptor (TrkA) [11], which in turn may induce sprouting of both these fibers. In the SNI model the sprouting ratio suggests that the formation of new branches mostly occurs in the dermis. Because NGF is also produced by the epidermal cells (e.g. keratinocytes) and plays a role in the proliferation and maintenance of the epidermis [43], we hypothesize that peripheral nerve injury increases the level of NGF significantly in the denervated epidermis. This not only affects the epidermal cells but also diffuses into the upper dermal area spreading in lateral directions and subsequently inducing sprouting of CGRP-IR fibers. These then enter both the normal as well as the denervated epidermis. The hyperinnervation of normal skin and the as yet unexplained enhanced invasion of CGRP-IR fibers into the footpads may also be related to the development of neuropathy.

REFERENCES

1.
Lauria, G. and Devigili, G., Skin biopsy as a diagnostic tool in peripheral neuropathy. Nat Clin Pract Neurol 2007; 3(10): 546-57.

2.
Lauria, G., Borgna, M., Morbin, M., et al., Tubule and neurofilament immunoreactivity in human hairy skin: markers for intraepidermal nerve fibers. Muscle Nerve 2004; 30(3): 310-6.

3.
Baron, R., Mechanisms of disease: neuropathic pain--a clinical perspective. Nat Clin Pract Neurol 2006; 2(2): 95-106.

4.
Ishida-Yamamoto, A., Senba, E., and Tohyama, M., Distribution and fine structure of calcitonin gene-related peptide-like immunoreactive nerve fibers in the rat skin. Brain Res 1989; 491(1): 93-101.

5.
Fundin, B.T., Arvidsson, J., Aldskogius, H., et al., Comprehensive immunofluorescence and lectin binding analysis of intervibrissal fur innervation in the mystacial pad of the rat. J Comp Neurol 1997; 385(2): 185-206.

6.
Pezet, S. and McMahon, S.B., Neurotrophins: mediators and modulators of pain. Annu Rev Neurosci 2006; 29: 507-38.

7.
Lindenlaub, T. and Sommer, C., Epidermal innervation density after partial sciatic nerve lesion and pain-related behavior in the rat. Acta Neuropathol 2002; 104(2): 137-43.

8.
Peleshok, J.C. and Ribeiro-da-Silva, A., Delayed reinnervation by nonpeptidergic nociceptive afferents of the glabrous skin of the rat hindpaw in a neuropathic pain model. J Comp Neurol 2011; 519(1): 49-63.

9.
Oaklander, A.L. and Brown, J.M., Unilateral nerve injury produces bilateral loss of distal innervation. Ann Neurol 2004; 55(5): 639-44.

10.
Ma, W. and Bisby, M.A., Calcitonin gene-related peptide, substance P and protein gene product 9.5 immunoreactive axonal fibers in the rat footpad skin following partial sciatic nerve injuries. J Neurocytol 2000; 29(4): 249-62.

11.
Yen, L.D., Bennett, G.J., and Ribeiro-da-Silva, A., Sympathetic sprouting and changes in nociceptive sensory innervation in the glabrous skin of the rat hind paw following partial peripheral nerve injury. J Comp Neurol 2006; 495(6): 679-90.

12.
Lauria, G., Lombardi, R., Camozzi, F., and Devigili, G., Skin biopsy for the diagnosis of peripheral neuropathy. Histopathology 2009; 54(3): 273-85.

13.
Gopinath, P., Wan, E., Holdcroft, A., et al., Increased capsaicin receptor TRPV1 in skin nerve fibres and related vanilloid receptors TRPV3 and TRPV4 in keratinocytes in human breast pain. BMC Womens Health 2005; 5(1): 2.

14.
Clatworthy, A.L., Illich, P.A., Castro, G.A., and Walters, E.T., Role of peri-axonal inflammation in the development of thermal hyperalgesia and guarding behavior in a rat model of neuropathic pain. Neurosci Lett 1995; 184(1): 5-8.

15.
Maves, T.J., Pechman, P.S., Gebhart, G.F., and Meller, S.T., Possible chemical contribution from chromic gut sutures produces disorders of pain sensation like those seen in man. Pain 1993; 54(1): 57-69.

16.
Bennett, G.J. and Xie, Y.K., A peripheral mononeuropathy in rat that produces disorders of pain sensation like those seen in man. Pain 1988; 33(1): 87-107.

17.
Decosterd, I. and Woolf, C.J., Spared nerve injury: an animal model of persistent peripheral neuropathic pain. Pain 2000; 87(2): 149-58.

18.
Li, Y., Hsieh, S.T., Chien, H.F., et al., Sensory and motor denervation influence epidermal thickness in rat foot glabrous skin. Exp Neurol 1997; 147(2): 452-62.

19.
Hsieh, S.T., Choi, S., Lin, W.M., et al., Epidermal denervation and its effects on keratinocytes and Langerhans cells. J Neurocytol 1996; 25(9): 513-24.

20.
Chiang, H.Y., Huang, I.T., Chen, W.P., et al., Regional difference in epidermal thinning after skin denervation. Exp Neurol 1998; 154(1): 137-45.

21.
Reinisch, C.M. and Tschachler, E., The touch dome in human skin is supplied by different types of nerve fibers. Ann Neurol 2005; 58(1): 88-95.

22.
Kelly, E.J., Terenghi, G., Hazari, A., and Wiberg, M., Nerve fibre and sensory end organ density in the epidermis and papillary dermis of the human hand. Br J Plast Surg 2005; 58(6): 774-9.

23.
Ebara, S., Kumamoto, K., Baumann, K.I., and Halata, Z., Three-dimensional analyses of touch domes in the hairy skin of the cat paw reveal morphological substrates for complex sensory processing. Neurosci Res 2008; 61(2): 159-71.

24.
Ji, G., Zhou, S., Kochukov, M.Y., Westlund, K.N., and Carlton, S.M., Plasticity in intact A delta- and C-fibers contributes to cold hypersensitivity in neuropathic rats. Neuroscience 2007; 150(1): 182-93.

25.
Lee, D.H., Iyengar, S., and Lodge, D., The role of uninjured nerve in spinal nerve ligated rats points to an improved animal model of neuropathic pain. Eur J Pain 2003; 7(5): 473-9.

26.
Murinson, B.B. and Griffin, J.W., C-fiber structure varies with location in peripheral nerve. J Neuropathol Exp Neurol 2004; 63(3): 246-54.

27.
Murinson, B.B., Archer, D.R., Li, Y., and Griffin, J.W., Degeneration of myelinated efferent fibers prompts mitosis in Remak Schwann cells of uninjured C-fiber afferents. J Neurosci 2005; 25(5): 1179-87.

28.
Wu, G., Ringkamp, M., Murinson, B.B., et al., Degeneration of myelinated efferent fibers induces spontaneous activity in uninjured C-fiber afferents. J Neurosci 2002; 22(17): 7746-53.

29.
Obata, K., Yamanaka, H., Fukuoka, T., et al., Contribution of injured and uninjured dorsal root ganglion neurons to pain behavior and the changes in gene expression following chronic constriction injury of the sciatic nerve in rats. Pain 2003; 101(1-2): 65-77.

30.
Freeland, K., Liu, Y.Z., and Latchman, D.S., Distinct signalling pathways mediate the cAMP response element (CRE)-dependent activation of the calcitonin gene-related peptide gene promoter by cAMP and nerve growth factor. Biochem J 2000; 345 Pt 2: 233-8.

31.
Ma, W. and Quirion, R., The ERK/MAPK pathway, as a target for the treatment of neuropathic pain. Expert Opin Ther Targets 2005; 9(4): 699-713.

32.
Wang, L.X. and Wang, Z.J., Animal and cellular models of chronic pain. Adv Drug Deliv Rev 2003; 55(8): 949-65.

33.
Kupers, R.C., Nuytten, D., De Castro-Costa, M., and Gybels, J.M., A time course analysis of the changes in spontaneous and evoked behaviour in a rat model of neuropathic pain. Pain 1992; 50(1): 101-11.

34.
Luukko, M., Konttinen, Y., Kemppinen, P., and Pertovaara, A., Influence of various experimental parameters on the incidence of thermal and mechanical hyperalgesia induced by a constriction mononeuropathy of the sciatic nerve in lightly anesthetized rats. Exp Neurol 1994; 128(1): 143-54.

35.
Stiller, C.O., Cui, J.G., O'Connor, W.T., et al., Release of gamma-aminobutyric acid in the dorsal horn and suppression of tactile allodynia by spinal cord stimulation in mononeuropathic rats. Neurosurgery 1996; 39(2): 367-74; discussion 374-5.

36.
Gazelius, B., Cui, J.G., Svensson, M., Meyerson, B., and Linderoth, B., Photochemically induced ischaemic lesion of the rat sciatic nerve. A novel method providing high incidence of mononeuropathy. Neuroreport 1996; 7(15-17): 2619-23.

37.
Cui, J.G., Holmin, S., Mathiesen, T., Meyerson, B.A., and Linderoth, B., Possible role of inflammatory mediators in tactile hypersensitivity in rat models of mononeuropathy. Pain 2000; 88(3): 239-48.

38.
Huang, I.T., Lin, W.M., Shun, C.T., and Hsieh, S.T., Influence of cutaneous nerves on keratinocyte proliferation and epidermal thickness in mice. Neuroscience 1999; 94(3): 965-73.

39.
Benrath, J., Zimmermann, M., and Gillardon, F., Substance P and nitric oxide mediate would healing of ultraviolet photodamaged rat skin: evidence for an effect of nitric oxide on keratinocyte proliferation. Neurosci Lett 1995; 200(1): 17-20.

40.
Takahashi, K., Nakanishi, S., and Imamura, S., Direct effects of cutaneous neuropeptides on adenylyl cyclase activity and proliferation in a keratinocyte cell line: stimulation of cyclic AMP formation by CGRP and VIP/PHM, and inhibition by NPY through G protein-coupled receptors. J Invest Dermatol 1993; 101(5): 646-51.

41.
Hou, Q., Barr, T., Gee, L., et al., Keratinocyte expression of calcitonin gene-related peptide beta: implications for neuropathic and inflammatory pain mechanisms. Pain 2011; 152(9): 2036-51.

42.
Khodorova, A., Montmayeur, J.P., and Strichartz, G., Endothelin receptors and pain. J Pain 2009; 10(1): 4-28.

43.
Di Marco, E., Mathor, M., Bondanza, S., et al., Nerve growth factor binds to normal human keratinocytes through high and low affinity receptors and stimulates their growth by a novel autocrine loop. J Biol Chem 1993; 268(30): 22838-46.

44.
Pitcher, G.M., Ritchie, J., and Henry, J.L., Paw withdrawal threshold in the von Frey hair test is influenced by the surface on which the rat stands. J Neurosci Methods 1999; 87(2): 185-93.

45.
Yalcin, I., Charlet, A., Freund-Mercier, M.J., Barrot, M., and Poisbeau, P., Differentiating thermal allodynia and hyperalgesia using dynamic hot and cold plate in rodents. J Pain 2009; 10(7): 767-73.

46.
Allchorne, A.J., Broom, D.C., and Woolf, C.J., Detection of cold pain, cold allodynia and cold hyperalgesia in freely behaving rats. Mol Pain 2005; 1: 36.

47.
Ruigrok, T.J. and Apps, R., A light microscope-based double retrograde tracer strategy to chart central neuronal connections. Nat Protoc 2007; 2(8): 1869-78.

.

48.
Funk, K., Woitecki, A., Franjic-Wurtz, C., et al., Modulation of chloride homeostasis by inflammatory mediators in dorsal root ganglion neurons. Mol Pain 2008; 4: 32.

49.
Takahashi, Y. and Nakajima, Y., Dermatomes in the rat limbs as determined by antidromic stimulation of sensory C-fibers in spinal nerves. Pain 1996; 67(1): 197-202.

50.
Brenan, A., Jones, L., and Owain, N.R., The demonstration of the cutaneous distribution of saphenous nerve C-fibres using a plasma extravasation technique in the normal rat and following nerve injury. J Anat 1988; 157: 57-66.

51.
Carmichael, N.M., Dostrovsky, J.O., and Charlton, M.P., Enhanced vascular permeability in rat skin induced by sensory nerve stimulation: evaluation of the time course and appropriate stimulation parameters. Neuroscience 2008; 153(3): 832-41.

5

RE-INNERVATION PATTERNS BY PEPTIDERGIC SUBSTANCE-P, NON-PEPTIDERGIC P2X3, AND MYELINATED NF-200 NERVE FIBERS IN EPIDERMIS AND DERMIS OF RATS WITH NEUROPATHIC PAIN

L. S. Duraku [1,2]
M. Hossaini [2]
B. N. Schüttenhelm[1,2]
M. Baas [1]
J. C. Holstege [2]
T. J. H. Ruigrok [2]
E. T. Walbeehm [1]

1. Department of Plastic, Reconstructive and Hand Surgery, Erasmus MC, University Medical Center, Rotterdam, The Netherlands

2. Dept. of Neuroscience, Erasmus MC, University Medical Center, Rotterdam, The Netherlands

ABSTRACT

Nerve endings in the epidermis, termed nociceptors, conduct information on noxious stimuli to the central nervous system. The precise role of epidermal nerve fibers in neuropathic pain is however still controversial. Here, we have investigated the re-innervation patterns of epidermal and dermal nerve fibers in a rat neuropathic pain model. After applying the spared nerve injury (SNI) model, we determined the mechanical and thermal withdrawal thresholds in the uninjured lateral (sural) and medial (saphenous) areas of the affected hind paw and investigated the innervations patterns of Substance P (SubP), Neurofilament-200 (NF-200) and P2X3-immunoreactive (IR) nerve fibers in the epidermis and dermis. We found a significant loss in the density of peptidergic (Sub P and NF-200) and non-peptidergic (P2X3) nerve fibers in the center area of the foot sole at 2 weeks postoperatively (PO). The densities of Sub P-IR fibers in the epidermis and upper dermis, and the density of P2X3-IR fibers in the upper dermis were significantly increased at 10 weeks PO as compared to 2 weeks PO, but were still significantly lower than the densities in controls. However, the density of NF-200-IR fibers in the center area reached control levels at 10 weeks PO. No changes were found in the densities of any of the fibers in the medial and lateral parts of the foot sole. The present results suggest that after peripheral nerve injury, specific nerve fibers have different re-innervation patterns in the epidermis and dermis and that they might be involved in the development of neuropathic pain.

INTRODUCTION

There is increasing evidence for the involvement of the epidermis in the development and maintenance of neuropathic pain[1-3]. Changes in density of nerve fibers in the epidermis are often used as a diagnostic tool in patients suffering from neuropathic pain[4]. However, an unequivocal correlation between the density of epidermal nerve fibers and the severity of experienced neuropathic pain has not yet been established [5].

Epidermal nerve fibers are divided in slow conducting unmyelinated C-fibers and fast conducting, thinly myelinated A-δ, mainly for detecting noxious stimuli [6]. Unmyelinated C-fibers are either peptidergic and contain the neuropeptides calcitonin gene-related peptide (CGRP) and/or substance P (Sub P)[7] or are non-peptidergic and are identified by their expression of purinergic receptor P2X3 and RET[8]. A-δ fibers are exclusively peptidergic and contain CGRP but can be distinguished from unmyelinated CGRP fibers by their co-expression of the marker neurofilament 200 (NF-200). Previously, we have shown that the density of CGRP-immunoreactive (IR) fibers in the epidermis adjacent to the innervation area of the lesioned fibers is increased and correlates with neuropathic pain behavior[9]. The re-innervation found in the epidermal innervation area of the injured and degenerated fibers originated from the adjacent uninjured nerve fibers. It has been shown before, using electrophysiological and behavioral studies, that after nerve transection, the adjacent skin innervated by undamaged nerve fibers becomes sensitized to mechanical and thermal stimuli[10-13.] But by using the SNI model the delineation between the injured epidermal nerve fibers and the adjacent uninjured nerve fibers was very clear and the uninjured fibers are likely to play a considerable role in the development of neuropathic pain in animal models[14].

Other epidermal cells involved in the pathogenesis of neuropathic pain are the epidermal Langerhans cells (LCs)[15]. These bone marrow-derived cells are important in presenting antigens to the T- and B-cells of the immune system[16]. LCs produce the axonal marker protein gene product 9.5 (PGP9.5), and become intensely immunoreactive to PGP9.5 after peripheral nerve injury, possibly due to a rise in PGP9.5 synthesis[17]. Increased numbers of PGP9.5-IR LCs in epidermis have been found in patients with neuropathic pain[18-20] and in neuropathic pain animal models[21, 22].

However, the distribution pattern of LCs in the epidermal innervation areas of the injured and uninjured nerve fibers, which might contribute to neuropathic pain behavior, is not known.

In the present study, we describe the normal and pathological changes in distribution of sensory subgroups of epidermal and dermal nerve fibers (Substance P, P2X3 and NF-200) and of epidermal Langerhans cells, after various post-lesion time intervals.

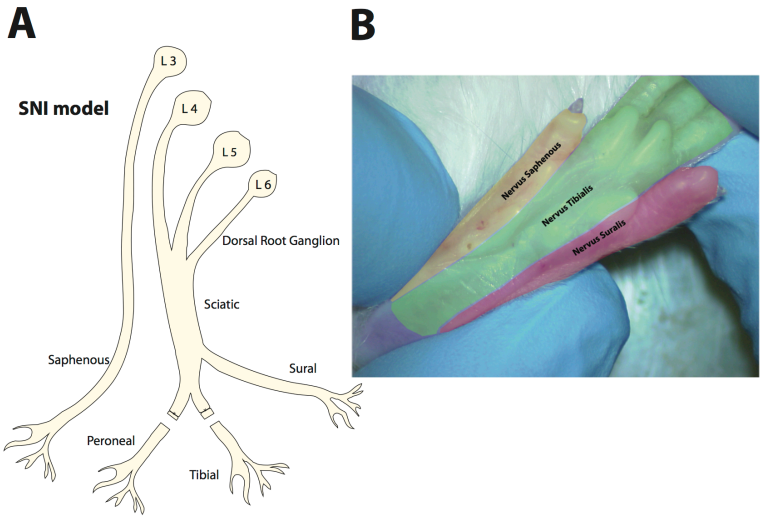

FIGURE 1 SNI MODEL:

Drawing and micrograph illustrating the spared nerve injury (SNI) model procedure. In this experiment, the tibial and common peroneal branches of the sciatic nerve were ligated and transected, while the sural branch, and the saphenous nerve, respectively at the medial and lateral side of the foot sole, were left intact (Fig. 1A). This method results in complete denervation of the tibial nerve area (center), without affecting the medial and lateral sides of the hind paw glabrous skin (Fig. 1B). The highlighted six areas on the foot sole represent the footpads (Fig. 1B).

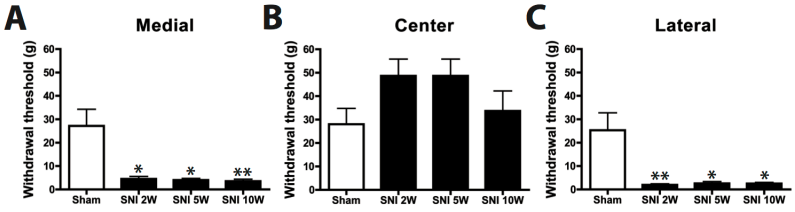

FIGURE 2 MECHANICAL WITHDRAWAL THRESHOLD:

Histograms showing the mechanical withdrawal thresholds in grams (± SEM) in the lateral, center and medial areas in the foot sole of the affected hind paws determined with Von Frey monofilaments. SNI-treated rats showed a significantly decreased mechanical withdrawal threshold in the medial and lateral foot soles areas at 2, 5 and 10 weeks PO as compared to the sham-treated rats. (: $p < 0.05$, **: $p< 0.01$, Kruskal-Wallis test).*

METHODS

ANIMALS

In the present study we used a total of 32 male Wistar rats weighing between 250-300 grams. All experiments were approved by the Dutch Ethical Committee on Animal Welfare (DEC) and all procedures were in adherence to the European guidelines for the care and use of laboratory animals (Council Directive 86/6009/EEC).

THE SPARED NERVE INJURY (SNI) MODEL

The SNI procedure was applied as described previously (see Decosterd and Woolf). In short, the three branches of the sciatic nerve i.e. the sural, common peroneal and tibial nerves were exposed under general anesthesia (2% Isoflurane). The tibial and common peroneal nerves were ligated together with 5.0 silk, and cut approximately 2 mm distal to the ligation while leaving the sural nerve intact (Fig 1.). The muscles and skin were closed using a 3.0 silk. In the sham-treated rats the sciatic branches were only exposed. This provides a model with clear delineation between innervated and denervated areas. Furthermore, since the ligation suture around the proximal stump has prevented regeneration, all fibers found in the central denervated area have to originate from the fibers of the uninjured saphenous and sural nerves.

MECHANICAL WITHDRAWAL THRESHOLD

The mechanical thresholds of the affected hind paws were measured using Von Frey monofilaments, ranging from 0.6 g to 300 g in a set of 14 filaments, at 2, 5 and 10 weeks postoperatively (PO). In this experiment, the rats were placed in a plastic box with a mesh floor in which they were able to move freely. For determining the withdrawal threshold, we started with the thinnest monofilament for producing the lowest force and increased the applied force in gradual steps. Each Von Frey hair was applied for 2 seconds (s) at 5 s intervals, and the response threshold was set at 3 responses, in a set of maximum of 5 applications. The withdrawal thresholds was determined in the medial and lateral sides of the foot sole at the transition points from glabrous to hairy skin, and in the center of the foot sole at the plantar midpoint.

HOT AND COLD PLATE TEST

The hot and cold plate tests were performed on an aluminum plate (21 x 21cm) encaged by see-through Plexiglas. The aluminum plate contained spiraling channels to provide a quick and homogenous adjustment of the plate temperatures. These channels are filled with water that is regulated by a water bath (HAAKE K20), with a temperature range from 0 to 50 °C, a maximum pressure of 300 mbar and a maximum flow rate of 12.5 L/min. The water bath is connected with PVC tubes to the

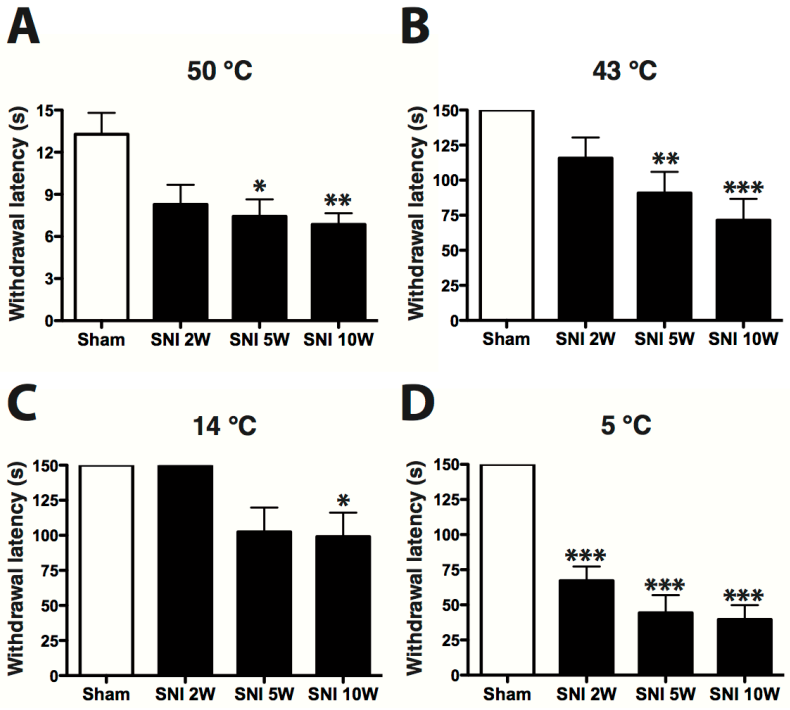

FIGURE 3 HOT AND COLD PLATE TEST:

*Histograms showing the withdrawal latency in seconds (± SEM) of the affected hind paw in the hot plate test (50 °C and 43 °C) and cold plate test (14°C and 5 °C) for sham- and SNI-treated rats. Note that only in the cold plate test at 5 °C, the withdrawal latency in the SNI-treated rats is significantly shorter at all time points as compared to sham-treated rats. *: $p < 0.05$, **: $p < 0.01$, ***: $p < 0.001$ (ANOVA).*

channels in the aluminium plate. The plate temperatures were measured with thermocouples (J-type: Fe/Cu-Ni) at the center of each plate. The plate temperatures corresponded with the water bath temperatures with a maximum discrepancy of ± 0.5 °C. The rats were placed on the hot or cold plates, and subsequently the paw withdrawal latency, defined as latency starting from the first contact of the hind paw with the plate until a positive response, was measured. A positive response was defined as a quick flutter or flinch of the affected hind paw.

TISSUE PREPARATION

After survival periods of 2, 5 and 10 weeks, the animals received an overdose of pentobarbital (100 mg/kg) and immediately thereafter the glabrous skin of the affected hind limb was dissected in a distal to proximal strip of tissue. The dissected skin was immersion-fixed in 2% paraformaldehyde-lysine-periodate (PLP) for 24 hours at 4˚C, and were thereafter embedded in gelatin blocks together with the rat's brainstem (10% sucrose) and post-fixed in 4% formaldehyde and 30 % sucrose [23]. Subsequently, transverse sections were cut at 40 µm using a freezing microtome and collected serially in 8 glycerol containing vials for long-term storage at –20 °C.

IMMUNOHISTOCHEMISTRY

Selected vials were distributed for the different immunohistochemical procedures. Sections were rinsed at least three times in phosphate buffered saline (PBS) for 40 minutes. Rinsing was performed after each incubation step with an antibody or other solution. To ensure minimal background staining, the sections were pretreated with 3% hydrogen peroxide solution at room temperature (RT) for 10 min. Thereafter, the sections were heated in at 80 ˚C for 40 minutes in a solution of 2.5 mM sodium citrate (pH 8.75), to unmask immunoreactivity 24. Subsequently, sections were pre-incubated (90 min, RT) in a blocking solution containing bovine serum albumin (BSA 2%) plus phosphate buffered saline (PBS, pH 7,4) with the addition of 0.5% Triton X-100 (Fraction V, Roche). After rinsing, the sections were incubated for 48 hours in a cocktail of 2% BSA or milk powder containing the diluted antibody at 4 ˚C. The primary antibodies were Substance P (1/500), which was raised against rabbit as described by Buijs et. al.25; P2X3 (1/25.000, guinea pig, Neuromics), NF-200 (1/15.000, rabbit, Chemicon), PGP 9.5 (1/10.000, rabbit, Biomol).

Subsequently, sections where incubated with the appropriate secondary biotinylated antibody (1/200, Biotine) for 90 min RT. Sections were further processed using a Vectastain Elite ABC kit (Vector, Burlingame, CA) (90 min at RT) and additional signal amplification was achieved by treating the sections with self-made biotin tyramide 26 for 12 minutes. The 3, -3δ diaminobenzidine (DAB) reaction enhanced by the glucose oxidase-nickel-DAB method [27] was used to reveal antigenic sites. Thereafter, the sections were mounted on gelatinized slides in sequential series and dehydrated

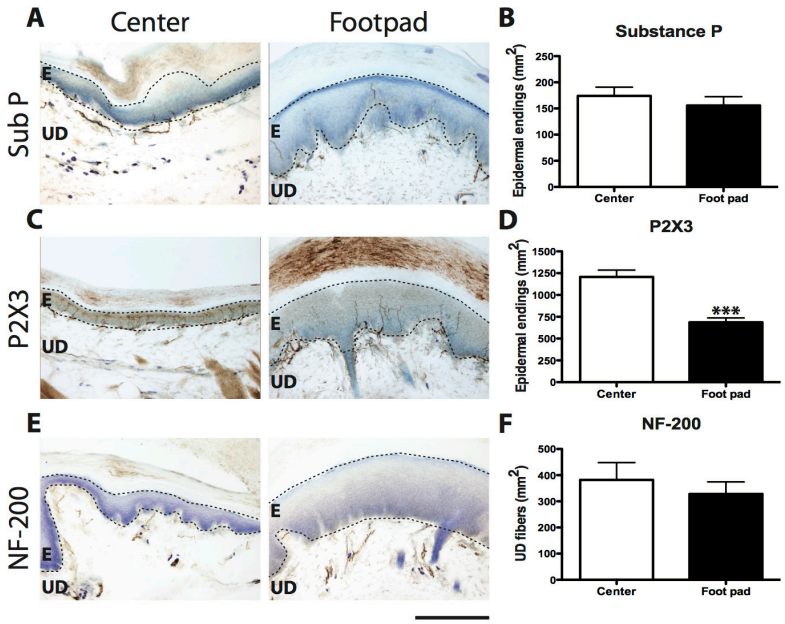

FIGURE 4 HOT AND COLD PLATE TEST:

*In Figure 4 the distribution pattern between the center non-footpad area and footpad is compared for the different subgroups of sensory skin fibers. For epidermal Sub P-IR and upper dermal NF-200-IR fibers there is an equal density of fibers in the center and footpad area suggesting a homogenous distribution over the foot sole of a rat. Whereas for epidermal P2X3-IR fibers there is a significant lower number of P2X3-IR fibers in the footpads as compared to the center non-footpad area, suggesting a heterogeneous distribution in the foot sole for this type of sensory fibers. N=5 per group. Unpaired t-test. ***: $p < 0.001$. Scale bar: 250 µm.*

using absolute ethanol (< 0.01% methanol), transferred to xylene and coverslipped with Permount (Fisher, Hampton, NH).

ANALYSIS

The sections from each vial were mounted on slides in a serial order from proximal to distal by using the brainstem as an anatomical marker [23]. The nerve fiber terminals within the epidermis and labeled nerve fibers in the upper dermis where counted in the sections using an Olympus BH microscope equipped with a Lucivid™ miniature monitor and Neurolucida™ software (MicroBrightField, Inc., Colchester, VT). In the epidermis only the terminal branches were counted and the minimal criterion for a labeled profile to be counted as an upper-dermal fiber was that it should be a clear non-interrupted single fiber and not e.g. interrupted fascicles. The fibers were identified using the 20x objective and were counted in a 750 µm wide region in the medial, center, and in the lateral side of the foot sole skin. For each rat, 8 sections of the proximal and 8 sections of the distal foot sole area were counted. From these counts the average number of nerve fibers per mm^2 were calculated for each rat. Per group (i.e. groups of rats with SNI-induced neuropathic pain with different survival periods), the results were averaged and compared with the results in the control group (i.e. sham-treated rats). For determining statistical differences, the one way-ANOVA with a Tukey post hoc test was used for intergroup comparisons, and for the data on mechanical withdrawal threshold (i.e. the Von Frey experiment), we used the Kruskal-Wallis test with a Dunn's post hoc test for the intergroup comparisons. Errors in variations were determined as standard error of the mean (SEM), and $p < 0.05$ was taken as significant.

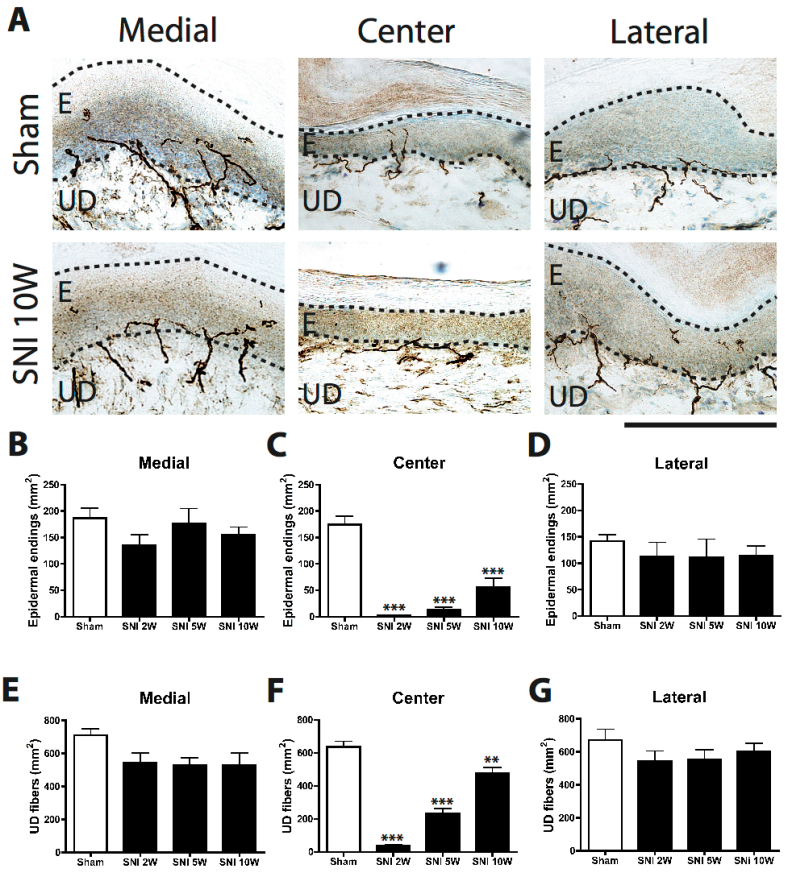

FIGURE 5 SUBSTANCE P IN THE SNI MODEL:

*Fig. 5A; Light microscopic micrographs showing nerve fibers labeled for Substance P (Sub P-IR) in the epidermis and upper dermis in the foot sole of SNI-treated (10 weeks postoperative) and sham-treated rats (2 weeks postoperative). The foot sole skin was divided in medial (innervated by saphenous nerve), center (tibial nerve) and lateral (sural nerve) areas. Fig. 5 B-G: histograms showing the number of epidermal (B-D) and upper dermal (E-G) Sub P-immunoreactive (IR) fibers per mm2 in the medial, center and lateral areas of the foot sole in SNI- and sham-treated rats at different time points. Note the significant decrease in Sub P-IR fibers in the foot sole center area of SNI-treated rats at all time points as compared to sham-treated rats (C and F). There were no significant differences in the medial and lateral areas between SNI- and sham-treated rats (B, D, E and G). . **: $p < 0.01$, ***: $p < 0.001$ (ANOVA). E = epidermis, UD = upper dermis. Scale bar: 250 µm.*

RESULTS

MECHANICAL THRESHOLD

The mechanical withdrawal thresholds in the medial and lateral parts of the foot sole determined with von Frey monofilaments were at all time points (2, 5 and 10 weeks PO) significantly lower in the SNI-treated animals as compared to the sham treated animals ($p < 0.05$) (Fig. 2A and C). This strongly suggests a rapid development and persistence of mechanical sensitization in the skin adjacent to the denervated area. The denervated central area of the SNI-treated rats showed no significant differences in the withdrawal thresholds at any time point as compared to sham-SNI (Fig. 2B).

HOT AND COLD PLATE TEST

In the hot plate (43 and 50 ºC) experiment, we found that the withdrawal latency of the affected hind paws in SNI treated rats was significantly shorter at 5 and 10 weeks PO but not at 2 weeks as compared to the affected hind paw in sham-treated rats (Fig. 3A and B). In the cold plate experiment set at 14 ºC, the withdrawal latency of the affected hind paw in the SNI-treated rats was significantly shorter at 10 weeks PO as compared to sham-treated rats ($p < 0.05$, ANOVA) (Fig. 3C), while at 5 ºC the withdrawal latency was significantly shorter at all time points (2, 5 and 10 weeks PO) ($p < 0.001$, ANOVA) (Fig. 3D).

EPIDERMAL AND DERMAL NERVE FIBERS IN THE SNI MODEL

The peripheral nociceptive sensory system can be divided into two classes, the peptidergic and non-peptidergic class. The peptidergic group consists of CGRP and Substance P, which includes unmyelinated C-fibers and myelinated A-δ fibers. However, because it is not possible to distinguish between the myelination states of the fibers with the peptidergic markers CGRP and Sub P, we have examined the innervation patterns of myelinated fibers with the antibody marker NF-200 and the non-peptidergic groups, which do not contain myelinated fibers with the P2X3 marker.

SUBSTANCE P IMMUNOREACTIVE NERVE FIBERS

In the sham-treated rats, numerous Sub P-IR nerve fibers were found in the upper dermis (Fig. 4A and 5A), some of which branched off in the upper dermal area and penetrated through the dermal-epidermal junction to terminate as free nerve endings in the epidermis. The density of epidermal Sup P-IR nerve fibers of the footpad area was not significantly different from that of the non-footpad area in the center region of the foot sole (Fig. 4A and B).

After the SNI procedure, the density of epidermal and upper dermal Sub P-IR nerve

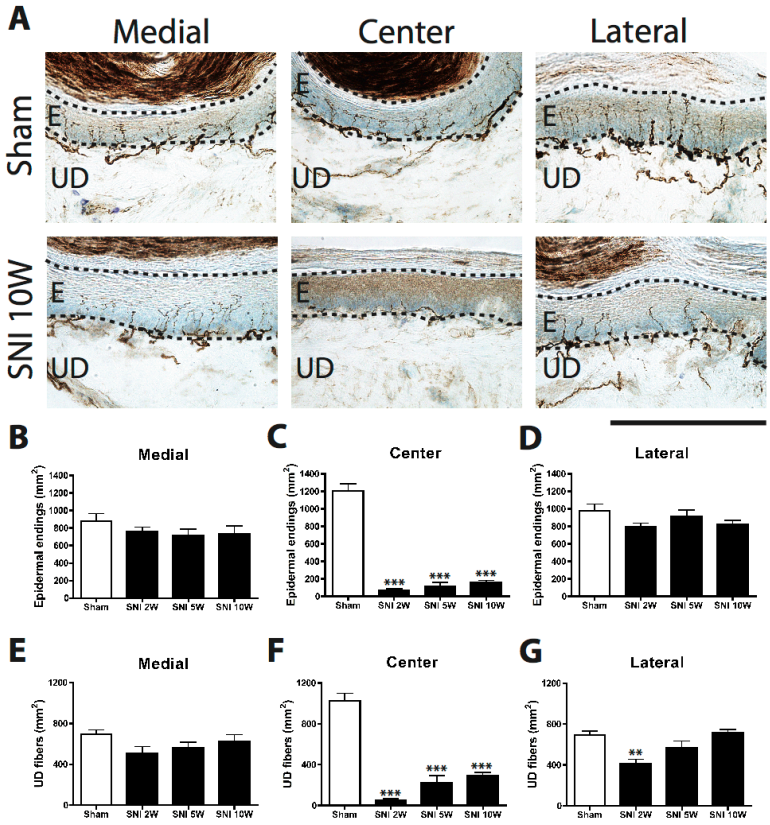

FIGURE 6 P2X3 IN THE SNI MODEL:

*Fig. 6A: Light microscopic micrographs showing nerve fibers labeled for P2X3 in the epidermis and upper dermis in the foot sole of SNI-treated (10 weeks postoperative) and sham-treated rats (10 weeks postoperative). The foot sole skin was divided in medial (innervated by saphenous nerve), center (tibial nerve) and lateral (sural nerve) areas. Fig. 6 B-G: histograms showing the number of epidermal (B-D) and upper dermal (E-G) P2X3-immunoreactive (IR) fibers per mm2 in the medial, center and lateral areas of the foot sole in SNI- and sham-treated rats at different time points. Note the significant decrease in P2X3-IR fibers in the foot sole center area of SNI-treated rats at all time points as compared to sham-treated rats (C and F). We found no significant differences in the medial and lateral areas between SNI- and sham-treated rats (B, D, E and G). **: $p < 0.01$, ***: $p < 0.001$ (ANOVA). E: epidermis, UD: upper dermis. Scale bar: 250 µm.*

fibers in the medial and lateral areas of the foot sole was at all time points not significantly different from sham-treated rats (Fig. 5A, B, D, E and G). However, in the center area, there was a significant decrease in the density of Sub P-IR nerve fibers as compared to sham-treated rats ($p < 0.01$) at all time points, with an almost complete depletion of epidermal fibers at 2 and 5 weeks PO and upper dermal fibers at 2 weeks PO (Fig. 5C and F). However, these results not only show a significant decrease in the Sub P-IR nerve fibers in the center area, but also indicate re-innervation of the center area at later time points (5 and 10 weeks PO). The density of Sub P-IR fibers is significantly increased at 10 weeks PO (epidermis: 31.85 % dermis: 74.75 % of control value) as compared to fiber density at 2 weeks PO (epidermis: 1.17 % dermis: 5.59 % of control value) (epidermis: $p < 0.05$; upper dermis: $p < 0.001$).

P2X3 IMMUNOREACTIVE NERVE FIBERS

Initially, isolectine B4 (IB4) was used as a marker for identifying unmyelinated non-peptidergic fibers, but due to binding to non-neuronal tissues (basal epidermal cells and vascular endothelial cells) identifying non-peptidergic fibers in the skin using IB4 was problematic [28, 29]. P2X3 has been shown to co-localize for more than 90% with IB4 positive nerve fibers is therefore a more suitable alternative, [8, 30]. Our data on P2X3-IR fiber density in the epidermis of the rat foot sole are in line with previous findings [8], which have shown that the density of P2X3 fibers in the epidermis is approximately four times that of Sub P-IR fiber density (Fig. 4B and 6A). We also found that there is a significantly lower density of epidermal P2X3-IR fibers in the footpads as compared to the non-footpad areas in the center of the foot sole ($p < 0.001$) (Fig. 4C and D).
In the SNI-treated rats, there were no significant changes in epidermal and upper dermal fiber density of P2X3-IR fibers in medial and lateral foot sole areas as compared to sham-treated rats (Fig. 6B, D, E and G). In the center area, similar to Sub P-IR fiber density, the P2X3-IR fiber density in the epidermis and upper dermis decreased significantly at all time points as compared to sham-treated rats ($p < 0.001$) (Fig. 6C and F). At 10 weeks PO (epidermis: 13.28 % dermis: 28.33 % of control value), the re-innervation of the center area resulted in a significant increase of P2X3-IR fiber density in upper dermis ($p < 0.05$) but not the epidermis as compared to 2 weeks PO (epidermis: 5.50 % dermis: 4.84 % of control value) (Fig. 6C and F).

NF-200 IMMUNOREACTIVE NERVE FIBERS

NF-200 stains both nociceptive (Aδ-fibers) and non-nociceptive (Aδ-fibers) myelinated fibers [7], and are therefore not exclusively nociceptive Aδ-fibers. In addition, myelinated fibers lose their myelin and Schwann cell sheaths when they penetrate the epidermis, and therefore we were only able to identify NF-200-IR fibers in the upper dermis [30, 31].
In sham-treated rats, we found NF-200-IF fibers in bundles located throughout the

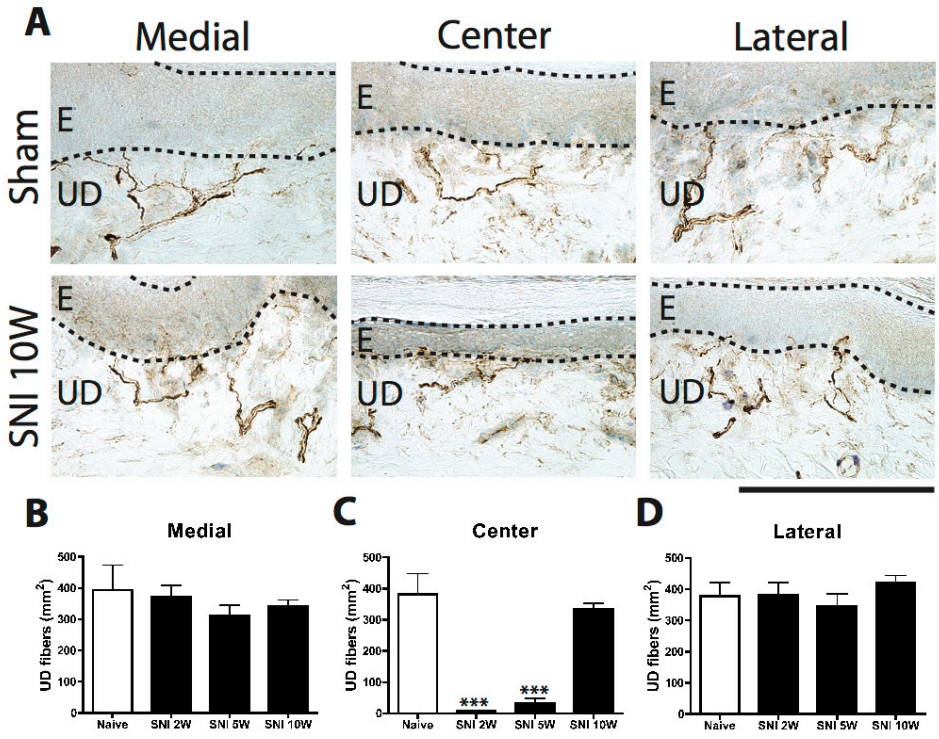

FIGURE 7 NF-200 IN THE SNI MODEL:

*Fig. 7A: Light microscopic micrographs showing nerve fibers labeled for NF-200 in the epidermis and upper dermis in the foot sole of SNI-treated (10 weeks postoperative) and sham-treated rats (10 weeks postoperative). The foot sole skin was divided in medial (innervated by saphenous nerve), center (tibial nerve) and lateral (sural nerve) areas. Note the absence of NF-200 immunoreactive (IR) fibers in the epidermis. Fig. 7 B-D: histograms showing the number of upper dermal P2X3-IR fibers per mm2 in the medial, center and lateral areas of the foot sole in SNI- and sham-treated rats at different time points. Note the significant decrease in P2X3-IR fibers in the foot sole center area of SNI-treated rats at 2 and 5 weeks postoperatively (PO) as compared to sham-treated rats, with a complete re-innervation at 10 weeks PO (C) We found no significant differences in the medial and lateral areas between SNI- and sham-treated rats (B and D). **: $p < 0.01$, ***: $p < 0.001$, (ANOVA). E: epidermis, UP: upper dermis. Scale bar: 250 µm.*

upper dermis without any NF-200-IR fibers penetrating the epidermis (Fig. 4E and 7A) in accordance with previous reports [30, 31]. No significant differences were found in NF-200-IR fiber densities between footpad and non-footpads areas (Fig. 4F).
Similar to Sub P-IR and P2X3-IR fiber densities, we noted that SNI surgery had no significant effect on the density of NF-200-IR fibers in the medial and lateral areas of the foot sole (Fig. 7A, B and D). In the center area, there was an almost complete absence of NF-200-IR fibers at 2 (1.96 %) and 5 (8.18 %) weeks PO ($p < 0.001$) as compared to sham-treated rats, while there was an almost complete re-innervation at 10 weeks PO (87.23%) (Fig. 7A and C). There was no significant difference between the densities of NF-200-fibers between the sham- and SNI-treated rats at 10 weeks PO.

LANGERHANS CELLS

Langerhans cells (LCs) were identified by using the pan-neuronal marker PGP-9.5 (Fig. 8A). We rarely found PGP-9.5 positive LCs in the epidermis of sham-treated rats in medial, center and lateral areas of the foot sole of the affected hind paw (Fig. 8C, D and E). In the medial and lateral area of SNI-treated rats there was a tendency towards a higher number of LCs, however this remained not significant at 10 weeks PO (Fig. 8C and E). On the contrary, in the center area there was a significant increase in the number of LCs per mm2 in SNI-treated rats at all time points as compared to sham-treated rats (Fig. 8D).

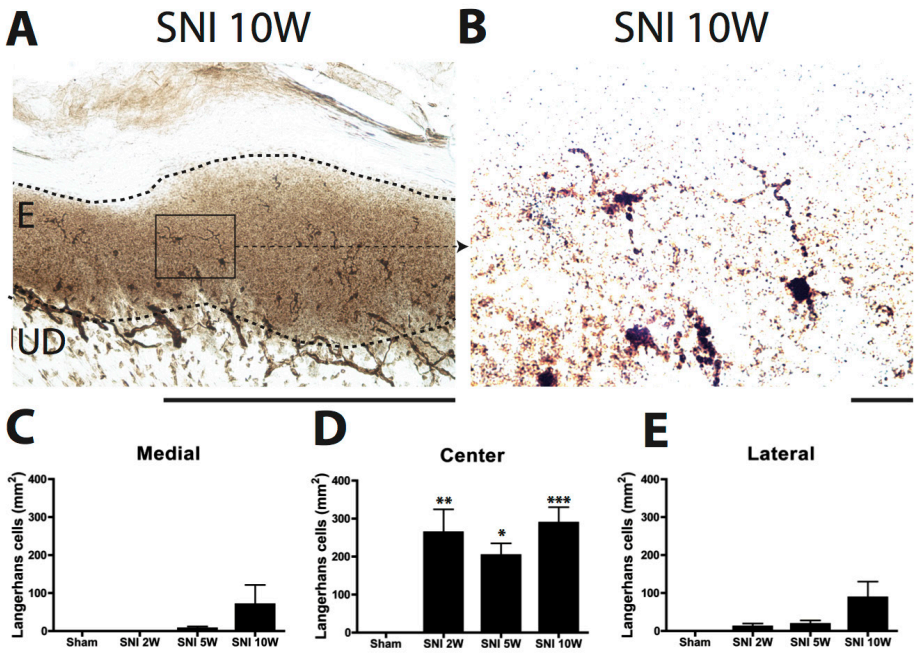

FIGURE 8 LANGERHANS CELLS IN THE SNI MODEL:

*Fig. A and B: Light microscopic micrographs showing labeling for PGP-9.5 in the foot sole (center area) of a SNI-treated rat 10 weeks after operation. Next to PGP-9.5 immunoreactive (IR) fibers, there are several PGP-9.5-IR Langerhans cells (LCs) located in the epidermis (arrowhead in B). C-E: histograms showing the number of PGP-9.5-IR LCs per mm2 in the epidermis of sham- and SNI-treated at different time points. The foot sole skin was divided in medial (innervated by saphenous nerve), center (tibial nerve) and lateral (sural nerve) areas. Note the significant increase in the number of LCs in the center area of the foot sole, whit no significant changes in the medial and lateral areas. *: p < 0.05, **: p < 0.01, ***: p < 0.001 (ANOVA), E: epidermis, UD: upper dermis. Scale bar: A; 250 µm, B; 25 µm.*

DISCUSSION

In the present study, potential changes in the density of nerve fibers immunoreactive for Sub P, P2X3 and NF-200 in the epidermis and upper dermis of the foot soles of rats with SNI-induced neuropathic pain were investigated. The main findings are that non-peptidergic P2X3 unmyelinated fibers show at best only mild changes in the skin after the SNI procedure, whereas peptidergic unmyelinated (Substance P) and peptidergic myelinated (NF-200) show a faster re-innervation pattern in the denervated areas as compared to the unmyelinated non-peptidergic fibers (P2X3). In addition, LCs showed a significant increase in the number of PGP-9.5-IR LCs in the center epidermal area at all time-points while there are very few LCs in sham-treated rats. In the medial and lateral area there was a, non-significant, tendency towards an increase at 10 weeks PO.

SUBSTANCE P IMMUNOREACTIVE PEPTIDERGIC FIBERS

Earlier studies have shown depletion of Sub P-IR fibers in the epidermis corresponding with neuropathic pain symptoms in rats with chronic constriction injury (CCI) [32]. This model involves placement of four loose cat-gut ligatures around the sciatic nerve [33]. CCI rats showed hypersensitivity to mechanical and thermal stimuli in the affected hind paw, which diminished after 2 to 3 months. Based on these findings, an inverse correlation between the density of Sub P-IR fibers and neuropathic pain behavior was suggested [32]. Interestingly, the skin biopsies were taken also at 7 months post-CCI, resulting in similar Sub P-IR fiber densities as the contralateral hind paw area [32]. However, because previous reports have shown that after a lesion changes of peripheral sensory nerve fibers may occur at the same region of the contralateral limb [34, 35], it seems possible that the changes of Sub P-IR fibers after 7 months CCI, when compared with the contralateral foot sole, are an under- or overestimation.

In our study, Sub P-IR fiber density is significantly decreased in the central area of the foot sole but without increased sensitivity to mechanical stimuli, while the medial and lateral areas show no change in fiber density but do present an enhanced sensitivity to mechanical and thermal stimuli. Thus, our data do not support the inverse correlation between Sub P-IR fiber density and neuropathic pain behavior. Whether the differences in outcome are due to the different neuropathic pain models, the different evaluative postoperative time points or differences in area examined by biopsy (footpad vs. non-footpad) is still to be determined.

NON-PEPTIDERGIC P2X3 IMMUNOREACTIVE FIBERS

In the present study, the numbers of epidermal and dermal P2X3 expressing fibers

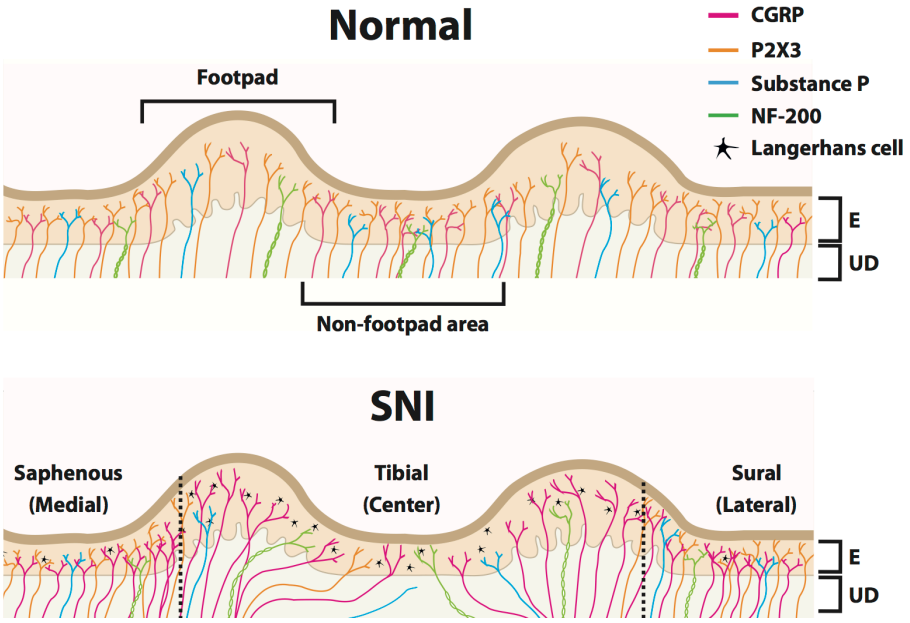

FIGURE 9 ILLUSTRATION OF THE SKIN INNERVATION IN NORMAL AND SNI SITUATION:

Illustration showing the innervation pattern of subgroups of sensory skin fibers in the normal situation and in the SNI model 10 weeks PO. In the naïve animals the peptidergic CGRP and non-peptidergic P2X3 fibers have a lower density in the footpads as compared to the non-footpad areas, while the Substance P and NF-200 fibers have an equal distribution over the complete foot sole. In the SNI model there is a significant increase of CGRP epidermal fibers in the medial and lateral area of the foot sole and there is a complete re-innervation of the center area. In addition the footpads in the SNI model are hyper-innervated with CGRP fibers. Substance P and P2X3 and NF-200 fibers show no increased density in the uninjured medial and lateral area after 10 weeks PO. In addition, Substance P and P2X3 fibers hardly re-innervate the center area, however the NF-200 fibers have the same density of fibers in the denervated area as in the normal situation. In the SNI model the medial, center and lateral area have all an increase in LC's, with the center area being the most prominent one. In addition the epidermis thickness of the SNI model has decreased significantly in all the three areas after 10 weeks PO.

show no substantial changes in the medial and lateral area of the foot sole after the SNI procedure. The center area of the paw shows a depletion of epidermal and upper dermal P2X3 fibers at 2 weeks PO, and re-innervation occurs minimally, with an increase of only 7.8 % in the epidermis and 23.49 % in the upper dermis at 10 weeks PO. This suggests that there is almost no sprouting of uninjured non-peptidergic fibers after an SNI injury. Similarly, minimal re-innervation for P2X3-IR fibers has been reported after the CCI procedure (16 weeks PO) [30] . Interestingly, the density of P2X3-IR fibers reached levels beyond that of control levels at 1.5 years PO in the CCI model.

These results are in contrast to P2X3 expression in dorsal root ganglion (DRG) cells in neuropathic pain models. The number of P2X3 expressing neurons in the DRG is increased after a CCI of the sciatic nerve [36], and after the SNI model there is an increase in P2X3 mRNA in intact neurons in the L4-5 DRG while there is decrease in P2X3 mRNA in axotomized neurons [37]. These changes in the DRG occur, as early as 2 weeks, and at 10 weeks there is still no substantial increase of P2X3-IR fibers in the skin. It is unclear why the increase in P2X3 expression in the DRG neurons is not reflected by an increase in peripheral expression of P2X3 in nerve fibers in the SNI and CCI models.

Despite this ambiguity, it is still possible that P2X3 fibers play a role in the development and maintenance of neuropathic pain. P2X3 receptors bind ATP, which is released in the epidermis by keratinocytes activated by mechanical and thermal stimuli, mediated by Transient Receptor Potential (TRP) channels [16, 38]. After peripheral nerve injury, the expression of TRP channels in epidermal cells is increased in skin areas that show behavioral signs of neuropathic pain [39, 40]. Thus, the interaction between P2X3 and ATP might be involved in producing neuropathic pain behavior, with or without possible increase in P2X3 expression in the non-peptidergic nerve fibers.

NF-200 IMMUNOREACTIVE FIBERS

Previous studies have shown a loss of NF-200-IR upper dermal fibers in the rat foot sole after the CCI model [30], with 25% regeneration at 16 weeks PO as compared to control group. We found that re-innervation by uninjured NF-200-IR upper dermal fibers in the central area reached 87.23 % of control levels at 10 weeks PO, without significant changes in the medial and lateral areas. The permanent loss of NF-200 fibers after a CCI procedure might be due to an inflammatory response to catgut ligatures [41, 42] that inhibits the NF-200 fiber regeneration, which is not present in the SNI model. Since it has been shown that uninjured Aδ-fibers contribute to neuropathic pain symptoms [10, 11], our finding of a complete re-innervation of NF-200-IR fibers might indicate that myelinated fibers, including Aδ-fibers, play a more prominent role in neuropathic pain behavior in the SNI model than in the CCI model.

FOOTPAD AND NON-FOOT PAD AREAS

In rodents, footpads are white cushion-like structures on the plantar surfaces of the fore and hind paws. We have shown that density of epidermal CGRP-IR fibers is significantly lower in the footpads compared to non-footpad areas, suggesting anatomical and possible functional distinctions between these regions [9]. The present study showed lower densities of P2X3-IR epidermal fibers in footpads as compared to non-footpad areas. These variations in density of nerve fibers of a rat's foot sole might cause distinct sensory perceptions in footpad and non-footpad areas, which may subsequently affect the results of behavioral experiments. For example, with the Von Frey test the non-footpad areas are mostly stimulated by applying the monofilaments, whereas in the thermal test such as the hot plate, the footpads are more likely to be in contact with the hot surfaces. Therefore, we propose that results of behavioral experiments that are based on sensory perceptions of a rodent's hind paw should consider the innervation characteristics of the specific foot sole regions that are stimulated.

LANGERHANS CELLS

In the present study, LCs were sparingly found in sham-treated animals. After the SNI procedure a significant increase in the number of LCs was only found in the denervated central area. There was a non-significant tendency towards an increase in the medial and lateral area at 10 weeks PO. Since LCs produce PGP-9.5 in denervated skin areas [43, 44], our finding of increased numbers of PGP-9.5 positive LCs might actually represent the number of already present LCs before SNI procedure. However, LCs have reproducing capabilities [45], and therefore an increase in the number of LCs after the SNI procedure is not excluded.

The precise role of LCs in neuropathic pain development is still to be determined. LCs have close appositions with epidermal nerve fiber terminals, and are capable of releasing nitric oxide (NO) and pro-inflammatory cytokines like tumor necrosis factor δ (TNF δ) and interleukin-1. These are known to sensitize injured and non-injured C-fibers and evoke spontaneous discharge of nociceptors ultimately resulting in neuropathic pain symptoms [44, 46-52].

Increased numbers of LCs have also been found in the CCI model and in a rat neuropathic pain model due to chemotherapy with paclitaxel and vincristine [15, 18-21]. The up-regulation of LCs is associated with a decrease in epidermal nerve fibers in these neuropathic pain models [15, 18-21]. Further, after crush injury of the sciatic nerve, initially resulting in a depletion of epidermal fibers, there was no increase in LCs [43]. Because the crush injury model does not result in neuropathic pain, the hypothesis that LCs may play a role in neuropathic pain is supported. However, in the current study using the SNI model, we found an increase in LCs in all three regions of the foot sole (i.e. of injured and uninjured areas) while there is an increase in epidermal fibers.

Previously we reported a complete re-innervation of epidermal CGRP fibers [9]. The unclear correlation between the LCs and epidermal fibers in the SNI model suggests a different mechanism for LCs in the development and maintenance of neuropathic pain as for example in the CCI model.

SIGNIFICANCE OF PEPTIDERGIC AND NON-PEPTIDERGIC FIBERS CHANGES IN THE SKIN.

The peptidergic (CGRP, SubP and NF-200)) and non-peptidergic (P2X3) unmyelinated fibers are known to terminate in distinct laminae in the dorsal spinal cord [53]. Interestingly, this distinct architecture between these two types of fibers is also seen in the skin. The majority of the non-peptidergic fibers terminate mostly in the epidermis [8, 54-56], whereas the peptidergic fibers mostly innervate skin, muscle and joint. More specifically it has been shown that non-peptidergic fibers terminate in the deeper layer of the epidermis, the stratum granulosum, whereas the peptidergic fibers terminate in the more superficial layer of the epidermis, the stratum spinosum [57]. This distinct organization suggests that peptidergic and non-peptidergic fibers convey distinct sensory information from the periphery, however this must still be determined. No changes in epidermal or upper-dermal Substance-P, P2X3 and upper-dermal NF-200 fiber density were observed, although there is a markedly enhanced sensitivity to mechanical and thermal stimuli. However, this does not exclude the possibility that these fiber subtypes may still play a role in the development and maintenance of neuropathic pain. Because electrophysiological changes accompanying neuropathic pain behavior have also been reported to occur in uninjured fibers as early as one week postoperatively in partial peripheral nerve injury models [11, 58], it seems likely that electrophysiological and behavioral changes may precede detectable changes in morphology [9]. We found no direct correlation between the virtually complete absence of Sub-P, P2X3 or dermal NF-200 fibers and the not statistically significant decline in mechanical withdrawal threshold of that region. In a previous study, epidermal CGRP fibers were also completely absent in the denervated central area in the SNI model, while we also failed to find a significant increase in the mechanical withdrawal threshold [9]. In explaining this phenomenon we have proposed that this could be due to indirect stimulation (i.e. skin contraction) of the already hypersensitive lateral and/or medial region of the foot sole, when stimulating the central region. Taken all toghether, it seems likely that peptidergic and non-peptidergic fibers play different roles in the development and maintenance of neuropathic pain [59].

CONCLUSION

Results presented in our previous report [9] and in the present study show that the CGRP peptidergic unmyelinated fibers have the most profound alterations in the skin upon induction of neuropathic pain. In contrast, the non-peptidergic P2X3 unmyelinated fibers show at best only mild changes in the skin after the SNI procedure, however, as indicated above, a role for P2X3 fibers in neuropathic pain cannot be ruled out. Peptidergic unmyelinated (Substance P) and peptidergic myelinated (NF-200) fibers show a faster re-innervation pattern in the denervated areas as compared to the unmyelinated non-peptidergic fibers (P2X3). Figure 9 shows an overview of the main findings presented here and from a previous study (Duraku et al.). The specific sprouting pattern of the SNI model provides additional insight in the role of peripheral nerve fibers in the development and maintenance of neuropathic pain, and therefore may be useful for diagnostic purposes in neuropathic pain patients.

REFERENCES

1.
Oaklander, A.L. and Siegel, S.M., Cutaneous innervation: form and function. J Am Acad Dermatol 2005; 53(6): 1027-37.

2.
Lauria, G., Cazzato, D., Porretta-Serapiglia, C., et al., Morphometry of dermal nerve fibers in human skin. Neurology 2011; 77(3): 242-9.

3.
Lauria, G., Lombardi, R., Camozzi, F., and Devigili, G., Skin biopsy for the diagnosis of peripheral neuropathy. Histopathology 2009; 54(3): 273-85.

4.
Hsieh, S.T., EFNS guidelines on the use of skin biopsy in the diagnosis of peripheral neuropathy. Eur J Neurol 2006; 13(12): e9.

5.
Lauria, G. and Devigili, G., Skin biopsy as a diagnostic tool in peripheral neuropathy. Nat Clin Pract Neurol 2007; 3(10): 546-57.

6.
Baron, R., Mechanisms of disease: neuropathic pain--a clinical perspective. Nat Clin Pract Neurol 2006; 2(2): 95-106.

7.
Ruscheweyh, R., Forsthuber, L., Schoffnegger, D., and Sandkuhler, J., Modification of classical neurochemical markers in identified primary afferent neurons with Abeta-, Adelta-, and C-fibers after chronic constriction injury in mice. J Comp Neurol 2007; 502(2): 325-36.

8.
Taylor, A.M., Peleshok, J.C., and Ribeiro-da-Silva, A., Distribution of P2X(3)-immunoreactive fibers in hairy and glabrous skin of the rat. J Comp Neurol 2009; 514(6): 555-66.

9.
Duraku, L., Hossaini, M., Hoendervangers, S., et al., Spatiotemporal dynamics of re-innervation and hyperinnervation patterns by uninjured CGRP fibers in the rat foot sole epidermis after nerve injury. Molecular Pain 2012; 8(1): 61.

10.
Ji, G., Zhou, S., and Carlton, S.M., Intact Adelta-fibers up-regulate transient receptor potential A1 and contribute to cold hypersensitivity in neuropathic rats. Neuroscience 2008; 154(3): 1054-66.

11.
Ji, G., Zhou, S., Kochukov, M.Y., Westlund, K.N., and Carlton, S.M., Plasticity in intact A delta- and C-fibers contributes to cold hypersensitivity in neuropathic rats. Neuroscience 2007; 150(1): 182-93.

12.
Wu, G., Ringkamp, M., Hartke, T.V., et al., Early onset of spontaneous activity in uninjured C-fiber nociceptors after injury to neighboring nerve fibers. J Neurosci 2001; 21(8): RC140.

13.
Wu, G., Ringkamp, M., Murinson, B.B., et al., Degeneration of myelinated efferent fibers induces spontaneous activity in uninjured C-fiber afferents. J Neurosci 2002; 22(17): 7746-53.

14.
Campbell, J.N. and Meyer, R.A., Mechanisms of neuropathic pain. Neuron 2006; 52(1): 77-92.

15.
Lindenlaub, T. and Sommer, C., Epidermal innervation density after partial sciatic nerve lesion and pain-related behavior in the rat. Acta Neuropathol 2002; 104(2): 137-43.

16.
Boulais, N. and Misery, L., The epidermis: a sensory tissue. Eur J Dermatol 2008; 18(2): 119-27.

17.
Lauria, G., Lombardi, R., Borgna, M., et al., Intraepidermal nerve fiber density in rat foot pad: neuropathologic-neurophysiologic correlation. J Peripher Nerv Syst 2005; 10(2): 202-8.

18.
Rodriguez, G. and Villamizar, R., Carcinoid tumor with skin metastasis. Am J Dermatopathol 1992; 14(3): 263-9.

19.
Springall, D.R., Karanth, S.S., Kirkham, N., Darley, C.R., and Polak, J.M., Symptoms of notalgia paresthetica may be explained by increased dermal innervation. J Invest Dermatol 1991; 97(3): 555-61.

20.
Calder, J.S., Holten, I., and McAllister, R.M., Evidence for immune system involvement in reflex sympathetic dystrophy. J Hand Surg Br 1998; 23(2): 147-50.

21.
Siau, C., Xiao, W., and Bennett, G.J., Paclitaxel- and vincristine-evoked painful peripheral neuropathies: loss of epidermal innervation and activation of Langerhans cells. Exp Neurol 2006; 201(2): 507-14.

22.
Ma, W. and Eisenach, J.C., Morphological and pharmacological evidence for the role of peripheral prostaglandins in the pathogenesis of neuropathic pain. Eur J Neurosci 2002; 15(6): 1037-47.

23.
Ruigrok, T.J. and Apps, R., A light microscope-based double retrograde tracer strategy to chart central neuronal connections. Nat Protoc 2007; 2(8): 1869-78.

24.
Jongen, J.L., Jaarsma, D., Hossaini, M., et al., Distribution of RET immunoreactivity in the rodent spinal cord and changes after nerve injury. J Comp Neurol 2007; 500(6): 1136-53.

25.
R M Buijs, C.W.P., J J Van Heerikhuize, A A Sluiter, P J Van Der Sluis, M Ramkema, T P Van Der Woude, E Van Der Beek, Antibodies to small transmitter molecules and peptides: production and application of antibodies to dopamine, serotonin, GABA, vasopressin, vasoactive intestinal peptide, neuropeptide Y, somatostatin and substance P. Biomedical research 1989; 10, Supplement 3: 213-221.

26.
Hopman, A.H., Ramaekers, F.C., and Speel, E.J., Rapid synthesis of biotin-, digoxigenin-, trinitrophenyl-, and fluorochrome-labeled tyramides and their application for In situ hybridization using CARD amplification. J Histochem Cytochem 1998; 46(6): 771-7.

27.
Kuhlmann, W.D. and Peschke, P., Glucose oxidase as label in histological immunoassays with enzyme-amplification in a two-step technique: coimmobilized horseradish peroxidase as secondary system enzyme for chromogen oxidation. Histochemistry 1986; 85(1): 13-7.

28.
Petruska, J.C., Streit, W.J., and Johnson, R.D., Localization of unmyelinated axons in rat skin and mucocutaneous tissue utilizing the isolectin GS-I-B4. Somatosens Mot Res 1997; 14(1): 17-26.

29.
Schaumburg-Lever, G., Alroy, J., Ucci, A., and Lever, W.F., Distribution of carbohydrate residues in normal skin. Arch Dermatol Res 1984; 276(4): 216-23.

30.
Peleshok, J.C. and Ribeiro-da-Silva, A., Delayed reinnervation by nonpeptidergic nociceptive afferents of the glabrous skin of the rat hindpaw in a neuropathic pain model. J Comp Neurol 2011; 519(1): 49-63.

31.
Lauria, G., Borgna, M., Morbin, M., et al., Tubule and neurofilament immunoreactivity in human hairy skin: markers for intraepidermal nerve fibers. Muscle Nerve 2004; 30(3): 310-6.

32.
Ma, W. and Bisby, M.A., Calcitonin gene-related peptide, substance P and protein gene product 9.5 immunoreactive axonal fibers in the rat footpad skin following partial sciatic nerve injuries. J Neurocytol 2000; 29(4): 249-62.

33.
Bennett, G.J. and Xie, Y.K., A peripheral mononeuropathy in rat that produces disorders of pain sensation like those seen in man. Pain 1988; 33(1): 87-107.

34.
Oaklander, A.L. and Brown, J.M., Unilateral nerve injury produces bilateral loss of distal innervation. Ann Neurol 2004; 55(5): 639-44.

35.
Koltzenburg, M., Wall, P.D., and McMahon, S.B., Does the right side know what the left is doing? Trends Neurosci 1999; 22(3): 122-7.

36.
Novakovic, S.D., Kassotakis, L.C., Oglesby, I.B., et al., Immunocytochemical localization of P2X3 purinoceptors in sensory neurons in naive rats and following neuropathic injury. Pain 1999; 80(1-2): 273-82.

37.
Tsuzuki, K., Kondo, E., Fukuoka, T., et al., Differential regulation of P2X(3) mRNA expression by peripheral nerve injury in intact and injured neurons in the rat sensory ganglia. Pain 2001; 91(3): 351-60.

38.
Lumpkin, E.A. and Caterina, M.J., Mechanisms of sensory transduction in the skin. Nature 2007; 445(7130): 858-65.

39.
Facer, P., Casula, M.A., Smith, G.D., et al., Differential expression of the capsaicin receptor TRPV1 and related novel receptors TRPV3, TRPV4 and TRPM8 in normal human tissues and changes in traumatic and diabetic neuropathy. BMC Neurol 2007; 7: 11.

40.
Gopinath, P., Wan, E., Holdcroft, A., et al., Increased capsaicin receptor TRPV1 in skin nerve fibres and related vanilloid receptors TRPV3 and TRPV4 in keratinocytes in human breast pain. BMC Womens Health 2005; 5(1): 2.

41.
Clatworthy, A.L., Illich, P.A., Castro, G.A., and Walters, E.T., Role of peri-axonal inflammation in the development of thermal hyperalgesia and guarding behavior in a rat model of neuropathic pain. Neurosci Lett 1995; 184(1): 5-8.

42.
Maves, T.J., Pechman, P.S., Gebhart, G.F., and Meller, S.T., Possible chemical contribution from chromic gut sutures produces disorders of pain sensation like those seen in man. Pain 1993; 54(1): 57-69.

43.
Stankovic, N., Johansson, O., and Hildebrand, C., Increased occurrence of PGP 9.5-immunoreactive epidermal Langerhans cells in rat plantar skin after sciatic nerve injury. Cell Tissue Res 1999; 298(2): 255-60.

44.
Hsieh, S.T., Choi, S., Lin, W.M., et al., Epidermal denervation and its effects on keratinocytes and Langerhans cells. J Neurocytol 1996; 25(9): 513-24.

45.
Czernielewski, J.M. and Demarchez, M., Further evidence for the self-reproducing capacity of Langerhans cells in human skin. J Invest Dermatol 1987; 88(1): 17-20.

46.
Qureshi, A.A., Hosoi, J., Xu, S., et al., Langerhans cells express inducible nitric oxide synthase and produce nitric oxide. J Invest Dermatol 1996; 107(6): 815-21.

47.
Deng, L., Ding, W., and Granstein, R.D., Thalidomide inhibits tumor necrosis factor-alpha production and antigen presentation by Langerhans cells. J Invest Dermatol 2003; 121(5): 1060-5.

48.
Andersson By, U., Tani, E., Andersson, U., and Henter, J.I., Tumor necrosis factor, interleukin 11, and leukemia inhibitory factor produced by Langerhans cells in Langerhans cell histiocytosis. J Pediatr Hematol Oncol 2004; 26(11): 706-11.

49.
Watkins, L.R. and Maier, S.F., Beyond neurons: evidence that immune and glial cells contribute to pathological pain states. Physiol Rev 2002; 82(4): 981-1011.

50.
Shubayev, V.I. and Myers, R.R., Upregulation and interaction of TNFalpha and gelatinases A and B in painful peripheral nerve injury. Brain Res 2000; 855(1): 83-9.

51.
Sommer, C., Marziniak, M., and Myers, R.R., The effect of thalidomide treatment on vascular pathology and hyperalgesia caused by chronic constriction injury of rat nerve. Pain 1998; 74(1): 83-91.

52.
Sommer, C., Schmidt, C., and George, A., Hyperalgesia in experimental neuropathy is dependent on the TNF receptor 1. Exp Neurol 1998; 151(1): 138-42.

53.
Molliver, D.C., Radeke, M.J., Feinstein, S.C., and Snider, W.D., Presence or absence of TrkA protein distinguishes subsets of small sensory neurons with unique cytochemical characteristics and dorsal horn projections. J Comp Neurol 1995; 361(3): 404-16.

54.
Plenderleith, M.B. and Snow, P.J., The plant lectin Bandeiraea simplicifolia I-B4 identifies a subpopulation of small diameter primary sensory neurones which innervate the skin in the rat. Neurosci Lett 1993; 159(1-2): 17-20.

55.
Bennett, D.L., Dmietrieva, N., Priestley, J.V., Clary, D., and McMahon, S.B., trkA, CGRP and IB4 expression in retrogradely labelled cutaneous and visceral primary sensory neurones in the rat. Neurosci Lett 1996; 206(1): 33-6.

56.
Perry, M.J. and Lawson, S.N., Differences in expression of oligosaccharides, neuropeptides, carbonic anhydrase and neurofilament in rat primary afferent neurons retrogradely labelled via skin, muscle or visceral nerves. Neuroscience 1998; 85(1): 293-310.

57.
Zylka, M.J., Rice, F.L., and Anderson, D.J., Topographically distinct epidermal nociceptive circuits revealed by axonal tracers targeted to Mrgprd. Neuron 2005; 45(1): 17-25.

58.
Lee, D.H., Iyengar, S., and Lodge, D., The role of uninjured nerve in spinal nerve ligated rats points to an improved animal model of neuropathic pain. Eur J Pain 2003; 7(5): 473-9.

59.
Taylor, A.M., Osikowicz, M., and Ribeiro-da-Silva, A., Consequences of the ablation of nonpeptidergic afferents in an animal model of trigeminal neuropathic pain. Pain 2012; 153(6): 1311-9.

6

CONTRALATERAL PEPTIDERGIC SKIN FIBER CHANGES AFTER INDUCTION OF IPSILATERAL NEUROPATHIC PAIN: POSSIBLE MECHANISM FOR NERVE INJURY INDUCED MIRROR IMAGE PAIN IN THE RAT.

L. S. Duraku [1,2]
M. Hossaini [2]
S. Kambiz [1,2]
J. C. Holstege [2]
E. T. Walbeehm [1]
T. J. H. Ruigrok [2]

1. Department of Plastic, Reconstructive and Hand Surgery, Erasmus MC, University Medical Center, Rotterdam, The Netherlands

2. Dept. of Neuroscience, Erasmus MC, University Medical Center, Rotterdam, The Netherlands

ABSTRACT

Neuropathic pain that develops in a specific part of the body may also develop similar but usually less severe symptoms in the same body part on the uninjured contralateral side, a condition termed ‘mirror image pain’. This phenomenon has been reported in patients with different neuropathic pain states, but also in various animal models of neuropathic pain. In the present study, we have investigated the innervation patterns of different subgroups of sensory nerve fibers in the epidermal and upper dermal skin areas in the contralateral hind paw of rats with neuropathic pain that was induced in the ipsilateral paw by the spared nerve injury (SNI) procedure. The mechanical threshold in the contralateral hind paw was determined and correlated with the changes in the innervation patterns of different sensory subgroups of nerve fibers in the contralateral hind paw. For this approach, we have used immunohistochemistry to identify peptidergic nerve fibers containing calcitonin gene-related peptide (CGRP), substance P (Sub P), and myelinated NF-200 positive, and non-peptidergic fibers containing the purinergic receptor P2X3. Our results show that the SNI procedure results in mechanical allodynia of the contralateral foot sole that is accompanied by an increase in the dermal density of CGRP immunoreactive fibers.

INTRODUCTION

In some patients with traumatic peripheral nerve injury, the experienced pain does not subside and may even progress as the patients develops neuropathic pain [1]. The main symptoms of neuropathic pain are spontaneous pain in the absence of noxious stimuli, pain induced by normally non-painful stimuli (allodynia), and the experience of exaggerated pain (hyperalgesia) following a pain stimulus as compared to pre-neuropathic state [2, 3]. These behavioral signs of neuropathic pain are usually not limited to the area innervated by the injured nerve, but they may also be evoked in the surrounding area innervated by non-injured nerves [4].

Patients that develop neuropathic pain in a specific part of the body, may also develop similar but usually less severe symptoms in the same body part on the uninjured contralateral side, a condition termed 'mirror image pain' [5, 6]. This phenomenon has been reported in patients with different inflammatory and neuropathic pain states, most notably in patients that developed neuropathic pain after peripheral nerve trauma [5, 7]. In addition, mirror image pain has also been reported in various animal models of neuropathic pain [5], such as the chronic constriction injury (CCI) procedure [8], the spared nerve injury (SNI) [9, 10], and the spinal nerve ligation (SNL) models [11]. These findings indicate that chronic pain on one side of the body may induce pain in the corresponding contralateral body part in the absence of injury on that side.

Both peripheral and central mechanisms are involved in the development and maintenance of neuropathic pain, suggesting that this is also true for the development of mirror image pain [5, 6]. Indeed, after peripheral nerve injury ipsilateral, several studies have shown sprouting of motor, sympathetic, and sensory fibers on the contralateral side [6]. However, others have found a decrease in the number of sensory nerve fibers on the contralateral side in both humans and rats after ipsilateral nerve damage [12, 13]. Therefore, the nature and role of these changes in the development of mirror image pain are far from resolved.

In the present study, we have investigated the innervation patterns of different subgroups of sensory nerve fibers in the epidermal and upper dermal skin areas in the contralateral hind paw of rats with neuropathic pain that was induced in the ipsilateral hind paw by the SNI procedure. The SNI procedure requires ligation and dissection of the tibial and peroneal branches of the sciatic nerve which results in mechanical allodynia and hyperalgesia of the foot sole area that is innervated by the intact sural and saphenous nerve branches [9]. This model not only uses the transection of nerves, which is representative of the most common cause of nerve injury induced neuropathic pain in humans, but it also results in a pain behavior that is very similar to neuropathic pain behavior in humans [14, 15]. The mechanical threshold in the contralateral hind paw was determined and correlated with the changes in the innervation

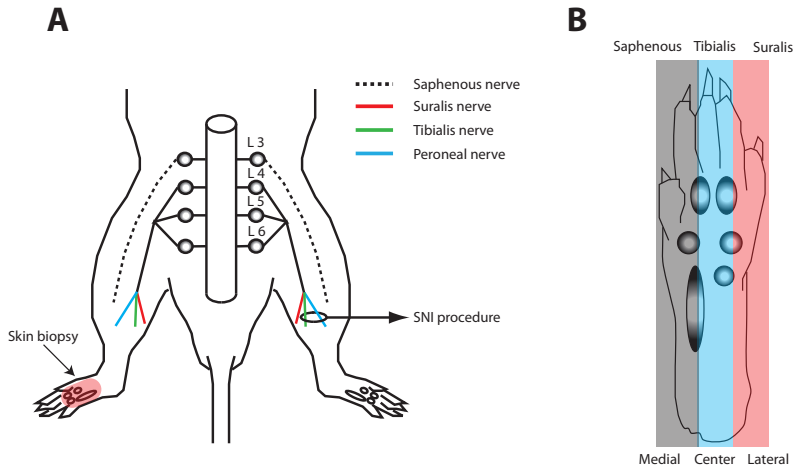

FIGURE 1:

Figure 1 A shows a drawing of the SNI procedure and the location where the skin biopsy is taken from the contralateral foot sole. Figure 1 B displays a drawing of the cutaneous innervation pattern of the saphenous, tibial and sural nerve in the hind foot sole of a rat.

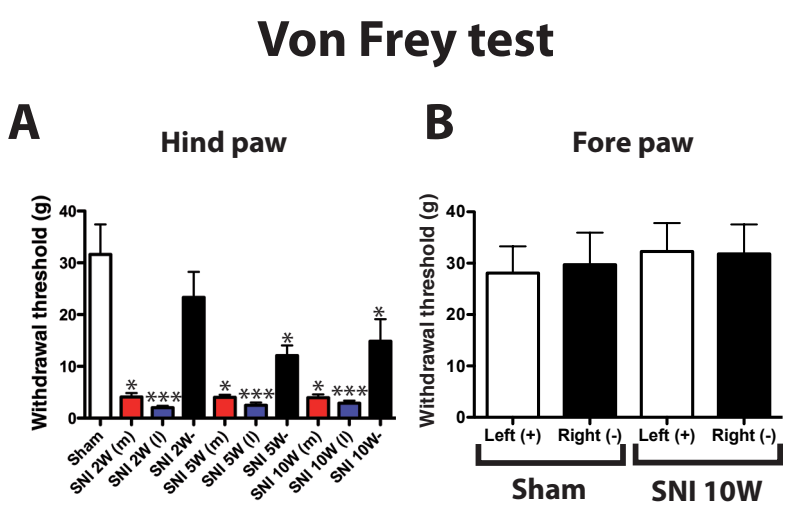

FIGURE 2:

*A histogram showing the mechanical withdrawal threshold in grams (g) of the ipsilateral medial (m) and lateral (l) part of the foot sole and the contralateral hind limb foot sole (-) of the sham and SNI-treated group after a unilateral nerve injury (Fig. 2 A) (n=13 per group). The significant differences depicted in Figure 2 A are the differences between the SNI-treated group and the shams. Figure 2 B shows the ipsi- (Left+) and contralateral (Right-) front paw mechanical sensitivity of sham and SNI-treated rats. Kruskal-Wallis test with Dunn's post-hoc test. *: p <0.05, ***: p <0.001.*

patterns of different nerve fiber in the contralateral hind paw. For this approach, we have used immunohistochemistry to identify peptidergic nerve fibers containing calcitonin gene-related peptide (CGRP), substance P (Sub P), and myelinated NF-200 positive, and non-peptidergic fibers containing the purinergic receptor P2X3. Our results show that the SNI procedure results in mechanical allodynia of the contralateral foot sole that is accompanied by an increase in the upper dermal density of CGRP immunoreactive fibers.

METHODS

ANIMALS

For the following experiments, we used 26 male Wistar rats of same age and weighing 250-350 grams. All experiments were approved by the Dutch Ethical Committee on Animal Welfare (DEC) and all procedures were in adherence to the European guidelines for the care and use of laboratory animals (Council Directive 86/6009/EEC).

THE SPARED NERVE INJURY (SNI) MODEL

We applied the SNI procedure [9] as follows: under general isoflurane (2%) anesthesia, the three branches of the sciatic nerve i.e. the sural, common peroneal and tibial nerves were exposed with minimal damage to the overlaying muscles. The tibial and common peroneal nerves were ligated together with a 5.0 silk (Ethicon) suture, and cut approximately 2 mm distal to the ligation (Fig. 1 A), while the sural nerve was left intact. For sham surgery the sciatic branches were only exposed. The rats recovered uneventful and did not display signs of autotomy at any of the survival times.

MECHANICAL THRESHOLD

The mechanical thresholds in the ipsi- and contralateral fore- and hind paws were determined using Von Frey hairs at 2, 5 and 10 weeks postoperatively (PO). For this experiment, rats were placed in a Plexiglas box (15cmx15cm) with a mesh floor, in which they were able to move freely. Before start of the experiment, all rats were habituated to the experimenter, the experiment room and the Plexiglas box for 5 days. Moreover, at each time point, prior to each measurement the rats were habituated for 30 min to the experiment room, and subsequently for 10 min to the transparent cage. Each Von Frey hair was applied for 2 s at 5 s intervals, and the threshold was set at 3 evoked responses in a set of 5 applications maximum. The medial and lateral side of the contralateral paw was stimulated at the transition point from glabrous skin to hairy skin and the center of the foot sole was stimulated approximately at halfway of the anterior to posterior midline. Previous studies have shown that in animals with

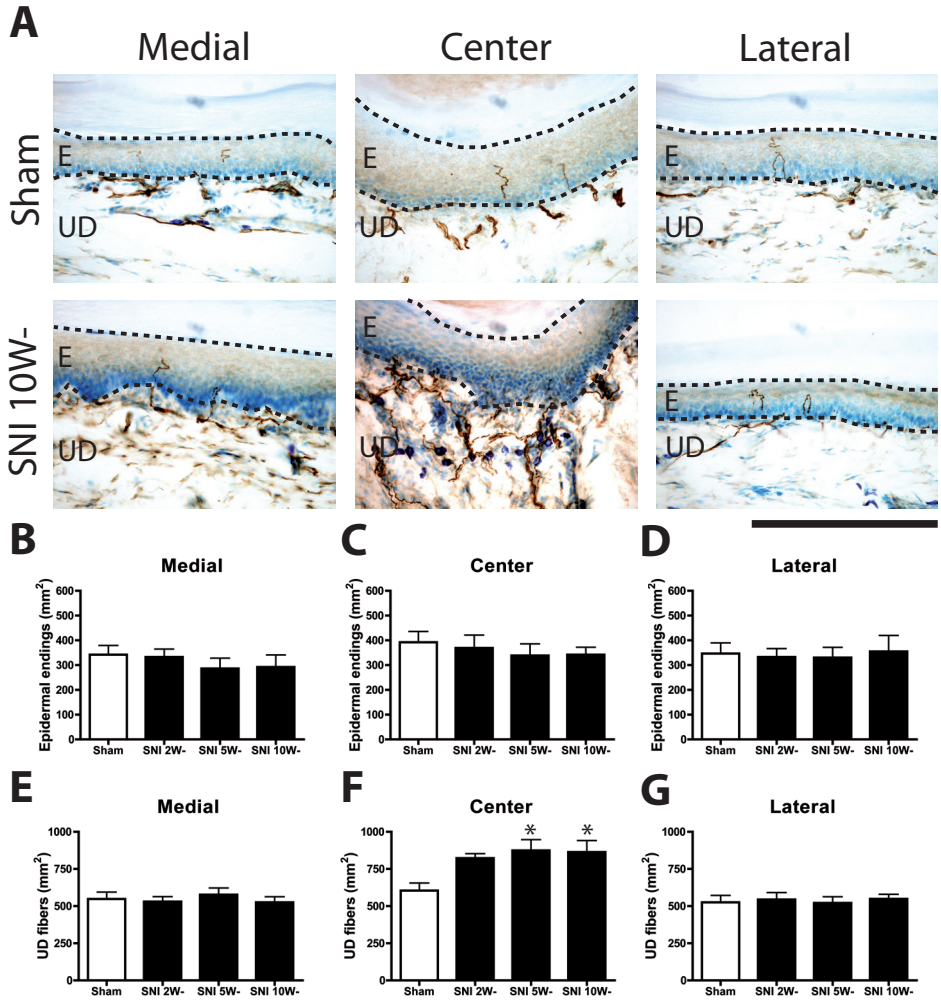

FIGURE 3:

*Microphotographs showing CGRP-IR fibers in skin biopsies taken from the medial (saphenous), center (tibial) and lateral (sural) part of the foot sole contralateral to the SNI or sham-operated side (Fig. 3 A). Fig. 3 B-D displays histograms of the number of CGRP-IR fibers (mm2) in the epidermis (E) and fig. 3 E-G shows the number of CGRP-IR fibers (mm2) in the upper dermis (UD). Note the significant increase ($p < 0.05$) of upper dermal CGRP-IR fibers in the center (tibial) area of the contralateral foot sole at 5 and 10 weeks PO (Fig. 3 A and F). One-way ANOVA with post-hoc Tukey test; *: $p < 0.05$, Scale bar: 250 µm.*

mirror image pain induced by inflammation [16, 17] or nerve injury [10, 18], the response threshold in the contralateral hind paw is only significantly decreased to mechanical and chemical stimuli, whereas the response threshold to (noxious) thermal stimuli remained unchanged. Therefore, in the present study, we decided not to investigate the thermal response threshold in the contralateral hind paw and we only focused on the mechanical response threshold.

TISSUE PREPARATION

Following survival periods of 2, 5 and 10 weeks, all animals received an overdose of pentobarbital (100 mg/kg). Two naïve animals were compared to the sham animals in mechanical behavior as well as in the number of epidermal and upper dermal CGRP, Substance P, P2X3, NF-200 and PGP 9.5 fibers in the foot sole (data not shown). There was no significant difference between sham animals and naïve rats and we therefore assumed that the results are comparable. Under deep anesthesia the glabrous skin of the contralateral foot sole was dissected in a distal to proximal strip of tissue (Fig 1 A and B), which was immersion-fixed in 2% paraformaldehyde-lysine-periodate solution for 24 hours on 4˚C. After fixation, the skins (suggestive: the flaps of skin) where embedded in gelatin mixture containing 10% gelatin, 4% formaldehyde and 30 % sucrose [19]. Thereafter, transverse sections were cut at 40 µm in a freezing microtome and collected free-floating in glycerol anti-freeze solution for long-term storage at –20 °C.

IMMUNOHISTOCHEMISTRY

First, sections were washed in PBS for 40 minutes, and this was repeated after hydrogen peroxide, heating, and antibody incubation steps. To ensure minimal background due to red blood cells in the skin, we incubated the sections after the first washing step in 3 % hydrogen peroxide solution for 10 minutes at room temperature (RT). Subsequently, the sections were heated for 40 minutes at 80 ˚C in a solution of 2.5 mM sodium citrate. Sections were then pre-incubated (90 min, RT) in a blocking solution containing bovine serum albumin (BSA 2%) or milk powder (Nutricia Profitar) (1/200) phosphate buffered saline (PBS, pH 7,4) and 0.5% Triton X-100 (Fraction V, Roche). After pre-incubation, the sections were incubated for 48 hours in a cocktail of 2% BSA or milk powder containing the primary antibody (table 1). Substance P was raised against rabbit as described previously [20]. Subsequently, sections were incubated in a 2% BSA of milk powder cocktail containing the secondary antibody (Vector Laboratories) for 90 min (RT). The primary antibodies were CGRP (1/30.000, rabbit, Calbiochem); Substance P (1/500); P2X3 (1/25.000, guinea pig, Neuromics) and NF-200 (1/15.000, rabbit, Chemicon); PGP 9.5 (1/10.000, rabbit, Biomol). Sections were further processed using a Vectastain Elite ABC kit (Vector, Burlingame, CA) (90 min at RT) and thereafter washed with PB (40 minutes). Further signal am-

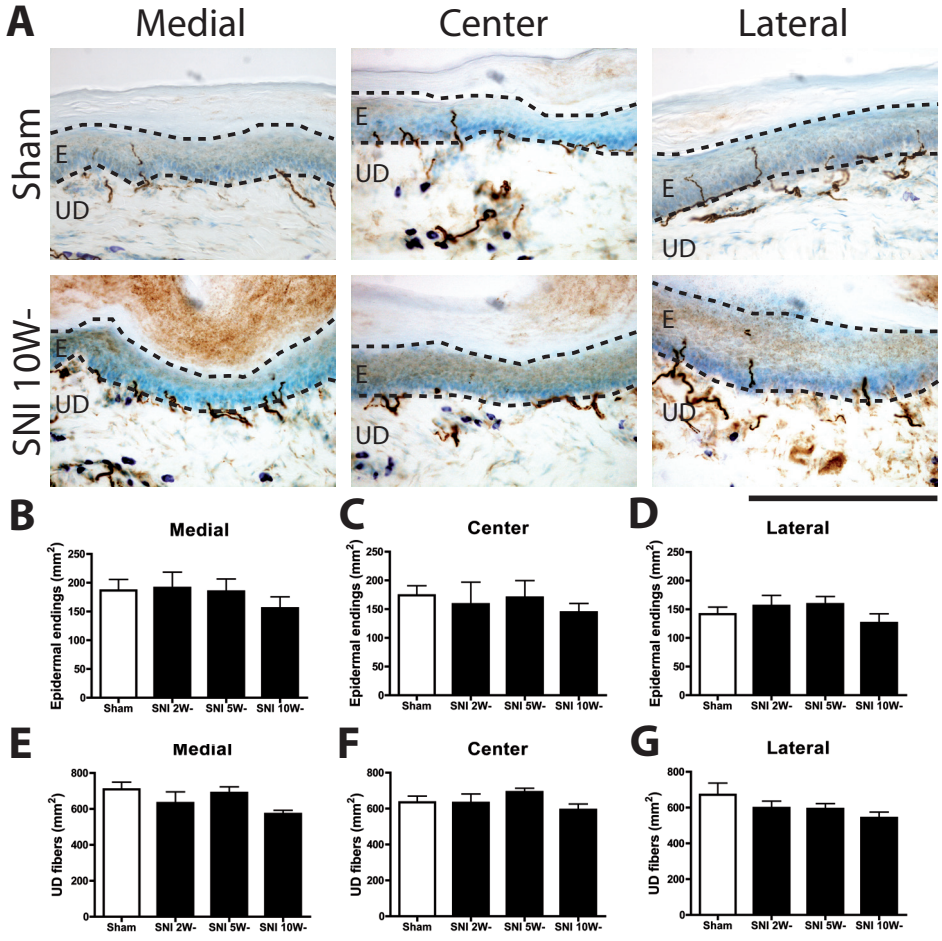

FIGURE 4:

Microphotographs showing staining for Substance P-IR fibers in skin biopsies taken from the medial (saphenous), center (tibial) and lateral (sural) part of the foot sole contralateral to the SNI or sham operated side (Fig. 4 A). Fig. 4 B-D displays histograms of the number of Substance P-IR fibers per mm2 in the epidermis (E) and fig. 4 E-G shows the number of Substance P-IR fibers (mm2) in the upper dermis (UD). Scale bar: 250 µm.

plification was achieved by applying biotin tyramide amplification [21]. Finally, 3,-3δ diaminobenzidine (DAB) enhanced by the glucose oxidase-nickel-DAB method [22] was used to reveal antibody location. The sections were mounted on gelatinized slides; air dried overnight, dehydrated using absolute ethanol (< 0.01% methanol), and transferred to xylene and coverslipped with Permount (Fisher, Hampton, NH).

ANALYSIS

Eight series of sections of the complete foot sole were used for analysis, making a selection in lateral, center and medial side. For each antibody, we analyzed sections from the proximal to distal parts of the foot sole by using the imbedded rat's brainstem as an anatomical position marker [19]. For each rat, eight sections from the proximal and eight sections from the distal part of the foot sole were analyzed. Analysis was conducted with an Olympus BH microscope (20x objective) equipped with a Lucivid™ miniature monitor and Neurolucida™ software (MicroBrightField, Inc., Colchester, VT). The number of labeled fibers was determined in the epidermis and upper dermis in the most medial, center, and most lateral side of the section by an experimenter who was blinded to the experiment. In the epidermis only the terminal branches were counted and the minimal criterion for a labeled profile to be counted as an upper-dermal fiber was that it should be a clear non-interrupted single fiber and not e.g. interrupted fascicles. Each area was 750µm in length with an approximate surface area of 0.03 mm^2, resulting in the number of labeled fibers per mm^2. Per group (n=6), the results were averaged and compared with the average results in the control-sham group. Errors in the variations were assessed as the standard error of the mean (SEM). We used the one way-ANOVA with a post hoc Tukey for statistical comparison of the number of labeled fibers between the SNI and control-sham treated groups. The results of the Von Frey test were analyzed using the non-parametric Kruskal-Wallis test with a Dunn's post-hoc test. Differences were considered significant only if $p < 0.05$.

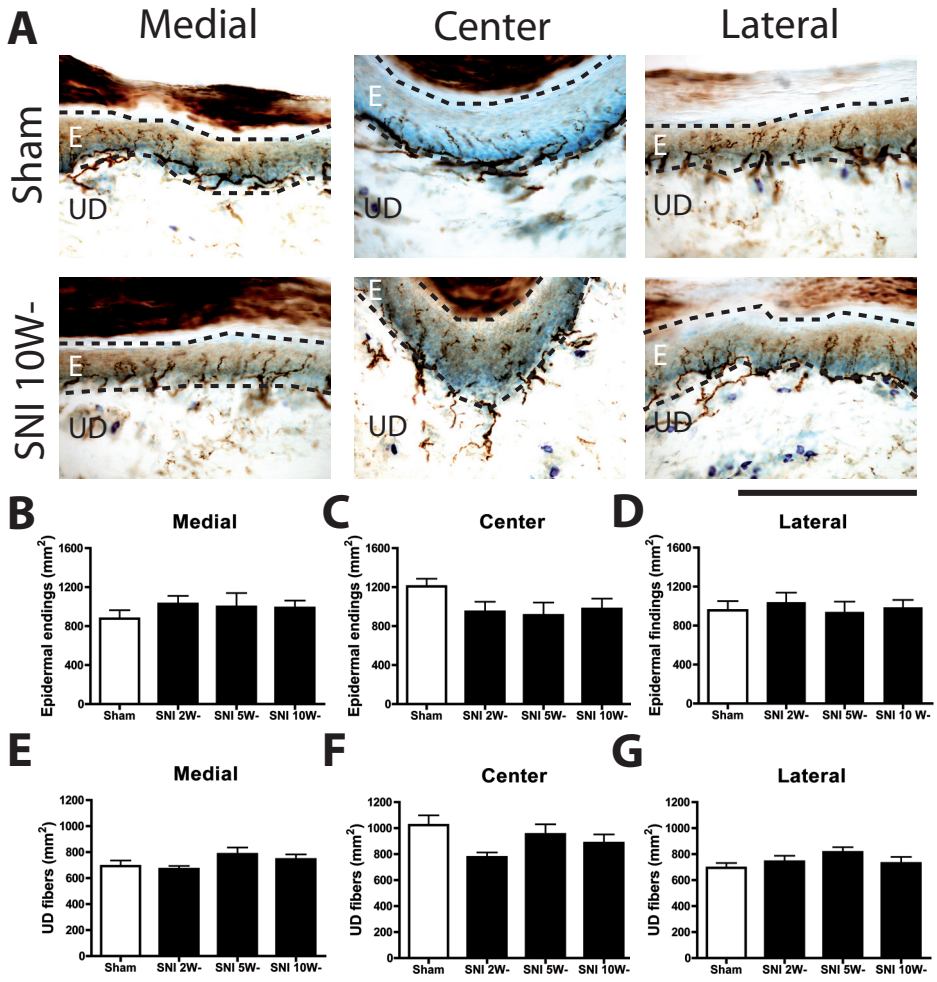

FIGURE 5:

Microphotographs showing staining for P2X3-IR fibers in skin biopsies taken from the medial (saphenous), center (tibial) and lateral (sural) part of the foot sole contralateral to the SNI or Sham operated side (Fig. 5 A). Fig. 5 B-G displays histograms of the number of P2X3-IR fibers per mm2 in the epidermis (E) and fig. 5 E-G shows the number of P2X3-IR fibers (mm2) in the upper dermis (UD). Scale bar: 250 µm.

RESULTS

MECHANICAL WITHDRAWAL THRESHOLD

In SNI-treated rats, the mechanical withdrawal threshold was significantly decreased in the affected medial ($p < 0.05$) and lateral ($p < 0.001$) hind paw as compared to sham-treated animals (Fig. 2 A). A significant decrease ($p < 0.05$) in the mechanical withdrawal threshold was also found in the contralateral hind paw of SNI-treated animals as compared to the sham group at 5 and 10 weeks PO (Fig. 2 A). Because there was no difference in mechanical sensitivity between the medial, center and lateral areas of the contralateral foot of SNI animals (data not shown), we present only the center area of the SNI-treated rats. Between the ipsilateral and contralateral foot sole of SNI-treated rats, the lateral ($p < 0.001$) and medial ($p < 0.01$) ipsilateral part showed a significant lower mechanical withdrawal threshold as compared to the contralateral foot sole at 2 weeks PO. At 5 and 10 weeks PO only the lateral ipsilateral part of the SNI-treated rats exhibited a significant lower mechanical withdrawal threshold ($p<0.01$) as compared to the contralateral hind paw (Fig. 2 A). We also compared the mechanical withdrawal thresholds in the ipsi- and contralateral forepaws, which were not significantly different from each other both within the SNI and sham-treated rats, as well as between the SNI- and sham-treated rats (Fig. 2 B).

INNERVATION OF THE FOOT SOLE AFTER CONTRALATERAL SNI

The SNI procedure induces mechanical and temperature hypersensitivity of the ipsilateral hind limb, which [9], at least to some extent, relates to changes in the innervation and re-innervation of the affected foot sole [23]. In order to determine if the mechanical hypersensitivity induced by an ipsilateral executed SNI procedure, also induces corresponding changes in the innervation of the contralateral foot sole, the density of several classes of nerve fibers was determined (i.e. CGRP, Substance P, P2X3, NF200 and PGP 9.5). Because the ipsilateral changes in the innervation of the foot sole, due to the nature of the SNI, are different in its medial, center and lateral part, we will describe the main features of the SNI effects at the contralateral side separately for the central part of the foot sole as well as for its edges (i.e. medial and lateral part).

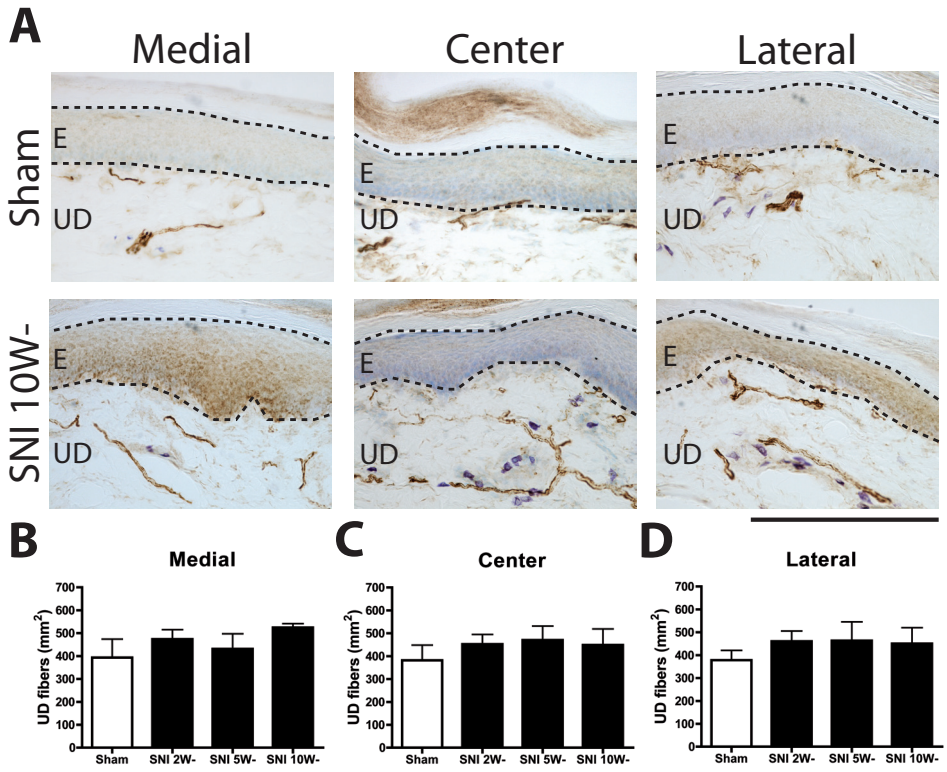

FIGURE 6:

Micrographs showing staining for NF-200-IR fibers in skin biopsies taken from the medial (saphenous), center (tibial) and lateral (sural) part of the foot sole (Fig. 6 A). Fig. 6 B-D displays histograms of the number of NF-200-IR fibers per mm2 in the upper dermis (UD). Scale bar: 250 µm.

INNERVATION OF THE CENTRAL SKIN AREA

CGRP

CGRP-IR fibers formed thick fiber fascicles in the superficial and deeper dermis, and most of these fibers penetrated the epidermis (Fig. 3 A), a characteristic morphology that was found in the ipsi- and contralateral hind paws of both SNI- and sham-treated rats. In SNI-treated rats, no significant changes were found in the number of epidermal CGRP-IR fibers in the central foot sole area of the contralateral hind paw as compared to the same foot sole area in the contralateral hind paw of sham-treated rats (Fig. 3 A and C). However, we found an increase in the density of upper dermal CGRP-IR fibers in the center area at 2 weeks PO, which became significant ($p < 0.05$) at 5 and 10 weeks PO as compared to the same foot sole area in the sham-treated group (Fig 3 A and F). At 10 weeks this corresponded to a 42,83% increase in the density of CGRP fibers in the contralateral foot sole (Fig. 3 F).

SUBSTANCE P

In the contralateral hind paw of both the sham- and SNI-treated rats, we found that the density of Substance P-IR fibers was significantly higher in the upper dermal region as compared to the epidermal region ($p < 0.05$) (Fig. 4). Further, the contralateral density of upper dermal and epidermal Substance P-IR fibers after ipsilateral SNI treatment were not different from the values found in the sham-treated animals. (Fig. 4 B-G).

P2X3

Numerous P2X3-IR fibers in the epidermis and upper dermis, representing the non-peptidergic fiber category, are present in the normal foot sole as observed in the contralateral hind limb of sham-treated rats (Fig 5A). Although the densities of epidermal and upper dermal P2X3-IR fibers were higher in the center area of the foot sole as compared to the medial and lateral areas, this difference was not significant at any PO time point (Fig. 5 B-G). The density of epidermal P2X3-IR fibers of animals subjected to the SNI procedure was somewhat lower (on average 21.69 %) as compared to the sham-group (Fig. 5 C). This value, however, was not significantly different from sham-treated animals. A similar, non-significant tendency towards a reduction in density of P2X3-IR fibers was also noted for the upper dermis at 2 weeks PO only (Fig. 5 F).

NF-200

As expected, NF-200-IR fibers, representing myelinated fibers, were distributed in the upper dermis but not in the epidermis (Fig. 6 A) [24, 25]. Moreover, the distribution pattern of upper dermal NF-200-IF fibers in the center area was fully comparable be-

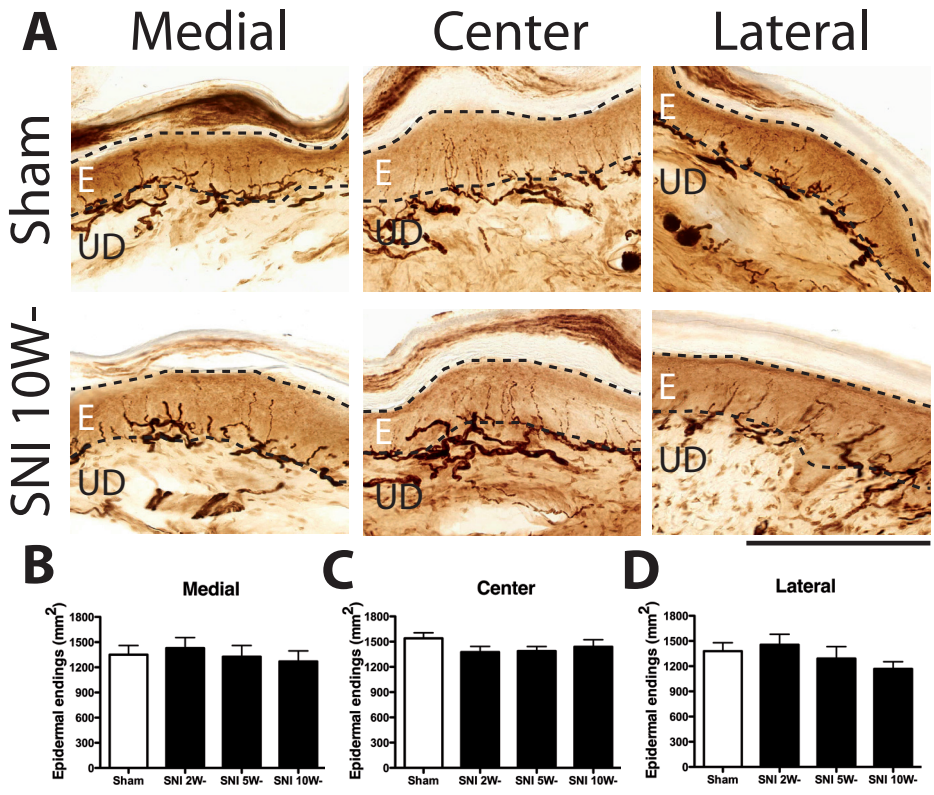

FIGURE 7:

Micrographs showing staining for PGP 9.5-IR fibers in skin biopsies taken from the medial (saphenous), center (tibial) and lateral (sural) part of the foot sole (Fig. 7 A). Fig. 7 B-D displays histograms of the number of PGP 9.5-IR fibers per mm2 in the epidermis (E). Scale bar: 250 µm.

tween the contralateral foot soles of sham- and SNI-treated rats (Fig. 6 A). Therefore, we found no significant changes in the number of NF-200-IR fibers contralateral after SNI at any time point PO as compared to sham treatment (Fig. 6 B-D).

PGP 9.5.
We used PGP 9.5, which is a pan-neuronal marker, to stain all the nerve fibers in the skin (Fig. 7 A). We found no significant changes in the epidermal density of PGP 9.5-IR fibers in the central area of the contralateral foot soles between sham- and SNI-treated rats at any time point PO (Fig. 7 B-D).

INNERVATION OF THE CONTRALATERAL MEDIAL AND LATERAL SKIN AREAS.
The medial and lateral skin areas of the contralateral foot soles after applying ipsilateral the SNI procedure, showed no changes in any of the subgroups of skin nerve fibers that were investigated in the current experiment (See also Fig. 3-7).

DISCUSSION

In the present study, we have investigated the epidermal and upper dermal innervation pattern of CGRP, Subtance P, P2X3, NF-200 and PGP 9.5 nerve fibers in the contralateral foot sole after SNI-induced neuropathic pain in the ipsilateral hind paw. Our main findings were: 1) a significant decrease in mechanical withdrawal thresholds in the contralateral hind paw of SNI-treated rats as compared to the sham-treated rats; 2) the only significant changes in the densities of the investigated fiber groups was found in the upper dermis in the central area of the foot sole for CGRP-IR fibers at 5 and 10 weeks PO, which was significantly higher than in the sham-treated group.

SNI AS A MODEL FOR MIRROR IMAGE PAIN
In the present study, we used the SNI-model for induction of neuropathic pain because of the clear anatomical distinctions between the affected and non-affected skin areas in the foot sole of the SNI-treated hind paw [9]. In addition, the neuropathic pain that develops following the SNI procedure can solely be ascribed to transection of the tibial and common peroneal branches. This enables a straightforward comparison of the homologous areas between sham- and SNI-treated rats.
We found that after SNI procedure, the mechanical withdrawal threshold is significantly decreased in the contralateral naïve hind paw as compared to the contralateral hind paw of sham-treated rats, a finding in line with previous studies [18, 26]. However, some studies have shown no changes in mechanical response thresholds of the contralateral hind paw [6, 12]. A factor that might play a substantial role in the

development of mirror image pain in neuropathic pain models is the use of different strains of rats, since the genetic background of rats has a considerable impact on the severity of neuropathic pain [27, 29]. In addition, the type of neuropathic pain, which is a major determinant of neuropathic pain behavior, may also be of importance in the development of mirror image pain [30]. Taken together, the factors that influence the development of neuropathic pain, may contribute to the development of mirror image pain, and therefore they should be taken into consideration when comparing different neuropathic pain animal models with each other.

THE MECHANICAL WITHDRAWAL THRESHOLD

Presently, we found no changes in the mechanical withdrawal thresholds in the forepaws, suggesting that the changes in the contralateral hind paw are indicative of mirror image pain and are produced by ipsilateral SNI treatment rather than systemic effects. In the ipsilateral hind paw, SNI results in sensitization to mechanical stimuli in the lateral and medial areas of the foot sole only, and corresponds to changes in the innervation patterns of these areas [23]. In contrast, the mechanical sensitization of the contralateral hind paw is enhanced in medial, central and lateral areas of the foot sole, indicating that SNI-induced mirror image pain is not a one-to-one mimic of the behavioral signs of the ipsilateral hind paw. An explanation for this discrepancy might be that on the contralateral central area, in contrast to the ipsilateral paw, is still innervated by the tibial nerve, which may participate in the development of neuropathic pain on that side.

EPIDERMAL AND UPPER DERMAL NERVE FIBERS

The density of CGRP-IR fibers was significantly increased in the center area of the upper dermis in the contralateral naïve foot sole of SNI-treated rats, whereas no changes were found in the density of Substance P-, P2X3-, NF-200- or PGP-9.5-IR fibers. Interestingly, in earlier studies we have shown that in the hypersensitive ipsilateral SNI-treated foot sole the density of CGRP-IR fibers [23] also was increased without any changes in the density of substance P-, NF-200- and P2X3-IR fibers [31]. However, here the increase in the density of CGRP-IR fibers was specifically found in the medial and lateral areas of the foot sole, areas that are innervated by uninjured nerve fibers. These findings suggest that one-sided nerve lesion leads to changes in the peripheral innervation patterns of CGRP-IR fibers on both the ipsilateral and the contralateral side, which correlate well with the behavioral signs of neuropathic pain. Whether peripheral and/or central mechanisms are responsible for the changes in the CGRP-IR fiber density on the contralateral side remains to be investigated.

Sprouting of contralateral peripheral nerve fibers following ipsilateral nerve injury has been found for motor, sensory and sympathetic fibers. E.g. ipsilateral section of an efferent motor nerve resulting in degeneration of ipsilateral neuromuscular junctions

has been shown to cause sprouting of nerve endings at neuromuscular junctions of the same muscle on the contralateral side [32, 33]. In addition, there was also an increase in neurotransmitter release at these neuromuscular junctions [34]. Further, sprouting of sympathetic fibers, which innervate dorsal-root ganglion (DRG) blood vessels, has been shown to occur bilaterally after unilateral peripheral nerve injury [35, 36]. Finally, contralateral sprouting of sensory nerve fibers has been described after infra-orbital and inferior alveolar nerve injuries in ferrets and rats [37, 38].

In order to determine whether the increase in the number of CGRP-IR fibers reflects growth of new CGRP-IR fibers or implies an up-regulation of CGRP expression in nerve fibers, we used the pan neuronal marker protein gene product 9.5 (PGP.9.5), which stains all the nerve fibers in the skin. Oaklander et. al. [12], showed a near-total loss of PGP 9.5-IR epidermal fibers in the ipsilateral foot sole of SNI-treated rats, but also a decrease of 54% in the center territory of the contralateral foot sole at 1 week PO. However, in the present study we only observed a limited and non-significant decrease in the density of PGP-9.5-IR epidermal fibers in the center area of the contralateral foot sole. Possible explanations for this discrepancy could be the use of rats with different genetic backgrounds (Sprague Dawley vs. Wistar), the different sampling and quantification methods (skin punches vs. large skin), and potential variations in sampling areas (footpad vs non-footpad areas). The bundling of upper dermal PGP 9.5-IR fibers made quantification in the present study not possible, however semi-quantitative analysis exhibited no changes in the density of upper dermal fibers in the contralateral foot sole. Based on our findings, we suggest that the increase in the number of CGRP-IR fibers is most likely due to up-regulation of CGRP expression in existing nerve fibers rather than by a gain of new CGRP-IR fibers. Although we do not have a clear explanation for the increase of CGRP-IR fibers in the dermis without a similar increase of terminals endings in the epidermis we note that the epidermis is constructed by a dense network of keratinocytes, which could make it more difficult for the anterograde CGRP to terminate in the epidermal nerve endings. However, this has to be elucidated in future studies.

An increase in the density of peptidergic CGRP-IR fibers in the contralateral foot sole may be induced by nerve growth factor (NGF). It is known that NGF, which is normally expressed at low levels in the epidermis, is involved in the pathogenesis of neuropathic pain and it initiates sprouting of nerve fibers via the tyrosine kinase receptor A (trkA) [39, 40]. After peripheral nerve injury, Schwann cells and non-neuronal cells such as keratinocytes that are located distal to the nerve injury secrete high amounts of NGF [41]. It has been shown that injection of NGF in the foot sole results in up-regulation of CGRP ipsilateral as well as in the contralateral sensory neurons in the dorsal root ganglion (DRG) and sciatic nerve [42, 43]. Furthermore, animals lacking the neurotrophin receptor p75 (low-affinity receptor for NGF), have a reduced sprouting ability of sympathetic fibers on the contralateral side, which is consistent

with the possible involvement of neurotrophic factors in regulating nerve fiber growth [44]. Because peptidergic fibers are highly responsive to NGF and are thought to play a pivotal role in the development of neuropathic pain, we propose that CGRP fibers and/or their change in expression may play a role in the development of mirror image pain on the contralateral site.

CONCLUSION

There are two major categories of explanatory mechanisms for mirror image pain, namely the immune and neural activation theory. The systemic activation mechanism suggests that, following unilateral lesion, factors released by damaged nerve or denervated tissue might induce changes on the contralateral side via the bloodstream [5, 6]. The neuronal activation mechanism suggests that unilateral nerve injury results in contralateral sprouting of the homonymous neuron due to connections via the central nervous system [5, 6].

In the present study, we have shown that after the SNI procedure, the withdrawal threshold in the contralateral naïve hind paw is significantly decreased as compared to control. In addition, the number of CGRP-IR fibers is also increased in the contralateral foot sole. As such, our findings not only shows that nerve injury on one side initiates the development of mirror image pain on the contralateral uninjured site but also supports the neuronal activation theory for the development of mirror image pain. The underlying mechanisms for the development of mirror image pain and its benefits for protecting the body remain however unclear.

REFERENCES

1.
Baron, R., Mechanisms of disease: neuropathic pain--a clinical perspective. Nat Clin Pract Neurol 2006; 2(2): 95-106.

2.
Costigan, M., Scholz, J., and Woolf, C.J., Neuropathic pain: a maladaptive response of the nervous system to damage. Annu Rev Neurosci 2009; 32: 1-32.

3.
Campbell, J.N. and Meyer, R.A., Mechanisms of neuropathic pain. Neuron 2006; 52(1): 77-92.

4.
Campbell, J.N., Nerve lesions and the generation of pain. Muscle Nerve 2001; 24(10): 1261-73.

5.
Huang, D. and Yu, B., The mirror-image pain: an unclered phenomenon and its possible mechanism. Neurosci Biobehav Rev 2010; 34(4): 528-32.

6.
Koltzenburg, M., Wall, P.D., and McMahon, S.B., Does the right side know what the left is doing? Trends Neurosci 1999; 22(3): 122-7.

7.
Konopka, K.H., Harbers, M., Houghton, A., et al., Bilateral sensory abnormalities in patients with unilateral neuropathic pain; a quantitative sensory testing (QST) study. PLoS One 2012; 7(5): e37524.

8.
Bennett, G.J. and Xie, Y.K., A peripheral mononeuropathy in rat that produces disorders of pain sensation like those seen in man. Pain 1988; 33(1): 87-107.

9.
Decosterd, I. and Woolf, C.J., Spared nerve injury: an animal model of persistent peripheral neuropathic pain. Pain 2000; 87(2): 149-58.

10.
Li, D., Yang, H., Meyerson, B.A., and Linderoth, B., Response to spinal cord stimulation in variants of the spared nerve injury pain model. Neurosci Lett 2006; 400(1-2): 115-20.

11.
Kim, S.H. and Chung, J.M., An experimental model for peripheral neuropathy produced by segmental spinal nerve ligation in the rat. Pain 1992; 50(3): 355-63.

12.
Oaklander, A.L. and Brown, J.M., Unilateral nerve injury produces bilateral loss of distal innervation. Ann Neurol 2004; 55(5): 639-44.

13.
Oaklander, A.L., Romans, K., Horasek, S., et al., Unilateral postherpetic neuralgia is associated with bilateral sensory neuron damage. Ann Neurol 1998; 44(5): 789-95.

14.
Facer, P., Casula, M.A., Smith, G.D., et al., Differential expression of the capsaicin receptor TRPV1 and related novel receptors TRPV3, TRPV4 and TRPM8 in normal human tissues and changes in traumatic and diabetic neuropathy. BMC Neurol 2007; 7: 11.

15.
Ruijs, A.C., Jaquet, J.B., van Riel, W.G., Daanen, H.A., and Hovius, S.E., Cold intolerance following median and ulnar nerve injuries: prognosis and predictors. J Hand Surg Eur Vol 2007; 32(4): 434-9.

16.
Chacur, M., Milligan, E.D., Gazda, L.S., et al., A new model of sciatic inflammatory neuritis (SIN): induction of unilateral and bilateral mechanical allodynia following acute unilateral peri-sciatic immune activation in rats. Pain 2001; 94(3): 231-44.

17.
Schreiber, K.L., Beitz, A.J., and Wilcox, G.L., Activation of spinal microglia in a murine model of peripheral inflammation-induced, long-lasting contralateral allodynia. Neurosci Lett 2008; 440(1): 63-7.

18.
Paulson, P.E., Morrow, T.J., and Casey, K.L., Bilateral behavioral and regional cerebral blood flow changes during painful peripheral mononeuropathy in the rat. Pain 2000; 84(2-3): 233-45.

19.
Ruigrok, T.J. and Apps, R., A light microscope-based double retrograde tracer strategy to chart central neuronal connections. Nat Protoc 2007; 2(8): 1869-78.

20.
Voorn, P. and Buijs, R.M., An immuno-electronmicroscopical study comparing vasopressin, oxytocin, substance P and enkephalin containing nerve terminals in the nucleus of the solitary tract of the rat. Brain Res 1983; 270(1): 169-73.

21.
Hopman, A.H., Ramaekers, F.C., and Speel, E.J., Rapid synthesis of biotin-, digoxigenin-, trinitrophenyl-, and fluorochrome-labeled tyramides and their application for In situ hybridization using CARD amplification. J Histochem Cytochem 1998; 46(6): 771-7.

22.
Kuhlmann, W.D. and Peschke, P., Glucose oxidase as label in histological immunoassays with enzyme-amplification in a two-step technique: coimmobilized horseradish peroxidase as secondary system enzyme for chromogen oxidation. Histochemistry 1986; 85(1): 13-7.

23.
Duraku, L., Hossaini, M., Hoendervangers, S., et al., Spatiotemporal dynamics of re-innervation and hyperinnervation patterns by uninjured CGRP fibers in the rat foot sole epidermis after nerve injury. Molecular Pain 2012; 8(1): 61.

24.
Peleshok, J.C. and Ribeiro-da-Silva, A., Delayed reinnervation by nonpeptidergic nociceptive afferents of the glabrous skin of the rat hindpaw in a neuropathic pain model. J Comp Neurol 2011; 519(1): 49-63.

25.
Lauria, G., Borgna, M., Morbin, M., et al., Tubule and neurofilament immunoreactivity in human hairy skin: markers for intraepidermal nerve fibers. Muscle Nerve 2004; 30(3): 310-6.

26.
Erichsen, H.K. and Blackburn-Munro, G., Pharmacological characterisation of the spared nerve injury model of neuropathic pain. Pain 2002; 98(1-2): 151-61.

27.
Rode, F., Thomsen, M., Brolos, T., et al., The importance of genetic background on pain behaviours and pharmacological sensitivity in the rat spared serve injury model of peripheral neuropathic pain. Eur J Pharmacol 2007; 564(1-3): 103-11.

28.
Ziv-Sefer, S., Raber, P., Barbash, S., and Devor, M., Unity vs. diversity of neuropathic pain mechanisms: Allodynia and hyperalgesia in rats selected for heritable predisposition to spontaneous pain. Pain 2009; 146(1-2): 148-57.

29.
Mogil, J.S., Animal models of pain: progress and challenges. Nat Rev Neurosci 2009; 10(4): 283-94.

30.
Wang, L.X. and Wang, Z.J., Animal and cellular models of chronic pain. Adv Drug Deliv Rev 2003; 55(8): 949-65.

31.
Duraku, H., Schüttenhelm, Holstege, Baas, Ruigrok, Walbeehm, Re-innervation patterns by peptidergic Substance-P, non-peptidergic P2X3, and myelinated NF-200 nerve fibers in epidermis and dermis of rats with neuropathic pain. Experimental Neurology (Accepted for publication 30 november 2012, YEXNR11327) 2013.

32.
Rotshenker, S. and Tal, M., The transneuronal induction of sprouting and synapse formation in intact mouse muscles. J Physiol 1985; 360: 387-96.

33.
Ring, G., Reichert, F., and Rotshenker, S., Sprouting in intact sartorius muscles of the frog following contralateral axotomy. Brain Res 1983; 260(2): 313-6.

34.
Herrera, A.A. and Grinnell, A.D., Contralateral denervation causes enhanced transmitter release from frog motor nerve terminals. Nature 1981; 291(5815): 495-7.

35.
McLachlan, E.M., Janig, W., Devor, M., and Michaelis, M., Peripheral nerve injury triggers noradrenergic sprouting within dorsal root ganglia. Nature 1993; 363(6429): 543-6.

36.
Chung, K., Kim, H.J., Na, H.S., Park, M.J., and Chung, J.M., Abnormalities of sympathetic innervation in the area of an injured peripheral nerve in a rat model of neuropathic pain. Neurosci Lett 1993; 162(1-2): 85-8.

37.
Chiaia, N.L., Allen, Z., Carlson, E., MacDonald, G., and Rhoades, R.W., Neonatal infraorbital nerve transection in rat results in peripheral trigeminal sprouting. J Comp Neurol 1988; 274(1): 101-14.

38.
Doubleday, B. and Robinson, P.P., The role of nerve growth factor in collateral reinnervation by cutaneous C-fibres in the rat. Brain Res 1992; 593(2): 179-84.

39.
Grelik, C., Bennett, G.J., and Ribeiro-da-Silva, A., Autonomic fibre sprouting and changes in nociceptive sensory innervation in the rat lower lip skin following chronic constriction injury. Eur J Neurosci 2005; 21(9): 2475-87.

40.
Peleshok, J.C. and Ribeiro-da-Silva, A., Neurotrophic factor changes in the rat thick skin following chronic constriction injury of the sciatic nerve. Mol Pain 2012; 8: 1.

41.
Anand, P., Neurotrophic factors and their receptors in human sensory neuropathies. Prog Brain Res 2004; 146: 477-92.

42.
Amann, R., Sirinathsinghji, D.J., Donnerer, J., Liebmann, I., and Schuligoi, R., Stimulation by nerve growth factor of neuropeptide synthesis in the adult rat in vivo: bilateral response to unilateral intraplantar injections. Neurosci Lett 1996; 203(3): 171-4.

43.
Donnerer, J., Amann, R., Schuligoi, R., and Skofitsch, G., Complete recovery by nerve growth factor of neuropeptide content and function in capsaicin-impaired sensory neurons. Brain Res 1996; 741(1-2): 103-8.

44.
Ramer, M. and Bisby, M., Reduced sympathetic sprouting occurs in dorsal root ganglia after axotomy in mice lacking low-affinity neurotrophin receptor. Neurosci Lett 1997; 228(1): 9-12.

7

RE-INNERVATION OF SUBGROUPS OF SPECIFIC SENSORY NERVE FIBRES OF THE SKIN FOLLOWING NERVE AUTOGRAFT RECONSTRUCTION IN A RAT MODEL

L. S. Duraku [1,2*]
T. H.J. Nijhuis [1*]
C. A. Hundepool [1]
J. W. van Neck [1]
T. J.H. Ruigrok [2]
S. E.R. Hovius [1]
E. T. Walbeehm [1]

*Both authors contributed equally

1. Department of Plastic, Reconstructive and Hand Surgery, Erasmus MC, University Medical Center, Rotterdam, The Netherlands

2. Dept. of Neuroscience, Erasmus MC, University Medical Center, Rotterdam, The Netherlands

ABSTRACT

For large peripheral nerve injuries the nerve autograft is still considered the best strategy for reconstruction. Visualization of the skin epidermal sensory nerve fibres is useful to show the regeneration in the most distal terminals of the injured nerve. Both peptidergic and non-peptidergic fibres are responsible for signalling noxious stimuli and termed nociceptors. The Aδ-fibres are responsible for fast pain signalling. This study investigates the re-innervation of these different types of cutaneous fibres in the rat foot sole, 12 weeks after reconstructing a nerve defect with an autograft. In 5 animals, a 15 mm sciatic nerve defect was reconstructed using an autograft. Five healthy animals served as control. Von Frey hairs were used to assess the mechanical threshold and sensibility after reconstruction. Twelve weeks after grafting, the sole of the foot of the operated hind paw was excised and incubated for CGRP, Substance P (both peptidergic fibres), P2X3 (non-peptidergic fibres) and NF200 (Aδ-fibres). Control staining involved incubation with PGP 9.5 (a pan-neuronal marker). Twelve weeks after reconstruction of the nerve defect, the withdrawal response of the operated paw was significantly delayed as compared to the healthy control response. PGP 9.5 staining demonstrated a 70% re-innervation of the skin sensory nerve fibres. Compared to control, the peptidergic fibres re-innervated the skin for 70%, whereas only up to 35% of the non-peptidergic fibres were regenerated. Myelinated fibres (Aδ-fibres) showed 80% re-innervation. The present findings are helpful in understanding neural regeneration after grafting a nerve defect with the autologous nerve graft. Especially the particular findings that illustrate a stronger regeneration of the peptidergic fibres compared to the non-peptidergic fibres 12 weeks post operative and that the overall regeneration percentage is approximately 70% as compared to the healthy control.

INTRODUCTION

Full recovery from peripheral nerve injuries still is a frequent problem. In lengthy nerve gaps therapeutic repair strategies preclude direct end-to-end coaptation of the nerve ends, since traction on coaptation can result in ischemia and fibrosis, and therefore negatively influences nerve regeneration. Clinically, the gold standard for reconstructing nerve defects is the use of a nerve autograft [1-4]. Considering the significant risk of donor site morbidity, the need for multiple nerve grafts and complications after reconstruction, such as neuroma formation and/or loss of sensibility, the urge for autograft replacement is still present [5, 6]. However to do so, it is of importance to understand the regeneration process distally from the nerve autograft, especially in the terminal endings of the regenerated nerve, where external stimuli are transduced into sensory information.

Previous studies investigating the regeneration across large peripheral nerve defects, when bridging the gap with other grafts than an autograft, incorporate extensive functional and histological evaluation of the nerve itself [7-9]. To the best of our knowledge there are no reports that examine the re-innervation of the terminal sensory fibres of a nerve (i.e. the nerve fibres in a rat foot sole) that was reconstructed by a nerve autograft.

Sensory fibres innervating the skin can be subdivided into two major groups; the unmyelinated C fibres and myelinated A-delta fibres (Aδ-fibres). The unmyelinated C fibres can be further subdivided in peptidergic and non-peptidergic fibres. The peptidergic fibres contain the neuropeptides calcitonin gene-related peptide (CGRP) and substance P. The non-peptidergic fibres express P2X purinoceptor [3] (P2X3). The Aδ-fibres are solely peptidergic and more specifically purely CGRP positive and can be visualized with a Neurofilament 200 (NF200) antibody.

Peptidergic fibres are responsive to the neurotrophic factor Nerve Growth Factor (NGF), and non-peptidergic fibres to Glial cell line-Derived Nerve Factor (GDNF). These neurotrophins are secreted in substantial quantities after peripheral nerve injury and ultimately assist the regeneration of the peptidergic and non-peptidergic fibres [10, 11].

The goal of the present study is to investigate the re-innervation pattern of epidermal nerve fibres in the rat foot sole, 12 weeks after reconstructing a 15mm nerve defect with an autograft. These data are correlated with the behavioural responses to mechanical stimuli.

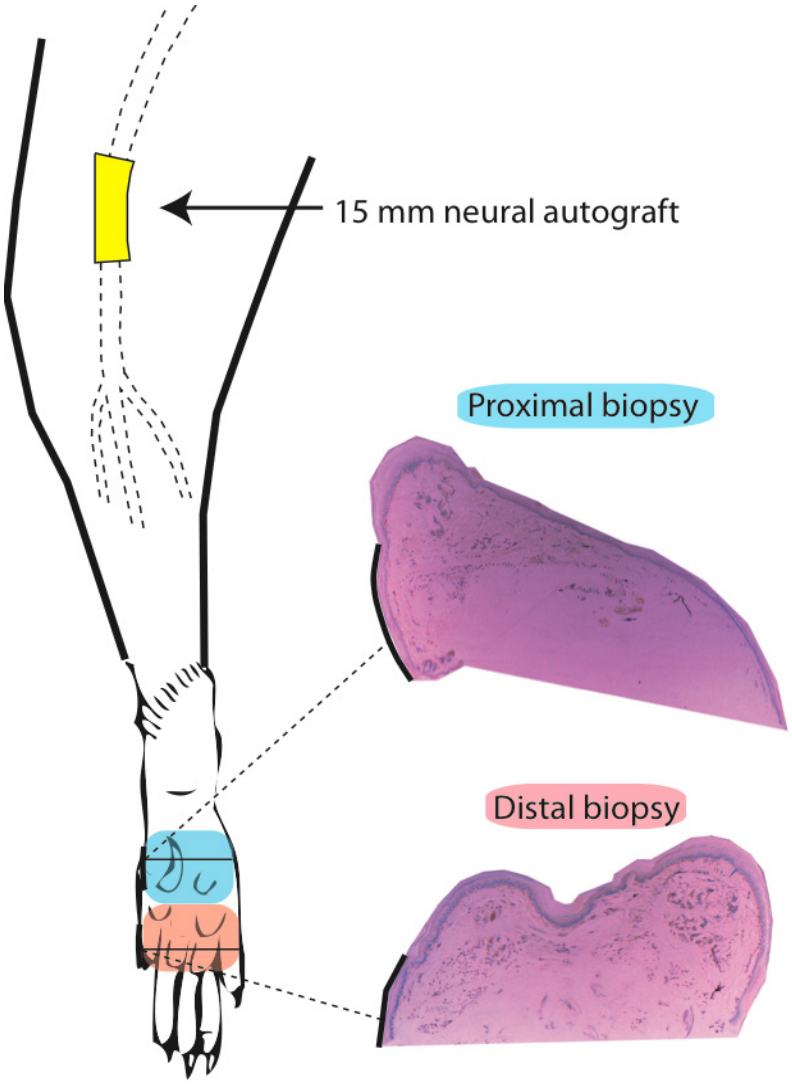

FIGURE 1:

Detailed image illustration of our model. Depicted are the 15 mm nerve autograft reconstruction and the biopsies taken at 12 weeks for both proximal and distal segments in the rat foot sole.

METHODS

ANIMALS

Ten isogenic adult female Lewis rats, weighing 180 – 200 grams, were used. Animals were pair-housed in hooded cages at room temperature on a 12-hour light/dark schedule, and were given food and water ad libitum. Surgical procedures and electrophysiological evaluations were performed under general anaesthesia (Isoflurane, 1-2% in a mixture of O2/N20).

SURGICAL TECHNIQUE

In five animals a 15mm sciatic nerve defect was reconstructed using an autograft by the same surgeon using standard aseptic microsurgical techniques under the operating microscope (Zeiss OP-MI 6-SD; Carl Zeiss, Goettingen, Germany). The autograft was retrieved from an isogenic donor animal and connected to the nerve stumps using 6 10/0 Ethilon sutures (Ethicon, Johnson & Johnson, Amersfoort, the Netherlands) at each coaptation site. Five healthy animals served as a control and didn't receive any treatment.

EVALUATION OF MECHANICAL HYPERSENSITIVITY

Twelve weeks postoperatively (PO), the mechanical threshold of the hind paws was measured using Von Frey hairs, ranging from 0.6 g to 300 g in a set of 14 filament steps. In the current experiment we used down-up testing by starting with low force and then increasing. For this part of the experiment, rats were placed in a plastic box with a mesh floor, in which they were able to move freely. Each Von Frey hair was applied for 2 s at 5 s intervals, and the response threshold was set at 3, indicating the numbers of evoked responses in 5 applications. Responses were the number of flinches and flutters of the affected hind paw that the rats express. The medial and lateral side where stimulated at the transition point from glabrous to hairy skin. The center foot sole was stimulated at the plantar lateral mid-point of the foot sole.

IMMUNOHISTOCHEMISTRY

Regarding the tissue preparation and immunohistochemical staining, the protocols were similar to our earlier published study [12, 13].

ANALYSIS

The foot sole of a rat can be divided into footpads (i.e. touch cushions) and intermediate thin skin. For quantification of the skin nerve fibres we used the intermediate thin area. A total of 16 series of sections of the complete foot sole were used for analysis. The sections were put in serial order from proximal to distal by using

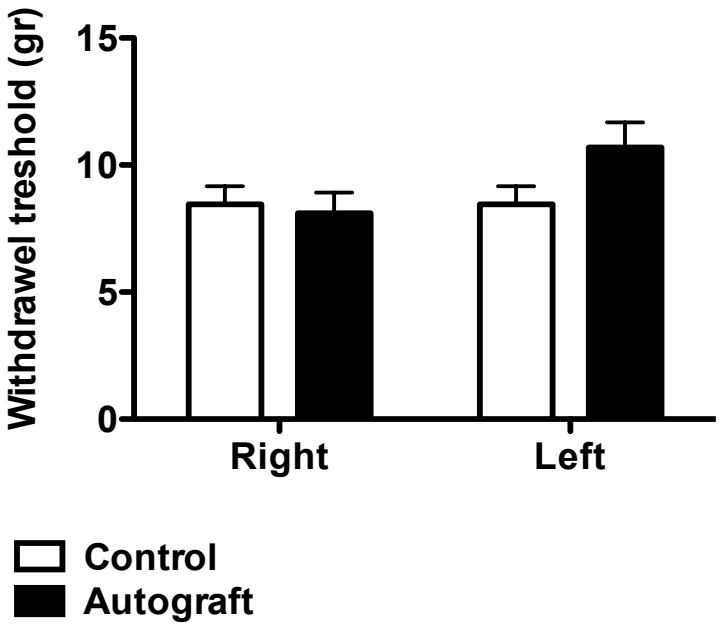

FIGURE 2:

This figure illustrates the results from the Von Frey Test. Depicted is the mean force (in grams) for the different groups to establish a withdrawal reaction.

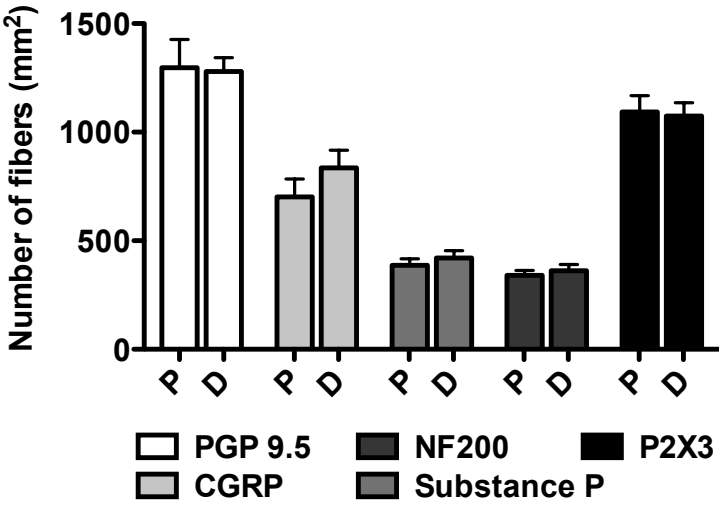

FIGURE 3:

Illustration of the normal distribution of the different sensory nerve fibres in the rat foot sole for the proximal and distal segment. SEM is visualised with the error bars.

the anatomy of the simultaneously embedded brain as an anatomical marker. This resulted in the selection of 8 proximal and 8 distal sections. Each selection was divided in a lateral and central sector. The sectors within the sections were analysed systematically to visualize the location of the labelled fibres in the dermis and the number of (apparently) terminal fibres within the epidermis using an Olympus BH microscope equipped with a Lucivid miniature monitor and Neurolucida™ software (MicroBrightField, Inc., Colchester, VT). The fibres were quantified using a 20 x 10 objective. The fibres in two sectors (i.e. the upper dermis and epidermis) of the central and lateral side of the foot sole were counted for analysis in all 16 sections. From these counts the average number of nerve fibres per mm2 was calculated for each rat. Per group, the results were averaged and compared with the average results in the control group. Errors in the variations were assessed as the standard error of the mean (SEM). An unpaired t-test was performed for all evaluations. An illustration of our study model is depicted in Figure 1.

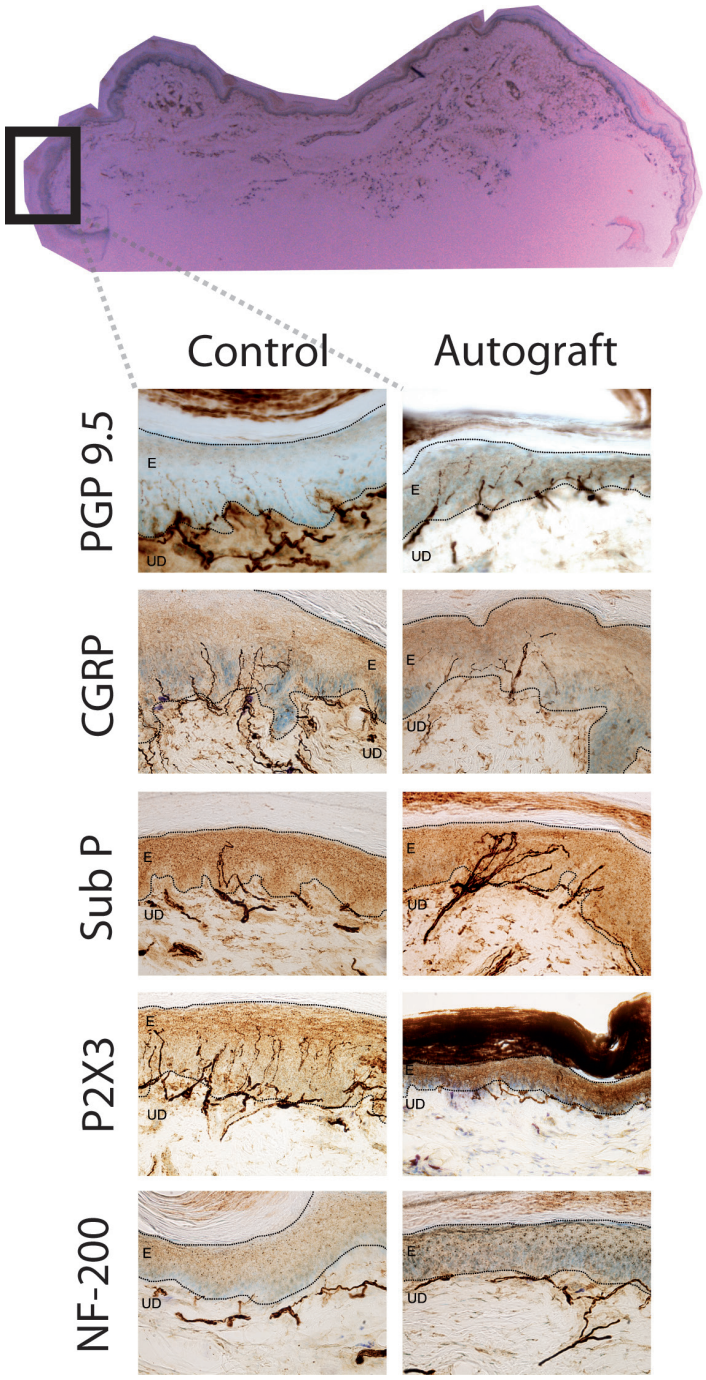

FIGURE 4:

An overview of the micrographs of the different markers used. Pictures are taken with a 20x10 objective.

RESULTS

EVALUATION OF MECHANICAL HYPERSENSITIVITY

The mechanical withdrawal of the operated paw was determined with von Frey hairs. The operated leg showed a significant increase at 12 weeks in the withdrawal threshold, compared to the healthy control ($p = 0.019$). The mean threshold for the animals treated with the autograft was 10.7 gram (SEM ± 3.38) versus 8.5 gram (SEM ± 2.68) for healthy animals (Figure 2). These results suggest that the autograft has less sensory efferent innervation to convert mechanical pressure into withdrawal reflex.

IMMUNOHISTOCHEMISTRY

Normal innervation of the sensory nerve skin fibres is plotted in Figure 3. Figure 4 depicts an example of our staining in the two groups for the markers used. Figure 5 illustrates the regrowth of fibres in all three layers (i.e. the upper dermis, dermal-epidermal junction and epidermis). A regeneration percentage was only given for the epidermal area, since this area is considered to be the most important for sensory transmission. As myelinated fibres loose their myelin sheath in the epidermis, we used the data of the crossing layer to determine the regeneration percentage (Table 1). Table 2 shows the average number of fibres per mm2 for the five markers in the two groups. Figure 6 and 7 illustrates the main findings of this study in a comprehensive matter.

PGP 9.5

Epidermis

Based on the data (see Table 2) the percentage of fibres regenerating in the lateral side of the foot sole for the proximal and distal segment was slightly below 70%. For the central sector a percentage of 77% and 61% was found for the proximal and distal areas. A statistical trend was found comparing the autograft to the healthy controls ($p < 0.09$). This indicates that the autograft still had less fibres compared to the healthy control for the epidermal part of the skin. In addition, the PGP 9.5-IR fibres in the autograft group appeared thinner and penetrated less deep into the epidermis as compared to the control group (Fig. 4).

Upper dermis

The first of the three most outer layers of the skin had, 12 weeks after the nerve autograft reconstruction, no significant difference for both the lateral and central regions between the two groups were noted ($p > 0.129$). Nevertheless, the distal segment of the central area was significantly lower from the proximal segment ($p < 0.001$).

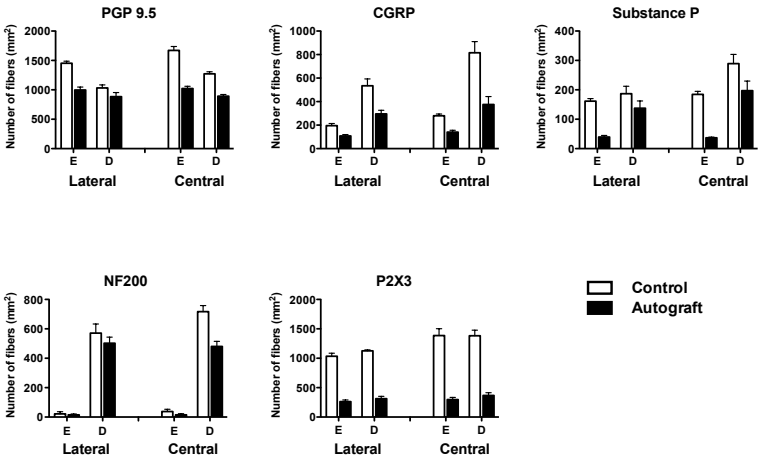

FIGURE 5:

The re-innervation of the distal skin nerve fibres, 12 week post operatively. SEM is visualised with the error bars.

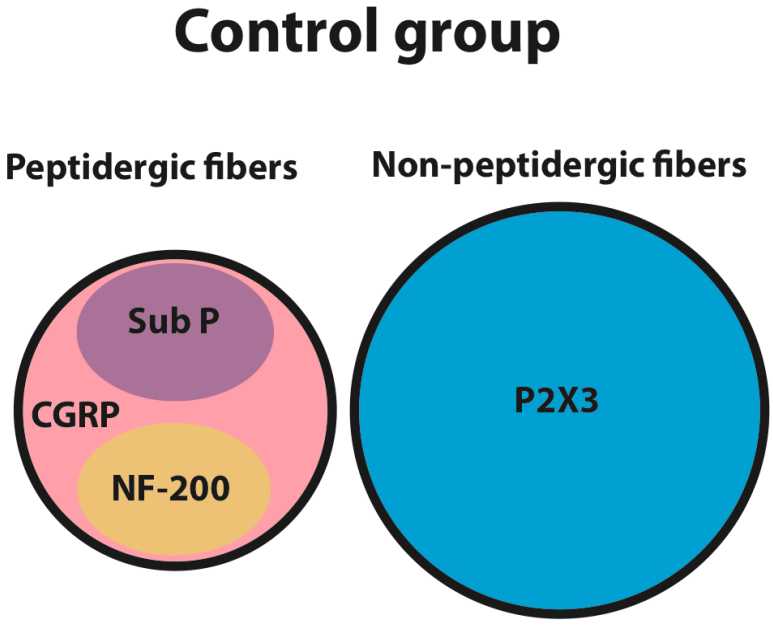

FIGURE 6:

Distribution of the five different subgroups of sensory nerve fibres in the rat foot sole 12 weeks after reconstructing the 15 mm nerve defect using an autograft. Distribution of the five different subgroups of sensory nerve fibres in the healthy rat foot sole.

CGRP

Epidermis

The density of epidermal fibres containing CGRP was notably lower in the lateral region of the foot as compared to the central regions as noted both in the proximal and distal parts of the foot sole (Fig. 5). The percentage of recovery was proximally 72% and 56% for the two sections, distally a recovery of 64% and 59% for the lateral and central sections was encountered. All segments were significantly different from the healthy controls ($p<0.006$).

Upper dermis

The upper dermis, as the most proximal of the three outer layers, showed still significantly fewer fibres in all areas of the proximal and distal sections compared to the control group ($p < 0.045$).

SUBSTANCE P

Epidermis

The most distal layer of the skin -after the auto graft reconstruction- had regarding the re-innervations of the subtype of peptidergic fibres a regenerative percentage of 68% and 45% proximal. Distally percentages of 56% and 74% were found. Without statistical significance, it should be mentioned that the results indicated that the autograft did not suffice enough re-innervation to equal the healthy nerve regarding the Substance P labelled fibres.

Upper dermis

For the upper dermis the lateral area was comparable in both groups for both segments. The central area in the autograft group was not comparable to the control group for both segments ($p < 0.018$).

NF-200

Epidermis

For the epidermis, all comparisons between the autograft reconstruction and the healthy control were not significantly different ($p > 0.231$), except for the central part of the proximal footpad where the density of NF200-positive fibres was significantly lower in the autograft group as compared to the control group ($p = 0.036$).

Upper dermis

In the upper dermis, the central area showed significant less fibres in the autograft group in both the proximal and distal segment ($p<0. 009$). In contrast, all other segments were not significantly different.

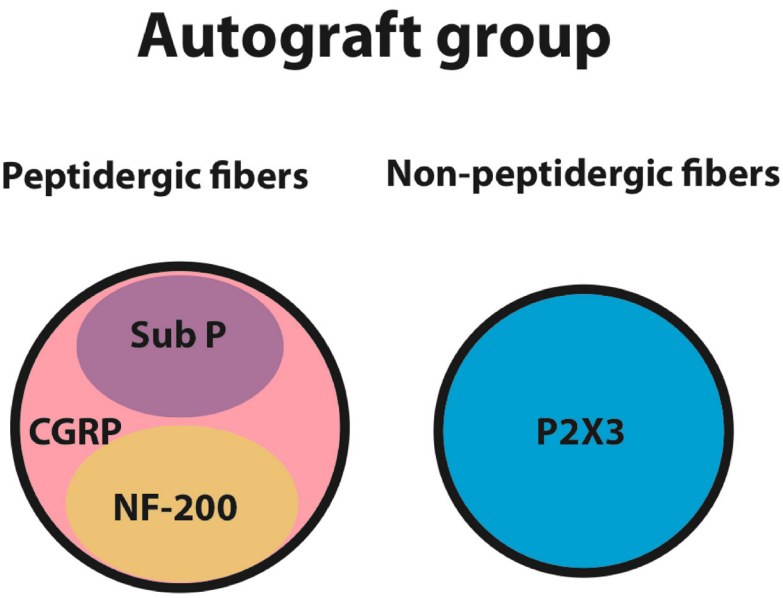

FIGURE 7:

Distribution of the five different subgroups of sensory nerve fibres in the rat foot sole 12 weeks after reconstructing the 15 mm nerve defect using an autograft. Distribution of the five different subgroups of sensory nerve fibres in the healthy rat foot sole.

	Proximal (%)		Distal (%)	
	Lateral	Central	Lateral	Central
Pgp 9.5	68	77	69	61
CGRP	72	56	64	59
Subst P	68	45	56	74
NF200	69	47	58	55
P2X3	36	32	25	22

TABLE 1:

Regeneration percentage of the sensory nerve fibre subgroups, as reflected by their AB staining pattern, 12 weeks post operative and compared to the respective control. PgP 9.5 is a pan neuronal marker. The calcitonin gene-related peptide (CGRP) marker stains the peptidergic fibres. Substance P (Sub P) also stains the peptidergic fibres. Neurofilament 200 (NF200) stains the Aδ-fibres. The P2X purinoceptor 3 (P2X3) staining visualizes all non-peptidergic fibres.

P2X3

Epidermis

For the non-peptidergic fibres the regeneration percentage for the proximal segment was 36% and 32%, distal percentages of 25% and 22% were found. All areas of both sections showed significant difference compared to the healthy control ($p<0.0001$).

Upper dermis

For the most proximal layer of the three investigated layers, all areas in all segments had significantly fewer fibres in the autograft group compared to the healthy control group ($p<0.020$).

DISCUSSION

This study examined the re-innervation of sensory nerve fibres of the glabrous skin in a rat hind paw at 12 weeks postoperatively (PO), after reconstructing a 15 mm gap using a neural autograft.

Oaklander et. al. showed that a transection of the tibial nerve (responsible for the innervation of the centre area of the foot sole) resulted in poor collateral re-innervation form the saphenous nerve (15%) at 5 months [14]. Therefore, we assume that the re-innervated fibres in the centre and lateral area of the foot sole originate from the reconstructed sciatic nerve. In addition, it was not possible to ligate the saphenous nerve, because this leads to severe auto-mutilation as seen in our lab and also described by others [12, 15, 16].

PGP 9.5

At 12 weeks post-operatively approximately 70% of all epidermal fibres re-innervated the foot sole, as demonstrated with the pan neuronal marker PGP 9.5.

Previous studies have shown that after a crush injury to the sciatic nerve, there is an almost complete re-innervation of PGP 9.5-IR fibres in the epidermis at 12 weeks [17-19]. The rate of nerve regeneration in rats is estimated at 2-3 mm / day.[20] Hence, most studies investigating nerve regeneration in a rodent model use 12 weeks as a legitimate cut-off point for evaluation. An explanation for the different re-innervation density and rate might have multiple reasons 1) In a crush lesion, the axons can follow their original basal lamina, usually with a 100% return of function, while graft reconstructions have a mismatching autograft to the original nerve and a mismatch due to the approximation of two nerve anastomoses 2) Crushed nerves hardly have a delay in regeneration following the injury, and regenerating axons in a transection usually have a delay of 1-2 weeks before regeneration starts 3) By the time the regenerating axons have reached the second, distal anastomosis, scar tissue might

PROXIMAL		Control		Autograft	
		Lateral *(SEM)*	Central *(SEM)*	Lateral *(SEM)*	Central *(SEM)*
PGP9.5	Epi	1516 *(191.5)*	1279 *(175.1)*	1025 *(32.6)*	1307 *(115.2)*
	EpiDerm	1197 *(112.2)*	1461 *(168.0)*	907 *(28.1)*	1107 *(64.9)*
	Derm	1088 *(115.3)*	1279 *(137.9)*	883 *(38.6)*	1056 *(67.8)*
CGRP	Epi	159 *(12.5)*	237 *(26.2)*	98 *(5.2)*	112 *(9.0)*
	EpiDerm	667 *(46.1)*	913 *(139.4)*	440 *(34.4)*	569 *(52.0)*
	Derm	497 *(57.5)*	606 *(119.6)*	304 *(39.3)*	301 *(45.7)*
Sub P	Epi	132 *(12.5)*	185 *(13.2)*	39 *(4.7)*	37 *(2.4)*
	EpiDerm	315 *(33.6)*	516 *(39.5)*	208 *(9.0)*	299 *(30.0)*
	Derm	138 *(17.0)*	310 *(29.3)*	87 *(24.7)*	179 *(32.8)*
NF200	Epi	13 *(9.4)*	46 *(11.9)*	5 *(2.4)*	10 *(8.0)*
	EpiDerm	272 *(24.1)*	433 *(36.1)*	187 *(50.4)*	205 *(41.8)*
	Derm	528 *(34.4)*	677 *(34.9)*	452 *(85.7)*	497 *(40.5)*
P2X3	Epi	1036 *(43.0)*	1402 *(112.8)*	369 *(40.3)*	447 *(38.0)*
	EpiDerm	981 *(44.6)*	1322 *(109.6)*	375 *(39.2)*	419 *(43.9)*
	Derm	1083 *(34.6)*	1425 *(86.2)*	388 *(41.7)*	457 *(38.7)*

TABLE 2A:

The mean number of fibres (±SEM) for the five different markers in the lateral and central sections of the proximal part of the rat footsole in both the control and operated groups.

have started to form, inhibiting outgrowth of axons across the second anastomosis, 4) Previous studies used Sprague Dawley male rats, however the present study uses Lewis female rats. Testosterone is known to accelerate nerve regeneration and therefore may explain the better regeneration rate in the previous reports that used male rats instead of female rats [21].

Stankovic et. al [17] employed a direct end-to-end suture after transection and showed a re-innervation density of only 30% at 12 weeks of PGP9.5-IR epidermal fibres, which conflicts with the current study. However, Stankovic et al. used the glabrous skin of a digit for evaluation, which is more distal for the regenerating nerve fibres than the foot sole and, therefore, could explain the lower re-innervation percentage. In our study we found that the regenerated PGP 9.5 fibres were thinner and penetrated less deep into the epidermis as compared to the control group.

PEPTIDERGIC FIBRES: CGRP AND SUBSTANCE P

CGRP and Substance P are peptidergic neuropeptides, which play a role in sensation as transducers of pain in unmyelinated C nerve and thinly myelinated Aδ fibres (only CGRP). CGRP and Substance P have also been implicated in other functions, but a discussion on these falls outside the scope of this paper and we refer to Brain and Cox for a detailed overview [22]. The regenerative process of CGRP and Substance P peptidergic fibres is mediated by the neurotrophic factor Nerve Growth Factor (NGF), which is secreted during peripheral nerve injury by Schwann cells, keratinocytes and other non-neuronal cells. NGF acts as a guidance cue for embryonic mammalian dorsal root ganglions and in the adult as a target-derived maintenance factor.

In the current study an average regeneration percentage of 70% was found for CGRP and for Substance P of approximately 60%. Although Substance P is always co-localized with CGRP, the reverse is not the case. Nevertheless, a significant difference in regeneration rate was unexpected [23].

Local axon synthesis of CGRP is critical for the Schwann cell proliferation during regeneration in adult peripheral nerve regrowth [24, 25]. Previous reports showed that CGRP expression increased substantially in regenerative growth cones after nerve injury [24-26]. This might be an explanation for the faster re-innervation rate of CGRP fibres as compared to Substance P.

NF-200

To evaluate the regeneration percentage of the NF-200 myelinated fibres (i.e. Aδ/Aβ fibres) the number of fibres in the upper dermis was quantified, since these fibres lose their myelin sheet in the dermal-epidermal crossing [27]. The low number of epidermal NF-200 counts in the present study confirm this. It should be stressed that the NF-200 marker does not discriminate between Aδ and Aβ fibres. However,

DISTAL		Control		Autograft	
		Lateral *(SEM)*	Central *(SEM)*	Lateral *(SEM)*	Central *(SEM)*
PGP9.5	Epi	1453 *(35.8)*	1670 *(67.8)*	998 *(48.6)*	1023 *(37.3)*
	EpiDerm	1208 *(46.1)*	1427 *(65.9)*	889 *(34.5)*	933 *(38.4)*
	Derm	1033 *(52.3)*	1273 *(33.6)*	884 *(70.3)*	892 *(29.0)*
CGRP	Epi	195 *(17.9)*	280 *(15.0)*	108 *(11.7)*	141 *(15.3)*
	EpiDerm	738 *(69.7)*	1026 *(125.2)*	468 *(42.6)*	679 *(94.1)*
	Derm	534 *(58.5)*	815 *(95.2)*	295 *(31.5)*	375 *(67.8)*
Sub P	Epi	162 *(8.4)*	185 *(10.0)*	39 *(5.5)*	59 *(4.5)*
	EpiDerm	348 *(28.4)*	490 *(34.5)*	262 *(27.0)*	347 *(20.8)*
	Derm	187 *(25.4)*	289 *(31.4)*	138 *(24.7)*	140 *(21.5)*
NF200	Epi	22 *(14.6)*	38 *(15.4)*	15 *(6.0)*	15 *(8.0)*
	EpiDerm	337 *(33.2)*	395 *(14.9)*	194 *(29.1)*	216 *(24.1)*
	Derm	571 *(62.4)*	717 *(41.7)*	503 *(41.4)*	480 *(35.1)*
P2X3	Epi	1034 *(50.8)*	1387 *(116.1)*	262 *(29.1)*	298 *(36.5)*
	EpiDerm	984 *(11.0)*	1297 *(110.8)*	280 *(43.3)*	318 *(31.1)*
	Derm	1126 *(16.0)*	1383 *(94.4)*	313 *(40.3)*	368 *(45.5)*

TABLE 2B:

The mean number of fibres (±SEM) for the five different markers in the lateral and central section of the distal part of the rat foot sole in both the control and operated groups.

because Aβ fibres terminate in the end-organs in the lower dermis and only the Aδ fibres are known to run as free nerve endings in the upper dermis [28], we presume that quantifying the amount of these fibres correlates well with the amount of Aδ fibres.
The NF-200-IR density of fibres reached approximately 75% of the normal value, which was similar to the 70% regeneration noted with the pan-neuronal marker and the 70% noted for CGRP containing fibres. The successful regeneration rate of the myelinated fibres is consistent with the notion that a nociceptive stimulus is the first sense that recovers during the regeneration process. Aδ fibres are essential for transducing acute pain, and therefore are essential to recover as soon as possible to protect the tissue against possible harm. Especially high levels are to be expected after re-innervation of the target organs since myelinisation of the nerve will than start.

P2X3

Few studies have considered the re-innervation pattern of non-peptidergic fibres [29], whereas these fibres account for more than 60% of the unmyelinated C-fibres innervating the skin. In the present study we found a re-innervation pattern of only 35% of skin P2X3-IR fibres in the autograft group 12 weeks after surgery. Clearly, the re-innervation process of the non-peptidergic fibres has not progressed as far as that of the peptidergic fibres.
One theory is that the non-peptidergic fibres are not responsive to NGF, but are responsive to the glial cell-line-derived neurotrophic factor (GDNF). GDNF has been shown to be a trophic factor for sensory and motor neurons, which promotes axonal outgrowth, neuronal survival and re-myelination. Matthew et. al.[30] found that delivery of GDNF via the affinity-based delivery system, promoted regeneration. However, another study reported no improved regeneration after administrating GDNF by osmotic pump into the silicone tube in a 5 mm nerve gap. [31] The poor re-innervation of non-peptidergic fibres might imply that there are low levels of GDNF secretion during the regeneration process. In vitro studies show that DRG neurons with a lesion to the sciatic nerve secrete much lower levels of GDNF compared to NGF in culture. Riberio et al. also supports these findings [10,32]. As such, this might be a possible explanation for the slow re-innervation of non-peptidergic fibres.

CONCLUSIONS

The present study found that 84 days PO the foot sole is not fully re-innervated with skin nerve fibres. The overall regeneration percentage is only 70% of the control situation and the non-peptidergic fibres show a distinctly less regenerative capacity compared to the peptidergic fibres. This incomplete regeneration was further strengthened by our Von Frey test, which still showed a somewhat higher mechanical withdrawal threshold in the autograft reconstruction group as compared to the control group.

The present findings are helpful in understanding neural regeneration after grafting a nerve defect with the autologous nerve graft. Especially the particular findings that illustrate a stronger regeneration of the peptidergic fibres compared to the non-peptidergic fibres 12 weeks post operative and that the overall regeneration percentage is approximately 70% as compared to the healthy control. In particular, we propose that the dissatisfactory recovery of sensation after nerve reconstruction could be explained by these different regeneration percentages of the different subgroups of sensory fibres.

REFERENCES

1.
Colen KL, Choi M, Chiu DT. Nerve grafts and conduits. Plast Reconstr Surg. 2009;124:e386-94.

2.
Deumens R, Bozkurt A, Meek MF, Marcus MA, Joosten EA, Weis J, et al. Repairing injured peripheral nerves: Bridging the gap. Prog Neurobiol. 2010;92:245-76.

3.
Matsuyama T, Mackay M, Midha R. Peripheral nerve repair and grafting techniques: a review. Neurol Med Chir (Tokyo). 2000;40:187-99.

4.
Wolford LM, Stevao EL. Considerations in nerve repair. Proc (Bayl Univ Med Cent). 2003;16:152-6.

5.
Stokvis A, van der Avoort DJ, van Neck JW, Hovius SE, Coert JH. Surgical management of neuroma pain: a prospective follow-up study. Pain. 2010;151:862-9.

6.
Lundborg G. Enhancing posttraumatic nerve regeneration. J Peripher Nerv Syst. 2002;7:139-40.

7.
Sunderland IR, Brenner MJ, Singham J, Rickman SR, Hunter DA, Mackinnon SE. Effect of tension on nerve regeneration in rat sciatic nerve transection model. Ann Plast Surg. 2004;53:382-7.

8.
Moore AM, Kasukurthi R, Magill CK, Farhadi HF, Borschel GH, Mackinnon SE. Limitations of conduits in peripheral nerve repairs. Hand (N Y). 2009;4:180-6.

9.
Mackinnon SE. Technical use of synthetic conduits for nerve repair. J Hand Surg Am. 2011;36:183.

10.
Peleshok JC, Ribeiro-da-Silva A. Delayed reinnervation by nonpeptidergic nociceptive afferents of the glabrous skin of the rat hindpaw in a neuropathic pain model. J Comp Neurol. 2011;519:49-63.

11.
Verdu E, Navarro X. Comparison of immunohistochemical and functional reinnervation of skin and muscle after peripheral nerve injury. Exp Neurol. 1997;146:187-98.

12.
Duraku LS, Hossaini M, Hoendervangers S, Falke LL, Kambiz S, Mudera VC, et al. Spatiotemporal dynamics of re-innervation and hyperinnervation patterns by uninjured CGRP fibers in the rat foot sole epidermis after nerve injury. Mol Pain. 2012;8:61.

13.
Duraku LS, Hossaini M, Schuttenhelm BN, Holstege JC, Baas M, Ruigrok TJ, et al. Re-innervation patterns by peptidergic Substance-P, non-peptidergic P2X3, and myelinated NF-200 nerve fibers in epidermis and dermis of rats with neuropathic pain. Exp Neurol. 2013;241:13-24.

14.
Oaklander AL, Brown JM. Unilateral nerve injury produces bilateral loss of distal innervation. Ann Neurol. 2004;55:639-44.

15.
Wall PD, Devor M, Inbal R, Scadding JW, Schonfeld D, Seltzer Z, et al. Autotomy following peripheral nerve lesions: experimental anaesthesia dolorosa. Pain. 1979;7:103-11.

16.
Zeltser R, Beilin B, Zaslansky R, Seltzer Z. Comparison of autotomy behavior induced in rats by various clinically-used neurectomy methods. Pain. 2000;89:19-24.

17.
Stankovic N, Johansson O, Hildebrand C. Occurrence of epidermal nerve endings in glabrous and hairy skin of the rat foot after sciatic nerve regeneration. Cell Tissue Res. 1996;284:161-6.

18.
Valero-Cabre A, Navarro X. Functional impact of axonal misdirection after peripheral nerve injuries followed by graft or tube repair. Journal of neurotrauma. 2002;19:1475-85.

19.
Navarro X, Verdu E, Wendelschafer-Crabb G, Kennedy WR. Immunohistochemical study of skin reinnervation by regenerative axons. J Comp Neurol. 1997;380:164-74.

20.
Lundborg G. Nerve Injury and Repair. Philadelphia, PA: Elsevier; 2004.

21.
Jones KJ, Brown TJ, Damaser M. Neuroprotective effects of gonadal steroids on regenerating peripheral motoneurons. Brain Res Brain Res Rev. 2001;37:372-82.

22.
Brain SD, Cox HM. Neuropeptides and their receptors: innovative science providing novel therapeutic targets. Br J Pharmacol. 2006;147 Suppl 1:S202-11.

23.
Ruscheweyh R, Forsthuber L, Schoffnegger D, Sandkuhler J. Modification of classical neurochemical markers in identified primary afferent neurons with Abeta-, Adelta-, and C-fibers after chronic constriction injury in mice. J Comp Neurol. 2007;502:325-36.

24.
Li XQ, Verge VM, Johnston JM, Zochodne DW. CGRP peptide and regenerating sensory axons. J Neuropathol Exp Neurol. 2004;63:1092-103.

25.
Toth CC, Willis D, Twiss JL, Walsh S, Martinez JA, Liu WQ, et al. Locally synthesized calcitonin gene-related Peptide has a critical role in peripheral nerve regeneration. J Neuropathol Exp Neurol. 2009;68:326-37.

26.
McLachlan EM, Keast JR, Bauer M. SP- and CGRP-immunoreactive axons differ in their ability to reinnervate the skin of the rat tail. Neurosci Lett. 1994;176:147-51.

27.
Lauria G, Borgna M, Morbin M, Lombardi R, Mazzoleni G, Sghirlanzoni A, et al. Tubule and neurofilament immunoreactivity in human hairy skin: markers for intraepidermal nerve fibers. Muscle Nerve. 2004;30:310-6.

28.
Oaklander AL, Siegel SM. Cutaneous innervation: form and function. J Am Acad Dermatol. 2005;53:1027-37.

29.
Duraku LS, Ruigrok T, Walbeehm ET. Innervation patterns of uninjured peptidergic, non-peptidergic and meylinated intra-epidermal fibers after a spared nerve injury. Submitted. 2011.

30.
Wood MD, Moore AM, Hunter DA, Tuffaha S, Borschel GH, Mackinnon SE, et al. Affinity-based release of glial-derived neurotrophic factor from fibrin matrices enhances sciatic nerve regeneration. Acta Biomater. 2009;5:959-68.

31.
Unezaki S, Yoshii S, Mabuchi T, Saito A, Ito S. Effects of neurotrophic factors on nerve regeneration monitored by in vivo imaging in thy1-YFP transgenic mice. J Neurosci Methods. 2009;178:308-15.

32.
Leclere PG, Norman E, Groutsi F, Coffin R, Mayer U, Pizzey J, et al. Impaired axonal regeneration by isolectin B4-binding dorsal root ganglion neurons in vitro. J Neurosci. 2007;27:1190-9.

8

RE-INNERVATION PATTERN OF PEPTIDERGIC, NON-PEPTIDERGIC AND MYELINATED PERIPHERAL NERVE FIBRES OF THE SKIN AFTER A VEIN-MUSCLE GRAFT RECONSTRUCTION SUPPORTED WITH BONE MARROW STROMAL CELLS (BMSCS) IN A RAT MODEL

L. S. Duraku [1,2*]
T. H.J. Nijhuis [1*]
C. A. Hundepool [1]
J. W. van Neck [1]
T. J.H. Ruigrok [2]
S. E.R. Hovius [1]
E. T. Walbeehm [1]

*Both authors contributed equally

1. Department of Plastic, Reconstructive and Hand Surgery, Erasmus MC, University Medical Center, Rotterdam, The Netherlands

2. Dept. of Neuroscience, Erasmus MC, University Medical Center, Rotterdam, The Netherlands

ABSTRACT

INTRODUCTION

A proposed alternative to the autograft in experimental nerve reconstruction is the vein-muscle graft supported with Bone Marrow Stromal Cells (BMSCs). However, the specific contributing effects of the BMSCs to successful regeneration are not completely understood. Visualizing skin epidermal nerve fibres illustrates the regeneration of the most distal sensory branches. This study investigates the re-innervation, by means of immunohistochemistry, of various classes of epidermal fibres in the rat foot sole. Regeneration of peptidergic, non-peptidergic and myelinated fibres is quantified 12 weeks after reconstruction of a nerve defect using either a plain vein-muscle graft or a vein-muscle graft filled with BMSCs.

METHODS

Peptidergic fibres were visualized by Calcitonin Gene Related Peptide (CGRP) and Substance-P (SubP) and the non-peptidergic fibres in the epidermis by P2X3. Neurofilament (NF)-200 was used to visualize all the myelinated fibres and control labelling was performed with Protein Gene Product (PGP)-9.5 (pan-neuronal marker) to stain all nerve fibres.

RESULTS AND CONCLUSION

The number of non-peptidergic P2X3 and myelinated NF-200 fibres had a significant increase in re-innervation favouring the vein-muscle graft with BMSCs as opposed to the plain vein-muscle graft group. The vein-muscle graft with the BMSCs showed no significant regenerative increase of the peptidergic (CGRP and SubP) fibres when compared to the vein-muscle graft. Twelve weeks after reconstructing a nerve defect using a vein-muscle graft with BMSCs, strong indications for the beneficial effect of the BMSCs were found, especially illustrated by the regeneration of the non-peptidergic P2X3 and myelinated NF-200 fibres.

INTRODUCTION

Peripheral nerve injury is a common problem in trauma. Especially larger nerve defects that cannot be reconstructed directly are in need for an appropriate technique to restore innervation of the end organs.[1-3]

The golden standard for bridging large nerve defects in clinical practise, is the use of an autologous nerve graft. Disadvantages of this technique are the inevitable donor site morbidity and limited length of available graft material. [2, 4-6] An experimental alternative, introduced by our group, is the vein-muscle graft supported with Bone Marrow Stromal Cells (BMSCs). [7] The rationale for using an inserted muscle in the already accepted vein graft is to prevent the vein from collapsing. [8-10] A tendency was found that a vein-muscle graft filled with BMSCs (VMG+) outperformed the conventional vein-muscle graft, which was reflected in functional (both sensory and motor function) and histological improvement. [7]

Previously, our group demonstrated the re-innervation of peptidergic, non-peptidergic and myelinated subgroups of fibres in the skin after an autograft reconstruction. [11] However, to our knowledge, no literature describes the re-innervation pattern of sensory nerve fibres in the skin following reconstruction using a conventional vein-muscle graft (VMG) or the vein-muscle graft filled with BMSCs (VMG+). Consequently, no studies have been reported about the beneficial effect of BMSCs on the re-innervation of the skin after vein-muscle graft reconstruction.

The present study has visualised subgroups of sensory fibres in the foot sole three months postoperatively using different immunohistochemical markers. PGP 9.5 is a pan neural marker that stains all sensory nerve fibres and thus can visualize the total ingrowth of the fibres. Subsequently, one can differentiate between the two major classes of sensory fibres in the skin, i.e. peptidergic and non-peptidergic fibres. Peptidergic fibres were labelled with Calcitonin Gene-Related Peptide (CGRP) and Substance P (SubP), visualising the unmyelinated C nerve fibres. [11-13] The 200-kDA Neurofilament protein staining (NF200-IR) visualizes all the peptidergic myelinated fibres in the skin. These fibres are only visible in the upper dermal area because they lose their myelination in the dermal/epidermal junction and –hence- only very few NF-200 stained fibres should be visualised in the epidermis. The P2X3 staining stains all non-peptidergic purinergic C nerve fibres. Both unmyelinated and myelinated fibres, which terminate in the epidermis, are responsible for the transduction of pain and temperature. [13]

Our hypothesis is that the BMSCs enhance neural re-innervation in the rat foot sole skin. Therefore, injection of these cells in the lumen of the graft is expected to result in better regeneration as compared to conventional neural reconstruction using a vein-muscle graft alone.

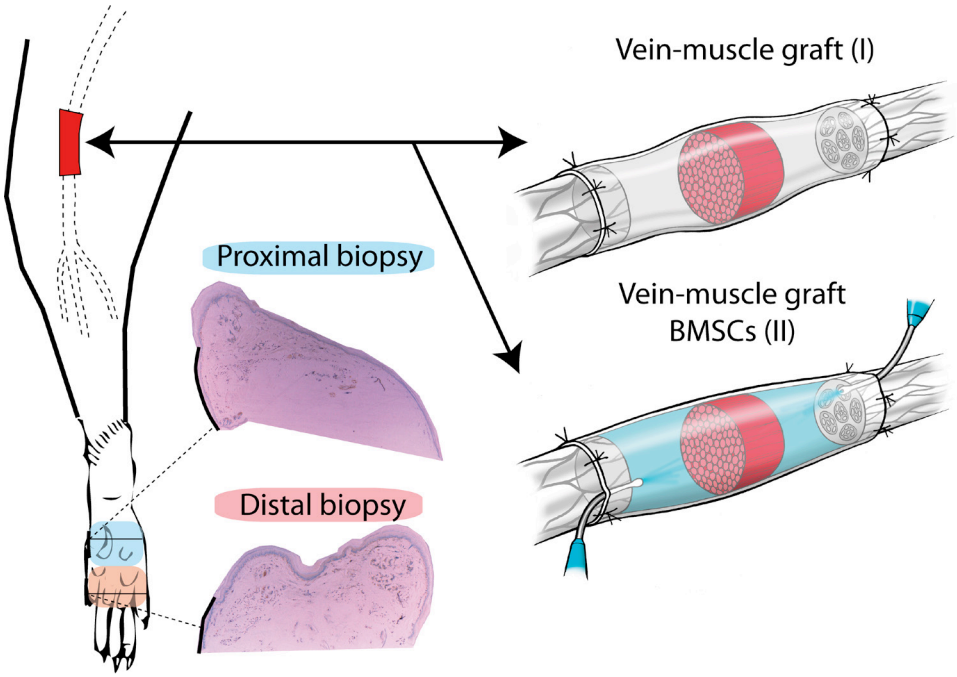

FIGURE 1:

Detailed illustration of the surgical model of the vein-muscle grafts used and the location of the skin biopsies.

METHODS

ANIMALS

The experimental protocol was approved by the Animal Experiments Committee according to the National Experiments on Animals Act and conducted according to this law that serves the implementations of Directive 86/609/EC of the Council of Europe. Ten isogenic adult female Lewis rats, weighing 180 – 200 grams, were used. Animals were pair-housed in hooded cages at room temperature on a 12-hour light/dark schedule, and were given food and water ad libitum. Surgical procedures and electrophysiological evaluations were performed under general anaesthesia (Isoflurane, 1-2% in a mixture of O2).

SURGICAL TECHNIQUE

The surgical procedure was performed by the same surgeon and assistant using standard aseptic microsurgical techniques under the operating microscope (Zeiss OP-MI 6-SD; Carl Zeiss, Goettingen, Germany) on the sciatic nerve of the left hind limb. Both groups contained 5 animals. After an oblique skin incision was made in the left gluteal region of the donor, the sciatic nerve was exposed through a gluteal muscle-splitting incision and externally dissected to isolate a 15-mm segment of the nerve. The nerve was transected proximally and distally to obtain the 15-mm segment. The jugular vein served as the conduit, which was harvested through a longitudinal mid-line incision of 35 mm in the neck. The left external jugular vein was dissected and both the proximal and the distal end of the vein were ligated. A small muscle fragment of 1½x 1½ mm2, was cut out of the gluteal muscle and placed inside the lumen of the vein using a straight irrigator. Next, the graft I (i.e. the VMG) was connected to the nerve stumps using 6 10/0 Ethilon sutures (Ethicon, Johnson & Johnson, Amersfoort, the Netherlands) at each coaptation side. The muscle was closed using 2 6/0 Vicryl Rapide sutures, followed by closing the skin using 6/0 Vicryl Rapide Sutures (Ethicon, Johnson & Johnson, Amersfoort, the Netherlands). In group II (VMG+) the cells were injected after connecting the graft to both the proximal and distal nerve stumps. A detailed illustration is depicted in Figure 1.

BONE MARROW STROMAL CELL PREPARATION

A detailed presentation of our preparation can be found in an earlier published study by our group.[7]

FIGURES

	Proximal (%)		Distal (%)	
	BMSCs-	**BMSCs+**	**BMSCs-**	**BMSCs+**
Pgp 9.5-IR	30	44	28	37
CGRP-IR	70	70	61	59
Subst P	53	67	42	48
NF200-IR	36	57	26	59
P2X3-IR	14	22	5	14

TABLE 1:

Regeneration percentage of the sensory nerve fiber subgroups, as reflected by their AB staining pattern, 12 weeks post operative and compared to the respective control. PGP 9.5-IR is a pan neuronal marker. The calcitonin gene-related peptide (CGRP-IR) marker stains the peptidergic fibres. Substance P-IR (Sub P) also stains the peptidergic fibres. Neurofilament 200 (NF200-IR) stains the Aδ-fibres. The P2X purinoceptor 3 (P2X3-IR) staining visualizes all non-peptidergic fibres.

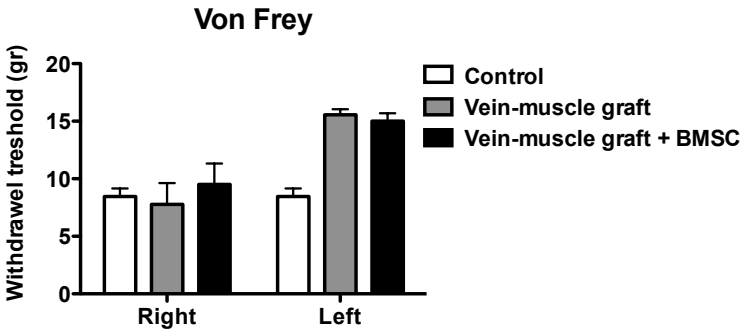

FIGURE 2:

The Von Frey test illustrating the mechanical withdrawal of the animals in both groups. The left side is the operated side for all animals. Error bars indicate standard deviation

EVALUATION OF MECHANICAL HYPERSENSITIVITY

Twelve weeks postoperative; the mechanical threshold of the hind paws was measured using the Von Frey hairs. Each Von Frey hair was applied for 2 s at 5 s intervals, with a maximum of 5 repeated measures. The threshold was set at 3 paw lifts. During testing the rats were placed in a plastic box (perforated floor) and able to move freely. The medial and lateral sides were stimulated at the transition point from glabrous skin to hairy skin. The center foot sole was stimulated at the very centre point of the foot sole. The mechanical withdrawal response was noted and used for analysis.

PREPARATION OF TISSUE

After sacrificing the animal, the complete foot sole of the left and right hind paws were surgically resected. The foot sole were then placed in a 10% sucrose solution for 24hrs, washed and rinsed with glycerol solution and placed in freezer. [11, 14]

IMMUNOHISTOCHEMICAL STAINING

After embedding in gelatin the foot sole was sectioned with a freeze microtome at 40µm. Immunohistochemistry was performed free-floating according to the protocol described by Duraku et al. [14] Briefly, sections were pre-incubated (90 min at room temperature (RT)) in a mixture containing bovine serum albumin (BSA 2%) phosphate buffered saline (PBS, pH 7,4). (Fraction V, Roche) and 0.5% Triton X-100. Thereafter, the sections were rinsed in PBS and incubated for 48 hours in a cocktail of 2% BSA containing antibody; CGRP-IR antibody (1/30.000, rabbit, Calbiochem), NF200-IR (1/35.000, rabbit, Chemicon), Substance P-IR (1/500, rabbit) [15] P2X3-IR (1/25.000, guinea pig, Neuromics), PGP 9.5-IR (1/15.000, rabbit, Chemicon). Subsequently, sections where incubated with a secondary antibody rabbit anti-goat for 90 min room temperature. Sections were further processed using a Vectastain Elite ABC kit (Vector, Burlingame, CA) (90 min at RT). Finally, 3,-3′ diaminobenzidine (DAB) enhanced by the glucose oxidase-nickel-DAB method [16] was used to reveal antigenic sites. The sections were mounted on gelatinized slides, air dried overnight, dehydrated using absolute ethanol (< 0.01% methanol), transferred to xylene and coverslipped with Permount (Fisher, Hampton, NH). Immunoreactivity for all immunohistochemical markers was completely abolished when primary antibodies were omitted.

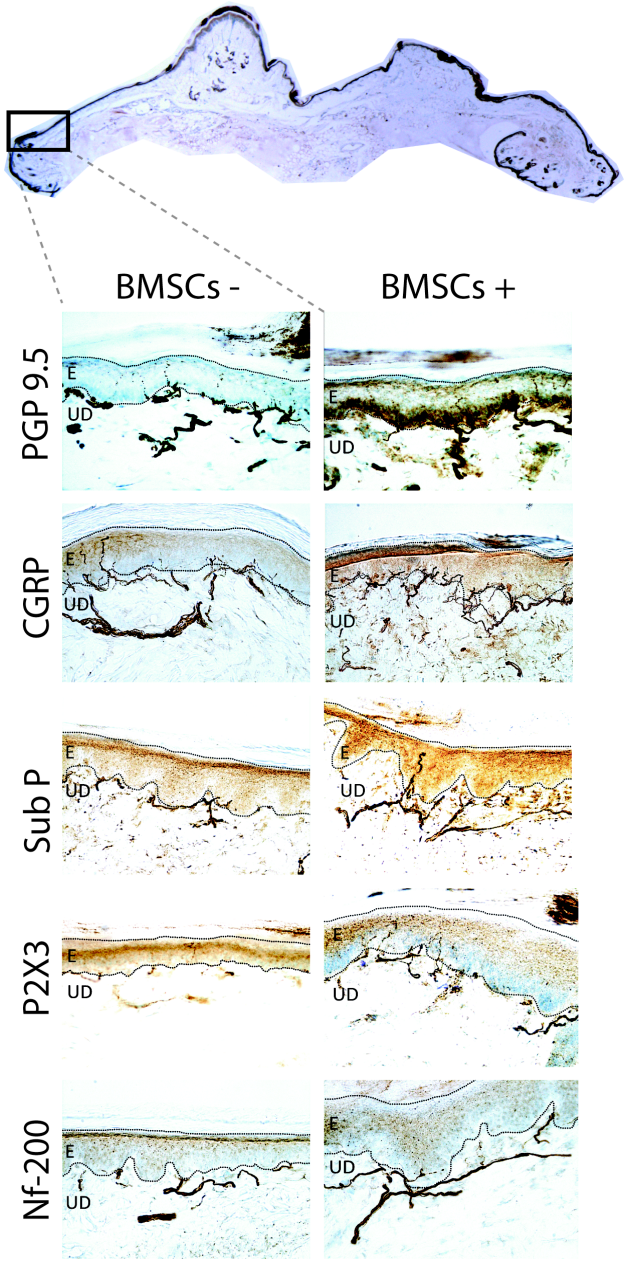

FIGURE 3:

An overview with example of the micrographs of the different markers used. Pictures are taken with a 20x10 objective for both the proximal and distal segment. PGP 9.5-IR is a pan neuronal marker. The calcitonin gene-related peptide (CGRP-IR) marker stains the peptidergic fibres. Substance P-IR (Sub P) also stains the peptidergic fibres. Neurofilament 200 (NF200-IR) stains the Aδ-fibres. The P2X purinoceptor 3 (P2X3-IR) staining visualizes all non-peptidergic fibres.

ANALYSIS

Important to state is that the control group we used is the same as used in our earlier publication. Since the investigated parameters are similar, we decided not to sacrifice animals for exactly the same goal as in the previous study. [11] Regarding the analysis of our animals, a total of 16 series of sections of the complete footpad per animal was used. The sections where put in serial order from proximal to distal by using the brain as an anatomical marker as described by Duraku et al. [14] This results in 8 proximal and 8 distal sections. Each section was divided in a lateral and central area. The sections were analysed systematically to visualize the location of the labelled fibres in the dermis, between the dermis and epidermis (crossing fibres) as well as the number of (apparently) terminal fibres within the epidermis using an Olympus BH microscope equipped with a Lucivid miniature monitor and Neurolucida™ software (MicroBrightField, Inc., Colchester, VT). The fibres were systematically counted using the 20 x 10 objective. The fibres in all two sections (i.e. the upper dermis and epidermis) of the center and of the lateral side were counted. To determine the number of fibres per square mm, we divided the counted fibres by the surface area (0,24 mm2). Per group, the results were averaged and compared with the average results in the control group. Variations are represented as standard error of the mean (SEM). Also, the data of our previous published manuscript regarding the re-innervation of the skin after autograft reconstruction was implemented in this analysis, since we used the same control group.[11] An unpaired t-test was performed for all evaluations. An illustration of our study model is depicted in Figure 1.

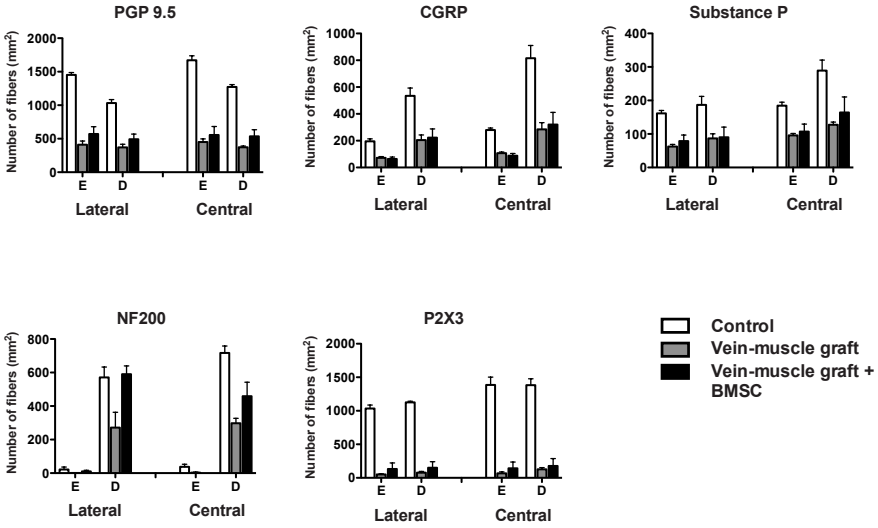

FIGURE 4:

The re-innervation of the skin nerve fibres, 12 week post operatively. SEM is visualised with the error bars. PgP 9.5-IR is a pan neuronal marker. The calcitonin gene-related peptide (CGRP-IR) marker stains the peptidergic fibres. Substance P-IR (Sub P) also stains the peptidergic fibres. Neurofilament 200 (NF200-IR) stains the Aδ-fibres. The P2X purinoceptor 3 (P2X3-IR) staining visualizes all non-peptidergic fibres. SEM is visualised with the error bars.

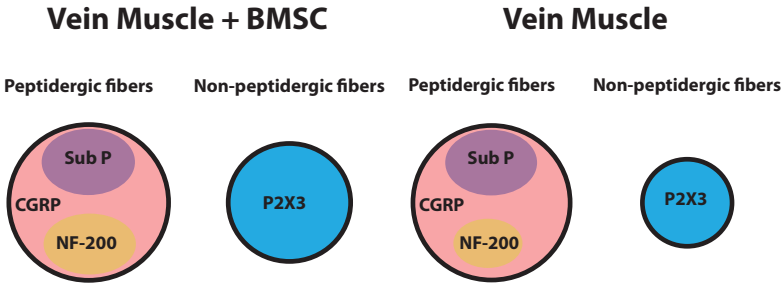

FIGURE 5:

A schematic illustration of the different stainings in proportion to each other. PgP 9.5-IR is a pan neuronal marker. The calcitonin gene-related peptide (CGRP-IR) marker stains the peptidergic fibres. Substance P-IR (Sub P) also stains the peptidergic fibres. Neurofilament 200 (NF200-IR) stains the Aδ-fibres. The P2X purinoceptor 3 (P2X3-IR) staining visualizes all non-peptidergic fibres

RESULTS

EVALUATION OF MECHANICAL HYPERSENSITIVITY

The mechanical withdrawal of both the operated and the non-operated paws was determined. The mean threshold for the animals treated with the vein-muscle graft was 15.6 gram (SEM ± 0,7) and was not significantly different from the animals with the vein-muscle graft with BMSCs showed a withdrawal reaction at 15.0 gram (SEM ± 1.0) 12 weeks postoperative (Figure 2).

IMMUNOHISTOCHEMISTRY

Fibre regeneration is shown by five immunohistochemical markers for nerve fibres: (1) PGP 9.5-immunoreactive (IR), (2) CGRP-IR, (3) Substance P-IR, (4) NF200-IR and (5) P2X3-IR. Figure 3 depicts the representative microphotographs of the resulting labelling. In Figure 4, a quantification of the number of labelled fibres in both layers (i.e. the epidermis and upper dermal area) of the distal part is presented. We only present the distal part as this part shows the clear difference between all groups, which is in line with our rationale that the more distal from the lesion the more outstanding the differences can be expected. Regeneration percentages were only given for the epidermal areas, as this is the area important for sensory transmission. For the myelinated fibres we used the dermal/epidermal crossing as the target area to measure regeneration percentage (Table 1), because they loose their myelination in the dermal/epidermal border.

PGP 9.5

Epidermis

Twelve weeks after surgery the skin innervation in both graft groups was still significantly below the control situation. The VMG group after 12 weeks showed on average a re-innervation percentage of 29% proximally and 28% distally. Although the VMG+ group on average showed an enhanced average percentage of re-innervated fibers (44% and 37% for proximal and distal foot sole, respectively), this was not significantly different from the vein-muscle group (p=0,163).

Upper dermis

In the central proximal segment, the VMG+ group showed a trend to outperform the vein-muscle graft alone (p = 0,086). Distally, both groups were not significantly different (p = 0,139). All segments in the vein-muscle group with or without BMSCs had a significant lower density of PGP 9.5-IR upper dermal fibres as compared to the healthy control group (p< 0,05).

CGRP

Epidermis

The CGRP-IR peptidergic nerve fibres innervated the skin after vein-muscle grafting with 61% proximally and 56% distally. In the VMG+ group proximally 69% re-innervation was encountered, distally 56% re-innervation was seen. For all sections no significant difference in results were found ($p > 0.318$). Compared with the control group all segments of both groups had a significant lower density of epidermal CGRP-IR fibres.

Upper dermis

The total number of fibres was not significantly different between the VMG group and the VMG+ group. All segments of both groups were significant different from the healthy control group.

SUBSTANCE P

Epidermis

The peptidergic SubP-IR fibres in the vein-muscle graft group re-innervated the skin proximally with 52% and distally with 47% of the normal values. No significant differences in the number of fibres between the two groups were found ($p = 0,204$). In the group supported with BMSCs in the proximal footpad area a re-innervation of 69% was found. Distally 50% of the fibres are re-innervated as compared to the healthy control foot sole area. Compared with the healthy control group all segments of both groups had a significant lower amount of fibres , except the lateral side of the proximal segment of the vein-muscle graft group supported with BMSCs ($p = 0.610$).

Upper dermis

No significant differences in the number of fibres between the two groups were found ($p = 0,309$). The VMG group had a significant lower number of upper dermal SubP-IR fibres as compared to the healthy control group except the lateral area of the distal segment ($p=0.108$). The vein-muscle graft group with BMSCs showed a non-significantly lower number of upper dermal SubP-IR fibres in the central area and in the lateral area of both proximal ($p=0.775$) and distal segment ($p=0.187$).

NF200-IR

Upper dermis

In the lateral segment of the distal section the VMG+ group significantly outperformed the group without BMSCs ($p = 0.016$). The other segments were not significantly different comparing the two groups ($p = 0.126$).

All segments of the vein-muscle graft group showed a significantly lower amount of fibres as compared to the healthy control group except for the lateral area of the

proximal segment (p=0.109). The vein-muscle graft group supported with BMSCs showed a significantly lower number of upper dermal NF200-IR fibres as compared to the healthy control group except for the lateral area of both the proximal (p=0.145) and the distal (p=0.817) segment.

P2X3-IR

Epidermis

The non-peptidergic fibres, proximally, had a 6% re-innervation in the vein-muscle graft group. Distally 2% re-innervation was seen. In the group supported by BMSCs, 17% proximally and 12% distally re-innervation was measured. Only for the lateral segment of the proximal section, the VMG+ group significantly outperformed the group without BMSCs (p=0.038) while no difference between both graft groups was observed for the other segments (p = 0.292).

Compared with the control group all segments of both groups had significantly less epidermal P2X3-IR fibres. The results show that the lateral proximal area of the foot sole has significant more epidermal P2X3-IR fibres in the VMG+ group as compared to the group without the BMSCs.

Upper dermis

In the upper dermis there were no significant differences in the density of the P2X3 labelled fibres between both graft groups, but both were close to a significant lower number of fibres compared to the control situation (p = 0.057).

DISCUSSION

The current study examined the re-innervation pattern of sensory nerve fibres in a rat hind paw glabrous skin 12 weeks postoperatively, after reconstructing a 15 mm gap using a vein-muscle graft and a vein-muscle graft supported with BMSCs. The main findings were: 1) the BMSCs treated vein grafts show a near significant approximately 30% increased epidermal re-innervation of PGP 9.5-immunoreactivity (IR) fibres in the skin as compared to the vein-muscle graft (p=0.086). 2) in the group with the vein-muscle graft with BMSCs, the number of peptidergic (CGRP-IR and Sub P-IR) did not show substantial changes as compared to the vein-muscle graft alone 12 weeks postoperatively; 3) the vein-muscle graft filled with BMSCs showed a significantly higher number of NF200-IR (myelinated fibres) and non-peptidergic P2X3-IR fibres as compared to the vein-muscle graft at 12 weeks postoperatively.

PGP 9.5-IR

Addition of BMSCs to the venous muscle conduit resulted in a marginal improvement in innervation of epidermal fibres.

We showed in a previous report that the autograft as a conduit resulted in a significantly higher PGP 9.5-IR density (i.e. up to 70%) in the foot sole as compared to the two conduits examined in the present study. [11] This finding is confirmed by our functional results comparing these conduits. [7] These results suggest that the nerve environment in the autograft, being rich in fascicles, nerve sustainable factors and cytokines [17] represents a favourable matrix for regeneration. If the vein does not have any supportive matrix at all can be discussed, but nevertheless the vein-muscle graft provides a metabolically supportive environment for the regenerating axons. As such, Schwann cells from the proximal part of the lacerated nerve will invade the vein and start proliferating after reconstruction, ultimately resulting in a comparable regeneration process as in the nerve autograft [18, 19]. Yet, with respect to the density of nerve fibres innervating the epidermis, the nerve autograft clearly outperforms the vein-muscle grafts both with and without BMSCs.

Peptidergic fibres: CGRP-IR and Substance P-IR

The vein-muscle graft and vein-muscle graft filled with BMSCs demonstrated a similar re-innervation density of the CGRP-IR fibres at 12 weeks postoperatively. Interestingly, the quantity of regenerated peptidergic sensory skin fibres was similar in the autograft group, as described in our previous study[11], and in the vein-muscle graft group regardless of the BMSCs filling. Supporting the superiority of the autograft group, is the total amount of skin nerve fibres (PGP 9.5-IR), which showed a different regeneration pattern, favouring the autograft group and thus is in accordance with

the functional data presented previously.[7] The addition of BMSCs did not seem to influence the regeneration of the CGRP-IR fibres in this matter. This could suggest that the regenerative rate of sensory CGRP-IR fibres is independent of the conduit used, at least for both the autograft and both vein-muscle grafts. Hence, it can be concluded that intra-axonal translation of CGRP-IR is of critical importance for the regeneration of injured nerve fibres, since it regulates Schwann cell proliferation, and will therefore be synthesised and translated independently of the conduit used.[20, 21]
The other peptidergic fiber group, Substance P-IR, showed similar re-innervation densities in the vein-muscle graft supported without and with BMSCs at 12 weeks postoperatively. In the present study we found a lower number of re-innervated Substance P-IR skin fibres in the vein-muscle graft group –with/without BMSCs, as compared to the number of CGRP-IR fibres. This is confirmed by McLachlan et. al., which showed that after peripheral nerve lesion the cutaneous Substance P-IR fibers show a slower reinnervation rate as compared to CGRP-IR fibers. However this study was performed in the rat tail, after proximal lesions of collector nerves, without reconstruction of the defect. We assume that the presence of Schwann cells is of critical importance for the regeneration of Substance P-IR fibres. This could also explain the delayed re-innervation of Substance P-IR as compared to the CGRP-IR fibres, as it has been shown that CGRP-IR up-regulates Schwann cell proliferation.[20, 21] Schwann cells up-regulate the p75 receptor and secrete Nerve Growth Factor (NGF) in substantial quantity.[22] These differentiated Schwann cells are essential for the guidance and ultimately for the direction of regenerated axons. This could explain the slower regeneration rate of Substance P-IR fibres, since the guidance of Schwann cell is absent in the vein-muscle graft. There is a trend for a better regeneration pattern of peptidergic skin fibres in the vein-muscle group supported with BMSCs as compared to the group without the BMSCs. This beneficial effect can be explained by the theory that BMSCs have the capability to trans-differentiate to Schwann-like cells and therefore may enhance the regeneration of sensory Substance P-IR skin fibres.[7, 22-25]

NF200-IR

To evaluate the re-innervation percentage of the NF200-IR myelinated fibres (i.e. Aδ/Aβ fibres) the number of fibres in the upper dermis was quantified, since these fibres lose their myelin sheet in the dermal-epidermal crossing.[14] The low number of epidermal NF200-IR counts in the present study confirms this. It should be stressed that the NF200-IR marker does not discriminate between Aδ and Aβ fibres. However, because Aβ fibres terminate in the end-organs in the lower dermis and Aδ fibres run as free nerve endings in the upper dermis[26], we presume that quantifying the amount of these fibres correlates mostly with the density of Aδ fibres.
We found a significantly higher number of NF200-IR fibres in the VMG+ group

as compared to the VMG group. A possible explanation for this difference is the trans-differentiation of BMSCs into Schwann cells, which would evidently support the regeneration rate. These trans-differentiated Schwann cells are of pivotal importance for the myelinisation of the axons. Therefore it is uncertain if the lower numbers of NF200-IR fibres, in the empty vein-muscle group are due to an incomplete myelinisation or to a lower number of myelinated fibres. In addition, the BMSCs produce substantial amounts of NGF as shown in an earlier study.[7] Furthermore, conduits filled with NGF also induce more myelinated fibres, thicker myelin sheaths, and higher conduction velocities.[27] Interestingly, the number of re-innervated NF200-IR fibres in the BMSCs group (58%) is comparable to the number found in the autograft group (51%) as studied in a previous report.[11] Regarding the pure histological regeneration of the myelinated fibres, the VMG+ treated group seems to be as good as the autograft. Nevertheless, evaluating the regeneration at whole, the reason for the inferiority of the BMSCs group might lie in both the regeneration of the other subgroups of fibres and the motor re-innervation..

P2X3

Few studies have considered the re-innervation pattern of non-peptidergic fibres [14] whereas these fibres account for more than 60% of the unmyelinated C-fibres innervating the epidermis. In the current study the non-peptidergic P2X3-IR fibres had the lowest re-innervation percentage as compared to their counterpart peptidergic sensory fibres (CGRP-IR, Substance P-IR and NF200-IR). Non-peptidergic fibres are not responsive to NGF but to the glial cell-line-derived neurotrophic factor (GDNF) [28]. It is believed that growth factor production by denervated Schwann cells in the distal nerve segment is crucial for successful peripheral nerve regeneration [21, 29]. Since, these denervated Schwann cells produce, apart from growth factors like NGF, also GDNF. In the current study, the vein-muscle graft supported with the BMSCs outperformed the empty vein-muscle graft, resulting in a significantly higher re-innervation percentage (18 vs 9.5 %, respectively). This supports the hypothesis that denervated Schwann cells are of critical importance for the regeneration of non-peptidergic fibres, using the earlier mentioned theory about trans-differentiation as explanation. Be that as it may, the regeneration of non-peptidergic fibres after implantation of an autograft group (27%) still remains better as when compared to the BMSCs group (18%). Despite the improved regeneration in the VMG+ group, it still remains interesting why non-peptidergic fibres have a dramatic slower regeneration rate compared to peptidergic fibres.[13, 30]

CONCLUSIONS

We would like to introduce Figure 5 in our conclusion, since this figure summarizes our data in a very comprehensive way. Taking these findings in consideration we can conclude that peptidergic fibres proliferate more dominant than non-peptidergic fibres as judged by the density of regenerated fibres within a specific timeframe (i.e. 12 weeks). Another finding is the more successful re-innervation of the NF200 and of the non-peptidergic P2X3 fibres in the vein-muscle conduit filled with BMSCs as compared to the conduit without BMSCs.

REFERENCES

1.
Colen KL, Choi M, Chiu DT. Nerve grafts and conduits. Plast Reconstr Surg. 2009;124:e386-94.

2.
Deumens R, Bozkurt A, Meek MF, Marcus MA, Joosten EA, Weis J, et al. Repairing injured peripheral nerves: Bridging the gap. Prog Neurobiol. 2010;92:245-76.

3.
Matsuyama T, Mackay M, Midha R. Peripheral nerve repair and grafting techniques: a review. Neurol Med Chir (Tokyo). 2000;40:187-99.

4.
Wolford LM, Stevao EL. Considerations in nerve repair. Proc (Bayl Univ Med Cent). 2003;16:152-6.

5.
Stokvis A, van der Avoort DJ, van Neck JW, Hovius SE, Coert JH. Surgical management of neuroma pain: a prospective follow-up study. Pain. 2010;151:862-9.

6.
Lundborg G. Enhancing posttraumatic nerve regeneration. J Peripher Nerv Syst. 2002;7:139-40.

7.
Sunderland IR, Brenner MJ, Singham J, Rickman SR, Hunter DA, Mackinnon SE. Effect of tension on nerve regeneration in rat sciatic nerve transection model. Ann Plast Surg. 2004;53:382-7.

8. Moore AM, Kasukurthi R, Magill CK, Farhadi HF, Borschel GH, Mackinnon SE. Limitations of conduits in peripheral nerve repairs. Hand (N Y). 2009;4:180-6.

9.
Battiston, B., Tos, P., Geuna, S., Giacobini-Robecchi, M. G., Guglielmone, R. Nerve repair by means of vein filled with muscle grafts.

10.
Brunelli, G. A., Battiston, B., Vigasio, A., Brunelli, G., Marocolo, D. Bridging nerve defects with combined skeletal muscle and vein conduits. Microsurgery 1993;14:247-251.

11.
Nijhuis, T. H. J., Duraku, L. S., Hundepool, C. A., et al. Distribution of subgroups of specific sensory nerve fibers of the skin following nerve autograft reconstruction in a rat model. Submitted 2011.

12.
Duraku, L. S., Hossaini, M., Hoendervangers, S., et al. Spatiotemporal dynamics of re-innervation and hyperinnervation patterns by uninjured CGRP fibers in the rat foot sole epidermis after nerve injury. Mol Pain 2012;8:61.

13.
Duraku, L. S., Hossaini, M., Schuttenhelm, B. N., et al. Re-innervation patterns by peptidergic Substance-P, non-peptidergic P2X3, and myelinated NF-200 nerve fibers in epidermis and dermis of rats with neuropathic pain. Exp Neurol 2012.

14.
Duraku, L. S., Ruigrok, T., Walbeehm, E. T. Innervation patterns of uninjured peptidergic, non-peptidergic and meylinated intra-epidermal fibers after a spared nerve injury. Submitted 2011.

15.
R M Buijs, C. W. P., J J Van Heerikhuize, A A Sluiter, P J Van Der Sluis, M Ramkema, T P Van Der Woude, E Van Der Beek. Antibodies to small transmitter molecules and peptides: production and application of antibodies to dopamine, serotonin, GABA, vasopressin, vasoactive intestinal peptide, neuropeptide Y, somatostatin and substance P. Biomedical research 1989;10, Supplement 3:213-221.

16.
Kuhlmann, W. D., Peschke, P. Glucose oxidase as label in histological immunoassays with enzyme-amplification in a two-step technique: coimmobilized horseradish peroxidase as secondary system enzyme for chromogen oxidation. Histochemistry 1986;85:13-17.

17.
Boyd, J. G., Gordon, T. Neurotrophic factors and their receptors in axonal regeneration and functional recovery after peripheral nerve injury. Mol Neurobiol 2003;27:277-324.

18.
Fornaro, M., Tos, P., Geuna, S., Giacobini-Robecchi, M. G., Battiston, B. Confocal imaging of Schwann-cell migration along muscle-vein combined grafts used to bridge nerve defects in the rat. Microsurgery 2001;21:153-155.

19.
Geuna, S., Raimondo, S., Nicolino, S., et al. Schwann-cell proliferation in muscle-vein combined conduits for bridging rat sciatic nerve defects. J Reconstr Microsurg 2003;19:119-123; discussion 124.

20. Li, X. Q., Verge, V. M., Johnston, J. M., Zochodne, D. W. CGRP peptide and regenerating sensory axons. J Neuropathol Exp Neurol 2004;63:1092-1103.

21.
Toth, C. C., Willis, D., Twiss, J. L., et al. Locally synthesized calcitonin gene-related Peptide has a critical role in peripheral nerve regeneration. J Neuropathol Exp Neurol 2009;68:326-337.

22.
Walsh, S., Midha, R. Use of stem cells to augment nerve injury repair. Neurosurgery 2009;65:A80-86.

23.
Chen, X., Wang, X. D., Chen, G., Lin, W. W., Yao, J., Gu, X. S. Study of in vivo differentiation of rat bone marrow stromal cells into schwann cell-like cells. Microsurgery 2006;26:111-115.

24.
Nijhuis, T. H., Brzezicki, G., Klimczak, A., Siemionow, M. Isogenic venous graft supported with bone marrow stromal cells as a natural conduit for bridging a 20 mm nerve gap. Microsurgery 2010.

25.
Tohill, M., Mantovani, C., Wiberg, M., Terenghi, G. Rat bone marrow mesenchymal stem cells express glial markers and stimulate nerve regeneration. Neurosci Lett 2004;362:200-203.

26.
Oaklander, A. L., Siegel, S. M. Cutaneous innervation: form and function. J Am Acad Dermatol 2005;53:1027-1037.

27.
Bu, S., Li, J., Hu, C. [The influence of nerve growth factor on inferior alveolar nerves regeneration in the silicone tubes]. Zhonghua Kou Qiang Yi Xue Za Zhi 1999;34:217-219.

28.
Anand, P. Neurotrophic factors and their receptors in human sensory neuropathies. Prog Brain Res 2004;146:477-492.

29.
Webber, C., Zochodne, D. The nerve regenerative microenvironment: early behavior and partnership of axons and Schwann cells. Exp Neurol 2010;223:51-59.

30.
Peleshok, J. C., Ribeiro-da-Silva, A. Delayed reinnervation by nonpeptidergic nociceptive afferents of the glabrous skin of the rat hindpaw in a neuropathic pain model. J Comp Neurol 2011;519:49-63.

9

ROTTERDAM ADVANCED MULTIPLE PLATE: A NOVEL METHOD TO MEASURE COLD HYPERALGESIA AND ALLODYNIA IN FREELY BEHAVING RODENTS.

L. S. Duraku [1,2]
S. P. Niehof [3]
Y. Misirli [1]
M. Everaers [1]
S. Hoendervangers [1]
H. J. Boele [2]
S. K.E. Koekkoek [2]
E. S. Smits [1]
R. W. Selles [1,4]
E. T. Walbeehm [1]

1. Department of Plastic, Reconstructive and Hand Surgery, Erasmus MC, University Medical Center, Rotterdam, The Netherlands

2. Dept. of Neuroscience, Erasmus MC, University Medical Center, Rotterdam, The Netherlands

3. Pain Treatment Centre, Erasmus MC, University Medical Centre Rotterdam, Rotterdam, The Netherlands

4. Dep. of Rehabilitation Medicine, Erasmus MC, University Medical Centre Rotterdam, Rotterdam, The Netherlands

ABSTRACT

To investigate the pathophysiology of temperature hypersensitivity in neuropathic pain rodent models, it is essential to be able to quantify the phenotype as objective as possible. Current temperature sensitivity measuring paradigms are performed during exposure to external factors, i.e. light, sound and smell, which modulate behavior significantly. In addition the present outcome measure for temperature hypersensitivity in rodents is the examination of the hind paw lift upon exposure to a certain temperature, which reflects more a reflex-flexion than an experience of pain. Therefore the Rotterdam Advanced Multiple Plate (RAMP) was developed to assess cold hyperalgesia and allodynia objectively in freely behaving neuropathic pain rats. The RAMP measures the avoidance for certain temperatures, by switching temperatures on four plates independently and monitoring the location of the rat continuously with an infrared camera while excluding external environmental influences such as light and sound. In the current study, spared nerve injury (SNI) rat models were used to induce long-lasting neuropathic pain behavior. Compared to sham rats, the SNI rats demonstrated a higher preference for the comfortable plate (27 ºC) when the other three plates were set at 5 ºC, 14 ºC, 17 ºC and 19 ºC. We were unable to detect heat hyperalgesia and allodynia with the RAMP. The results indicate that the RAMP is able to quantify cold hyperalgesia and allodynia in neuropathic pain rats while resolves some of the problems of conventional temperature sensitivity measuring paradigms in rodents.

INTRODUCTION

Neuropathic pain is a debilitating disease with a wide range of symptoms, including spontaneous pain and hypersensitivity to mechanical and temperature stimuli [1]. The temperature hypersensitivity, includes heat or cold hyperalgesia (an increased sensitivity to a normally painful heat or cold stimuli) and heat or cold allodynia (pain due to a heat or cold stimulus that does not normally provoke pain) [2].

With the identification of the thermo-sensitive ion channels, the Transient Receptor Potential (TRP) channels, it is now possible to investigate the pathophysiology of temperature hypersensitivity in neuropathic pain animal models [3]. However, despite the identification of these TRP channels, the pathophysiology of temperature hypersensitivity after peripheral nerve injury remains elusive [4-6], which partly may be attributed to the difficulty in determining temperature hypersensitivity objectively in rodents.

The current method to examine heat or cold hypersensitivity is to measure the time between the first contact of the hind paw with a heat or cold plate and the first paw withdrawal, the so-called 'paw lift' latency [7]. This 'paw lift' technique, however, is not always performed or scored similarly. For example, some reports measure the total number of 'paw lifts' [8], while others measure the cumulative 'paw lifts' [9] or the latency to the first 'paw lift' [9, 10].

The Rotterdam Advanced Multiple Plate (RAMP) is a novel device that measures the preference of the animals to avoid plates with specific temperatures and is therefore an alternative to measuring paw lifts. The RAMP consists of four plates, with always one plate at a comfortable temperature. The temperatures of the other three plates are systematically manipulated during the experiment; subsequently, the preference of the animal for the comfortable plate is used as a measure of temperature hypersensitivity. Thus, the philosophy of the RAMP is that neuropathic pain rats will have a higher preference for the comfortable plate as compared to control rats, avoiding the other colder or hotter plates. By design, the RAMP has a number of theoretical advantages over the paw lift method. Since the animal is free to move, it can avoid painful stimuli. In addition, reflex action does not play a role as it may during paw stimulation in the paw lift technique [11]. Furthermore, since neuropathic pain animal models do not only develop temperature hypersensitivity but also spontaneous pain [12] and hypersensitivity to mechanical stimuli [13, 14], it is uncertain if a 'paw lift' is only caused by temperature hypersensitivity or is also due to the spontaneous pain that might be enhanced during the test. Besides these confounders, there may be intra-individual differences in scoring the paw lift because of the subjective nature of scoring the paw lifts.

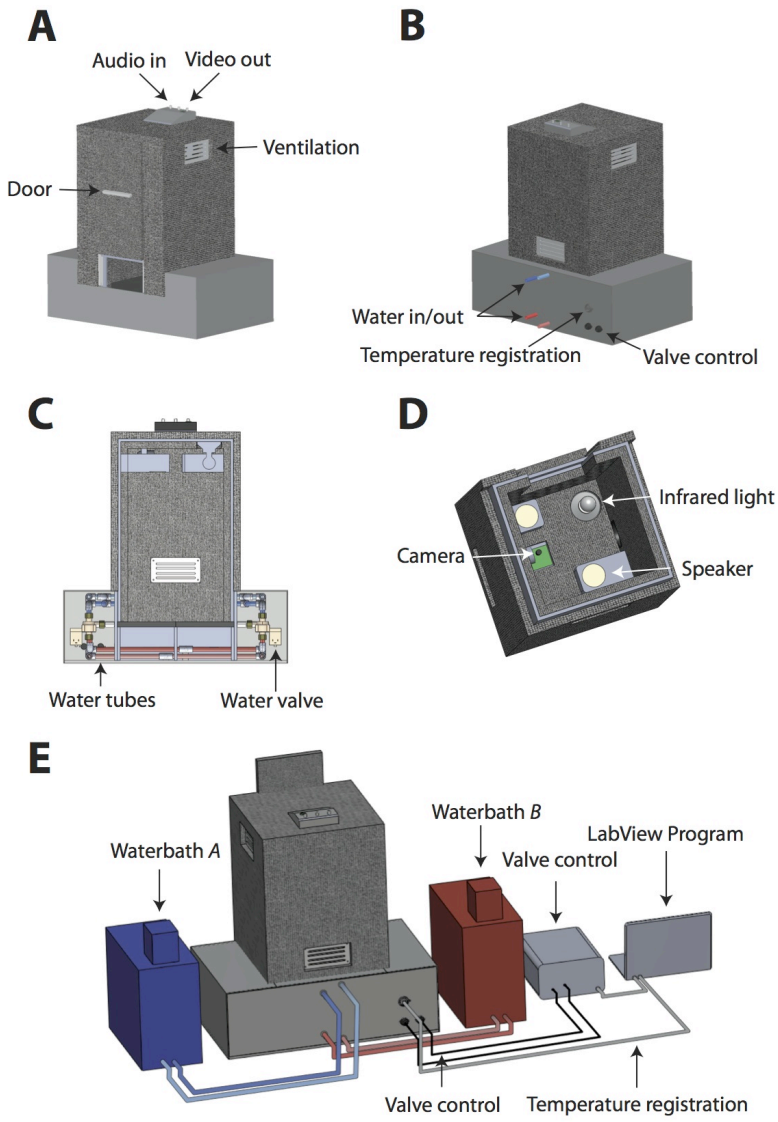

FIGURE 1:

The RAMP consists of two parts, the dark grey box and the four plates, which are connected by water tubes and are suited in a light grey Plexiglas case (Fig. 1A-C). On the roof of the RAMP, wiring is suited which enables plugging of the audio for the speakers and the video output for tracking the rat (Fig. 1A). The light grey base functions as the case for the plates and water tubes. Furthermore, the hardware for the valve control and temperature registration is located here (Fig. 1C). The main purpose of the dark grey box is that it is sound- and lightproof and the camera, which records the movement of the rat, is housed in the box (Fig. 1D). Next to the camera, an infrared light is placed to detect the animal in the dark. In addition, speakers are positioned to produce background noise for the rats during the experiment to minimize stress (Fig. 1D).

In the current study, we used the spared nerve injury (SNI) model [15], which is a well-established neuropathic pain animal model that is known to develop long-term cold and heat hypersensitivity. The hypothesis of the current experiments was that the SNI group would have a higher preference for the comfortable plate as compared to the sham group, indicating that the RAMP can objectively measure hyperalgesia and allodynia for cold and heat in the SNI rat model.

METHODS

All experiments were approved by the Dutch Ethical Committee on Animal Welfare (DEC) and all procedures adhered to the European guidelines for the care and use of laboratory animals (Council Directive 86/6009/EEC). We used 35 Male Wistar rats weighing 250 gram. These were divided into an SNI (n=20) and a sham group (n=15). All 20 SNI rats and 15 sham group rats were used for all the RAMP experiments and were also followed in time, meaning the same animals were used to test for the different time points. Two rats per cage were housed with free access to water and food and maintained on a 12h dark-light cycle.

SNI-SURGERY

Under isoflurane (2%) anesthesia the skin on the left lateral surface of the thigh was incised and the biceps femoris muscle was divided and spread lengthwise to expose the three branches of the sciatic nerve: i.e. the sural, common peroneal and tibial nerves. Two of the three terminal branches, the common peroneal and the tibial nerves were tight ligated with 5.0 silk sutures. Great care was taken to avoid any contact with or stretching of the intact sural nerve. For sham controls we performed the same surgery without the ligatures and lesions, leaving the nerves intact. The skin was sutured and the animals were allowed to recover. In all cases, postoperative analgesia was provided by subcutaneous administration of buprenorphine (0.05-0.1 mg/kg; Temgesic; Schering-Plough BV, Utrecht, the Netherlands). Animals were monitored daily for signs of stress or discomfort but in all cases recovered uneventfully with no autotomy.

PAW LIFT THERMAL TEST

As a reference for the RAMP measurements, we used the conventional paw lift method with the hot and cold plate test device. Before testing, all animals were habituated for 5 days by the same person placing the animals in the box during 10 minutes, with the plates at room temperature. The device consisted of an aluminum plate (21 x 21 cm of surface and 2 cm thick) coiled with PVC tubes that circulated water with 50% methanol diluted and a see-through Plexiglas around it. The rat was

Fig. 1E shows a drawing of the complete set-up of the RAMP. Two water baths (A and B) are connected to the plates to provide circulated water, which is constantly on specific temperatures. Also a power box is suited to provide the water valves of power and to switch the valves between the two water baths by means of the LabView 8.5 program in the computer (Fig. 1E). Also the temperature sensors, which are suited under every plate, are linked to the computer to monitor if the plates have the right temperature (Fig. 1E).

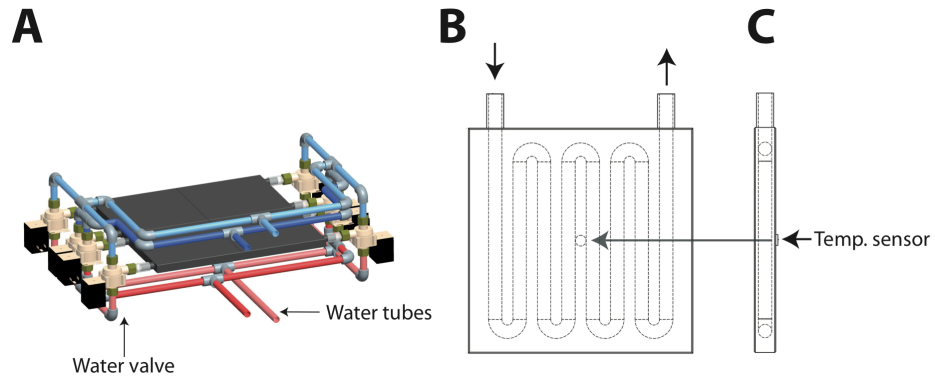

FIGURE 2:

Fig. 2A displays a detailed drawing of the four plates, water valves and water tubes. Each of the eight-water valves is connected to the two water baths and a plate, which enables switching between the two water baths (Fig. 2A). Fig. 2B and C shows a schematic drawing of the internal structure of the plates in transversal and sagittal orientation. The four temperature sensors are placed under each of the four plates in the center point (Fig. 2B and C).

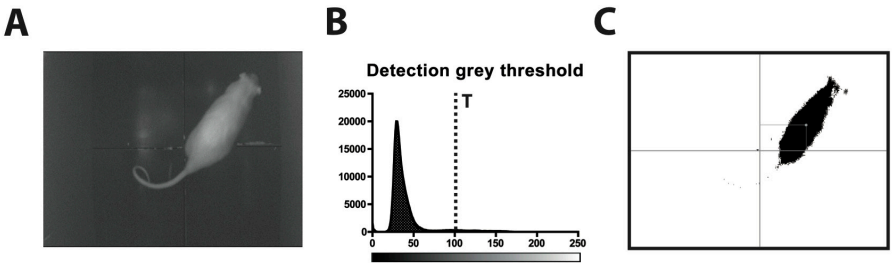

FIGURE 3:

Fig. 3A shows an image acquired with the infrared camera. Fig. 3B depicts the graph on which the threshold is determined (T>100) for detection of the rat. On the Y-axis the amount of pixels are displayed and on the X-axis the gray scale. Finally Fig. 3C shows that, after thresholding, only the rat is visualized. The center location of the rat is used for further data analysis.

placed on the hot (37˚C, 40˚C, 43˚C and 50˚C) or cold plate (5˚C, 14˚C, 17˚C and 19 ˚C). A paw lift was taken as a positive response, which is defined as a quick flutter or flinch of the affected hind paw. The time difference between the start of the paw contact with the plate until a positive response was noted, was called the latency time. A maximum cut off time of 150 seconds was used to prevent tissue damage at the lower and higher temperatures. Each rat was only tested once on any given test day to avoid any possible anesthetic or tissue damage effects that could be produced by repeated exposure to a cold or hot surface. The tester performing the paw withdrawal test was blind to the treatment. In the first week postoperatively we examined the animals daily with the paw lift thermal test. However, because we did not observe evidential differences between the sham and SNI group in the first week, the decision was made to take 1 week as the first time-point post-surgery.

THE ROTTERDAM ADVANCED TEMPERATURE MULTIPLE PLATE (RAMP)

The Rotterdam Advanced Multiple Plate consists of 4 aluminum plates, each 21 x 21 x 2 cm (L x W x H) (Fig. 1). The plates contain fluid channels, which are connected to water bath A and water bath B (both Haake K20) through polyvinyl chloride (PVC) tubes and 8 valves (three way Solenoid valve-dry 3/2 - NC). Each water bath is set at a different electronically controlled temperature (for example: water bath A cold, water bath B warm) in the range from 0 to 50 ˚C (with an accuracy of ± 1 ˚C). Distilled water is continuously pumped through the system at a maximum flow rate of 12,5 L/min and at a maximum pressure of 300 mbar. The valves are controlled by a computer program developed in LabVIEW 8.5 (National Instruments) via a NI-6008 I/O hardware card and solid-state relays to provide power to the valves. A pair of valves for each plate determines from whether water from the warm or cold bath flows through a plate. In this way, each plate adapts the temperature of one of the two water baths homogeneously and fast. In order to avoid learning behavior of the rats, the pairs of three way valves are switched randomly to provide random surface temperatures of the plates. To reduce stress factors for the rats, we built a box surrounding the plates to avoid light and sound entering the box using sound-isolating foam (Fig. 1). Given that complete silence induces stress in rats, we installed speakers in the box to generate background noise (white noise) of 68 dB. The background noise was equal for all animals. The box has two ventilators and louvers for ventilation. We installed an infrared camera and infrared light to track the movements (from above) of the animal. On the front a shutter was placed to access the box.

The plate temperatures are measured with thermocouples (J-type: Fe/Cu-Ni) at the center of each plate (using a MCC DAQ TM USB-TC measuring device) (Fig. 2). The plate temperatures were continuously monitored throughout the experiments with thermocouples with a measuring range from 50 to 250 °C that were isolated from all external conditions. The accuracy of the thermocouples is ± 0,6 ˚C between 15-35

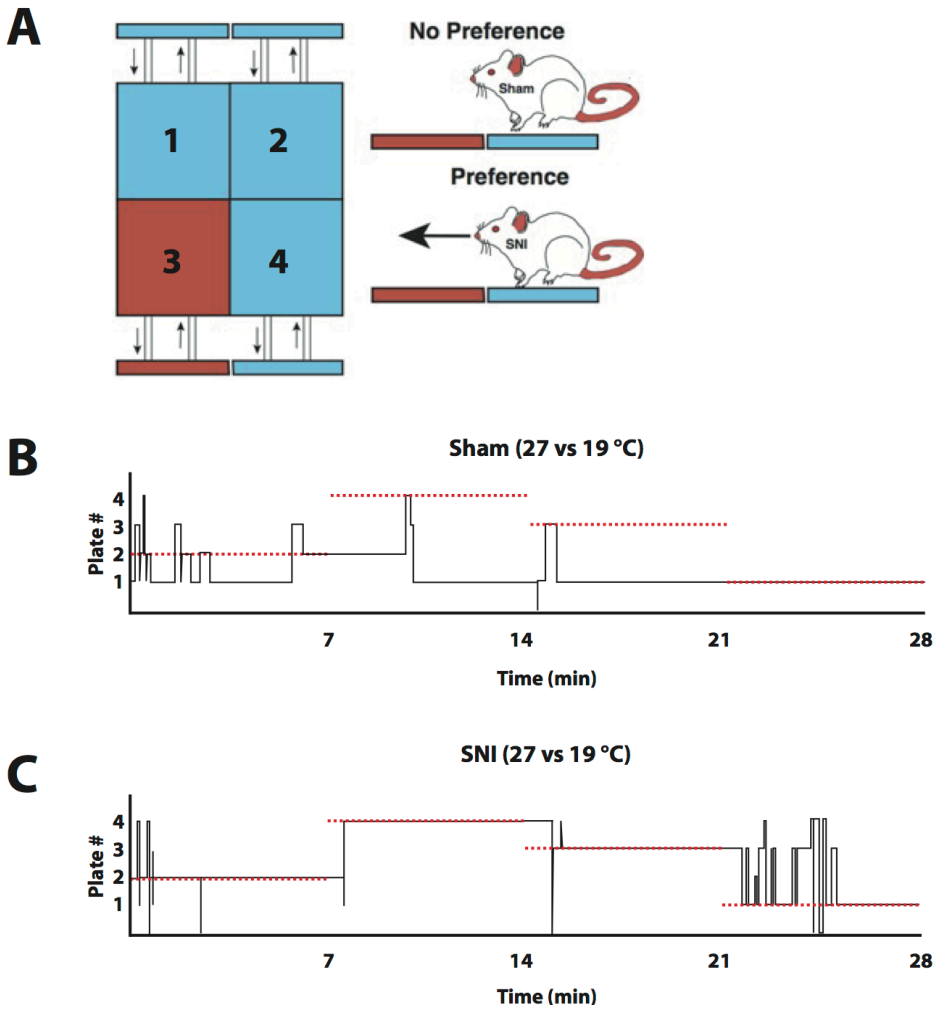

FIGURE 4:

Fig. 4A shows a schematic drawing of the RAMP. There is one comfortable plate (red) and three plates (blue) with a hot or cold temperature. The concept of the RAMP is that the SNI group shows a stronger preference for the comfortable plate. In Fig. 4B we display typical data of a sham and SNI rat (3 weeks postoperatively) during an experiment with the comfortable at 27 °C and the other three plates are 19 °C. The red dotted line displays which plate is at 27 °C and the black line exhibits the location of the SNI or sham rat. It is evident that the SNI rat displays a strong preference for the comfortable plate (27°C) while the sham-treated rat does not show a clear preference for the comfortable plate.

˚C; outside this range the maximum error is ± 1,1 ˚C. To correlate the plate surface temperature to the water bath temperature, the temperature of a water bath was increased in steps of 5 ˚C. The plate temperatures corresponded with the water bath temperatures with a maximum discrepancy of ± 0,5 ˚C.

DIGITAL IMAGE PROCESSING

To determine the position of a rat, grey-scale images acquired by the infrared camera were processed with a technique based on thresholding (Fig. 3). The animal can be separated from the plates because of the contrast between the white animal and the black plates. Each pixel in the image is compared to a threshold grey value: if its value is lower than the threshold, the pixel is considered to be 'background' and is set to white. Otherwise, if its value is higher than the threshold, the pixel is considered to be the 'foreground' and is set to black. If a black object exceeds a predefined minimal object size it is considered to be the animal. The center mass of the animal is calculated and is used as its position on either plate P1, P2, P3 or P4.

RAMP MEASUREMENTS

The rats were tested for temperature hypersensitivity with the RAMP, 5 days a week from week 2 till week 10 postoperatively. Before testing, all animals were habituated for 5 days by the same person by placing the animals in the box for 10 minutes, with the plates at room temperature. During the measurement, one of the four plates is set at the comfortable temperature, while the other three plates have a more uncomfortable temperature. The testing temperatures of the three cold plates for cold allodynia were 14°C or 17°C or 19°C while the remaining comfortable plate was set at 27°C. In cold hyperalgesia testing, we used 5°C as the temperature for the cold plates, with 24°C for the comfortable plate. The paradigm of the RAMP experiments is that one plate has a comfortable plate and the other three plates have a test temperature. In a range of critical temperatures, the sham rats will have no preference for a certain plate, while the SNI rats have a preference for the comfortable plate (Fig. 4A). In Fig. 4B we display typical data of a sham and SNI rat (3 weeks postoperatively) during an experiment with the comfortable on 27 °C and the other three plates are 19 °C. The red dotted line displays which plate is 27 °C and the black line exhibits the location of the SNI or sham rat. It is evident that the SNI rat displays a strong preference for the comfortable plate (27°C) while the sham-treated rat does not show a clear preference for the comfortable plate. For heat allodynia testing, the temperatures of the three hot plates were 35°C or 37°C while the comfortable plate was set at 33°C. The heat hyperalgesia testing was performed at 40°C or 43°C with the comfortable temperature at 33°C. The RAMP plate temperatures for cold and heat allodynia and hyperalgesia in this study were founded on previous literature. These temperatures for evaluating the presence of cold hyperalgesia and allodynia

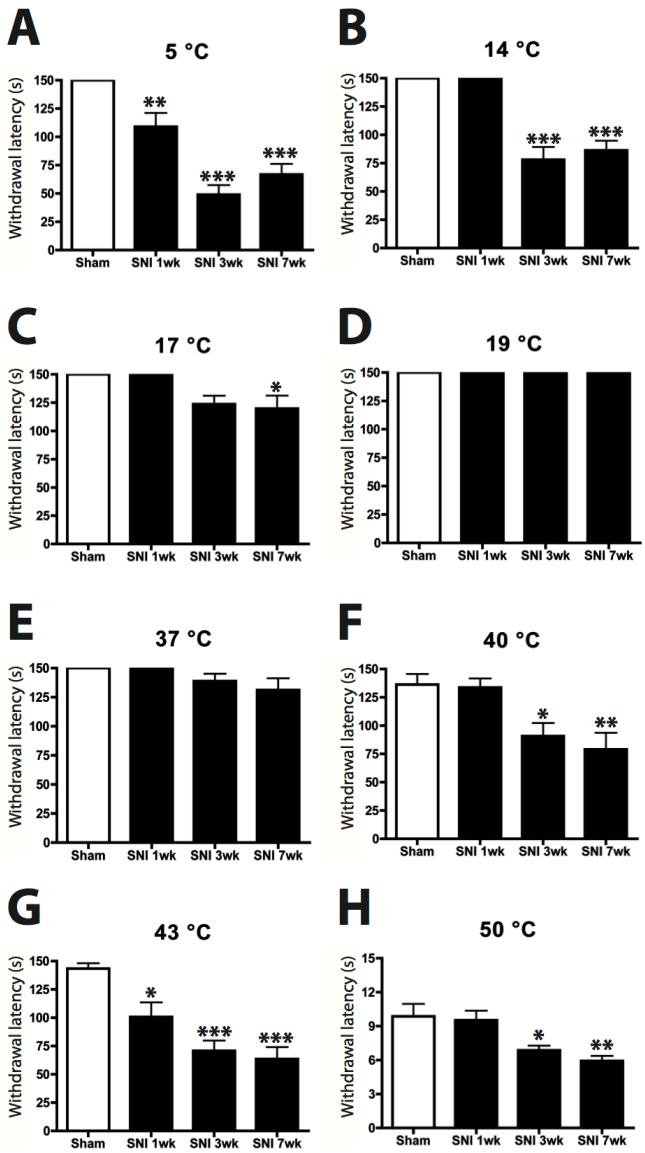

FIGURE 5:

*The results of the paw lift experiment. The Y-axis represents the withdrawal thresholds in seconds and the X-axis displays the different groups tested. The SNI group display a significant lower withdrawal threshold at 5 °C at all the postoperatively time points as compared to the sham group (Fig. 5A). At 14 °C and 17 °C the SNI group shows also a significant lower withdrawal threshold, however only at 3 and 7 weeks for 14 °C and at 7 weeks postoperatively for 17 °C (Fig. 5B and C). During the hot plate test the SNI group showed a significant lower withdrawal threshold for 40 °C (3 and 7 weeks postoperatively), 43 °C (1,3 and 7 weeks postoperatively) and for 50 °C (3 and 7 weeks) as compared to the sham (Fig. 5F-H). SNI: N=15, sham: N=15; *: p<0.05 **: p<0.01 ***: p<0.001*

were based on studies showing that temperatures ≤ 5 °C elicited cold pain in rodent studies [16] and ≥14 °C was presumed to be innocuous [10, 17]. For the RAMP heat testing, we chose 37 °C as innocuous heat temperature [8], and ≥ 40 °C for heat pain [8, 18]. The comfortable temperatures 27 °C and 33 °C were chosen based on the paper which described the double plate technique [17], in which the comfortable plate was set at 30 °C. However, when we used 30 °C as the comfortable plate for the cold allodynia test we observed that the sham-treated rats also exhibited a higher preference for the comfortable plate as opposed to the 27 °C (Supplementary Fig. 1). A similar phenomenon applies for the heat allodynia test. When we used the 30 °C as the comfortable plate for the heat allodynia test we observed that the sham-rats showed a higher preference for the comfortable plate as opposed to the 33 °C when the hot plate was set at 35°C. An explanation for this may be that rats have more difficulty losing their heat through their tail at 33 °C as compared to 30 °C.
The plate temperatures are switched every 7 minutes and each of the four plates is switched on once as the comfortable temperature, resulting in three switches and a total measuring time of 28 minutes. The switches were performed randomly for every experiment, therefore none of the animals had the same order of location for the comfortable plate during all RAMP experiments. To investigate the importance of the temperature plate switches in the RAMP experiments, we repeated the experiment but with a 5-minute duration and without switching the location of the comfortable plate.

ANALYSIS

After placing the animal in the box, the preference for the comfortable temperature was measured. For the analysis, a computer program was developed in Labview 8.5 and Labview Vision 10.0 to measure the preference of an animal by comparing the configuration of the plates and the position of an animal in time. With the program we switched the temperatures of the plates every 7 minutes. Meanwhile, we tracked the location of the animal and determined whether an animal is on a comfortable plate or on a non-comfortable plate. Simultaneously, the data output was given as a text file. We analyzed this data with custom-made software in Python. This program analyzed the total percentage that the animal spent on the comfortable plate and the number of switches, which is the number of crossings over the particular plates. All the experiments were tested with the One-way ANOVA. If there was a significant main effect, a Bonferroni-corrected post-hoc was performed. The values are means ± SEM and $p<0.05$ was taken as significant.

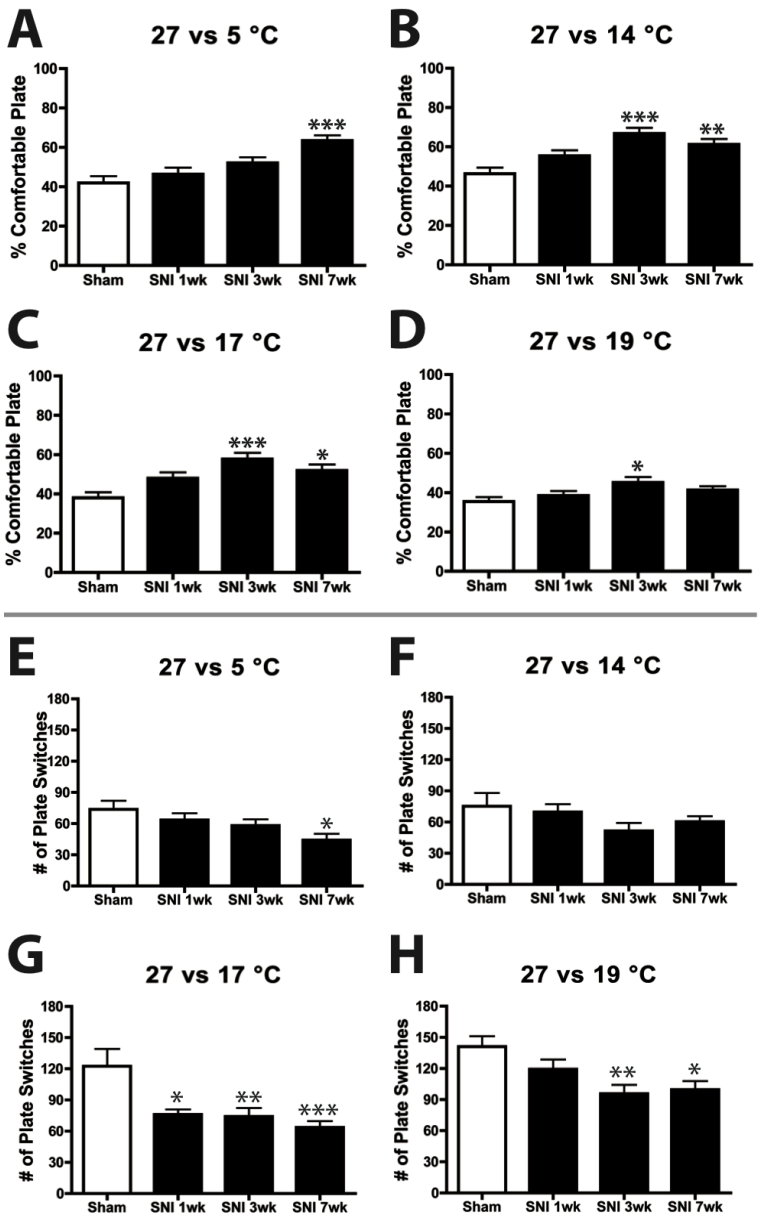

FIGURE 6:

*Fig. 6A-D: The total time (%) spent on the comfortable plate during the RAMP cold test. The SNI group showed a significant stronger preference for the comfortable plate (27°C) at 5 °C (7 weeks postoperatively), 14 °C (3 and 7 weeks postoperatively), 17 °C (3 and 7 weeks postoperatively) and 19 °C (3 weeks postoperatively) compared to the sham group. Fig. 6E-F: Number of switches during the RAMP cold test, indicating that when the SNI group show a preference for the comfortable plate (27°C), they display less switches as compared to the sham group (Fig. 6E-F). SNI: N=20, sham=15. *: p<0.05 ** : p<0.01 *** : p<0.001*

RESULTS

PAW LIFT THERMAL TEST

During the cold paw lift experiments, a reference was used to determine if the SNI group indeed developed cold and heat hypersensitivity. We found that the SNI group had a significantly ($p<0.01$) reduced paw withdrawal latency at 5 °C at all postoperatively time-points compared to the sham group (Fig. 5). At 14 °C, there was a significantly ($p<0.001$) lower paw withdrawal latency at 3 and 7 weeks postoperatively. At 17 °C, at 3 and 7 weeks postoperatively, the SNI group had a decreased paw withdrawal latency as compared to the sham group, however this was only significantly ($p<0.05$) for 7 weeks postoperatively. No paw withdrawal reactions during the 150 seconds of the experiment at 19 °C where observed. During the hot plate experiments, the SNI group showed a significantly reduced paw withdrawal latency at 40 °C (3 and 7 weeks postoperatively), 43 °C (all postoperatively time-points) and 50 °C (3 and 7 weeks postoperatively) ($p<0.05$) (Fig. 5).

TECHNICAL VALIDATION OF THE RAMP TEMPERATURES

During the RAMP experiments, the plate surface temperatures adjusted to the target temperatures with a maximum discrepancy of 1.0 ˚C (Supplementary Fig. 2). After every switch, the temperature of the aluminum plates adjusted in less than one minute to the new temperature. The adjustment time was slightly shorter in the heat experiments compared to the cold experiments.

RAMP COLD TESTING

Based on the percentage of time that the animals were on the comfortable plate, we found that the SNI group had a significant higher preference for the comfortable plate after 7 weeks at 5 °C ($p<0.001$) than the sham group (Fig. 6). The sham group also had an increased preference for the comfortable plate at 5 °C compared to 14 °C ($p<0.05$) (Fig. 6 A-D). At 14 °C and 17 °C we found a significantly ($p<0.001$) higher preference for the comfortable plate in the SNI group after 3 and 7 weeks compared to the sham group. The SNI group also showed a significantly ($p<0.05$) higher preference for the comfortable plate compared to the sham group at 19 °C after 3 weeks. In the results of the RAMP experiments, we find a transient increase in time in the preference for the comfortable plate of the SNI group at 5 °C, whereas the preference for the comfortable plate in the SNI group at the temperatures 14 °C, 17 °C and 19 °C only show a peak after 3 weeks.

We saw a decrease in the number of switches as the preference for the comfortable plate increased in the SNI group (Fig. 6 E-H). At 5°C, the number of switches in the SNI group was significantly smaller than in the sham group after 7 weeks ($p<0.05$).

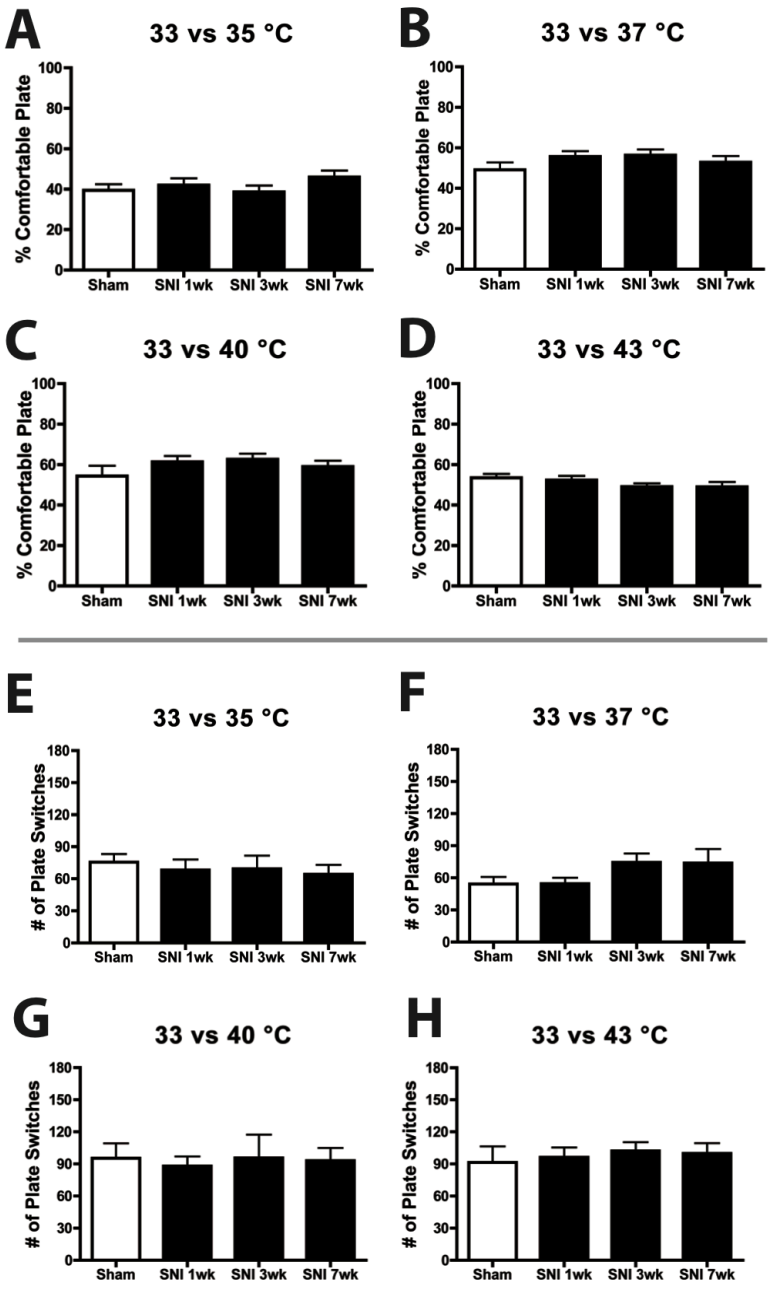

FIGURE 7:

*Fig. 7 A-D: The total time (%) spent on the comfortable plate during the RAMP heat test. No significant higher preference for the SNI group as compared to the sham groups was found at all postoperatively time points. Fig. 7E-H: The numbers of switches during the RAMP heat test. There were no differences between the number of switches between the SNI and sham group (Fig. 7E-H). SNI: N=20, sham: N=15. *: p<0.05 ** : p<0.01 *** : p<0.001*

At 17°C, we saw a significantly ($p<0.05$) decreased number of switches in the SNI group compared to the sham group at all postoperatively time-points and at 19 °C, we saw a significantly ($p<0.01$) smaller number of switches in the SNI group after 3 and 7 weeks.

RAMP HEAT TESTING

We saw higher preferences for the comfortable plate in the sham group during heat experiments compared to the sham group showed for the comfortable plate during cold experiments. During our heat experiments with the RAMP we saw a tendency at 37 °C and 40 °C towards a higher preference for the comfortable plate in the SNI group compared to the sham group (Fig. 7 A-D). We found no significant differences in the numbers of switches in the SNI group compared to the sham group in heat experiments (Fig. 7 E-H).

RESULTS OF THE RAMP WITHOUT TEMPERATURE PLATE SWITCHES

The preference of the SNI group for the comfortable plate was not significantly different from the control group in the 5–minute experiment in which the location of the comfortable plate was not altered, except for a significant increase in the SNI group at 17°C after 3 weeks ($p<0.05$) (Fig. 8). During the heat experiments, we did not find any significant differences between the preference of the SNI group and the sham group (Fig. 8).

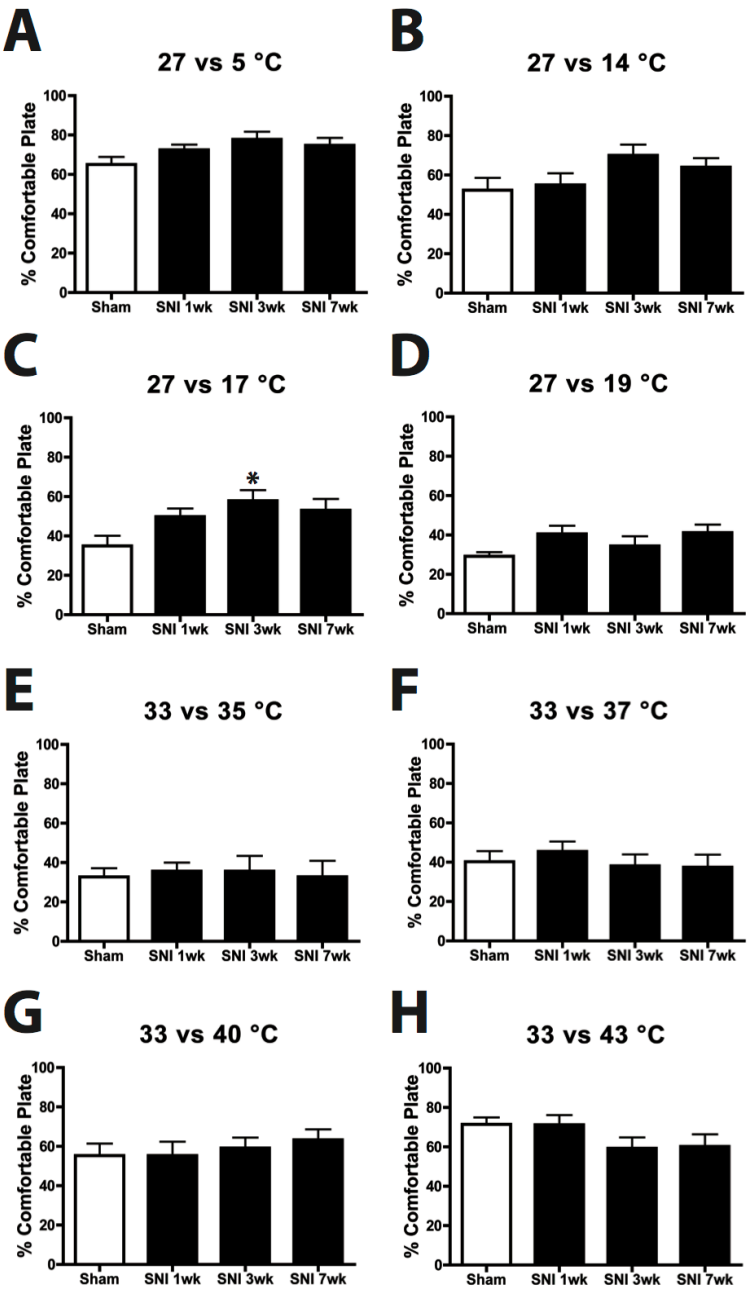

FIGURE 8

*In the current figure, the first seven minutes from the RAMP are displayed without switches. There is only during the 27 °C vs. 17 °C at 3 weeks postoperatively a higher preference for the SNI group as compared to the sham group. During the RAMP heat test there was also no higher preference for the SNI group. SNI: N=20, sham: N=15 *: p<0.05 **: p<0.01 ***: p<0.001*

DISCUSSION

In this study, we introduced a novel universal device, the RAMP, to measure temperature sensitivity in freely behaving rats. The RAMP measures the preference of the rats for plates with specific temperatures and is an alternative for measuring the flexion-reflex after a temperature stimulus of the affected hind paw in the commonly used paw lift test. The RAMP measurement is based on a precisely controlled environment, excluding interfering noise and light from outside. To evaluate the ability of the RAMP to detect changes in temperature sensitivity, we used the SNI-model, which is known to display cold and heat hypersensitivity, as was confirmed with the paw lift method in the present study. The main findings with the RAMP were that 1) the SNI group displayed a transient peak in cold allodynia (measured at 19-14°C) at 3 weeks postoperatively, still persisting at 7 weeks postoperatively (17 and 14°C), 2) the SNI group showed a slowly developing cold hyperalgesia (measured at 5°C) that emerged at 7 weeks postoperatively 3) the number of plate switches that the rats made decreased when the rats had a higher preference for the comfortable plate during cold testing, which only applies to 17 °C and 19 °C and not to 14 °C. A possible explanation might be that at lower temperatures the sham rats show less movement to conserve energy and heat, therefore showing the same amount of switches as the SNI group at 14 °C. Finally 4) while the SNI group did display heat hypersensitivity during the paw withdrawal test, we did not find differences in heat allodynia or hyperalgesia with the RAMP between SNI and the sham group.

While in the last two decades several research paradigms have been designed to test thermal sensitivity in rodents based on measuring a paw reflex, these methods all have important limitations. The most common method is assessing the paw withdrawals responses from a cold or hot plate, as was also performed in the current study as a control measure. However, as discussed in the Introduction, this method has a number of limitations. It does not reflect directly thermal pain perception but more a spinal reflex [11, 19]. Furthermore, spontaneous pain and mechanical hyperalgesia and allodynia, may also influence the paw withdrawal, which neuropathic animal models also experience [12, 13, 20]. Another extensively-used evaluation method for cold sensitivity in rodents is simulating cooling by evaporation of acetone [21, 22] or ethyl chloride [23] and measuring subsequent paw elevations. In the original paper [15] in which the SNI model is described, it was shown that the SNI-rats presented symptoms of cold allodynia as early as one day post-surgery by means of the acetone test. However, the rate of evaporation of acetone or ethyl chloride is difficult to standardize, because of confounding factors like ambient and body temperature of the rodents. In addition, the liquid may cause a chemical, olfactory or mechanical

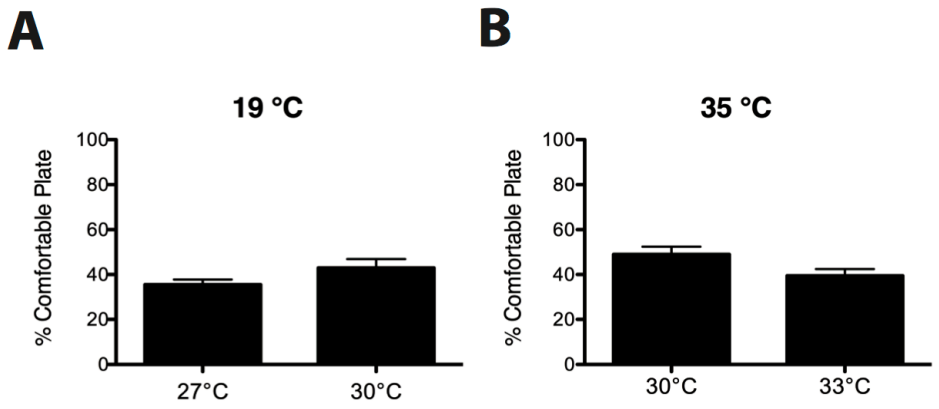

SUPPLEMENTARY FIGURE 1

Supplementary Fig. 1A shows the preference of sham rats during the RAMP cold test when the testing temperature is at 19 °C and the comfortable plate at 27 °C or 30 °C. The sham rats have a slightly higher preference for the 30 °C plate as opposed to the 27 °C plate during the testing temperature 19 °C. In Supplementary Fig. 1B the same experiment has been performed only then the testing temperature was set at 35 °C and the comfortable plates at 30 °C and 33 °C. When 30 °C was used as the comfortable plate for the heat allodynia test we observed that the sham-rats showed a higher preference for the comfortable plate as opposed to the 33 °C as compared to the hotter plate (35°C).

stimulus that could, independent of the temperature, provoke a flexion reflex [10]. In the current study, we found that the SNI-rats did not elicit any paw withdrawal reaction in the first week postoperatively during examination of cold allodynia, which makes the development of cold allodynia in the first day postoperatively unlikely. A third method is assessing the dipping of the animals foot in cooled water and measuring the reflex [24, 25]. However, this may produce high levels of stress, which in turn can change behavioral reflex responses in neuropathic pain models [26].

As an alternative to paw lift testing, systems have been developed that measure the preference of a rodent for a certain temperature, similar to the RAMP. The Escapetest, measures latency and duration of escape from a compartment where the floor is heated or cooled [19]. However, during the Escapetest, control rats showed similar escape latencies for 1 °C and 20 °C floors, implicating that these rats escaped in similar fashion form a noxious or an innocuous temperature [19]. A confounding factor, which may explain these results, is that these animals are conditioned to escape. Therefore, in RAMP experiments, the comfortable plate is switched randomly every 7 minutes to exclude conditioning. The double plate test has some similarity to the RAMP. However, this technique uses only two plates instead of four and the preference is measured during 5 minutes without switching the location of the cold or warm plate [17]. Walczak and Beaulieu et al. found on the double plate that neuropathic pain mice, due to chronic constrictive injury of the sciatic nerve (CCI), had a higher preference for the comfortable plate (31°C) than for the cold plates (22 °C and 18 °C) [17]. In the present study, we tested the same paradigm as in the double plate technique by excluding the plate switches in the RAMP and measuring for only 5 minutes. In contrast to the previous study [17], however, we did not find a stronger preference in the SNI-treated rats for the comfortable plate compared to the sham group for both cold and heat temperatures. While both studies use different species (mice vs. rat) and different neuropathic pain models (CCI vs. SNI), a more essential difference may be the use of more plates and randomized plate selection, reducing chance migration of the animal to the comfortable plate and reducing conditioning for specific plates. A possible explanation for the difference between behavior with or without alteration of the location of comfortable plate is the preference of the sham-treated rats. During the first explorative minutes the sham-treated rats may have a higher preference for the comfortable plate as compared to the colder plates, reducing the difference in preference between the sham and SNI rats for the comfortable plate. When the location of the comfortable plate is altered, aversion for the other three plates is tested, showing a difference in behavior between the SNI-rats and the sham-rats. Another explanation might be that the SNI rats instinctively show explorative behavior due to the fact that they do not remain constantly on the comfortable plate. It may take several seconds for SNI rats to perceive noxious stimuli as painful, therefore making it possible to explore also the remaining three plates

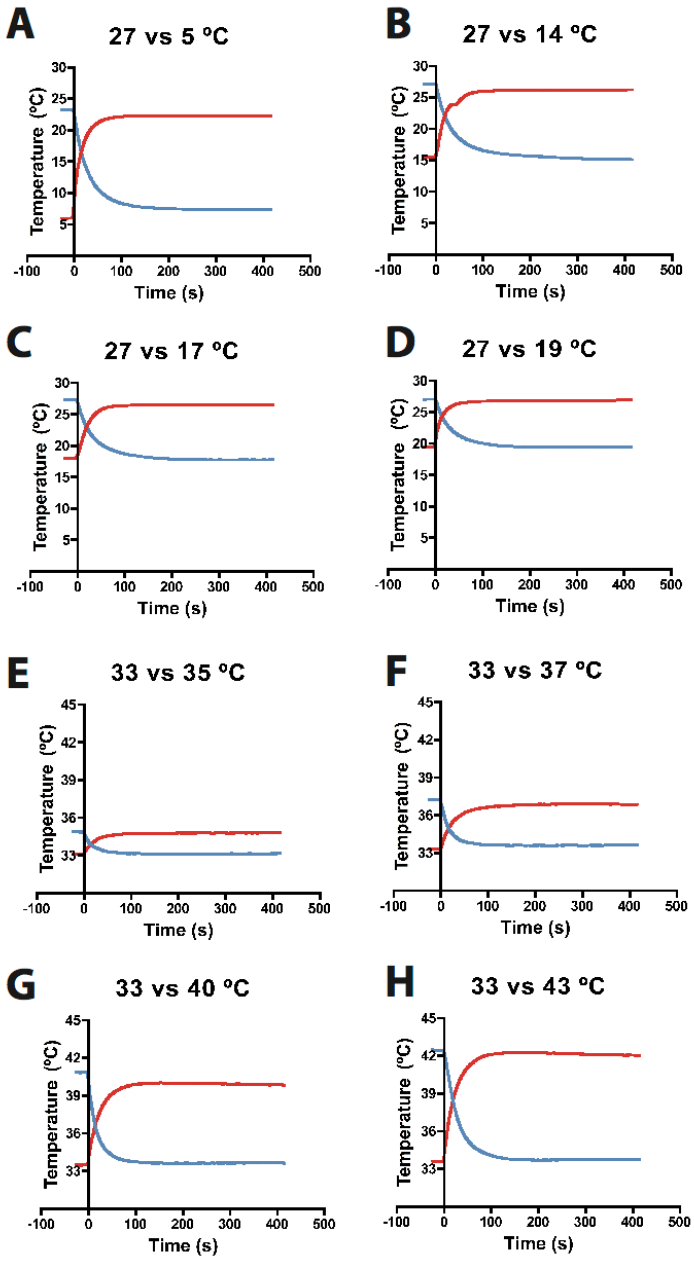

SUPPLEMENTARY FIGURE 2

The temperature adjustment times of the RAMP plates after a switch. The red line in Supplementary Fig. 2 A-D represents the plate that is switched to 27 °C and the blue line represents the plates that are switched to the colder temperatures. In Fig. 2 E-H, the red line characterizes the plate that was 33 °C, which is switched to hotter temperatures and the blue line represents the plate that is switched to 33°C.

that result in less preference for the comfortable plate. However, if the location of the comfortable plate is altered, SNI rats are forced to move and hence have less explorative behavior, which explains partly the difference between with or without alteration of the comfortable plate.

The presence of cold allodynia and hyperalgesia in the SNI model is in line with previous studies on this model [15, 10, 27] and with other neuropathic [4, 28] and inflammatory models [7]. The SNI-treated rats show a tendency towards a higher preference at 3 weeks postoperatively during the 5 °C test and a significant higher preference at 7 weeks after surgery. This suggests that SNI-treated animals develop cold hyperalgesia only at 7 weeks postoperatively, while with the paw lift method they exhibit lower paw withdrawal latency after 1 week as compared to the sham group. An explanation for this discrepancy may be that the heightened flexion-reflex in the SNI-rats at 1 week postoperative may present in an early stage of neuropathic pain.
We were unable to detect heat hyperalgesia or allodynia with the RAMP although a trend was present. Interestingly, there are no reports of heat allodynia in nerve injury-induced neuropathic pain rodents due to peripheral nerve injury, while there is clear evidence that these animals develop cold allodynia. An explanation might be that thresholds for innocuous heat and heat pain lie more closely together than for cold in rodents. For example, it has been shown that at >39 °C, control rats experience heat pain while rats with inflammatory pain already had a response at 37 °C 8, a reduction of 2 °C. In comparison, with cold plate test, control rats experience cold pain at 5 °C while inflammatory and neuropathic pain rats have a positive response threshold at 15 °C [8, 10], showing a difference of 10 °C. Also, the findings that we were not able to measure heat hyperalgesia with the RAMP might be explained by the heightened preference of the sham-treated rats for the comfortable plate, therefore being unable to detect a difference. Some reports used 50 °C to measure heat hyperalgesia with the paw lift method [29, 30], as we also did in the current study, lasting only 15 seconds to prevent any foot sole damage. However, when we performed a 50 °C experiment with the RAMP, we noticed that both SNI and sham rats displayed an immense degree of stress due to which detection of a comfortable plate was not possible.

The RAMP device also has limitations. A first limitation is that we cannot compare the ipsi- and contralateral sides. However, it is known that neuropathic pain model induced by a nerve injury can lead to contralateral neuropathic pain-like symptoms, also known as mirror image pain [31, 32]. Therefore, the contralateral side is not applicable as a control parameter in neuropathic pain models. Another limitation of the RAMP is that the rats may rest there neuropathic hind paw on the comfortable plate and the other paws on the other plates, which would be detected in our analyses

as preferring the uncomfortable plates. However, in general, we observed that rats preferred the corners of the box, which is typical for rodents. In these locations, these errors cannot occur. A third important limitation is that a RAMP experiment takes more time (approximately 30 minutes) compared to the paw lift test (about 5 minutes). However, the RAMP has the advantage of being automated while the paw lift method is not.

CONCLUSION

The RAMP was made light- and soundproof with background noise creating a reproducible environment for noise, sight and smell, reducing stress for the animals. Furthermore, during RAMP experiments, rodents can escape possible painful stimuli, in accordance with ethical guidelines and minimizing suffering of animals. In conclusion, we have developed a novel device for objectively assessing cold hyperalgesia and allodynia in a completely controlled environment in freely behaving rats.

REFERENCES

1.
Baron, R., Mechanisms of disease: neuropathic pain--a clinical perspective. Nat Clin Pract Neurol 2006; 2(2): 95-106.

2.
Coutaux, A., Adam, F., Willer, J.C., and Le Bars, D., Hyperalgesia and allodynia: peripheral mechanisms. Joint Bone Spine 2005; 72(5): 359-71.

3.
Caterina, M.J., Transient receptor potential ion channels as participants in thermosensation and thermoregulation. Am J Physiol Regul Integr Comp Physiol 2007; 292(1): R64-76.

4.
Katsura, H., Obata, K., Mizushima, T., et al., Antisense knock down of TRPA1, but not TRPM8, alleviates cold hyperalgesia after spinal nerve ligation in rats. Exp Neurol 2006; 200(1): 112-23.

5.
Fleetwood-Walker, S.M., Proudfoot, C.W., Garry, E.M., et al., Cold comfort pharm. Trends Pharmacol Sci 2007; 28(12): 621-8.

6.
Xing, H., Chen, M., Ling, J., Tan, W., and Gu, J.G., TRPM8 mechanism of cold allodynia after chronic nerve injury. J Neurosci 2007; 27(50): 13680-90.

7.
Jasmin, L., Kohan, L., Franssen, M., Janni, G., and Goff, J.R., The cold plate as a test of nociceptive behaviors: description and application to the study of chronic neuropathic and inflammatory pain models. Pain 1998; 75(2-3): 367-82.

8.
Yalcin, I., Charlet, A., Freund-Mercier, M.J., Barrot, M., and Poisbeau, P., Differentiating thermal allodynia and hyperalgesia using dynamic hot and cold plate in rodents. J Pain 2009; 10(7): 767-73.

9.
Tanimoto-Mori, S., Nakazato-Imasato, E., Toide, K., and Kita, Y., Pharmacologic investigation of the mechanism underlying cold allodynia using a new cold plate procedure in rats with chronic constriction injuries. Behav Pharmacol 2008; 19(1): 85-90.

10.
Allchorne, A.J., Broom, D.C., and Woolf, C.J., Detection of cold pain, cold allodynia and cold hyperalgesia in freely behaving rats. Mol Pain 2005; 1: 36.

11.
Borszcz, G.S., Johnson, C.P., Anderson, M.E., and Young, B.J., Characterization of tailshock elicited withdrawal reflexes in intact and spinal rats. Physiol Behav 1992; 52(6): 1055-62.

12.
Wang, L.X. and Wang, Z.J., Animal and cellular models of chronic pain. Adv Drug Deliv Rev 2003; 55(8): 949-65.

13.
Mogil, J.S., Animal models of pain: progress and challenges. Nat Rev Neurosci 2009; 10(4): 283-94.

14.
Mogil, J.S., Graham, A.C., Ritchie, J., et al., Hypolocomotion, asymmetrically directed behaviors (licking, lifting, flinching, and shaking) and dynamic weight bearing (gait) changes are not measures of neuropathic pain in mice. Mol Pain 2010; 6: 34.

15.
Decosterd, I. and Woolf, C.J., Spared nerve injury: an animal model of persistent peripheral neuropathic pain. Pain 2000; 87(2): 149-58.

16.
Desmeules, J.A., Kayser, V., Weil-Fuggaza, J., Bertrand, A., and Guilbaud, G., Influence of the sympathetic nervous system in the development of abnormal pain-related behaviours in a rat model of neuropathic pain. Neuroscience 1995; 67(4): 941-51.

17.
Walczak, J.S. and Beaulieu, P., Comparison of three models of neuropathic pain in mice using a new method to assess cold allodynia: the double plate technique. Neurosci Lett 2006; 399(3): 240-4.

18.
Yeomans, D.C. and Proudfit, H.K., Nociceptive responses to high and low rates of noxious cutaneous heating are mediated by different nociceptors in the rat: electrophysiological evidence. Pain 1996; 68(1): 141-50.

19.
Mauderli, A.P., Acosta-Rua, A., and Vierck, C.J., An operant assay of thermal pain in conscious, unrestrained rats. J Neurosci Methods 2000; 97(1): 19-29.

20.
Klusakova, I. and Dubovy, P., Experimental models of peripheral neuropathic pain based on traumatic nerve injuries - an anatomical perspective. Ann Anat 2009; 191(3): 248-59.

21.
Vissers, K. and Meert, T., A behavioral and pharmacological validation of the acetone spray test in gerbils with a chronic constriction injury. Anesth Analg 2005; 101(2): 457-64, table of contents.

22.
Carlton, S.M., Lekan, H.A., Kim, S.H., and Chung, J.M., Behavioral manifestations of an experimental model for peripheral neuropathy produced by spinal nerve ligation in the primate. Pain 1994; 56(2): 155-66.

23.
Hama, A.T., Capsaicin-sensitive primary afferents mediate responses to cold in rats with a peripheral mononeuropathy. Neuroreport 2002; 13(4): 461-4.

24.
Perrot, S., Attal, N., Ardid, D., and Guilbaud, G., Are mechanical and cold allodynia in mononeuropathic and arthritic rats relieved by systemic treatment with calcitonin or guanethidine? Pain 1993; 52(1): 41-7.

25.
Pizziketti, R.J., Pressman, N.S., Geller, E.B., Cowan, A., and Adler, M.W., Rat cold water tail-flick: a novel analgesic test that distinguishes opioid agonists from mixed agonist-antagonists. Eur J Pharmacol 1985; 119(1-2): 23-9.

26.
Alexander, J.K., DeVries, A.C., Kigerl, K.A., Dahlman, J.M., and Popovich, P.G., Stress exacerbates neuropathic pain via glucocorticoid and NMDA receptor activation. Brain Behav Immun 2009; 23(6): 851-60.

27.
Zhao, C., Chen, L., Tao, Y.X., et al., Lumbar sympathectomy attenuates cold allodynia but not mechanical allodynia and hyperalgesia in rats with spared nerve injury. J Pain 2007; 8(12): 931-7.

28.
Vierck, C.J., Acosta-Rua, A.J., and Johnson, R.D., Bilateral chronic constriction of the sciatic nerve: a model of long-term cold hyperalgesia. J Pain 2005; 6(8): 507-17.

29.
Plone, M.A., Emerich, D.F., and Lindner, M.D., Individual differences in the hotplate test and effects of habituation on sensitivity to morphine. Pain 1996; 66(2-3): 265-70.

30.
Le Bars, D., Gozariu, M., and Cadden, S.W., Animal models of nociception. Pharmacol Rev 2001; 53(4): 597-652.

31.
Huang, D. and Yu, B., The mirror-image pain: an unclered phenomenon and its possible mechanism. Neurosci Biobehav Rev 2010; 34(4): 528-32.

32.
Koltzenburg, M., Wall, P.D., and McMahon, S.B., Does the right side know what the left is doing? Trends Neurosci 1999; 22(3): 122-7.

10

DISCUSSION

DISCUSSION

In this thesis, we have investigated peripheral thermoregulation by determining the cold-induced vasodilatation (CIVD) and rewarming patterns in rats with neuropathic pain during exposure to cold temperatures (chapter 2 and 3). Further, by employing immunohistochemistry, the innervation patterns of peptidergic, non-peptidergic and myelinated fibers in the epidermis and upper dermis were determined in rats with post-traumatic nerve injury by using the the Spared Nerve Injury (SNI) model (chapter 4, 5 and 6) (Fig.1). In addition, the reinnervation patterns of peptidergic, non-peptidergic and myelinated nerve fibers were investigated in the hind paw of rats with sciatic nerve transection after different methods of nerve reconstruction (chapter 7 and 8). Finally, we developed a novel device in order to improve the assessment of cold allodynia and hyperalgesia in rats with post-traumatic nerve injury (SNI model) (chapter 9).

In the following general discussion, we will first discuss the use of different animal models for investigating reinnervation patterns in the skin of rats with neuropathic pain (section 10.1). Next, we will focus on peripheral thermoregulation in the hind paws of rats with cold intolerance (section 10.2). Also the changes in the skin reinnervation of peptidergic, non-peptidergic and myelinated fibers (section 10.3), the role of uninjured fibers adjacent to injured fibers (section 10.3), sprouting mechanisms (section 10.4) and mirror image pain (section 10.5) in post-traumatic neuropathic pain rats will be reviewed. Additionally cutaneous reinnervation patterns of peptidergic, non-peptidergic and myelinated fibers will be elaborated after different methods of nerve reconstruction (section 10.6). Finally, we will focus on the Rotterdam Advanced Multiple Plate (RAMP) (section 10.7), a novel device to measure cold hypersensitivity in rodents. This discussion will end with our view on future perspectives (section 10.8) on the use of skin biopsies in diagnosing and distinguishing different forms of neuropathic pain in a bench-to-bedside approach.

10.1. ANIMAL NEUROPATHIC PAIN MODEL FOR SKIN FIBER RESEARCH

In the last three decades, several animal models of neuropathic pain have been developed. One of the first was developed by Bennet and Xie (1988) [1] who described the chronic constrictive injury (CCI) model [1]. The CCI model is based on four catgut ligatures loosely tied around the sciatic nerve in rats, resulting in behavioral signs consistent with neuropathic pain, such as protective behavior and hypersensitivity to thermal (cold and heat) and mechanical stimuli. However, a drawback of this model is that the four loosely tied catgut ligatures may induce a variable inflammation that results in intra-neural edema and a subsequent secondary strangulation of the sciatic nerve [2-5]. In the CCI model therefore, it is difficult to attribute both behavior

suggestive of neuropathic pain, as well as concurrent changes in skin nerve fibers to only inflammation, nerve injury or a combination of both factors. For example, it has been found that rats with inflammatory pain in the hind paws induced by Complete Freud's Adjuvant (CFA) show similar sensory fiber sprouting patterns as in the CCI neuropathic pain model [6]. Consequently it cannot be excluded that the morphological changes observed in the CCI model, at least to some extent, might be caused by inflammation. Further, in order to quantify changes in peripheral nerve fibers, it is essential to make use of a highly reproducible neuropathic pain model ensuring consistent changes in the periphery. The CCI model results in highly variable neuropathic pain symptoms, which are related to variability in the tightness of the four ligatures around the sciatic nerve [7]. Finally, in the CCI model, it is difficult to determine to what extent the changes in the distribution patterns of skin nerve fibers are due to reinnervation by injured fibers or to collateral sprouting of uninjured fibers from adjacent areas. Therefore, in our opinion the CCI model is unreliable for investigating skin nerve fibers in neuropathic pain.

In recent years, other neuropathic pain models have been developed that are more favorable for skin nerve fiber research. For example, the spinal nerve ligation (SNL) [8] model, in which one or more spinal nerves (L5-L6) are ligated, and the spared nerve injury (SNI) [9] model, for which the common peroneal and tibial branches of the sciatic nerve are ligated and cut while the sural nerve branch is spared. The procedures used in the SNL and SNI models are highly reproducible, and both consistently result in the development of long-term spontaneous pain, and hypersensitivity to thermal and mechanical stimuli. Further, these neuropathic pain models are based solely on axonotomy, thus excluding inflammation of the injured nerve in the development of neuropathic pain. In addition, since the innervation areas of a rat foot sole are rather sharply demarcated [10, 11], it is in these models also possible to distinguish whether the changes in the skin nerve fibers involve injured fibers or adjacent uninjured nerve fibers.

In conclusion, the SNL and SNI models are both suitable for skin nerve fiber research. In the current thesis, we have made use of the SNI model rather that the SNL model. The latter model, due to ligation of the spinal nerves at different sites, i.e. pre-ganglionic vs. post-ganglionic, and crush vs. nerve ligation have been shown to result in different neuropathic pain symptoms in rodents [12, 13]. In addition, it has been shown that the SNI model develops a more severe form of neuropathic pain as compared to the SNL model [14].

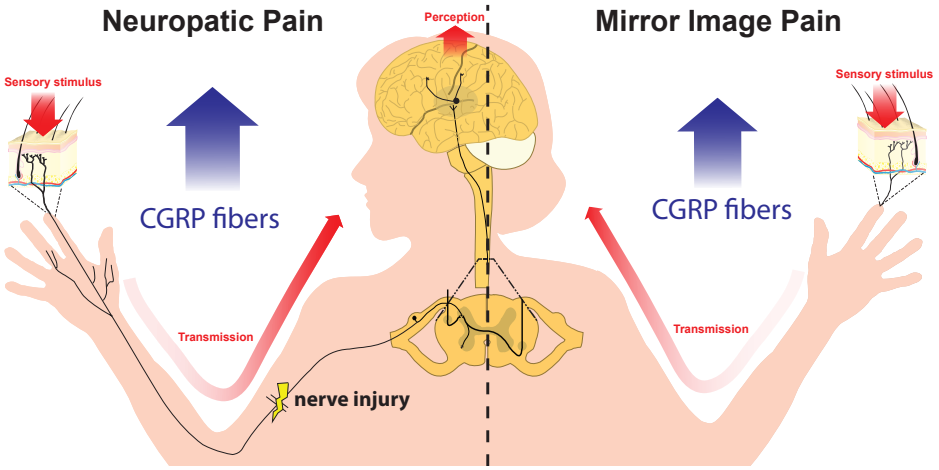

FIGURE 1:

Uninjured peptidergic CGRP fibers demonstrate the most profound alterations in their innervation pattern after ipsilateral induction of neuropathic pain, due to partial nerve injury, as compared to other subgroups of sensory fibers (Substance P, NF-200 and P2X3). Additionally, an increase in skin CGRP neuropeptide content on the contralateral side after ipsilateral induction of neuropathic pain might play a pivotal role in the pathophysiology of mirror image pain.

10.2. ALTERED THERMOREGULATION IN NEUROPATHIC PAIN

Approximately 80% of patients with peripheral nerve injury in the upper extremities develop cold intolerance, which is defined as an increased pain experience to mild or severe cold [15-18]. One of the proposed mechanisms underlying this symptom is a disrupted peripheral thermoregulation during cold exposure that results in cold intolerance [19, 20]. Peripheral thermoregulations during cold exposure are cold-induced cyclic vasodilatations [21, 22], a process that regulates blood flow during prolonged cooling of body parts and results in an active rewarming of these body parts [19, 23]. However, other factors may also lead to disturbed peripheral thermoregulation, which are not related to cold intolerance. For example, vascular damage might result in disturbed peripheral thermoregulation in patients with cold intolerance. Additionally age and gender might also disrupt peripheral thermoregulation [24]. As described in chapter 2 and 3, we found in SNI-treated rats no change in cold-induced vasodilatation (CIVD) and rewarming patterns after cold exposure, despite the development of profound intolerance to cold. This finding suggests that cold intolerance has rather a neurological than a thermoregulatory origin.

Recently, autonomic nerve fibers of the skin have been suggested to play an important role in neuropathic pain, especially in sympathetic maintained pain (SMP) [25]. SMP is defined as a form of neuropathic pain that specifically can be relieved by administrating sympathetic blocking agents or by performing sympathectomy [26]. In rats, it has been shown that a peripheral nerve injury of the mental or sciatic nerves results in a new innervation of the upper dermis with sympathetic and parasympathetic fibers [27-29]. In neuropathic pain, these sympathetic and parasympathetic fibers seem to be in close proximity with respectively peptidergic and non-peptidergic fibers [3, 28]. It has been suggested that after peripheral nerve injury, uninjured nociceptors in the skin develop de novo adrenergic agonist sensitivity and start to express adrenoceptors [30]. Subsequently, sympathetic fibers can modulate the peptidergic sensory fibers by releasing norepinephrine, which binds to these adrenoceptors and causes an intensely painful sensation in patients [30]. On the other hand, the involvement of the parasympathetic system in neuropathic pain remains elusive. However, one of the postulated mechanisms is that following nerve injury there may be an up-regulation or sensitization of muscarinic and/or nicotinic receptors on non-peptidergic sensory fibers by neurotransmitters released from sprouted parasympathetic fibers, such as acetylcholine [31, 32].

In SMP, sprouting of autonomic fibers results in an increased release of catecholamines, which in turn leads to modulation of the blood vessels in the upper dermis by activation of the adrenergic receptors [33-35]. This could alter peripheral thermoregulation, resulting in an altered CIVD or rewarming pattern after cold exposure. Therefore, patients with peripheral nerve injury-induced cold intolerance with altered peripheral thermoregulation might suffer from SMP. Consequently, a postulated hy-

pothesis might be that cold intolerant patients with altered thermoregulation suffer from SMP. Therefore, the examination of CIVD and rewarming patterns in patients with cold intolerance, but also other neuropathic pain symptoms, might help to make a distinction between SMP and sympathetic independent neuropathic pain (SIP).

10.3 CUTANEOUS PEPTIDERGIC, NON-PEPTIDERGIC AND MYELINATED FIBERS

The location of skin biopsy punctures has been an underestimated determinant of innervation patterns in animal models of neuropathic pain. Previously, it has been shown that the hairy skin is more densely innervated with the peptidergic PGP 9.5-immunoreactive (IR) and CGRP-IR fibers as compared to glabrous skin [36, 37], whereas the non-peptidergic fibers have a higher innervation density in glabrous skin [38]. In addition, it has been found that after crush injury of the sciatic nerve the number of fibers re-innervating the epidermis of the rat hind paw is significantly higher in hairy skin as compared to glabrous skin [39]. Thus, the distinction between hairy and glabrous skin is a necessity for a valid interpretation of skin biopsies in neuropathic pain research. Moreover, in the current thesis, we have demonstrated that the footpads, i.e. cushion-like white structures that contact the floor, not only have a considerably thicker epidermis than the surrounding non-footpad areas but also demonstrate a reduced density of peptidergic CGRP-IR and non-peptidergic P2X3-IR fibers in naïve rats. Remarkably, this difference was not observed for Sub P-IR and NF-200-IR fibers (chapter 4 and 5). This heterogeneous innervation pattern of the rat foot sole may considerably affect the outcome of behavioral experiments performed on the hind paw. For example, when performing the Von Frey test [40], non-footpad areas are, for their sheer size are more likely to be stimulated, whereas in the thermal plate test [41] the footpad areas, which are continuously in contact with the surface of the hot plate, are more likely to determine the animal's responsiveness. Thus, our data together with previous data strongly suggest that in both behavioral and non-behavioral experiments involving the foot sole, the area of investigation, i.e. footpad and/or non-footpad, should be taken into account. We believe that such an approach will result in more precise and reproducible results, which will aid in pinpointing the subtle characteristics in different types of neuropathic pain, and thus fine-tuning the therapeutic targets for a better treatment of neuropathic pain.

As previously described (see Introduction), evidence indicates that not only the injured fibers, but also the uninjured fibers play a substantial role in inducing and maintaining neuropathic pain [26, 42]. In this thesis, we have shown that the uninjured peptidergic CGRP fibers in the rat foot sole demonstrate the most profound alterations in their innervation pattern after induction of neuropathic pain (chapter 4) as compared to other subgroups of sensory fibers (chapter 5). In contrast, minimal changes were found in the innervation pattern of the non-peptidergic P2X3-IR fibers

after induction of neuropathic pain (chapter 5). These findings, however, do not exclude the involvement of P2X3 fibers in neuropathic pain e.g. by way of interacting with nearby keratinocytes [43]. There is emerging evidence that keratinocytes play a substantial role in the development and induction of neuropathic pain [44, 45]. Studies using electron microscopy have shown that epidermal fibers are in close vicinity of keratinocyte bodies, enabling rapid paracrine communication. Transient receptor potential channels (TRP), which are located on sensory fibers are also expressed by keratinocytes, and are activated by mechanical and thermal stimuli [46-48]. Upon activation, the epidermal cells release ATP that binds to the adjacent P2X3 receptors on epidermal fibers leading to their activation [49, 50]. Interestingly, peripheral nerve injury may induce an increased expression of various subtypes of TRP channels (TRPV1, TRPV3, TRPV4 and TRPA1) on epidermal cells as demonstrated in neuropathic pain patients [44]. This, in turn, may lead to an altered ATP-P2X3 communication, which may contribute to the development of behavioral signs of neuropathic pain. Therefore, apart from taking skin biopsies, information on the expression of receptors, such as TRP channels on keratinocytes, would be of substantial additional value in diagnosing and differentiating subtypes of neuropathic pain in both animal models and patients.

The results presented in the current thesis on the sprouting of epidermal fibers in rats with neuropathic pain may have implications for the site of skin biopsy puncture in patients. Currently, in patients with small-fiber or poly-neuropathies, the common sites for skin biopsy punctures are the distal parts of the lower extremities. The choice of these locations is based on the assumption that in these diseases the longer nerves are affected earlier than the shorter nerves [51]. Commonly, neuropathic pain symptoms in patients with small fiber or poly-neuropathy often start in the feet and progress upward, probably caused by the underlying systemic disease [52]. However, post-traumatic neuropathic pain patients not only experience neuropathic pain symptoms at the injury site but also in the surrounding tissue. Therefore, in nerve injury-induced neuropathic pain, skin biopsies should be obtained not only from the site of injury but also from the surrounding area. It is possible that the site of nerve injury and the surrounding areas are reinnervated by adjacent uninjured nerve fibers [53], which are known to contribute to the development of neuropathic pain. Whether skin biopsies taken from the symptomatic but also the non-symptomatic surrounding skin areas will be of value in diagnosing post-traumatic neuropathic pain in clinical settings is yet to be determined.

Another question that remains is whether it is possible to distinguish between different subtypes of post-traumatic neuropathic pain animal models, based on the analysis of skin fibers in skin biopsies. In the last decade, the innervation patterns of sensory fibers in the skin have been intensively studied in the CCI model. From the results it can be concluded that in this model the CGRP fibers particularly may

be involved in the induction of neuropathic pain symptoms, while non-peptidergic fibers might play a role at a later stage of the disease [54]. This pattern is similar to the SNI model as we show in chapter 4 and 5 of this thesis. However, the two models show a major difference in the reinnervation density of myelinated NF-200-IR fibers. In the CCI model, there is hardly any reappearance of myelinated fibers after 16 weeks [54], while in the SNI model the reinnervation densities of the myelinated fibers reach control levels at 10 weeks postoperatively (chapter 5). A possible explanation could be the inflammatory component induced by the catgut ligatures in the CCI model, which results in the permanent loss of myelinated fibers. Also in a clinical situation, it is not uncommon that an inflammatory component accompanies nerve injury in some patients with post-traumatic neuropathic pain, whereas it may be absent in other patients. Furthermore, mental nerve injury in rodents results in a faster recovery of both epidermal peptidergic and non-peptidergic fibers as compared to sciatic nerve injury [29, 55]. This finding led to the assumption that both peptidergic and non-peptidergic fibers are important in the induction and maintenance of mental nerve neuropathic pain in rodents. This could indicate that in patients with neuropathic pain, skin biopsies from the head and neck region, i.e. trigeminal innervation areas, should be interpreted differently than skin biopsies from the limbs.

10.4 ROLE OF NEUROTROPHIC FACTORS IN SENSORY SPROUTING AND PAIN MECHANISMS

Neurotrophic factors, working in the periphery, are essential for the survival of the sensory nervous system during embryonic development [56]. During development, all sensory neurons express the tyrosine kinase receptors, trkA, trkB and trkC, and are dependent on their ligands, the neurotrophic factors, nerve growth factor (NGF), brain-derived neurotrophic factor (BDNF) and/or neurotrophin-3 (NT-3), respectively. A phase of extensive proliferation is followed by a phase of rapid cell death, and only cells that have access to sufficient quantities of a particular neurotrophic factor survive into adulthood. Apart from their role in the development of the sensory nervous system, some neurotrophic factors are known to be involved in the initiation and maintenance of posttraumatic neuropathic pain [57, 58]. In this section we will discuss the role of neurotrophic factors in the changes of peptidergic and non-peptidergic sensory skin fibres and their effect on posttraumatic neuropathic pain.

NGF

Nerve Growth Factor (NGF) is one of the major growth factors that plays a pivotal role in the induction and maintenance of neuropathic pain. In the embryonic phase of life, NGF ensures the development and survival of sympathetic and sensory neurons, by binding to its high-affinity receptor trkA [58, 59]. These neurons are generally part of the small and medium diameter population of dorsal root ganglion cells (DRG), but

some larger cells also express trkA [60]. In adults, NGF is normally expressed in very low quantities in non-neuronal cells such as the keratinocytes, which are located in the epidermis [57]. However, after nerve injury, there is a substantial increase in the secretion of NGF by macrophages, fibroblasts, and Schwann cells proximal to the lesion site in the nerve, and by keratinocytes in the denervated areas [61, 62]. These large quantities of NGF bind to trkA receptors that are located on peptidergic (CGRP and Substance P) and sympathetic fibers, which in turn promote the sprouting of these fiber populations following nerve injury [57]. Interestingly, it has been shown that NGF sensitization is partially dependent on sympathetic neurons, as sympathectomy partly reduces the effect of NGF in causing hyperalgesia [63]. The peptidergic population also co-labels with the TRPV1 [64] and TRPA1 [65] channels that are thought to play a pivotal role in the development of nerve injury-induced heat [66] and cold hyperalgesia [67], respectively. A proposed mechanism for the development of these subtypes of neuropathic pain is that NGF is taken up by the high affinity receptor trkA, becomes internalized, and is subsequently transported to the cell body where it activates the p38 mitogen-activated protein kinase (MAPK) [68]. This pathway results in the upregulation of several receptors (for example TRPV1 [69] and TRPA1 [70]) in the peripheral nerve endings, which in turn results in the development of neuropathic pain. NGF also acts indirectly by activating mast cells and neutrophils, which subsequently release additional inflammatory mediators causing hypersensitivity [71, 72]. Given a clear role for NGF in sensory neuron sensitization and hyperalgesia, anti-NGF treatments may constitute an effective means of treating pain in humans [72-75]. These hypotheses, however, have not been extensively studied or verified [76]. Perhaps NGF only affects a small proportion of nociceptors in the DRG, and other molecules and neurotrophic factors are most certainly involved in hyperalgesia and overall sensory neuron sensitization.

GDNF

In contrast, non-peptidergic and parasympathetic fibers do not express trkA and therefore do not respond to NGF. However, they bind isolectin B4 (IB4) and respond to the neurotrophic factor glial cell-line-derived neurotrophic factor (GDNF) [56]. One of the main roles of GDNF is neuronal survival and maturation in early postnatal life [77-80]. During the first week of postnatal development a subset of small sensory neurons downregulates trkA and becomes dependent on GDNF for survival [81, 82]. Subsequently, the NGF- and GDNF-sensitive sensory neurons develop into separate populations. For example, the NGF- and GDNF-responsive group of sensory neurons terminates in slightly different regions of the skin and spinal cord (see Introduction) [81-87]. It has thus been hypothesized that these two populations of nociceptors are involved in different aspects of pain, but more data is necessary to confirm this. The delayed reinnervation of the non-peptidergic fibers in the SNI (**chapter 5**) and CCI

model [54] suggests that the concentration of GDNF released by surrounding cells is either lesser or in a later stage compared to NGF release. Although convincing data on this potential difference are currently not available. This notion was supported by a study that indicated that a hind limb injection of Complete Freuds Adjuvant (CFA), which induces inflammation, results in a rapid (1 day postoperatively) and transient increase of NGF concentration, whereas GDNF gradually increased over a period of a week in the DRG [66]. Nevertheless, this has not been confirmed in a model of nerve injury-induced neuropathic pain of the sciatic nerve with examination of GDNF levels in the skin. However, if the same CCI-procedure is performed on the mental nerve, the non-peptidergic (P2X3) and parasympathic fibers show the same sprouting pattern as the peptidergic fibers [55], which is accompanied with subsequent significant increase of GDNF in the skin [29]. This suggests that there is a different GDNF secretion mechanism in the trigeminal nervous system as compared to the rest of the body. Yet, it should be noted that contradictory ideas have been proposed for the function of GDNF, varying from playing a role in inducing neuropathic pain [88-90] to preventing it [91, 92]. Thus while GDNF may have a role in a sensory neuron sensitization, its role in pain processing is still unclear.

Determining the presence of NGF [45, 62, 93, 94] and GDNF [29] in skin biopsies as a possible tool for diagnosing neuropathic pain still needs examination. The temporal and spatial secretion of NGF and GDNF might be valuable for diagnosis of the possible development of neuropathic pain, in addition to the analysis of different sensory fibers in the skin. If increased concentrations of NGF and/or GDNF only occur in specific subtypes of neuropathic pain, it does not seem farfetched to develop new treatment strategies involving anti-NGF and anti-GDNF. Indeed, some promising results have been shown in rodent pain models [66, 95-97]. Nonetheless, these anti-trophic therapies may result in hypoalgesic conditions in humans, whereas it is difficult to explore these side-effects in rodents [57]. However, trophic factors such as NGF and GDNF may, at an early stage of nerve injury, form part of an adaptive response [57]. Failure to respond or produce a secondary adaptation in the dorsal spinal cord or higher up, may contribute to the development of neuropathic pain. Thus, NGF and GDNF manipulations may, in the future, serve as prophylaxis and treatment of neuropathic pain.

10.5 MIRROR IMAGE PAIN

Two possible hypotheses for the phenomenon of mirror image pain described in chapter 6 are the systemic theory and the neural theory. The systemic theory suggests that following a unilateral lesion, breakdown products from the damaged nerve or denervated tissue might circulate in the bloodstream and induce changes in the neuronal somata of the contralateral fibers in the contralateral DRG neuronal populations [98-100]. The neuronal theory proposes that when the ipsilateral afferent in tissue

with bilateral afferent input to the spinal cord is damaged, this results in sprouting of peripheral nerves not only on that side, but also in the contralateral undamaged tissue [101-103]. In chapter 6, we showed that SNI-treated rats developed hypersensitivity to mechanical stimuli in the hind paw contralateral to the lesion, without any changes in the mechanical threshold in the fore paws. Therefore, this fulfills the criteria for mirror image pain. Furthermore, we found an increase in CGRP neuropeptide content in the contralateral hind paw in the innervation area of the tibial nerve, which is a denervated area in the ipsilateral SNI-treated hind paw. This finding supports the neural theory as a possible mechanism for the development of mirror image pain in the SNI model. An anatomical correlate of this phenomenon may be the observation that fibers enter the dorsal horn and cross the mid-line through the posterior commissure, terminating in the superficial laminae of the contralateral dorsal horn [104]. Other fibers synapse ipsilateral but continue by decussating and supplying terminals to either the deep or superficial laminae of the contralateral dorsal horn. NGF might induce the increase of CGRP peptide content by the nociceptive pathways that are located contralateral [105, 106]. Therefore, we conclude that using the contralateral foot sole as a control in rats with ipsilateral SNI treatment is not justified since there are changes in the innervation pattern in the contralateral hind paw. Furthermore, in patients with one-sided post-traumatic neuropathic pain in a body part, the contralateral body part cannot be used as a control skin for analysis of peripheral innervation patterns [107]. However, skin biopsies taken from other body parts could be used as control if they have the same composition of sensory nerve fibers [51]. Ideally, a database of cutaneous sensory subgroups of healthy subjects should be generated, which in turn can be used as control values.

Interestingly, although mirror image pain is common in animal models, it is sporadic in humans. There are three possible explanations for this difference [108]: I) In humans, the threshold for experiencing pain on the ipsilateral damaged side is reduced to such levels that hyperalgesia and allodynia is experienced, while the pain experience on the contralateral side is much less, directing the attention of the patient mainly to the ipsilateral damaged side. In addition, most physicians are not familiar with mirror image pain, and therefore, they may underestimate the patient's complaints of pain experienced on the contralateral side, or fail to link contralateral pain to the primary neuropathic pain on the ipsilateral side. II) The underlying central processes for experiencing emotions such as pain are much more complicated in humans than in rodents such as the rat [109]. Further, the feeling of pain in humans is susceptible to factors as marital status, gender, and mental conditions, factors that are inappropriate or unknown in rodents. III) A key factor in the detection behavioral signs of neuropathic pain on the contralateral side is the duration of the follow-up. Clinical studies have shown that in some chronic (neuropathic) pain syndromes the appearance of mirror image pain is less intense and occurs later than the ipsilateral pain [108,

[110, 111]. Hence, mirror image pain is usually missed in early stages of the follow-up or is concealed after therapy. In conclusion, behavioral signs indicative of mirror image pain should be included in the diagnostic guidelines of neuropathic pain for improving therapeutic regimens and patient care. [108]

10.6 EPIDERMAL FIBERS AFTER NERVE RECONSTRUCTION

In chapter 7 and 8 we studied the reinnervation pattern of sensory skin fibers in the hind paw of rats with sciatic nerve transection after different reconstruction methods, i.e. autologous nerve graft, vein-muscle graft filled with bone marrow stem cells (BMSC's) and vein-muscle graft without BMSC's. We found that reinnervation by peptidergic CGRP-IR fibers was much faster when compared to the other sensory fibers. However, the CGRP-IR fibers did not sprout as excessively as they do in the SNI and CCI neuropathic pain models [28, 54], a reinnervation pattern that is specifically found in these pain models. This is also in accordance with their pain behavior, as rats with reconstructed sciatic nerve showed postoperatively no mechanical hypersensitivity, while SNI-treated rats do. For peripheral nerve regeneration to occur, the presence of Schwann cells (SC) that remain contiguous to the damaged axon with mutual interaction is a prerequisite [112]. It has been shown that after nerve transection, delicate processes of SCs are likely to facilitate interactions between SCs and the axon of the damaged nerve inducing axonal regrowth [113]. Furthermore, axonal regeneration without SC participation is substantially impaired. Interestingly, axon-SC interaction is triggered by an increase in local CGRP released by adjacent sprouting axons [114], hence ascribing fast reinnervation of CGRP fibers as a possible mechanism to induce nerve regeneration after nerve injury. Nerve reconstruction using vein-muscle graft with BMSC's results in significantly lower reinnervation densities of all investigated sensory fibers as compared to reconstruction with auto-graft, which is in agreement with the functional recovery examined earlier in these different nerve reconstruction models [115]. The vein-muscle graft supported with BMSC's showed higher reinnervation densities of NF-200 and P2X3 cutaneous nerve fibers as compared to the vein-muscle graft group without BMSC's. The advantage of including BMSCs might be due to their capability to differentiate into Schwann cells or their capability to produce cytokines such as NGF and GDNF [116], stimulating a faster reinnervation of myelinated peptidergic and non-peptidergic fibers. Taken together, the skin biopsy technique might be a valuable tool for investigating changes in the skin innervation pattern after nerve reconstruction. Since it is possible to take skin biopsies from the same skin area additional times, the functional and histological recovery of sensory fibers after nerve reconstruction may be monitored over time. Directing future studies towards such an approach would make it possible to investigate the advantage of growth factors in stimulating the delayed regeneration of specific sensory fibers for improving patient's recovery in peripheral sensory functioning.

10.7 RAMP

In chapter 9 we described a novel device, the Rotterdam Advanced Multiple Plate (RAMP), which enables us to objectively measure noxious cold thresholds in the rodent's hind paw by determining the avoidance behavior for nociceptive temperatures. The thermal plate of the RAMP is a construction of four separate plates, with one plate always set at a comfortable non-noxious temperature, while the temperature of the other three plates are manipulated by the experimenter. The seeking behavior of the animal for the comfortable plate is used as a measure of temperature hypersensitivity. Thus, the philosophy of the RAMP is that neuropathic pain rats will have a higher preference for the comfortable plate as compared to control rats, avoiding the other colder or hotter plates. The current gold standard to examine thermal hypersensitivity in rodents is to measure the elapsed time between the first contact of the affected hind paw with a hot or cold plate and the first paw withdrawal, the so-called paw lift latency [14, 41, 117, 118]. By design, the RAMP has a number of theoretical advantages over the paw lift method. Since the animal is free to move, it can avoid painful stimuli. In addition, reflex action does not play a role as it may during paw stimulation in the paw lift technique. Furthermore, since neuropathic pain animal models do not only develop temperature hypersensitivity but also spontaneous pain and hypersensitivity to mechanical stimuli, it is uncertain if a 'paw lift' is only caused by temperature hypersensitivity or is also due to the spontaneous pain that might be enhanced during the test [119]. Apart from these potential confounders, there may be intra-individual differences in scoring the paw lift due to the inherent subjective nature of its scoring.

One of the main struggles in pain research is to measure pain behavior objectively in neuropathic animal models. Consequently, it is difficult to compare behavior results between research labs worldwide. A silent and lightproof box, ensuring no environmental interferences during the experiment, encloses the thermal plate of the RAMP. In addition, because of the camera tracking system the results are independent of the researcher's observations. Therefore, we believe that the RAMP is the first universal device capable of objectively measuring cold hypersensitivity in freely behaving rodents. Consequently, we are confident that this will produce more reproducible results, which may help understand and eventually counter the devastating disease, which is neuropathic pain.

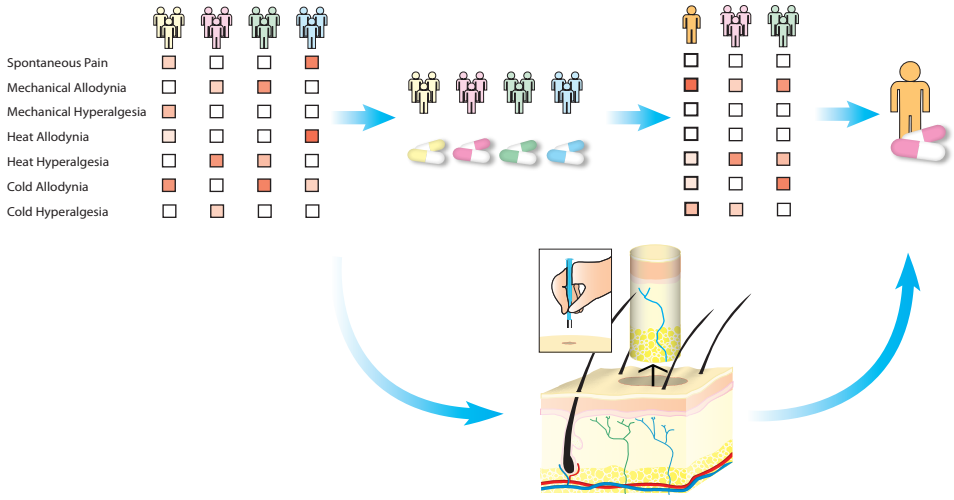

FIGURE 2:

Diagnosis of neuropathic pain is guided by the symptoms the patient is presenting with and the treatment of choice is based on a trial and error process. However, labeling of sensory skin fibers provides essential information for discriminating more efficiently nerve injury-induced neuropathic pain from other types of neuropathic pain.

10.8 FUTURE PERSPECTIVES

Presently, a consensus on objective diagnosis of neuropathic pain has not been reached. In many cases, the diagnosis of neuropathic pain is guided by the symptoms the patient is presenting with and the treatment of choice is based on a trial and error process (Fig.2), similar to the diagnosis and treatment of cancer a few decades ago. One of the main problems we are facing currently is our inability to differentiate between different forms of neuropathic pain based on their pathophysiology, and therefore challenging us in developing new therapies. In this thesis, we have shown that labeling of sensory skin fibers provides essential information for discriminating nerve injury-induced neuropathic pain from other types of neuropathic pain. Furthermore, we suggest that the inclusion of autonomic skin fibers in neuropathic pain together with peripheral thermoregulation measurements could be an additional and valuable tool to differentiate between Sympathic Maintained Pain (SMP) and Sympathic Independent Pain (SIP) in humans and animal studies. In addition, identifying keratinocytes and their expression of sensory receptors, and investigating the interaction between keratinocytes and both peptidergic and non-peptidergic fibers will provide even more information on the pathophysiology of the different forms of neuropathic pain. Therefore, at present we believe that analysis of skin biopsy is a powerful diagnostic tool and should be the mainstay for diagnosing neuropathic pain in the near future.

Another advantage of the skin biopsy-based approach is that it can be applied to both humans and animals with minimal modification since it is based on antibody reactions, which makes it highly suitable for ‘bench to bedside’ research. Data on skin biopsies from a human subject would provide new insights for adjusting and developing animal models of neuropathic pain, while research on animal models would provide an overall view of the underlying mechanisms and give insight into possible targets for new therapies. In our opinion, skin biopsy-based research brings science and patient care closer to each other, and, thus, is an effective counter-measure against the devastating and still elusive disease that is called neuropathic pain.

REFERENCES

1.
Bennett, G.J. and Y.K. Xie, A peripheral mononeuropathy in rat that produces disorders of pain sensation like those seen in man. Pain, 1988. 33(1): p. 87-107.

2.
Basbaum, A.I., et al., The spectrum of fiber loss in a model of neuropathic pain in the rat: an electron microscopic study. Pain, 1991. 47(3): p. 359-67.

3.
Clatworthy, A.L., et al., Role of peri-axonal inflammation in the development of thermal hyperalgesia and guarding behavior in a rat model of neuropathic pain. Neurosci Lett, 1995. 184(1): p. 5-8.

4.
Maves, T.J., et al., Possible chemical contribution from chromic gut sutures produces disorders of pain sensation like those seen in man. Pain, 1993. 54(1): p. 57-69.

5.
Myers, R.R., et al., The role of focal nerve ischemia and Wallerian degeneration in peripheral nerve injury producing hyperesthesia. Anesthesiology, 1993. 78(2): p. 308-16.

6.
Almarestani, L., G. Longo, and A. Ribeiro-da-Silva, Autonomic fiber sprouting in the skin in chronic inflammation. Mol Pain, 2008. 4: p. 56.

7.
Obata, K., et al., Contribution of injured and uninjured dorsal root ganglion neurons to pain behavior and the changes in gene expression following chronic constriction injury of the sciatic nerve in rats. Pain, 2003. 101(1-2): p. 65-77.

8.
Kim, S.H. and J.M. Chung, An experimental model for peripheral neuropathy produced by segmental spinal nerve ligation in the rat. Pain, 1992. 50(3): p. 355-63.

9.
Decosterd, I. and C.J. Woolf, Spared nerve injury: an animal model of persistent peripheral neuropathic pain. Pain, 2000. 87(2): p. 149-58.

10.
Takahashi, Y., et al., Dermatomes and the central organization of dermatomes and body surface regions in the spinal cord dorsal horn in rats. J Comp Neurol, 2003. 462(1): p. 29-41.

11.
Takahashi, Y., J. Hirayama, and Y. Nakajima, Segmental regulation pattern of body surface temperature in the rat hindlimb. Brain Res, 2002. 947(1): p. 100-9.

12.
Obata, K., et al., The effect of site and type of nerve injury on the expression of brain-derived neurotrophic factor in the dorsal root ganglion and on neuropathic pain behavior. Neuroscience, 2006. 137(3): p. 961-70.

13.
Lancelotta, M.P., et al., Severity and duration of hyperalgesia in rat varies with type of nerve lesion. Neurosurgery, 2003. 53(5): p. 1200-8; discussion 1208-9.

14.
Allchorne, A.J., D.C. Broom, and C.J. Woolf, Detection of cold pain, cold allodynia and cold hyperalgesia in freely behaving rats. Mol Pain, 2005. 1: p. 36.

15.
Irwin, M.S., et al., Cold intolerance following peripheral nerve injury. Natural history and factors predicting severity of symptoms. J Hand Surg Br, 1997. 22(3): p. 308-16.

16.
Ruijs, A.C., et al., Cold intolerance following median and ulnar nerve injuries: prognosis and predictors. J Hand Surg Eur Vol, 2007. 32(4): p. 434-9.

17.
Lenoble, E., et al., [Cold sensitivity after median or ulnar nerve injury based on a series of 82 cases]. Ann Chir Main Memb Super, 1990. 9(1): p. 9-14.

18.
Collins, E.D., et al., Long-term follow-up evaluation of cold sensitivity following nerve injury. J Hand Surg Am, 1996. 21(6): p. 1078-85.

19.
Ruijs, A.C., et al., Digital rewarming patterns after median and ulnar nerve injury. J Hand Surg Am, 2009. 34(1): p. 54-64.

20.
Ruijs, A.C., et al., Cold-induced vasodilatation following traumatic median or ulnar nerve injury. J Hand Surg Am, 2011. 36(6): p. 986-93.

21.
Daanen, H.A., Finger cold-induced vasodilation: a review. Eur J Appl Physiol, 2003. 89(5): p. 411-26.

22.
Bergersen, T.K., J. Hisdal, and L. Walloe, Perfusion of the human finger during cold-induced vasodilatation. Am J Physiol, 1999. 276(3 Pt 2): p. R731-7.

23.
Mason, H.J., K. Poole, and J. Saxton, A critique of a UK standardized test of finger rewarming after cold provocation in the diagnosis and staging of hand-arm vibration syndrome. Occup Med (Lond), 2003. 53(5): p. 325-30.

24.
van Marken Lichtenbelt, W.D. and H.A. Daanen, Cold-induced metabolism. Curr Opin Clin Nutr Metab Care, 2003. 6(4): p. 469-75.

25.
Raja, S.N., et al., Systemic alpha-adrenergic blockade with phentolamine: a diagnostic test for sympathetically maintained pain. Anesthesiology, 1991. 74(4): p. 691-8.

26.
Campbell, J.N. and R.A. Meyer, Mechanisms of neuropathic pain. Neuron, 2006. 52(1): p. 77-92.

27.
Grelik, C., G.J. Bennett, and A. Ribeiro-da-Silva, Autonomic fibre sprouting and changes in nociceptive sensory innervation in the rat lower lip skin following chronic constriction injury. Eur J Neurosci, 2005. 21(9): p. 2475-87.

28.
Yen, L.D., G.J. Bennett, and A. Ribeiro-da-Silva, Sympathetic sprouting and changes in nociceptive sensory innervation in the glabrous skin of the rat hind paw following partial peripheral nerve injury. J Comp Neurol, 2006. 495(6): p. 679-90.

29.
Taylor, A.M. and A. Ribeiro-da-Silva, GDNF levels in the lower lip skin in a rat model of trigeminal neuropathic pain: implications for nonpeptidergic fiber reinnervation and parasympathetic sprouting. Pain, 2011. 152(7): p. 1502-10.

30.
Ali, Z., et al., Uninjured C-fiber nociceptors develop spontaneous activity and alpha-adrenergic sensitivity following L6 spinal nerve ligation in monkey. J Neurophysiol, 1999. 81(2): p. 455-66.

31.
Akoev, G.N., Catecholamines, acetylcholine and excitability of mechanoreceptors. Prog Neurobiol, 1980. 15(4): p. 269-94.

32.
Coggeshall, R.E. and S.M. Carlton, Receptor localization in the mammalian dorsal horn and primary afferent neurons. Brain Res Brain Res Rev, 1997. 24(1): p. 28-66.

33.
Benedict, C.R., M. Fillenz, and S.C. Stanford, Plasma noradrenaline levels during exposure to cold [proceedings]. J Physiol, 1977. 269(1): p. 47P-48P.

34.
Brock, J.A., E.M. McLachlan, and S.E. Rayner, Contribution of alpha-adrenoceptors to depolarization and contraction evoked by continuous asynchronous sympathetic nerve activity in rat tail artery. Br J Pharmacol, 1997. 120(8): p. 1513-21.

35.
McCarty, R., Sympathetic-adrenal medullary and cardiovascular responses to acute cold stress in adult and aged rats. J Auton Nerv Syst, 1985. 12(1): p. 15-22.

36.
Povlsen, B., C. Hildebrand, and N. Stankovic, Functional projection of sensory lateral plantar and superficial peroneal nerve axons to glabrous and hairy skin of the rat hindfoot after sciatic nerve lesions. Exp Neurol, 1994. 128(1): p. 129-35.

37.
Verdu, E. and X. Navarro, Comparison of immunohistochemical and functional reinnervation of skin and muscle after peripheral nerve injury. Exp Neurol, 1997. 146(1): p. 187-98.

38.
Taylor, A.M., J.C. Peleshok, and A. Ribeiro-da-Silva, Distribution of P2X(3)-immunoreactive fibers in hairy and glabrous skin of the rat. J Comp Neurol, 2009. 514(6): p. 555-66.

39.
Stankovic, N., O. Johansson, and C. Hildebrand, Occurrence of epidermal nerve endings in glabrous and hairy skin of the rat foot after sciatic nerve regeneration. Cell Tissue Res, 1996. 284(1): p. 161-6.

40.
Lambert, G.A., G. Mallos, and A.S. Zagami, Von Frey's hairs--a review of their technology and use--a novel automated von Frey device for improved testing for hyperalgesia. J Neurosci Methods, 2009. 177(2): p. 420-6.

41.
Jasmin, L., et al., The cold plate as a test of nociceptive behaviors: description and application to the study of chronic neuropathic and inflammatory pain models. Pain, 1998. 75(2-3): p. 367-82.

42.
Campbell, J.N., Nerve lesions and the generation of pain. Muscle Nerve, 2001. 24(10): p. 1261-73.

43.
Lumpkin, E.A. and M.J. Caterina, Mechanisms of sensory transduction in the skin. Nature, 2007. 445(7130): p. 858-65.

44.
Facer, P., et al., Differential expression of the capsaicin receptor TRPV1 and related novel receptors TRPV3, TRPV4 and TRPM8 in normal human tissues and changes in traumatic and diabetic neuropathy. BMC Neurol, 2007. 7: p. 11.

45.
Gopinath, P., et al., Increased capsaicin receptor TRPV1 in skin nerve fibres and related vanilloid receptors TRPV3 and TRPV4 in keratinocytes in human breast pain. BMC Womens Health, 2005. 5(1): p. 2.

46.
Minke, B. and B. Cook, TRP channel proteins and signal transduction. Physiol Rev, 2002. 82(2): p. 429-72.

47.
Reaves, B.J. and A.J. Wolstenholme, The TRP channel superfamily: insights into how structure, protein-lipid interactions and localization influence function. Biochem Soc Trans, 2007. 35(Pt 1): p. 77-80.

48.
Denda, M. and M. Tsutsumi, Roles of transient receptor potential proteins (TRPs) in epidermal keratinocytes. Adv Exp Med Biol, 2011. 704: p. 847-60.

49.
Boulais, N. and L. Misery, The epidermis: a sensory tissue. Eur J Dermatol, 2008. 18(2): p. 119-27.

50.
Denda, M., et al., Epidermal keratinocytes as the forefront of the sensory system. Exp Dermatol, 2007. 16(3): p. 157-61.

51.
Lauria, G. and G. Devigili, Skin biopsy as a diagnostic tool in peripheral neuropathy. Nat Clin Pract Neurol, 2007. 3(10): p. 546-57.

52.
Devigili, G., et al., The diagnostic criteria for small fibre neuropathy: from symptoms to neuropathology. Brain, 2008. 131(Pt 7): p. 1912-25.

53.
Rajan, B., et al., Epidermal reinnervation after intracutaneous axotomy in man. J Comp Neurol, 2003. 457(1): p. 24-36.

54.
Peleshok, J.C. and A. Ribeiro-da-Silva, Delayed reinnervation by nonpeptidergic nociceptive afferents of the glabrous skin of the rat hindpaw in a neuropathic pain model. J Comp Neurol, 2011. 519(1): p. 49-63.

55.
Grelik, C., S. Allard, and A. Ribeiro-da-Silva, Changes in nociceptive sensory innervation in the epidermis of the rat lower lip skin in a model of neuropathic pain. Neurosci Lett, 2005. 389(3): p. 140-5.

56.
Pezet, S. and S.B. McMahon, Neurotrophins: mediators and modulators of pain. Annu Rev Neurosci, 2006. 29: p. 507-38.

57.
Anand, P., Neurotrophic factors and their receptors in human sensory neuropathies. Prog Brain Res, 2004. 146: p. 477-92.

58.
Huang, E.J., et al., Expression of Trk receptors in the developing mouse trigeminal ganglion: in vivo evidence for NT-3 activation of TrkA and TrkB in addition to TrkC. Development, 1999. 126(10): p. 2191-203.

59.
Patapoutian, A. and L.F. Reichardt, Trk receptors: mediators of neurotrophin action. Curr Opin Neurobiol, 2001. 11(3): p. 272-80.

60.
Wright, D.E. and W.D. Snider, Neurotrophin receptor mRNA expression defines distinct populations of neurons in rat dorsal root ganglia. J Comp Neurol, 1995. 351(3): p. 329-38.

61.
Mearow, K.M., Y. Kril, and J. Diamond, Increased NGF mRNA expression in denervated rat skin. Neuroreport, 1993. 4(4): p. 351-4.

62.
Peleshok, J.C. and A. Ribeiro-da-Silva, Neurotrophic factor changes in the rat thick skin following chronic constriction injury of the sciatic nerve. Mol Pain, 2012. 8(1): p. 1.

63.
Andreev, N., et al., Peripheral administration of nerve growth factor in the adult rat produces a thermal hyperalgesia that requires the presence of sympathetic post-ganglionic neurones. Pain, 1995. 63(1): p. 109-15.

64.
Caterina, M.J., et al., Impaired nociception and pain sensation in mice lacking the capsaicin receptor. Science, 2000. 288(5464): p. 306-13.

65.
Kobayashi, K., et al., Distinct expression of TRPM8, TRPA1, and TRPV1 mRNAs in rat primary afferent neurons with adelta/c-fibers and colocalization with trk receptors. J Comp Neurol, 2005. 493(4): p. 596-606.

66.
Amaya, F., et al., NGF and GDNF differentially regulate TRPV1 expression that contributes to development of inflammatory thermal hyperalgesia. Eur J Neurosci, 2004. 20(9): p. 2303-10.

67.
Katsura, H., et al., Antisense knock down of TRPA1, but not TRPM8, alleviates cold hyperalgesia after spinal nerve ligation in rats. Exp Neurol, 2006. 200(1): p. 112-23.

68.
Obata, K., et al., Differential activation of MAPK in injured and uninjured DRG neurons following chronic constriction injury of the sciatic nerve in rats. Eur J Neurosci, 2004. 20(11): p. 2881-95.

69.
Ji, R.R., et al., p38 MAPK activation by NGF in primary sensory neurons after inflammation increases TRPV1 levels and maintains heat hyperalgesia. Neuron, 2002. 36(1): p. 57-68.

70.
Obata, K., et al., TRPA1 induced in sensory neurons contributes to cold hyperalgesia after inflammation and nerve injury. J Clin Invest, 2005. 115(9): p. 2393-401.

71.
Cheng, J.K. and R.R. Ji, Intracellular signaling in primary sensory neurons and persistent pain. Neurochem Res, 2008. 33(10): p. 1970-8.

72.
Sena, C.B., et al., Cyclosporine A treatment of leprosy patients with chronic neuritis is associated with pain control and reduction in antibodies against nerve growth factor. Lepr Rev, 2006. 77(2): p. 121-9.

73.
Anand, P., et al., Endogenous NGF and CNTF levels in human peripheral nerve injury. Neuroreport, 1997. 8(8): p. 1935-8.

74.
Lowe, E.M., et al., Increased nerve growth factor levels in the urinary bladder of women with idiopathic sensory urgency and interstitial cystitis. Br J Urol, 1997. 79(4): p. 572-7.

75.
Jimenez-Andrade, J.M., et al., Nerve growth factor sequestering therapy attenuates non-malignant skeletal pain following fracture. Pain, 2007. 133(1-3): p. 183-96.

76.
Abdiche, Y.N., D.S. Malashock, and J. Pons, Probing the binding mechanism and affinity of tanezumab, a recombinant humanized anti-NGF monoclonal antibody, using a repertoire of biosensors. Protein Sci, 2008. 17(8): p. 1326-35.

77.
Treanor, J.J., et al., Characterization of a multicomponent receptor for GDNF. Nature, 1996. 382(6586): p. 80-3.

78.
Baloh, R.H., et al., TrnR2, a novel receptor that mediates neurturin and GDNF signaling through Ret. Neuron, 1997. 18(5): p. 793-802.

79.
Klein, R.D., et al., A GPI-linked protein that interacts with Ret to form a candidate neurturin receptor. Nature, 1997. 387(6634): p. 717-21.

80.
Translational Pain Research: From Mouse to Man, ed. L. Kruger and A.R. Light2010, Boca Raton, FL: Llc.

81.
Molliver, D.C. and W.D. Snider, Nerve growth factor receptor TrkA is down-regulated during postnatal development by a subset of dorsal root ganglion neurons. J Comp Neurol, 1997. 381(4): p. 428-38.

82.
Molliver, D.C., et al., IB4-binding DRG neurons switch from NGF to GDNF dependence in early postnatal life. Neuron, 1997. 19(4): p. 849-61.

83.
Coimbra, A., B.P. Sodre-Borges, and M.M. Magalhaes, The substantia gelatinosa Rolandi of the rat. Fine structure, cytochemistry (acid phosphatase) and changes after dorsal root section. J Neurocytol, 1974. 3(2): p. 199-217.

84.
Zylka, M.J., et al., Atypical expansion in mice of the sensory neuron-specific Mrg G protein-coupled receptor family. Proc Natl Acad Sci U S A, 2003. 100(17): p. 10043-8.

85.
Zylka, M.J., F.L. Rice, and D.J. Anderson, Topographically distinct epidermal nociceptive circuits revealed by axonal tracers targeted to Mrgprd. Neuron, 2005. 45(1): p. 17-25.

86.
Lindfors, P.H., et al., Deficient nonpeptidergic epidermis innervation and reduced inflammatory pain in glial cell line-derived neurotrophic factor family receptor alpha2 knock-out mice. J Neurosci, 2006. 26(7): p. 1953-60.

87.
Liu, Y., et al., Mechanisms of compartmentalized expression of Mrg class G-protein-coupled sensory receptors. J Neurosci, 2008. 28(1): p. 125-32.

88.
Malin, S.A., et al., Glial cell line-derived neurotrophic factor family members sensitize nociceptors in vitro and produce thermal hyperalgesia in vivo. J Neurosci, 2006. 26(33): p. 8588-99.

89.
Franck, M.C., et al., Essential role of Ret for defining non-peptidergic nociceptor phenotypes and functions in the adult mouse. Eur J Neurosci, 2011. 33(8): p. 1385-400.

90.
Joseph, E.K. and J.D. Levine, Hyperalgesic priming is restricted to isolectin B4-positive nociceptors. Neuroscience, 2010. 169(1): p. 431-5.

91.
Boucher, T.J., et al., Potent analgesic effects of GDNF in neuropathic pain states. Science, 2000. 290(5489): p. 124-7.

92.
Nagano, M., et al., Decreased expression of glial cell line-derived neurotrophic factor signaling in rat models of neuropathic pain. Br J Pharmacol, 2003. 140(7): p. 1252-60.

93.
Wu, C., et al., Nerve growth factor expression after plantar incision in the rat. Anesthesiology, 2007. 107(1): p. 128-35.

94.
Banik, R.K., et al., Increased nerve growth factor after rat plantar incision contributes to guarding behavior and heat hyperalgesia. Pain, 2005. 117(1-2): p. 68-76.

95.
Ro, L.S., et al., Local application of anti-NGF blocks the collateral sprouting in rats following chronic constriction injury of the sciatic nerve. Neurosci Lett, 1996. 218(2): p. 87-90.

96.
Ro, L.S., et al., Effect of NGF and anti-NGF on neuropathic pain in rats following chronic constriction injury of the sciatic nerve. Pain, 1999. 79(2-3): p. 265-74.

97.
Sabsovich, I., et al., Effect of anti-NGF antibodies in a rat tibia fracture model of complex regional pain syndrome type I. Pain, 2008. 138(1): p. 47-60.

98.
Hunt, J.L., et al., Repeated injury to the lumbar nerve roots produces enhanced mechanical allodynia and persistent spinal neuroinflammation. Spine (Phila Pa 1976), 2001. 26(19): p. 2073-9.

99.
Spataro, L.E., et al., Spinal gap junctions: potential involvement in pain facilitation. J Pain, 2004. 5(7): p. 392-405.

100.
Schreiber, K.L., A.J. Beitz, and G.L. Wilcox, Activation of spinal microglia in a murine model of peripheral inflammation-induced, long-lasting contralateral allodynia. Neurosci Lett, 2008. 440(1): p. 63-7.

101.
Oaklander, A.L. and A.J. Belzberg, Unilateral nerve injury down-regulates mRNA for Na+ channel SCN10A bilaterally in rat dorsal root ganglia. Brain Res Mol Brain Res, 1997. 52(1): p. 162-5.

102. Oaklander, A.L. and J.M. Brown, Unilateral nerve injury produces bilateral loss of distal innervation. Ann Neurol, 2004. 55(5): p. 639-44.

103.
Coderre, T.J. and R. Melzack, Increased pain sensitivity following heat injury involves a central mechanism. Behav Brain Res, 1985. 15(3): p. 259-62.

104.
Fitzgerald, M., The contralateral input to the dorsal horn of the spinal cord in the decerebrate spinal rat. Brain Res, 1982. 236(2): p. 275-87.

105.
Donnerer, J., et al., Complete recovery by nerve growth factor of neuropeptide content and function in capsaicin-impaired sensory neurons. Brain Res, 1996. 741(1-2): p. 103-8.

106.
Amann, R., et al., Stimulation by nerve growth factor of neuropeptide synthesis in the adult rat in vivo: bilateral response to unilateral intraplantar injections. Neurosci Lett, 1996. 203(3): p. 171-4.

107.
Oaklander, A.L., et al., Unilateral postherpetic neuralgia is associated with bilateral sensory neuron damage. Ann Neurol, 1998. 44(5): p. 789-95.

108.
Huang, D. and B. Yu, The mirror-image pain: an unclered phenomenon and its possible mechanism. Neurosci Biobehav Rev, 2010. 34(4): p. 528-32.

109.
Kramer, H.H., et al., Illusion of pain: pre-existing knowledge determines brain activation of 'imagined allodynia'. J Pain, 2008. 9(6): p. 543-51.

110.
Koltzenburg, M., P.D. Wall, and S.B. McMahon, Does the right side know what the left is doing? Trends Neurosci, 1999. 22(3): p. 122-7.

111.
Konopka, K.H., et al., Bilateral sensory abnormalities in patients with unilateral neuropathic pain; a quantitative sensory testing (QST) study. PLoS One, 2012. 7(5): p. e37524.

112.
Webber, C. and D. Zochodne, The nerve regenerative microenvironment: early behavior and partnership of axons and Schwann cells. Exp Neurol, 2010. 223(1): p. 51-9.

113.
Chen, Y.Y., et al., Axon and Schwann cell partnership during nerve regrowth. J Neuropathol Exp Neurol, 2005. 64(7): p. 613-22.

114.
Toth, C.C., et al., Locally synthesized calcitonin gene-related Peptide has a critical role in peripheral nerve regeneration. J Neuropathol Exp Neurol, 2009. 68(3): p. 326-37.

115.
Nijhuis, T.H., et al., Natural conduits for bridging a 15-mm nerve defect: Comparison of the vein supported by muscle and bone marrow stromal cells with a nerve autograft. J Plast Reconstr Aesthet Surg, 2012.

116.
de Ruiter, G.C., et al., Designing ideal conduits for peripheral nerve repair. Neurosurg Focus, 2009. 26(2): p. E5.

117.
Tanimoto-Mori, S., et al., Pharmacologic investigation of the mechanism underlying cold allodynia using a new cold plate procedure in rats with chronic constriction injuries. Behav Pharmacol, 2008. 19(1): p. 85-90.

118.
Yalcin, I., et al., Differentiating thermal allodynia and hyperalgesia using dynamic hot and cold plate in rodents. J Pain, 2009. 10(7): p. 767-73.

119.
Le Bars, D., M. Gozariu, and S.W. Cadden, Animal models of nociception. Pharmacol Rev, 2001. 53(4): p. 597-652.

11

SUMMERY
SAMENVATTING

SUMMERY

Post-traumatic neuropathic pain is one of the most crippling symptoms that occur after peripheral nerve trauma. The International Association for the Study of Pain (IASP) defines post-traumatic neuropathic pain as abnormal chronic pain arising as a direct consequence of a lesion affecting the somatosensory system. The discomfort is usually of a chronic nature and may be described by the patient as a burning sensation, a sharp, stabbing or shooting pain, or 'like an electric shock'. Other features may include allodynia, when seemingly harmless stimuli, such as light touch, provoke pain, and hyperalgesia - discomfort, which would otherwise be mild, felt as severe pain. One of the causes for the inability to treat post-traumatic neuropathic pain accurately is the elusive nature of the pathophysiology, despite extensive research. In addition, there is a lack of objective diagnostic tools. In the last decade there is emerging evidence that the skin plays a pivotal role in the pathophysiology of neuropathic pain.

There is some evidence that disturbed peripheral thermoregulation in the skin after peripheral nerve trauma may contribute to symptoms of neuropathic pain in patients suffering from post-traumatic cold intolerance. Peripheral thermoregulations during cold exposure are cold-induced cyclic vasodilatations (CIVD), a process that regulates blood flow during prolonged cooling of body parts and results in an active rewarming of these body parts. However, other factors may also lead to disturbed peripheral thermoregulation, which are not related to cold intolerance. For example, vascular damage might result in disturbed peripheral thermoregulation in patients with cold intolerance. Additionally age and gender might also disrupt peripheral thermoregulation. As described in chapter 2 and 3, we found no change in CIVD or rewarming patterns after cold exposure in rats with peripheral nerve injury, despite development of profound intolerance to cold. This finding suggests that cold intolerance has rather a neurological than a thermoregulatory origin.

Emerging evidence indicates epidermal nerve fibers play a pivotal role in the pathophysiology of neuropathic pain, especially uninjured nerve fibers adjacent to injured ones. The nerve fibers that terminate in the epidermis are fast conducting thinly myelinated A-delta (Aδ) fibers and slow conducting unmyelinated C-fibers. Epidermal Aδ and C-fiber nociceptors are subdivided into peptidergic and non-peptidergic fibers by their expression of different neurotrophic receptors: they show different peripheral and central terminations. Peptidergic nociceptors, in addition to the classical neurotransmitter glutamate, contain one or more neuropeptides, such as Substance P (SubP) (C-fibers), Calcitonin Gene-Related Peptide (CGRP) (Aδ and C- fibers). Non-peptidergic epidermal fibers (C-fibers) only use glutamate as a transmitter and express the P2X3 receptor.

Firstly, we demonstrated that the distribution of epidermal CGRP nerve fibers in glabrous skin of the rat is not homogeneous. Peptidergic CGRP and non-peptidergic P2X3 fibers showed a significantly lower density of epidermal fibers in footpads (i.e. cushion like structures) as compared to non-footpad areas, which have a significantly thinner epidermis (chapter 4 and 5). Peptidergic Substance-P and NF-200 fibers showed, on the other hand, a homogenous distribution on the glabrous skin. This is also the case in humans, for example evidence shows that on the palmar side of the hand there is a heterogeneous distribution of skin nerve fibers. This may imply that both for the study of epidermal fibers in humans and for animal studies, the location of the skin biopsy puncture should be accurately chosen, because it may result in biased outcomes. In the current thesis we have also investigated the reinnervation patterns of uninjured epidermal fibers in a spared nerve injury model. We have shown that the uninjured peptidergic CGRP fibers in the rat foot sole demonstrate the most profound alterations in their innervation pattern after induction of neuropathic pain (chapter 4) as compared to other subgroups of sensory fibers (Substance P, NF-200 and P2X3; chapter 5). In contrast, minimal changes were found in the innervation pattern of the non-peptidergic P2X3 fibers after induction of neuropathic pain (chapter 5). This may imply that after a partial peripheral nerve trauma without complications of inflammation, the uninjured (adjacent to injured) peptidergic CGRP fibers probably contribute the most to posttraumatic neuropathic pain symptoms.

In some patients with post-traumatic neuropathic pain in a body part, the same but uninjured body part on the contralateral side also develops symptoms of neuropathic pain, a condition known as ‘mirror image pain’. This phenomenon has been described in different neuropathic pain states, particularly those after peripheral nerve damage by trauma. However, previous studies have shown contradictory results concerning the morphological changes of nerve fibers in the contralateral body part after an ipsilateral nerve injury. In chapter 6, we showed that SNI-treated rats developed hypersensitivity to mechanical stimuli in the hind paw contralateral to the lesion, without any changes in the mechanical threshold in the fore paws. Therefore, this fulfills the criteria for mirror image pain. Furthermore, we found an increase in CGRP neuropeptide content in the contralateral hind paw in the innervation area of the tibial nerve, which is a denervated area in the ipsilateral SNI-treated hind paw. Therefore, we conclude that using the contralateral foot sole as a control in rats with ipsilateral SNI treatment is not justified since there are changes in the innervation pattern in the contralateral hind paw. Furthermore, in patients with one-sided post-traumatic neuropathic pain in a body part, the contralateral body part cannot serve as a control skin for analysis of peripheral innervation patterns. However, skin biopsies taken from other body parts could be used as control if they have the same composition of sensory nerve fibers. Ideally, a database of cutaneous sensory subgroups of healthy subjects should be generated, which in turn can be used as control values.

In chapter 7 and 8 we studied the reinnervation pattern of sensory skin fibers in the hind paw of rats with sciatic nerve transection after different reconstruction methods i.e. autologous nerve graft, vein-muscle graft filled with bone marrow stem cells (BMSC's) and vein-muscle graft without BMSC's. We found that the speed of reinnervation by peptidergic CGRP fibers was much faster than that by the other sensory fibers. However, the CGRP fibers did not sprout as excessively as they do in the SNI and CCI neuropathic pain models, a reinnervation pattern that is specifically found in these pain models. This is also in accordance with their pain behavior, as rats with a reconstructed sciatic nerve showed no mechanical hypersensitivity postoperatively, while SNI-treated rats did. The skin biopsy technique might be a valuable tool for investigating changes in the skin innervation pattern after nerve reconstruction. Since it is possible to take skin biopsies from the same skin area multiple times, the functional and histological recovery of sensory fibers after nerve reconstruction may be monitored over time. Directing future studies towards such an approach would make it possible to investigate the advantage of growth factors in stimulating the delayed regeneration of specific sensory fibers for improving patients' recovery of peripheral sensory functioning.

In chapter 9 we described a novel device, the Rotterdam Advanced Multiple Plate (RAMP), which enables us to objectively measure noxious cold thresholds in the rodent's hind paw by determining the avoidance behavior for nociceptive temperatures. The thermal plate of the RAMP is a construction of four separate plates, with one plate always set at a comfortable non-noxious temperature, while the investigator can manipulate the temperature of the other three plates. The urgency of seeking the comfortable plate by the animal serves as a measure of temperature hypersensitivity. Thus, the rationale of the RAMP is that neuropathic pain rats will have a higher preference for the comfortable plate as compared to control rats, avoiding the other colder or hotter plates to a greater extent. One of the main struggles in pain research is to measure pain behavior objectively in neuropathic animal models. Consequently, it is difficult to compare behavior results between research labs worldwide. A silent and lightproof box, ensuring no environmental interferences during the experiment, encloses the thermal plate of the RAMP. In addition, because of the camera tracking system the results are independent of the researcher's observations. As such, we claim that the RAMP is the first universal device capable of objectively measuring cold hypersensitivity in freely behaving rodents. Using this device will result in higher reproducibility, thereby ultimately not only decreasing the number of animal experiments but also in helping to understand and eventually counter the devastating disease, which is neuropathic pain.

In summary this thesis provides a detailed analysis of disturbed cold-induced vasodilatation and rewarming patterns during the neuropathic pain state in the rat. It has become evident that disturbed cold-induced vasodilatation and rewarming patterns

do not attribute to the symptoms of neuropathic pain during cold exposure. In addition, the distribution pattern of different subgroups of skin nerve fibers has been demonstrated in a neuropathic pain state after peripheral nerve injury, as well as after different reconstruction methods. Furthermore, we propose that lack of nerve reconstruction after trauma induces significant sprouting of uninjured (adjacent to injured) peptidergic CGRP skin fibers, which are causal to enhanced neuropathic pain. Finally, a novel device was built, the Rotterdam Advanced Multiple Plate (RAMP), which enables us to investigate cold hypersensitivity objectively and automatically for the first time. In conclusion the current thesis underlines the significant and dynamic role of skin innervation in the development of post-traumatic neuropathic pain.

SAMENVATTING

Post-traumatische neuropathische pijn is één van de meest invaliderende symptomen die na perifeer zenuwletsel kan ontstaan. “The International Association for the Study of Pain” (ISAP) definieert post-traumatische neuropathische pijn als een abnormale chronische pijn die ontstaat als direct gevolg van een laesie aan het somatosensorische systeem. Neuropathische pijn is chronisch van aard en wordt vaak beschreven door patiënten als een brandend gevoel, een scherpe, stekende of schietende pijn, of als “een elektrische schok”. Andere karakteristieken, zoals allodynie, waarbij een niet-pijnlijke stimulus pijn veroorzaakt, en hyperalgesie, waarbij een lichte pijn prikkel een heftige pijnsensatie veroorzaakt, kunnen ook aanwezig zijn. Ondanks veeltallig onderzoek blijft het achterliggend mechanisme van neuropathische pijn vrijwel onbekend. Dit is een van de redenen waarom neuropathische pijn op dit moment niet nauwkeurig behandeld kan worden. Daarnaast, ontbreekt er op dit moment een objectief diagnostisch instrument. In de laatste tien jaar is er toenemend bewijs gevonden dat de huid een cruciale rol speelt in de pathofysiologie van neuropathische pijn.

Er bestaat bewijs dat een gestoorde perifere thermoregulatie van de huid na perifeer zenuwletsel een rol zou kunnen spelen in het ontstaan van symptomen bij neuropathische pijnpatiënten die aan post-traumatische koude intolerantie lijden. Perifere thermoregulatie gedurende blootstelling aan kou zijn kou-geïnduceerde cyclische vasodilataties, oftewel “cold-induced cyclic vasodilations (CIVD). Dit is een proces dat de bloedtoevoer reguleert gedurende langdurige onderkoeling van lichaamsdelen, en veroorzaakt een actieve verwarming van de betreffende lichaamsdelen. Desalniettemin zijn er mogelijk ook andere factoren betrokken bij een verstoorde perifere thermoregulatie die niet gerelateerd zijn aan koude intolerantie zoals bijvoorbeeld vasculaire letsels. Daarnaast kunnen leeftijd en geslacht ook invloed hebben op gestoorde perifere thermoregulatie. Zoals beschreven in hoofdstuk 2 en 3, hebben we geen verandering in zowel CIVD als in opwarmingspatronen kunnen aantonen nadat ratten met perifeer zenuwletsel aan koude blootgesteld werden, ondanks het feit dat ze een aanzienlijke koude intolerantie ontwikkeld hadden. Deze bevindingen suggereren dat de oorzaak van koude intolerantie eerder neurologisch is dan thermoregulatief.

Er is toenemend bewijs dat de zenuwvezels van de epidermis een essentiële rol spelen in de pathofysiologie van neuropathische pijn en hoofdzakelijk in niet aangedane zenuwvezels nabij gelaedeerde zenuwvezels in de huid. Zenuwvezels die in de epidermis eindigen kunnen snel-geleidende dun gemyeliniseerde A-delta (Aδ) vezels of langzaam geleidende niet-gemyeliniseerde C-vezels zijn. Aδ-vezel en C-vezel nociceptoren zijn onderverdeeld in peptiderge en niet-peptiderge zenuwvezels doordat

ze verschillende neurotrofische receptoren tot expressie brengen en verschillen in hun perifere en centrale beëindigingen. Peptiderge nociceptoren bevatten, naast de neurotransmitter glutamaat, één of meerdere neuropeptiden zoals Substance P (SubP) (C-vezels) en Calcitonin Gene-Related Peptide (CGRP) (Aδ en C-vezels). Niet-peptiderge vezels van de epidermis (C-vezels) gebruiken strikt glutamaat als transmitter en brengen de receptor P2X3 tot expressie.

Ten eerste, hebben we aangetoond dat de distributie van CGRP zenuwvezels in de epidermis van de onbehaarde huid bij ratten niet homogeen is. De densiteit van peptiderge CGRP en niet-peptiderge P2X3 zenuwvezels in de epidermis was significant lager in de "footpad" (kussenachtige structuren) vergeleken met de "niet-footpad" delen, waarin de epidermis veel dunner is (**hoofdstuk 4 en 5**). Peptiderge Sustance-P en NF-200 vezels toonde daarentegen een homogene distributie in de onbehaarde huid aan. Dit is ook het geval in humane huid: er is aangetoond dat aan de palmaire zijde van de hand een heterogene distributie van zenuwvezels is. Dit suggereert dat voor zowel humane studies als voor dierenstudies de locatie waar gebiopteerd wordt nauwkeurig gekozen moet worden om zo onnauwkeurige resultaten te voorkomen.

In dit proefschrift beschrijven we daarnaast ook ons onderzoek naar het reïnnervatie patroon van onaangedane zenuwvezels in de epidermis in de "spared nerve injury model" (SNI). We hebben aangetoond dat onaangedane peptiderge CGRP zenuwvezels in de voetzool van de rat het meest verschillen in hun innervatiepatroon na inductie van neuropathische pijn (**hoofdstuk 4**) vergeleken met andere subgroepen van sensorische vezels (Substance P, NF-200 en P2X3; hoofdstuk 5). In contrast, toonde het innervatiepatroon van non-petiderge P2X3-IR zenuwvezels weinig verandering na inductie van neuropathische pijn (**hoofdstuk 5**). Dit suggereert dat er na partiële perifere zenuwletsels zonder complicaties of inflammatie, de onaangedane peptiderge CGRP vezels (die zich naast gelaedeerde zenuwvezels bevinden) het meest bijdragen aan post-traumatische neuropathische pijn symptomen.

In sommige patiënten met post-traumatische neuropathische pijn in een specifiek lichaamsdeel, ontwikkelt hetzelfde maar niet aangedane lichaamsdeel aan de contralaterale zijde ook symptomen van neuropathische pijn. Dit is ook wel bekend als "mirror image pain". Dit fenomeen is beschreven in verschillende neuropathische pijn toestanden, meer specifiek in neuropathische pijn die veroorzaakt is door trauma. Desalniettemin hebben voorgaande studies tegensprekende resultaten getoond betreffende de morfologische zenuwvezelveranderingen in het contralaterale lichaamsdeel na ipsilateraal zenuwletsel. In hoofdstuk 6, hebben we beschreven dat SNI-behandelde ratten hypersensitiviteit voor mechanische prikkels in de contralaterale achterpoot ontwikkelen zonder dat er veranderingen in mechanische hypersensitiviteit in de voorpoten ontstaat. Derhalve is dit een valide model voor "mirror image pain". Daarnaast, hebben we een toename in CGRP neuropeptide in het innervatiegebied van de nervus tibialis van de contralaterale achterpoot gevonden

welke een gedenerveerd gebied is in de ipsilaterale SNI-behandelde achterpoot. Hierdoor kunnen we concluderen dat de contralaterale voetzool geen goede controle is bij ratten met ipsilaterale SNI-behandeling omdat er veranderingen zijn in het innervatiepatroon in de contralaterale achterpoot. Daarnaast kan in patiënten met enkelzijdige post-traumatische neuropathische pijn in bepaalde lichaamsdelen de contralaterale zijde van het lichaamsdeel niet fungeren als controle voor de analyse van perifere innervatiepatronen. Desalniettemin, zouden huidbiopten van andere lichaamsgebieden wel als controle gebruikt kunnen worden mits ze dezelfde compositie van sensorische zenuwvezels hebben. Idealiter zou een database van cutane sensorische subgroepen van gezonden individuen gemaakt moeten worden om zo valide controles te hebben.
In hoofdstuk 7 en 8, hebben we het reïnnervatiepatroon van sensorische huidvezels in de achterpoot van de rat met een transsectie van de nervus ischiadicus onderzocht na verschillende reconstructiemethoden zoals autologe zenuwtransplantatie, vene-spiertransplantaten met beenmergstamcellen (BMSC's) en vene-spiertransplantaten zonder BMSC's. We hebben geobserveerd dat de snelheid van reïnnervatie door peptiderge CGRP zenuwvezels veel sneller was vergeleken met de andere zenuwvezelsubtypen. Desalniettemin, vertakken CGRP zenuwvezels in mindere mate in dit model vergeleken met de SNI en CCI neuropathische pijnmodellen waarbij dit een specifiek kenmerk is. Dit is ook gerelateerd aan hun pijngedrag waarbij ratten met een gereconstrueerde nervus ischiadicus geen postoperatieve mechanische hypersensitiviteit vertonen terwijl SNI-behandelde ratten dat wel laten zien. De huidbiopsietechniek zou een waardevol instrument kunnen zijn in het opsporen van veranderingen in het patroon van zenuwvezelinnervatie van de huid na zenuwreconstructie. Omdat het mogelijk is om huidbiopten van dezelfde huid meerdere malen af te nemen, zijn de veranderingen in zenuwinnervatie van de huid te volgen in tijd. Het aansturen van toekomstige studies naar een dergelijke aanpak zou het mogelijk maken om de voordelen van groeifactoren in de stimulatie van vertraagde regeneratie van specifieke sensorische vezels te achterhalen om zo het herstel van perifere zenuwen in patiënten te bevorderen.

In hoofdstuk 9 beschrijven we een nieuw apparaat, de Rotterdam Advanced Multiple Plate (RAMP), dat objectieve metingen van pijnlijke koude-drempels in de achterpoot van knaagdieren mogelijk maakt door het vermijdgedrag voor pijnlijke temperaturen te bepalen. De temperatuurplaat van de RAMP bestaat uit vier verschillende platen, waarbij één plaat altijd op een comfortabele niet-pijnlijke temperatuur ingesteld is terwijl de onderzoeker de temperatuur van de andere drie platen kan reguleren. De behoefte van het proefdier om de comfortabele plaat op te zoeken dient als meting voor de temperatuurgevoeligheid. Geconcludeerd kan worden dat, vergeleken met controleratten, ratten met neuropathische pijn een grotere voorkeur zullen hebben

voor de comfortabele plaat en vaker de andere koudere of warmere platen zullen vermijden wanneer deze op de RAMP geplaatst worden. Eén van de grootste problemen in pijnonderzoek is het objectief meten van pijngedrag in neuropathische proefdier modellen. Het is daardoor moeilijk om de gedragsmetingen van verschillende studies wereldwijd met elkaar te vergelijken.
Een geluidvrije en lichtvrije doos omvat de temperatuur platen van de RAMP zodat omgevingsfactoren het diergedrag niet kunnen beïnvloeden. Daarnaast, zijn de geobserveerde resultaten onafhankelijk van de onderzoekersobservaties omdat er een cameravolgsysteem in de RAMP ingebouwd is. Hierdoor, beweren we dat de RAMP het eerste universele apparaat is dat in staat is om koude intolerantie objectief te meten in vrij bewegende knaagdieren. Het veelvuldig gebruik van dit apparaat zal leiden tot hoge herhaalbaarheid van resultaten. Dit zal tot een verlaging van het aantal dierexperimenten leiden en zal daarnaast een significante invloed hebben op het begrijpen van het achterliggende mechanisme van neuropathische pijn en uiteindelijk leiden tot het ontwikkelen van nieuwe methoden om dit verwoestend ziektebeeld te begrijpen en te bestrijden.
Samenvattend, verschaft dit proefschrift een gedetailleerde analyse van verstoorde door kou geïnduceerde vasodilatatie en verstoorde opwarmingspatronen bij neuropathische pijn in verschillende ratmodellen. Het is duidelijk geworden dat een verstoorde door kou geïnduceerde vasodilatatie en verstoord opwarmingspatronen niet de oorzaak zijn voor neuropathische pijn bij blootstelling aan koude temperaturen. Daarnaast, beweren we dat zenuwschade na trauma significante vertakking veroorzaakt van niet aangedane peptiderge CGRP-IR zenuwvezels in de huid (die zich in de nabijheid van aangedane zenuwvezels bevinden) welke gecorreleerd is aan de toename van neuropathische pijn. Tenslotte, hebben we een nieuw apparaat ontwikkeld, namelijk het Rotterdam Advanced Multiple Plate (RAMP), welke het mogelijk maakt om op een objectieve wijze koude hypersensitiviteit op een geautomatiseerde wijze te meten. Concluderend onderstreept dit proefschrift de aanzienlijke dynamische rol die de huidinnervatie speelt in het ontwikkelen van post-traumatische neuropathische pijn.

12

APPENDICES

CURRICULUM VITAE
PhD PORTFOLIO
DANKWOORD

CURRICULUM VITAE

Liron Sabahet Duraku was born on August 7th 1986 in Bar, Montenegro. In 1994 he immigrated from Pristina, Kosovo, to the Netherlands with his parents and little sister. After graduating from the Da Vinci College (Atheneum) in Leiden in 2004, he started medical school at the Erasmus MC in Rotterdam. His first encounter with Plastic and Reconstructive Surgery was in his third year during which he attended several lectures from Prof.dr. S.E.R. Hovius and Dr. E.T. Walbheem about reconstructive surgery. During his Research Master in Neuroscience (Erasmus MC, 2007-2010) he started a novel skin research project in neuropathic pain, which was a collaboration between the department of Plastic and Reconstructive Surgery and Neuroscience, under the supervision of Dr. E.T. Walbheem and Dr. T.J.H. Ruigrok. In 2008 this Research Master project was converted into a PhD project with the supervision of Prof.dr. S.E.R. Hovius and Dr. E.T. Walbeehm, which resulted in several successful follow up projects and grants. Since this initial skin project there has been a strong cooperation between the department of Plastic and Reconstructive Surgery and Neuroscience that have led to successfully completed projects in neuropathic pain, nerve regeneration, diabetic neuropathy, neuropathic itch and burn research. Liron has published his work in several peer-reviewed journals and presented in several international conferences. In 2011 he was awarded by the International Brain Research Organization the European Young Scientist Award. Currently he is doing his internship and continues supervising Research Master Neuroscience students, expecting to finish his MD training in the beginning of 2014. His ambitions are to become a Plastic Surgeon in an academic setting with room for translational research, especially in post-traumatic pain conditions.

PhD PORTFOLIO

Name PhD student: Liron S. Duraku

Erasmus MC

Department: Plastic, Reconstructive and Hand Surgery

PhD period: November 2008 – February 2013

Promoter: Prof. S.E.R Hovius

Supervisor: Dr. E.T. Walbeehm, Dr. T.J.H. Ruigrok

PhD training

	Year	Workload (Hours)
General courses		
- Research Master of Neuroscience	2007-2010	
- Biomedical English Writing	2010	10 hrs.
Specific courses		
- Microsurgery; Mevr. JM Hekking	2009-2013	300 hrs.
Skillslab - Plastic and Reconstructive surgery		
Seminars and workshops		
- Advanced quantitive methods in optical imaging	2008	10 hrs.
- Linear systems	2008	10 hrs.
- Neuro histology	2008	10 hrs.
- F-MRI analysis techniques	2008	10 hrs.
- Molecular neurobiology	2009	10 hrs.
- Genetics and neurological diseases	2009	10 hrs.
- Tools and therapy in psychiatry	2009	10 hrs.
- Mouse behavioural phenotyping	2009	10 hrs.
- Elective workshop	2009	10 hrs.
Oral Presentations		
- Endo-Neuro-Psycho Meeting, Doorwerth, the Netherlands	2009	30 hrs.
3D reconstruction model of epidermal fibers: A novel approach for assessment of neuropathic pain		
- Annual Plexus and Brachial Injury Congress, Luxemberg, Luxemburg	2009	30 hrs.
Neuropathic pain after peripheral nerve injury: Role of the skin		
- European Conference for Scientist and Plastic Surgeons, Rotterdam, the Netherlands	2009	30 hrs.
Skin biopsy: A novel approach for assessment of neuropathic pain		
- Federation of European Societies for Surgery of Hand (FESSH), Boekarest, Romenia	2010	30hrs.
Role of peptidergic fibers in neuropathic pain		
- European Conference for Scientist and Plastic Surgeons, Helsinki, Finland	2010	30 hrs.
Role of peptidergic fibers in neuropathic pain		
- Annual meeting of the Dutch Society for Plastic Surgery (NVPC), Amsterdam, the Netherlands	2011	30 hrs.
Thermoregulation in cold intolerant rats		
- Annual meeting of the Dutch Society for Hand Surgery (NVvH), Amsterdam the Netherlands	2011	30 hrs.
Non-peptidergic fibers and neuropathic pain		

- Federation of European Societies for Surgery of Hand (FESSH), Oslo, Norway *Thermoregulation in cold intolerant rats*	2011	30 hrs.
- International Brain Research Organization (IBRO), Florence, Italy *Re-innervation patternd of CGRP fibers in neuropathic pain rats*	2011	30 hrs.
- Federation of European Societies for Surgery of Hand (FESSH), Antwerpen, Belgum *Re-innervation of skin in a vein-muscle graft with BMSCs*	2012	30 hrs.
- Annual meeting of the Dutch Society for Hand Surgery (NVvH), Amsterdam, the Netherlands *Rotterdam Advanced Multiple Plate: RAMP*	2012	30 hrs.
- Annual meeting of the Dutch Society for Plastic Surgery (NVPC, Amsterdam, the Netherlands *Contralateral neuropathic pain: The role of the skin*	2013	30 hrs.
Other		
- Organizing the 20th Esser Course: Masterclass Neuropathic Pain, Rotterdam, the Netherlands	2013	250 hrs
- Organizing the 17th Esser Course: Dupuytren's Contracture, Rotterdam, the Netherlands	2013	100 hrs.
Teaching		
Lecturing		
- Course "Anatomy of the Arm en Hand" (3th and 4th year students) *Supervising practical's and excursions*	2009-2012	60 hrs.
- Supervision Microsurgery course *Skillslab, Erasmus MC, Rotterdam*	2009-2013	120 hrs.
- Course "Basics in suture techniques" (3th year students)	2009-2011	16 hrs.
- Supervision Neuro-anatomy course (3th year students)	2009-2011	60 hrs.
Grants		
- Erasmus Trustfonds (€8.000)		
- Co-applicant Nuts-Ohra Foundation (€196.000)		

DANKWOORD

Prof.dr. S.E.R. Hovius, beste Professor,

Vijf jaar geleden heeft u mij de kans gegeven om een promotietraject in te gaan op een nieuw en risicovol onderwerp binnen de plastische chirurgie. Bij dezen wil ik u enorm bedanken voor deze mogelijkheid en de onvoorwaardelijke steun, motivatie en advies tijdens deze periode. Het gegeven dat u tijdens onze voortgangsgesprekken altijd op de hoogte bent en met nieuwe inzichten komt, terwijl het niet uw primaire aandachtsgebied is, vind ik nog steeds bewonderenswaardig. Één van de dingen die u mij geleerd heeft en mij altijd is bijgebleven; dat ik altijd strijdlustig moet zijn en 'no matter what' nooit moet opgeven. Nogmaals hartelijk dank Professor.

Erik Walbeehm, beste Erik,

Als de dag van gisteren herinner ik mij jouw college uit het derde jaar nog en dat ik nadien op jou afstapte met de vraag hoe ik plastisch chirurg zou kunnen worden. Waarop jij antwoordde dat het zeer lastig is om in opleiding te komen en dat ik eerst maar de Master of Neuroscience zou moeten volgen. Daarna zouden we wel verder praten. Eerlijk gezegd dacht ik dat we een relatief makkelijk onderwerp zouden starten, een retrospectieve klinische studie of iets dergelijks (met alle respect naar alle retrospectieve klinische studies). Deze gedachte verdween al snel na jouw eerste mail. Jouw idee was namelijk om veranderingen in Transient Receptor Potential kanalen te gaan bekijken bij koude intolerante ratten. Dit bovenstaande geeft een alomvattende beschrijving van jou; een echte wetenschapper met een scalpel. Oprecht zou ik mij geen betere begeleider/mentor kunnen voorstellen voor de afgelopen periode. Ik heb enorm genoten van onze spar sessies over potentieel nieuwe projecten tot in de late uurtjes onder het genot van whisky. Het is echt uitzonderlijk hoe goed jij mij kan motiveren, na elk gesprek met jou kan ik weer tegenaan. Jij hebt mij geleerd om nooit tevreden te zijn met een mogelijke verklaring of hypothese, maar je altijd af te vragen hoe het precies zit. Dit heeft zeker bijgedragen aan het succes dat wij tot nu toe hebben behaald. Wie had zes jaar geleden gedacht, toen wij met nagenoeg niks waren begonnen, dat we zouden uitgroeien tot een grote en succesvolle groep. Dit is allemaal te danken aan jouw kwaliteiten als mentor om ons zo optimaal mogelijk te motiveren en te stimuleren om het beste uit ons te halen. Erik, dank voor alles.

Tom Ruigrok, beste Tom,

Op de afdeling Neurowetenschappen word jij gezien als één van de beste onderzoekers, waardoor men altijd zegt dat er bij Tom's onderzoek geen speld tussen te krijgen is. Altijd heb je een kritische kijk op de uitvoering van experimenten en de analyse hiervan, waardoor je het huidonderzoek zeker op een hoger niveau hebt gebracht. Jij stond altijd klaar om te helpen met brainstormen over projecten waar we zeker de vruchten van hebben geplukt. Ook ben ik je eeuwig dankbaar voor je gastvrijheid ten aanzien van Shoista en mij, om ons vanuit de plastische chirurgie tot jouw onderzoeksgroep toe te laten met de bijbehorende begeleiding. Zonder jou was deze hele huid onderzoekslijn nooit van de grond gekomen. Dank voor alles Tom.

De manuscriptcommissie wil ik bedanken:
Prof.dr. F.J.P.M. Huygen, Prof.dr. E.P. Prens en Prof.dr. P.A. van Doorn,
hartelijk dank voor uw bereidheid zitting te nemen in de kleine commissie.

Chris de Zeeuw, beste Chris,

Enorm bedankt dat ik op je afdeling mijn promotieonderzoek mocht uitvoeren. De familiesfeer die je gecreëerd hebt op de 12de zal ik nooit vergeten en ik ben blij dat ik daar een onderdeel van mocht zijn.

Aram Hossaini, beste Aram,

Aram, jij was van onschatbare waarde voor mijn promotieonderzoek. Altijd behulpzaam om mee te denken en te helpen, terwijl je zelf genoeg te doen had. Ik weet nog dat we in het begin niet eens wisten waar de onderkant of bovenkant van de huidjes zich bevonden. Het vroeg beginnen en doorgaan tot in de late uurtjes heeft er uiteindelijk toe geleid dat wij met succes mooie publicaties hebben neergezet. Aram, beste vriend, bedankt.

Joan Holstege, beste Joan,

Met jou ben ik in contact gekomen via Aram en daar heb ik zeker geen spijt van gehad. Aan jouw kennis over het pijnsysteem lijkt geen eind te komen. Ik ben je enorm dankbaar voor jouw bijdrage aan het huidonderzoek en het doet mij zeer deugd dat jij er nu ook onderdeel van uitmaakt. Naast serieuze zaken kan ik altijd bij jou terecht om over zogezegd koetjes en kalfjes te praten waar ik enorm van geniet en dit maakt jou tegelijkertijd ook een top begeleider.

Sjoerd Niehof, Beste Sjoerd,

Keer op keer laat jij mij weer versteld staan door een oplossing paraat te hebben als wij er met een project niet uitkomen. Als wij een bepaald meetapparaat niet hebben, zeg jij altijd:" dan maken wij er toch gewoon één", waarop ik soms overrompeld ja knik. Dit is precies tekenend voor jou, waarbij jij van de uitdrukking ''the sky is the limit" jouw levensspreuk hebt gemaakt. Bedankt dat jij mij hebt geleerd om nooit in hokjes te denken, maar alle kennis uit de omgeving te gebruiken om tot nieuwe ideeën te komen.

Ruud Selles, Beste Ruud,

Jij voelt jezelf nooit te min om ons te helpen bij het bedenken van onderzoeksprojecten, het schrijven van artikelen t/m het organiseren van congressen. Jij bent zeer laagdrempelig in de communicatie en probeert ons (de studenten) altijd wat bij te brengen bij het adviseren, wat jou een top begeleider maakt. Wij hebben een aantal mooie publicaties neergezet en zonder jouw hulp was dit zeker niet gelukt. Ruud, bij dezen dankjewel dat jij altijd voor ons klaar staat.

Beste Elise en Erika,

Allereerst wil ik jullie mijn excuses aanbieden voor de mogelijke hoofdpijn die ik jullie soms bezorgd heb tijdens mijn verblijf op de 12de ;). Ik wil jullie graag enorm bedanken voor jullie behulpzaamheid en zorg tijdens dit verblijf. Eerlijk waar, ik zie jullie als mijn tantes waarbij ik altijd terecht kan met mijn problemen omtrent het onderzoek. Zonder jullie onschatbare ervaring zou dit hele proefschrift niet tot stand zijn gekomen.

Marnix Guijt en Thomas van Essen, beste Marnix en Thomas,

In de afgelopen jaren zijn wij beste maten geworden. Ik kan mij nog steeds niet voorstellen hoe wij in zo'n korte tijd zo'n hechte vriendschap hebben opgebouwd; echte familie. Ik kijk enorm tegen jullie op; van jullie perceptie op de wereld tot de karakters die jullie hebben. Daarom kan ik me geen betere paranimfen voorstellen die me vergezellen tijdens mijn verdediging. Met twee reuzen naast mijn zijde voel ik mij onoverwinnelijk, dank voor dat gevoel.

Lukas Jorrissen, Beste Luuk,

In Leiden achttien jaar geleden zaten we op het schoolpleintje American Ninja tegen elkaar te spelen. Ons enige communicatie middel, aangezien ik nog geen Nederlands sprak. Samen de middelbare school en studenten tijd trotseren. Nu achttien jaar later ben jij baas van een enorm succesvol bedrijf en vind het prachtig dat ik dat allemaal meegemaakt hebt. Luuk ben zo enorm trots op jou en wat jij gedaan hebt met jouw bedrijf Coqtail. Ik wil jou enorm bedanken voor de steun tijdens mijn promotie periode. Wij kunnen hier links of rechts voor keren; jij bent en blijft altijd mijn broer, L&L forever!

Ernst Smits, beste Ernst,

Ik ben jou enorm dankbaar dat jij naast collega in de loop der jaren ook een hele goede vriend bent geworden. Al moet ik wel zeggen dat ik mij nog steeds erg ongemakkelijk voel als jij mij buiten kantooruren aan jouw vrienden als collega voorstelt;). Zonder dollen Ernst, we hebben een top tijd gehad in de toren met als resultaat, twee prachtige artikelen en een fantastisch congres dat we samen organiseren. Beste vriend/collega (ben zelf nu ook in de war:p) dank voor de mooie tijd die we samen in de toren hebben doorgebracht en hopelijk gaan wij dit in de toekomst voortzetten.

Tim Nijhuis, beste Tim,

Zoals jij al in je proefschrift schreef, zaten we samen in hetzelfde schuitje. Beiden een compleet nieuwe onderzoekslijn beginnen en daarbij ook het dierexperimentele als overeenkomst. Wij hebben samen zoveel meegemaakt tijdens de periode in de toren, van mooie congressen tot samen aan projecten klussen. Weet jij nog die keer dat we de RAMP in het weekend aan het solderen waren…dat waren nog eens mooie tijden. Ik heb enorm veel respect en bewondering voor de onuitputbare energie die jij in jouw onderzoek steekt. Naast onze passie voor wetenschap, ben ik ook enorm blij dat we goede vrienden zijn geworden.

Carin Oostdijk, beste Carin,

Bedankt voor jouw inspanningen om de laatste loodjes van dit boekje te volbrengen en dat ik altijd bij jou terecht kon voor vragen.

Sieske Hoedervanger, Rashidi Rellum, Lucas Falke, Marco Vergere, Yesim Misirli, Martijn Baas, beste studenten,

Zonder jullie immense inzet en passie voor onderzoek zou een groot deel van dit onderzoek niet afgemaakt zijn. Dank voor jullie hulp.

Ineke Hekking, Beste Inneke,

Bedankt voor jouw hulp tijdens het onderzoek en voor de talloze micro sessies. Maar bovenal wil ik jou enorm bedanken voor de koffietijd waar ik mij altijd bij jou kon ontladen en voor jouw ongezouten mening en advies.

Ester Fijneman, Beste Esther,

Dank voor je immense hulp tijdens de experimenten in het skills lab.

Shoista Kambiz en Barthold Schüttenhelm, beste Shoista en Barthold,

Als masterstudent begonnen jullie met het voortzetten van het huidonderzoek en dat hebben jullie voortreffelijk gedaan. Shoista, ik heb zeer veel bewondering voor de manier waarop jij nu al het onderzoek managet en ben je ook zeer dankbaar voor de manier waarop jij de hele huidonderzoekslijn hebt opgepakt. Barthold jij hebt ook voortreffelijk werk verricht met het jeuk onderzoek. Heb enorm veel respect voor je doorzettingsvermogen en creativiteit, welke tot een nieuwe en succesvolle onderzoekslijn geresulteerd heeft. Shoista en Barthold, dank voor alles.

Gemb Duraku, Lyra Duraku en Deja Duraku,

Hoe kan ik jullie nou vergeten kleine boefjes. Ik ben zo enorm trots op jullie, elk afzonderlijk een sterk karakter, intelligent en mooi. Ben zeer dankbaar dat ik jullie broer ben en het spreekt natuurlijk voor zichzelf, maar je kan het natuurlijk niet vaak genoeg zeggen: Hou zo ontzettend veel van jullie en zal altijd voor jullie klaarstaan.

Sabahet Duraku en Aldiana Rexha-Duraku, beste Papa en Mama,

Nu ik aan het eind van mijn dankwoord ben gekomen, dacht ik dat het makkelijk zou worden om jullie te bedanken voor jullie hulp en etc. (de cliché zaken). Het tegendeel is waar, toen ik begon met typen overheerste een sterk en warm gevoel wat ervoor zorgde dat ik nauwelijks iets op papier kreeg. Ik ga het echter toch proberen. Hoe ouder je wordt des te meer je sommige zaken gaat relativeren en de omgeving in een ander perspectief zien. Als kind zijnde komt het vaak voor dat je opkijkt tegen mensen in jouw omgeving, maar naarmate je ouder wordt erachter komt dat dit echter wel meevalt. Bij jullie gaat dit absoluut niet op: Hoe ouder ik word, des te mooier en bewonderenswaardiger ik jullie ben gaan vinden. Het lijkt wel of ik met de dag steeds meer tegen jullie opkijk. De warmte die jullie uitstralen, reflecteert op het hele gezin, waardoor ik soms niet kan wachten wanneer wij met zijn zessen weer bij elkaar zitten als een echte 'full house' familie. Bovendien zijn jullie ook enorm cool en authentiek. Papa en mama, dank voor de onvoorwaardelijke liefde die jullie, dag in dag uit, aan Gemb, Lyra, Deja en mij geven en dit boekje is dan ook aan jullie opgedragen.

13

FULL COLOR IMAGES

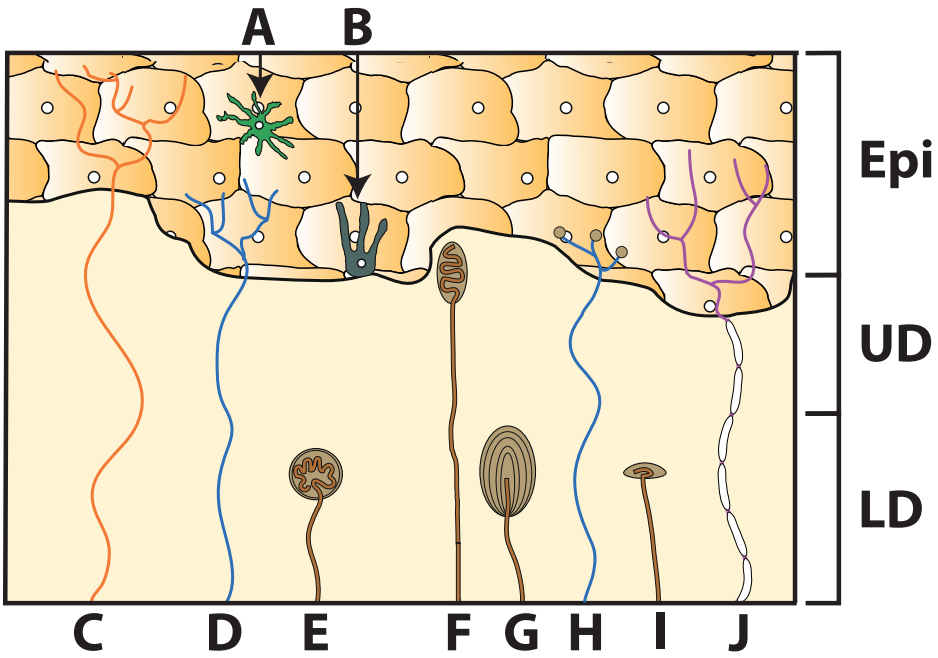

	Type	Location	Function
A	Langerhans cell	Stratum spinosum (epi)	Presents antigens
B	Melanocyte	Stratum basale (epi)	Produces melanine
C	Non-peptidergic C fiber	Mainly stratum granulosum (epi)	Transmits nociception and itch
D	Peptidergic C fiber	Mainly stratum spinosum (epi)	Transmits nociception and itch
E	Krause bulb	Lower Dermis	Detects low-frequency vibrations
F	Meissner corpuscule	Upper Dermis	Transmits light touch (rapidly adapting)
G	Pacini corpuscule	Lower Dermis	Detects vibrations and pressure
H	Merkel cell	Stratum basale (epi)	Transmits light touch (slowly adapting)
I	Ruffini corpuscule	Lower Dermis	Sensitive to skin stretch
J	Aδ fiber	Epidermis	Transmits nociception

FIGURE 1:

Figure 1 displays the architectural epidermal and dermal organization of the plantar side rat's hind limb foot sole.

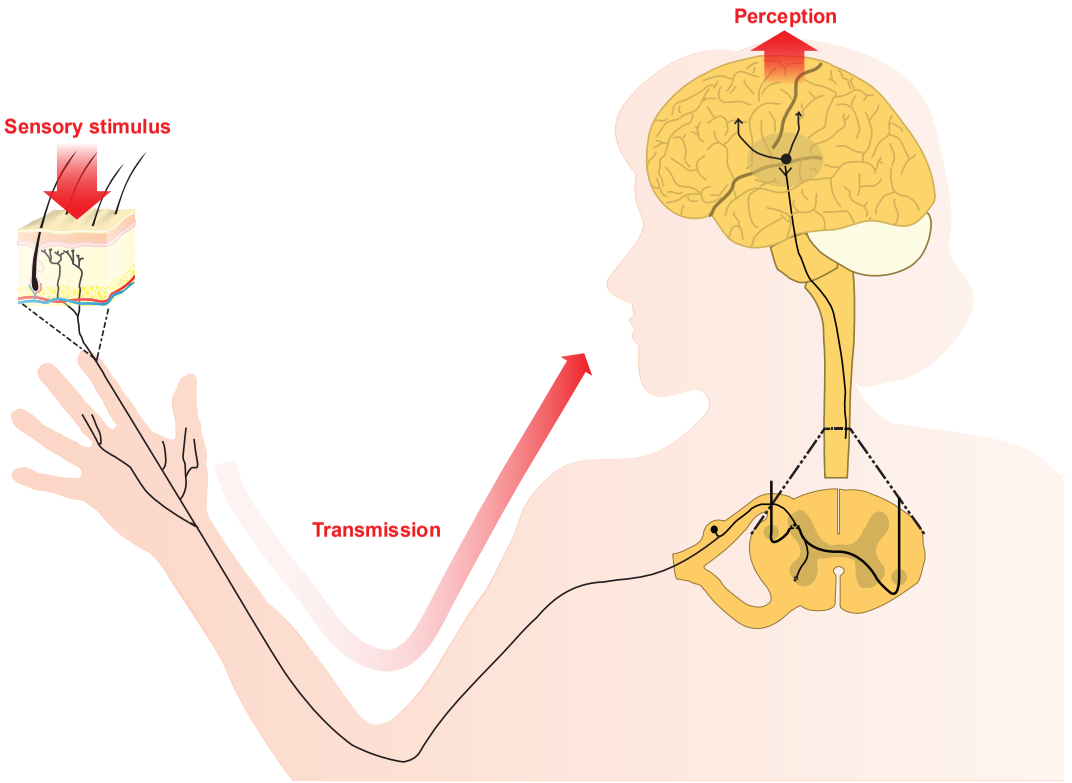

FIGURE 2:

The epidermis is capable of detecting noxious and non-noxious stimuli and transmitting this information to the spinal cord by specialized nerve fibers. In the spinal cord, sensory information is conveyed to higher structures in the central nervous system, eventually leading to perception of sensory stimuli.

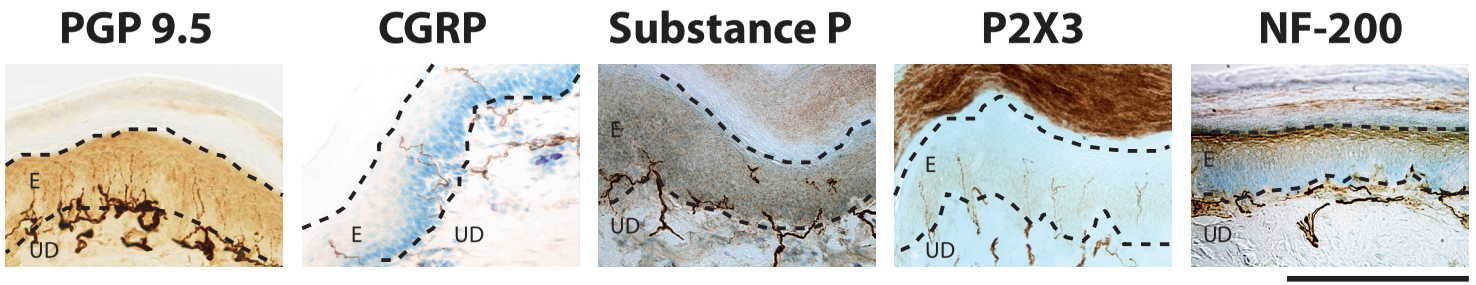

FIGURE 3:

Light microscopic micrographs showing nerve fibers for the immunomarkers that have been used in the current thesis to label the specific subclasses of sensory skin fibers. Epidermal nerve fibers are divided in slow conducting unmyelinated C-fibers and fast conducting, thinly myelinated A-δ, mainly for detecting noxious stimuli. PGP 9.5 is a pan-neuronal marker, which labels all the sensory skin fibers. Unmyelinated C-fibers are either peptidergic and contain the neuropeptides calcitonin gene-related peptide (CGRP) and/or Substance P or are non-peptidergic and are identified by their expression of purinergic receptor P2X3. A-δ fibers are exclusively peptidergic and contain CGRP but can be distinguished from unmyelinated CGRP fibers by their co-expression of the marker neurofilament 200 (NF-200). E: Epidermis, UD: Upper dermis. Scale bar: 250 um.

2

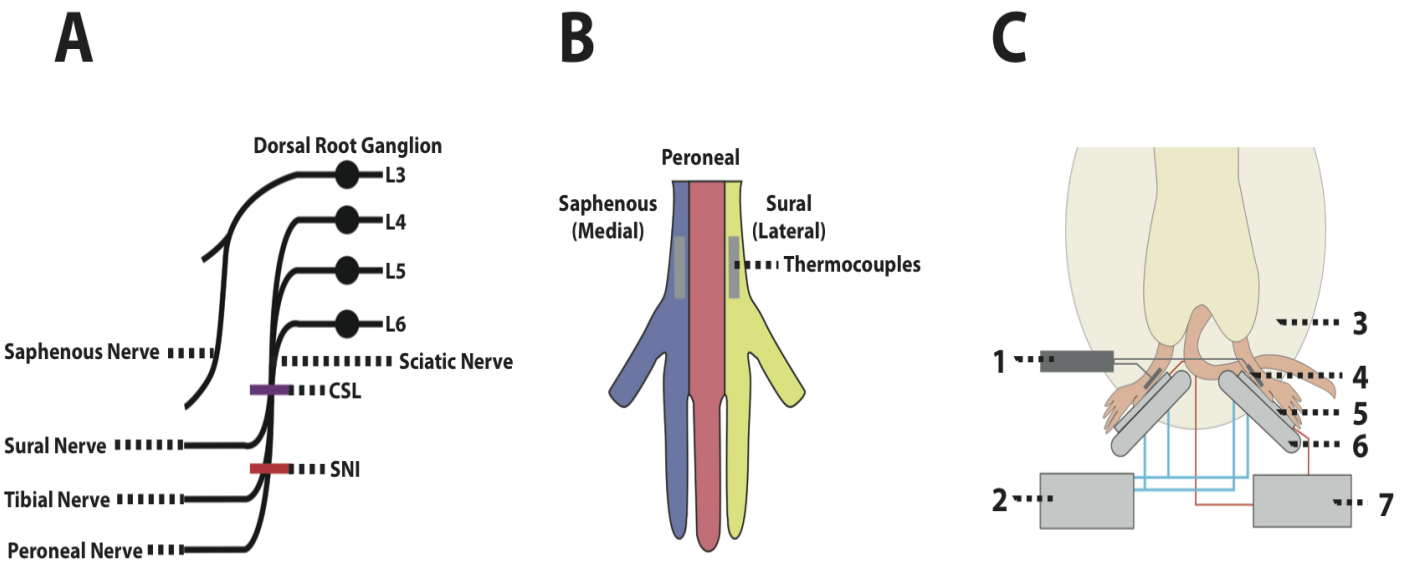

FIGURE 1:

1A: Operation methods of the Spared Nerve Injury (SNI) and the Complete Sciatic Lesion (CSL). The SNI procedure a ligation of the tibial and common peroneal nerves leaving the sural nerve intact. CSL compromised a ligation of the sciatic nerve, 1 cm above the three main branches of the sciatic nerve. Sham controls involved exposure of the sciatic nerve and its branches without any lesion. 1B: Positioning of the thermocouples on the hind limbs of the rat. Innervated areas of the nerves are colored on the hind limbs. 1C: Illustration of the cooling setup and positioning of the rat. 1: USB-based 8-channel thermocouple input module, 2: Thermostatic bath, 3: Heating mattress. 4: Thermocouples, 5: Peltier elements, 6: Water coolers, 7: Power supply.

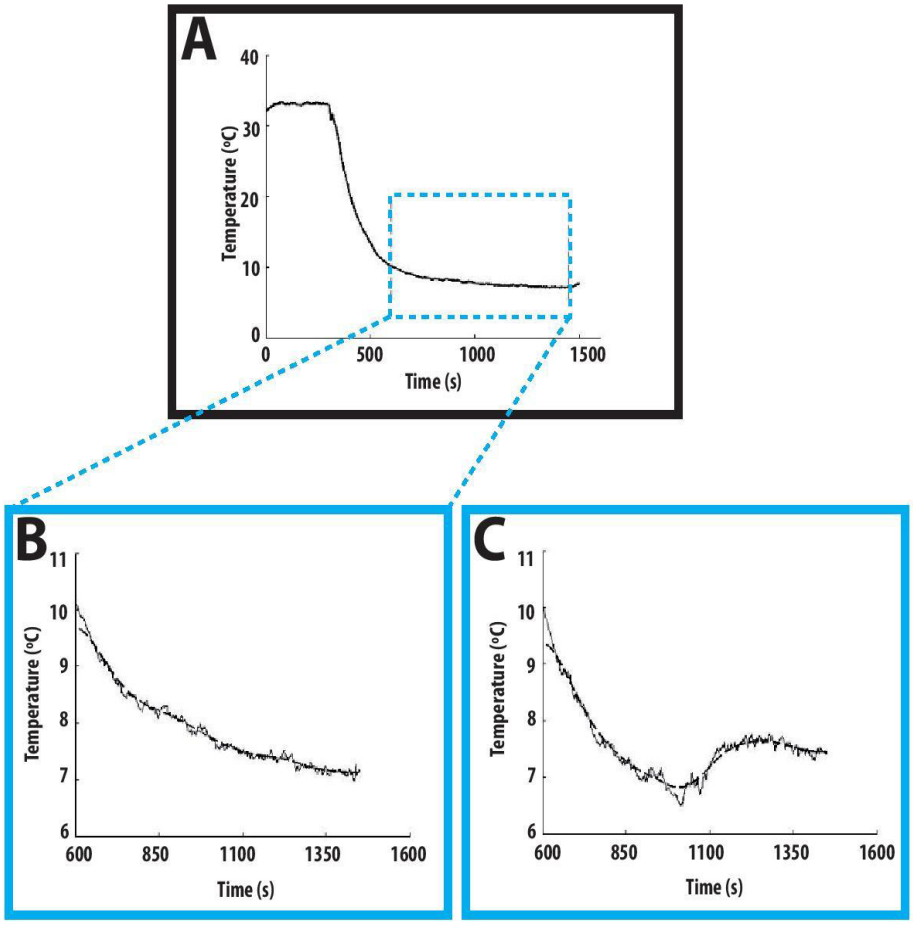

FIGURE 2:

Typical example of temperature during the cooling phase, illustration of the Cold Induced Vasodilatation, the so-called Hunting reaction, in one of the rats. A) Illustration of the total pre- and cooling phase. The analysis period started 375 seconds after the start of cooling and lasted for 850 seconds. The selected cooling phase in Figure 1B and 1C are raw and filtered data. B) A typical example of a cooling phase without CIVD reaction. C) A typical example of a CIVD reaction during the cooling phase. A CIVD was identified when the temperature of the filtered signal increased at least 0.4 °C during the cooling phase.

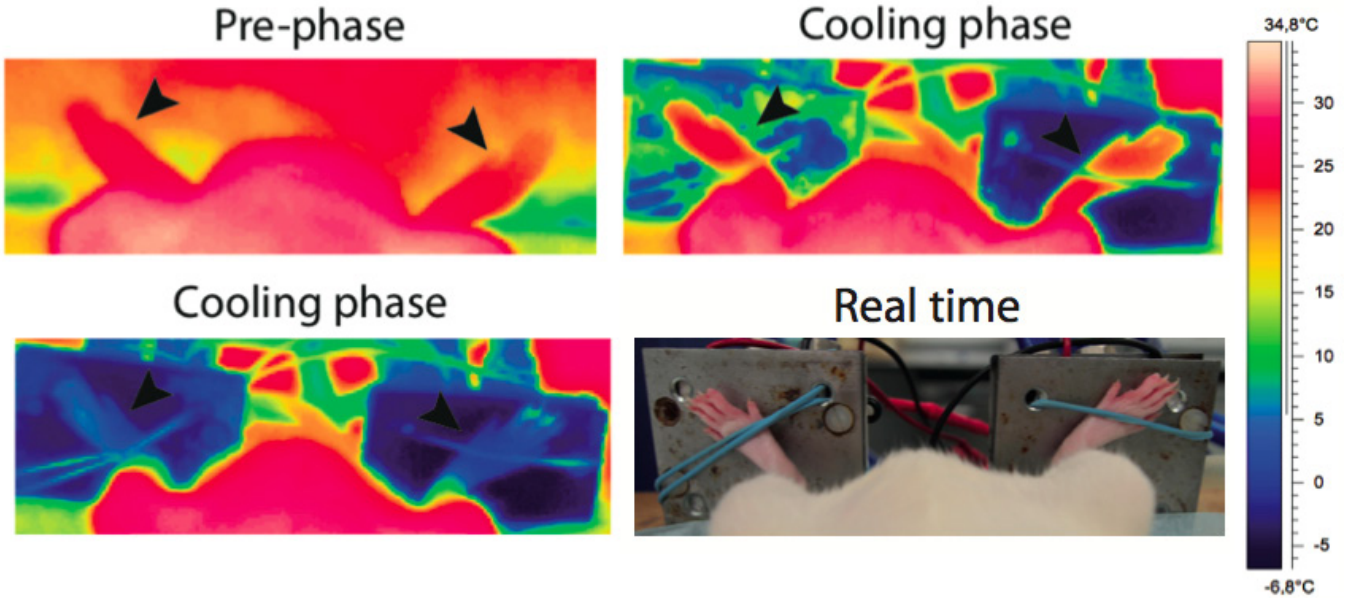

FIGURE 4:

Thermographic imaging and a real time photo of the body of the rat during the experiment, both hind limbs and the Peltier element. Pre-phase: Rat is dorsally positioned under anesthesia to measure baseline temperatures of the hind limbs. Cooling phase (20 min.): Both hind limbs are attached to the Peltier elements. The color indicates that both Peltier elements and hind limbs get equally cooled.

3

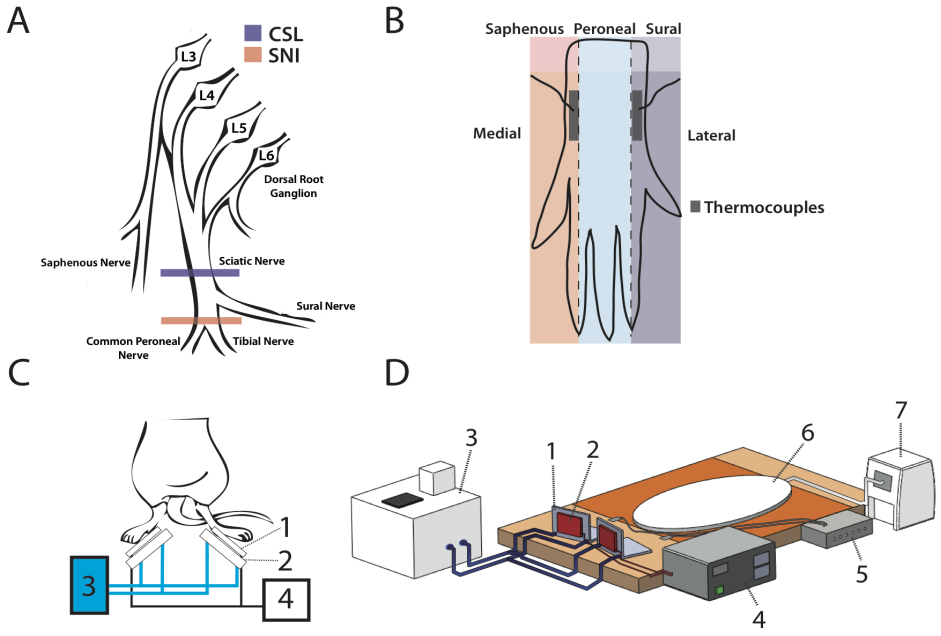

FIGURE 1:

Illustration of the experiment. A: The complete Sciatic Lesion model (CSL) comprises a lesion of the sciatic nerve while the Spared Nerve Injury model (SNI) comprises a lesion of the tibial and common peroneal nerve. B: Dorsal sides of a rat hind paw with its nerve innervations areas. Thermocouples are attached on the medial (saphenous) and lateral (sural) part of the paw. C: Illustration of the cooling set-up. 1: Peltier elements, 2: Water coolers, 3: Thermostatic bath, 4: Power supply. Under anesthesia the rat is positioned on the dorsal side with the hind paws placed on the Peltier elements for cooling. D: Illustration of the complete cooling set-up. 1: Peltier elements, 2: Water coolers, 3: Thermostatic bath, 4: Power supply, 5: USB-based 8-channel thermocouple input module, 6: Heating mattress, 7: Heating mattress regulator.

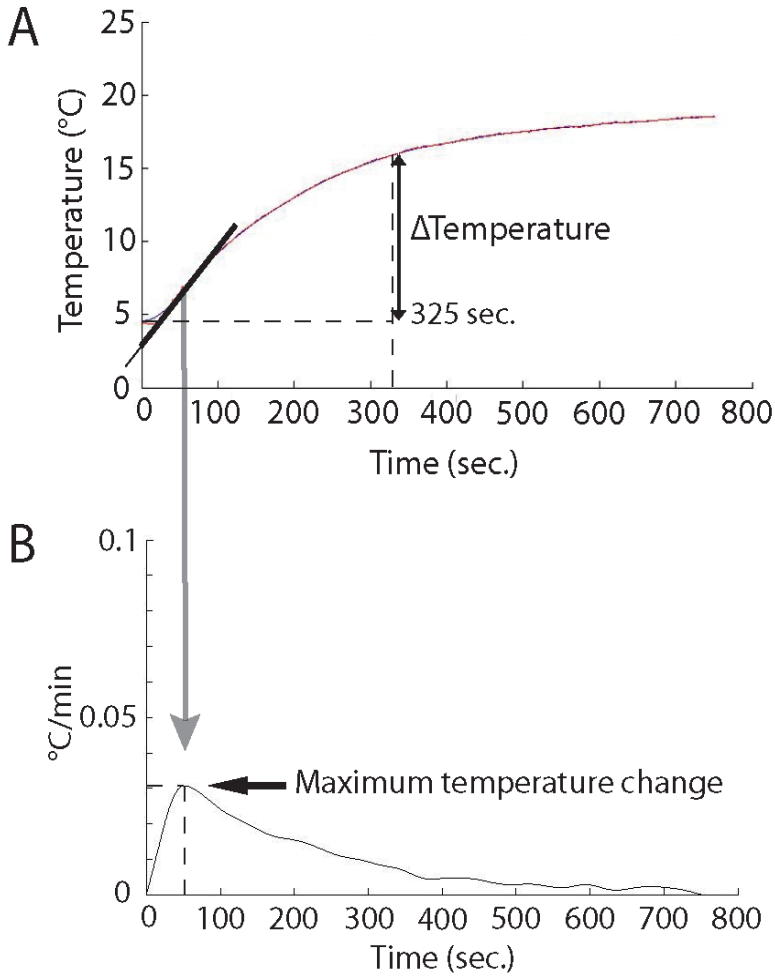

FIGURE 3:

Typical example of the temperature during the rewarming phase and illustration of the outcome measures. A: Increase in temperature is determined by calculating the difference between the lowest and highest temperature of the rewarming curve (Δ Temperature) during the first 325 seconds in the rewarming phase. B: Maximum rate of temperature increase was calculated by taking the first derivative of the time temperature curve. The highest point in the first derivative graph (°C/min.) is the maximum change in temperature during the rewarming phase.

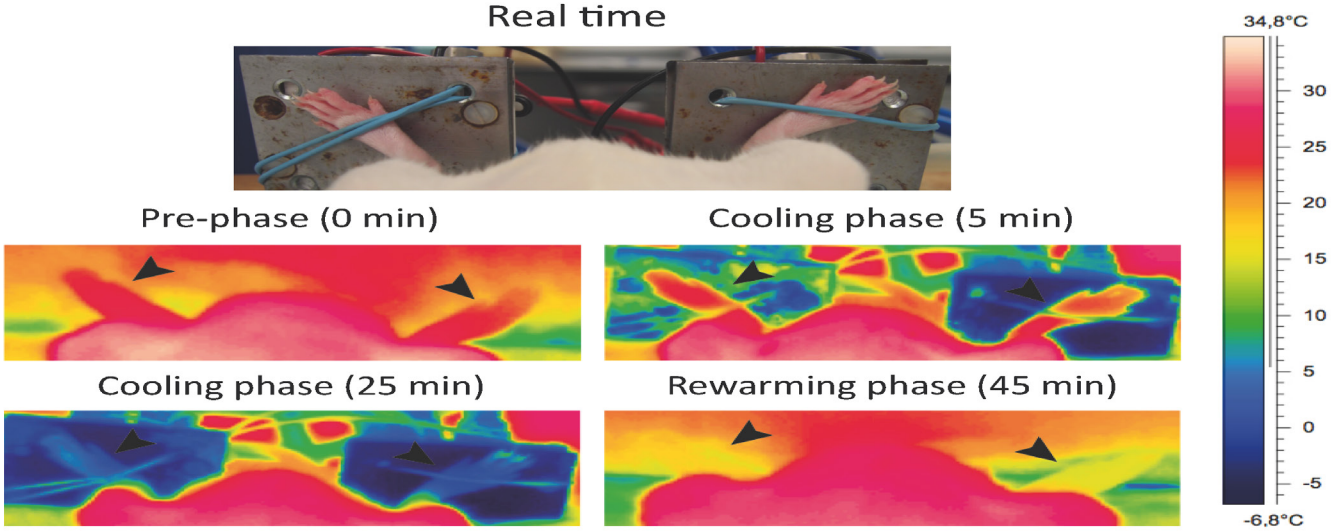

FIGURE 4:

Thermographic imaging of the experiment illustration the body of the rat, both hind paws and the Peltier element. Pre-phase (5 min.): Rat is dorsally positioned under anesthesia to measure baseline temperatures of the hind paws. Cooling phase (20 min.): Both hind paws are attached to the Peltier elements. The color indicates that both Peltier elements and hind paws get equally cooled. Rewarming phase (20 min.): Hind paws are detached from the Peltier elements and the elements are displaced, therefore not being able to affect the environmental temperature.

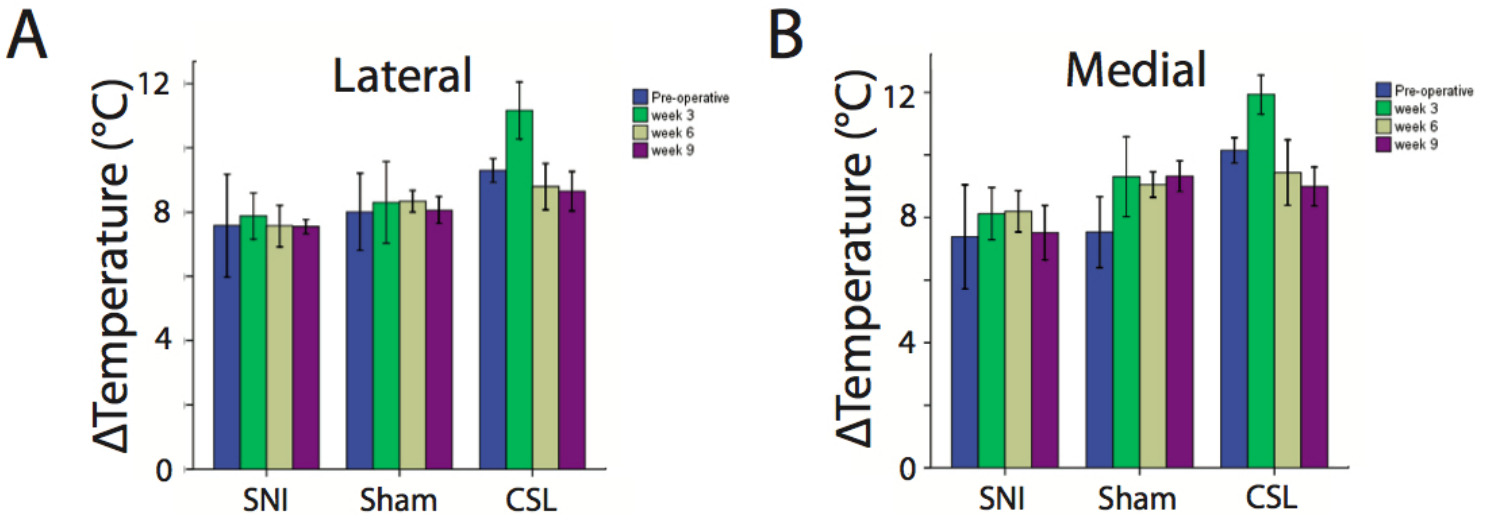

FIGURE 5:

Increase in Temperature: Graphs show the increase in temperature in the rewarming phase. There is no significant difference in the SNI group post-operatively compared to the Sham group. In the CSL group there is a tendency in higher increase in temperature on week 3, compared to the Sham and SNI group. There is no difference in increase of temperature between the measured medial and lateral side. On week 3 with the ANOVA test there was no significant difference between the CSL and Sham group on week 3.

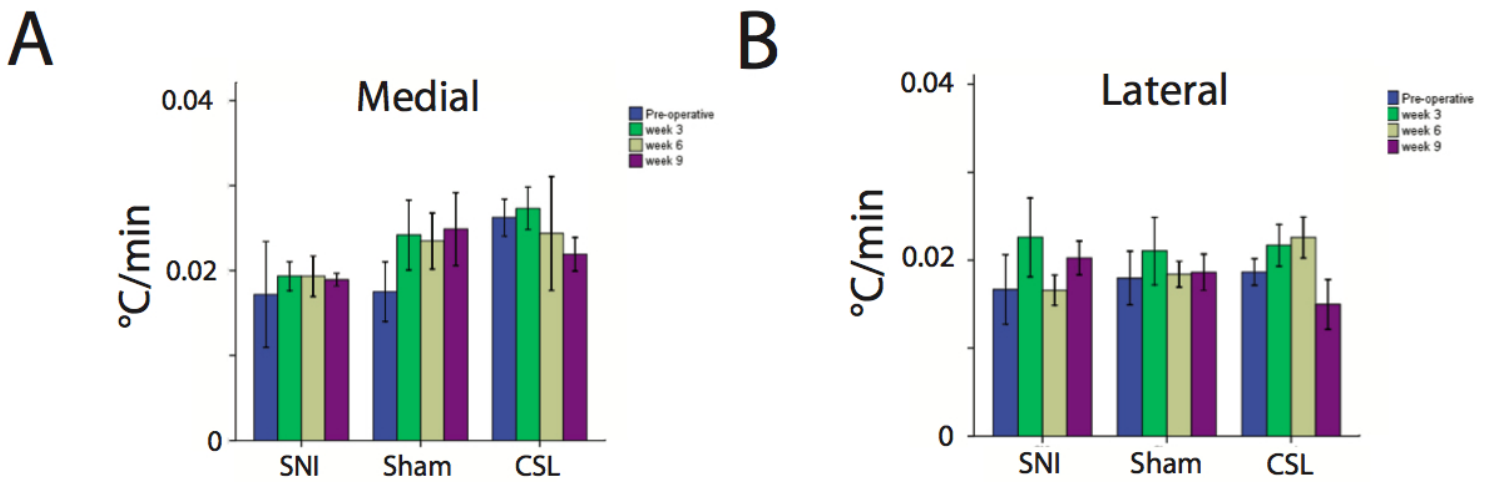

FIGURE 6:

Maximum Change in Temperature. We found no significant difference in maximum change in temperature between the different groups post-operatively and no difference in acceleration speed between the medial and lateral side.

4

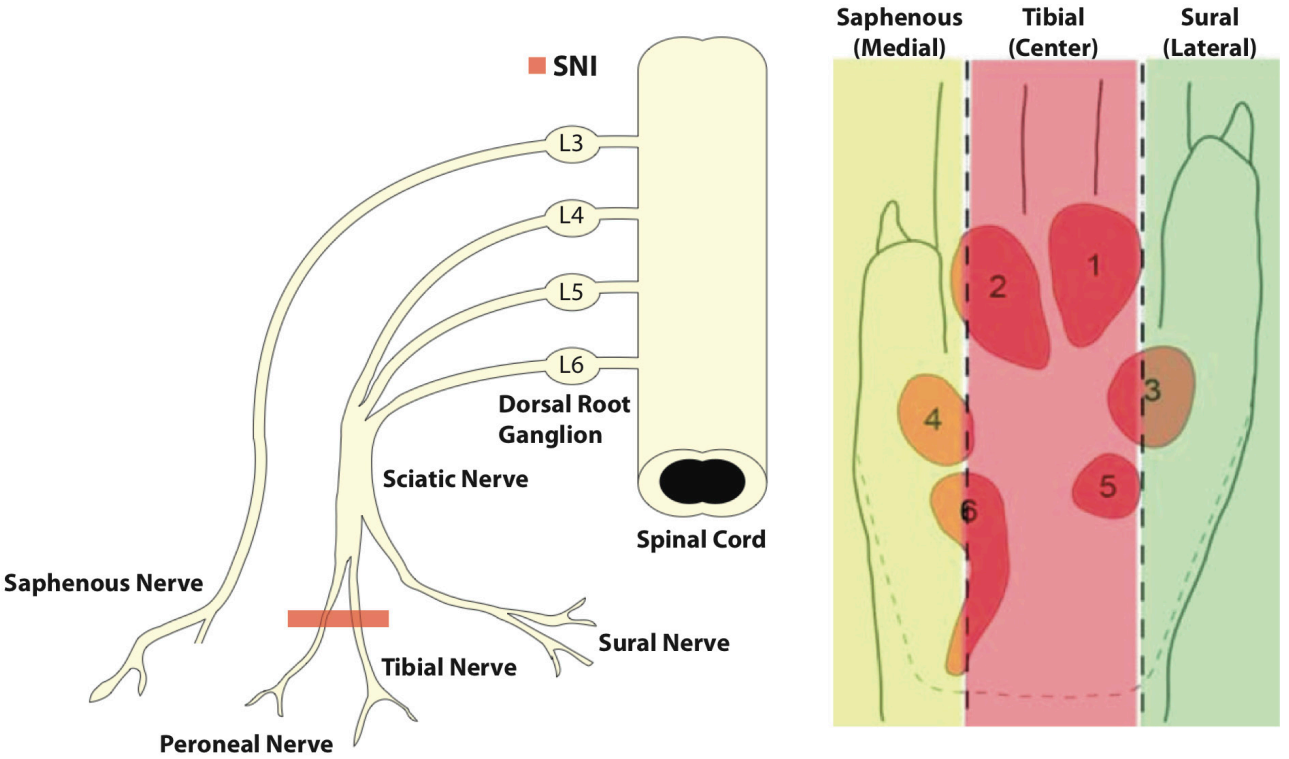

FIGURE 1:

The Spared Nerve Injury (SNI) procedure consists of transection and displacement of the tibial and common peroneal nerves, sparing the adjacent sural and saphenous nerves. This procedure leads to complete denervation of the tibial (central) innervated area (red), but leaves the medial (saphenous: yellow) and lateral (sural: green) sides of the hind paw glabrous skin intact.

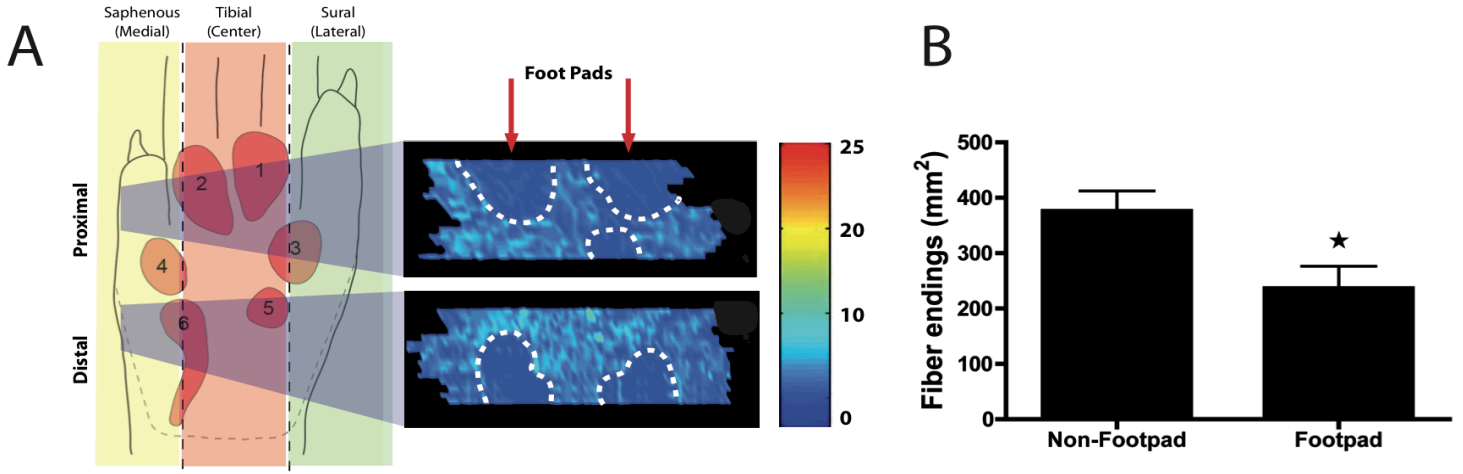

FIGURE 4:

*Epidermal CGRP-IR 2-D density profile of the hind paw glabrous skin. A: Two large skin biopsies (left hand panel, grey shaded areas) are taken from the distal and proximal foot sole and cut transversely. Serial sections were plotted, binned and the density of labeled profiles was visualized in a 2-D density profile that was made using Matlab routines (colorbar reflect number of labeled fibers.) The resulting plots indicate that the footpads are less densely innervated compared to non-footpad areas. B: Quantification shows a significant lower number of epidermal CGRP-IR fibers in the footpads compared to non-footpads. (N=5), student t-test, *P<0.05.*

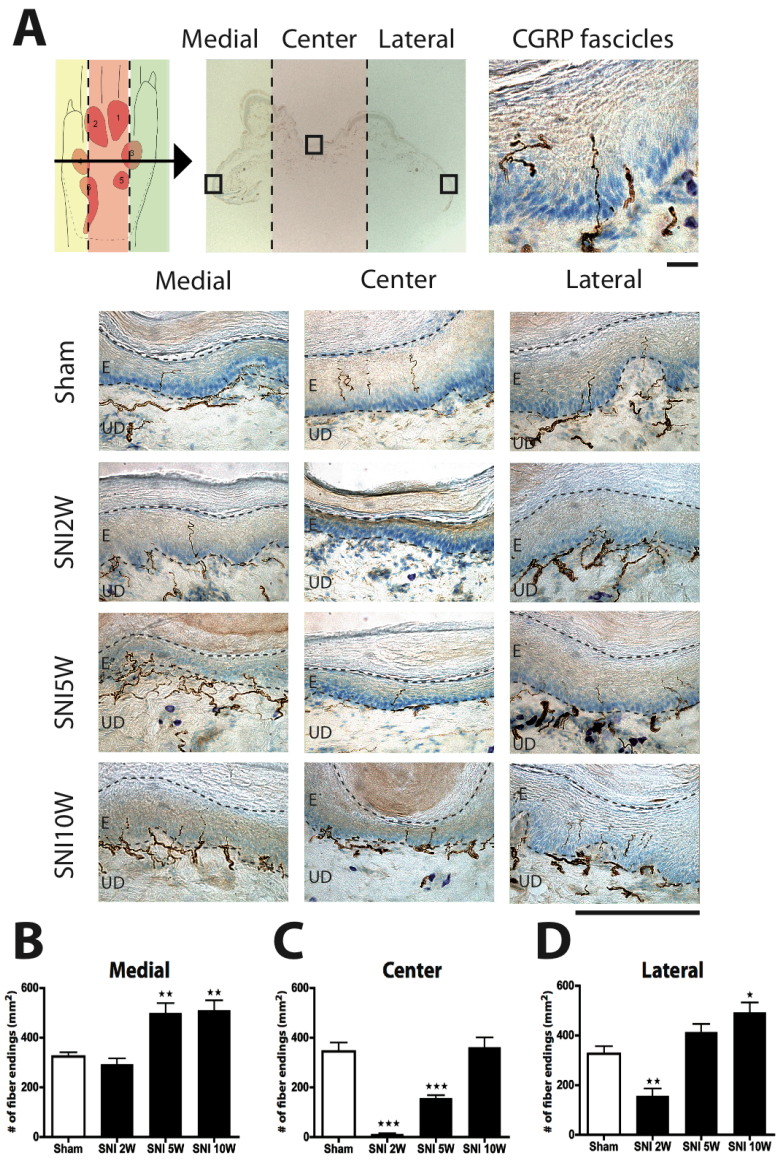

FIGURE 5:

Micrographs showing staining for CGRP-IR fibers in skin biopsies taken from the medial (saphenous), center (tibial) and lateral (sural) part of the foot sole (Fig. 5A). Note that two weeks after SNI a complete loss of CGRP-IR fibers is observed in the central part while preserving CGRP-IR fibers on the medial and lateral side. Five weeks PO, the SNI group shows an increase of CGRP-IR fibers in the medial and lateral part when compared to the sham group. Also, at this time a re-innervation of the center area is noted. Ten weeks PO, the SNI group shows CGRP-IR fibers in all three parts of the foot sole, suggesting complete re-innervation of CGRP-IR fibers in the foot sole. Upper scale bar: 25 µm, and lower scale bar: 250 µm. Diagrams showing

*CGRP-IR fiber endings (mm²) in the medial, center and lateral area of the hind paw glabrous skin. In the medial area there is a significantly higher density of epidermal CGRP-IR endings at 5 and 10 weeks PO (Fig. 5B-D). The center area shows a decreased number of CGRP-IR fibers at 2 weeks, which normalizes at sham levels at week 10. Lateral area shows an initial decrease of CGRP-IR fibers at 2 weeks that becomes significantly higher at 10 weeks PO. (n=6) One-way ANOVA with post Turkey test *: P<0.05, **:P<0.01, ***:P<0.001.*

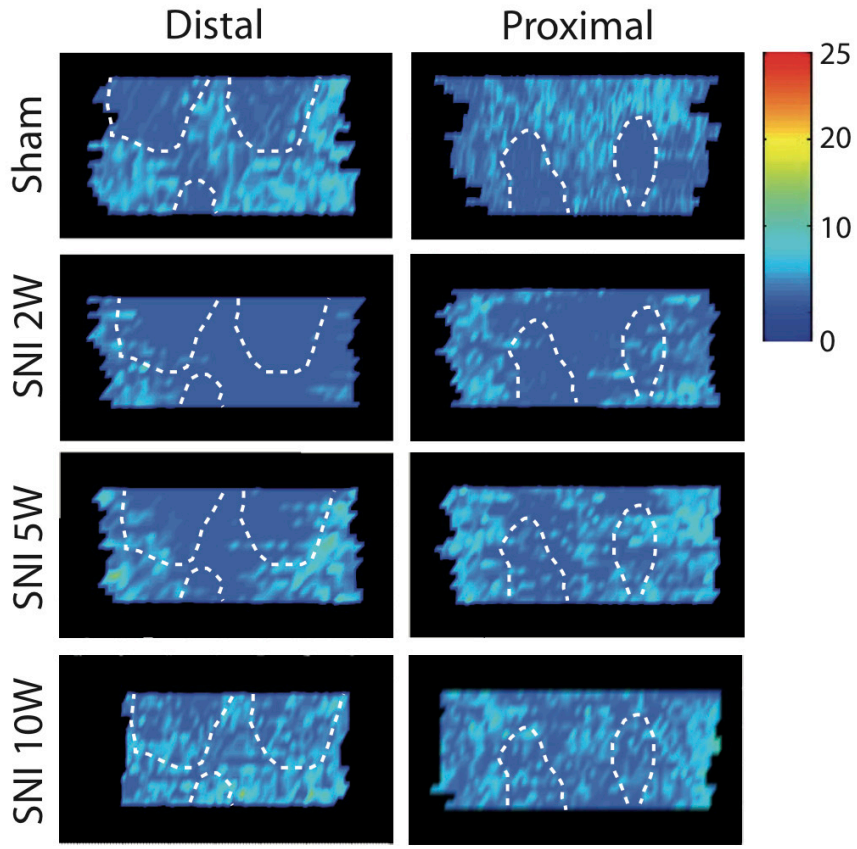

FIGURE 7:

Two-dimensional density profile of epidermal CGRP-IR fibers in the distal and proximal parts of the foot sole. Note patches with lower CGRP-IR density in the sham group, which represent the footpads. After 2 weeks PO there is a complete abolishment of CGRP-IR fibers in the center area (tibial). Five weeks PO an enhanced density of epidermal CGRP-IR fibers within the medial and lateral areas can be observed. Ten weeks PO the epidermal CGRP-IR fiber density profile shows re-innervation of fibers into the previously denervated center area (tibial). Note that the lower density in the footpads that is seen in the sham group is not observed at 10 weeks PO in the SNI group.

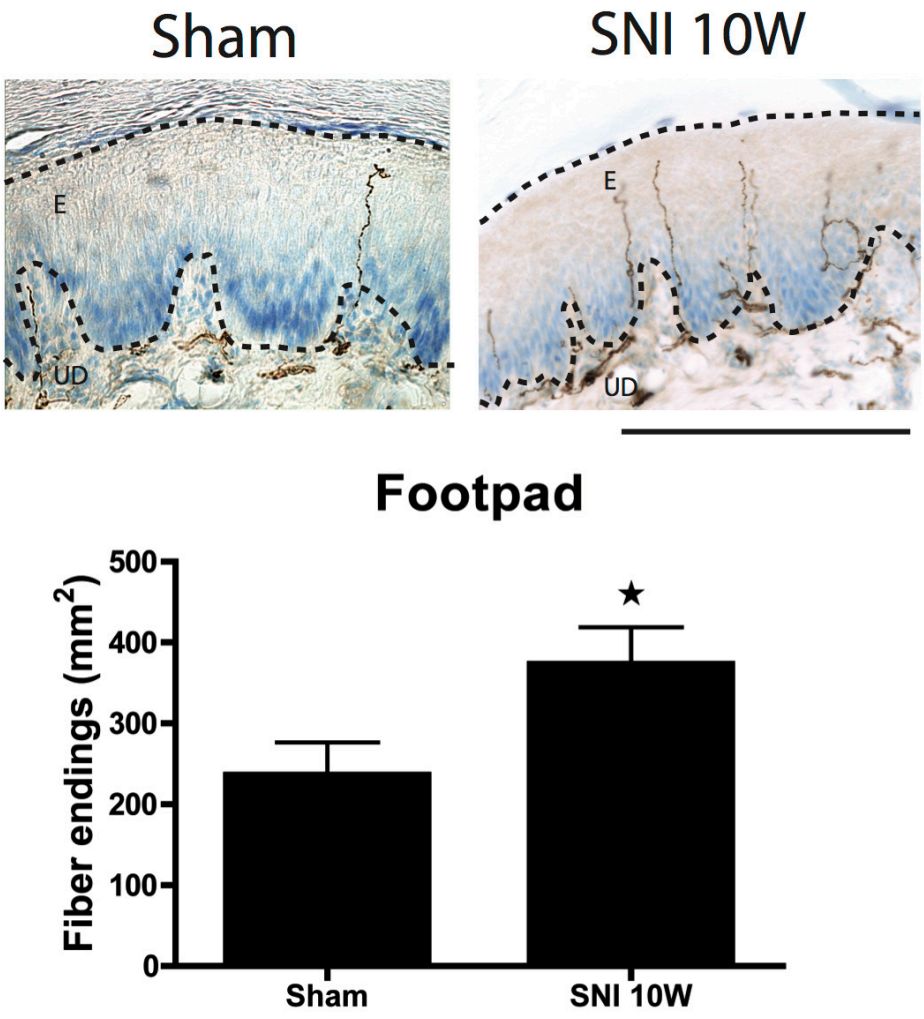

FIGURE 8:

*Micrographs showing footpad epidermal CGRP-IR fibers in the Sham versus SNI 10 week groups. There are a significant higher number of epidermal CGRP-IR fibers in the footpads of the SNI group compared to the Sham group. (n=5), student t-test, * :P<0.05. Scale bar: 250μm.*

5

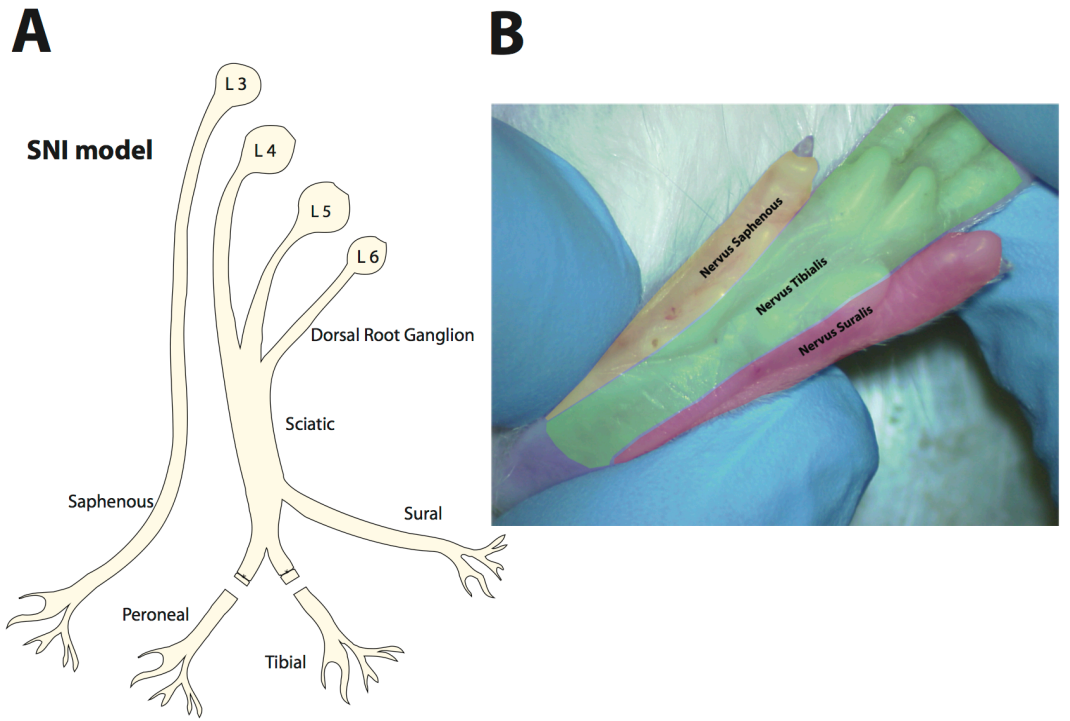

FIGURE 1 SNI MODEL:

Drawing and micrograph illustrating the spared nerve injury (SNI) model procedure. In this experiment, the tibial and common peroneal branches of the sciatic nerve were ligated and transected, while the sural branch, and the saphenous nerve, respectively at the medial and lateral side of the foot sole, were left intact (Fig. 1A). This method results in complete denervation of the tibial nerve area (center), without affecting the medial and lateral sides of the hind paw glabrous skin (Fig. 1B). The highlighted six areas on the foot sole represent the footpads (Fig. 1B).

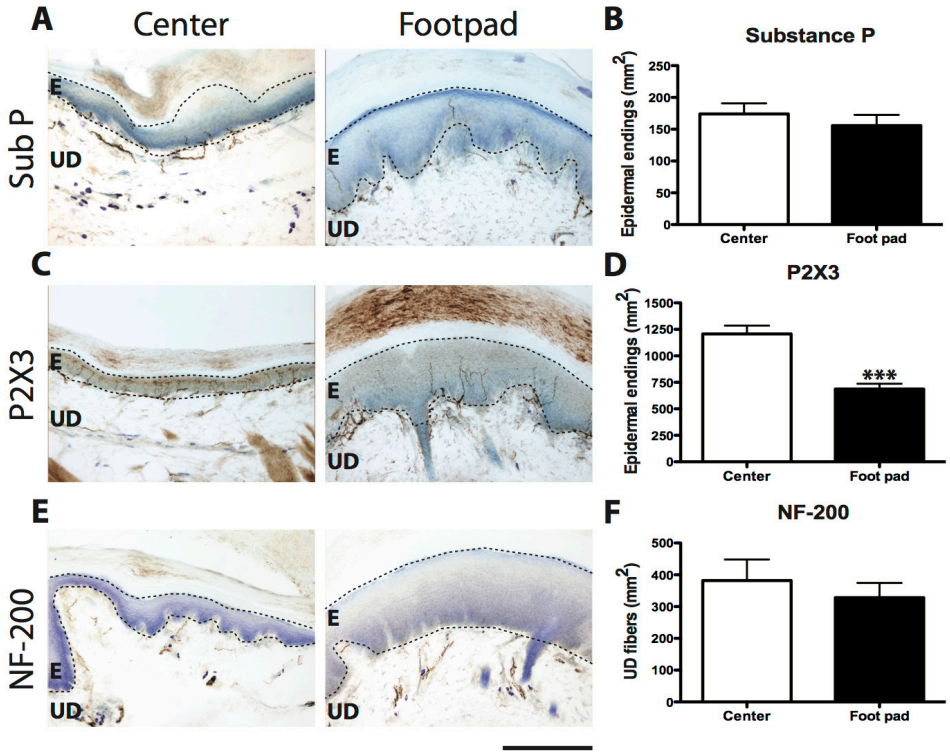

FIGURE 4 HOT AND COLD PLATE TEST:

*Histograms showing the withdrawal latency in seconds (± SEM) of the affected hind paw in the hot plate test (50 ºC and 43 ºC) and cold plate test (14ºC and 5 ºC) for sham- and SNI-treated rats. Note that only in the cold plate test at 5 ºC, the withdrawal latency in the SNI-treated rats is significantly shorter at all time points as compared to sham-treated rats. *: p < 0.05, **: p < 0.01, ***: p < 0.001 (ANOVA).*

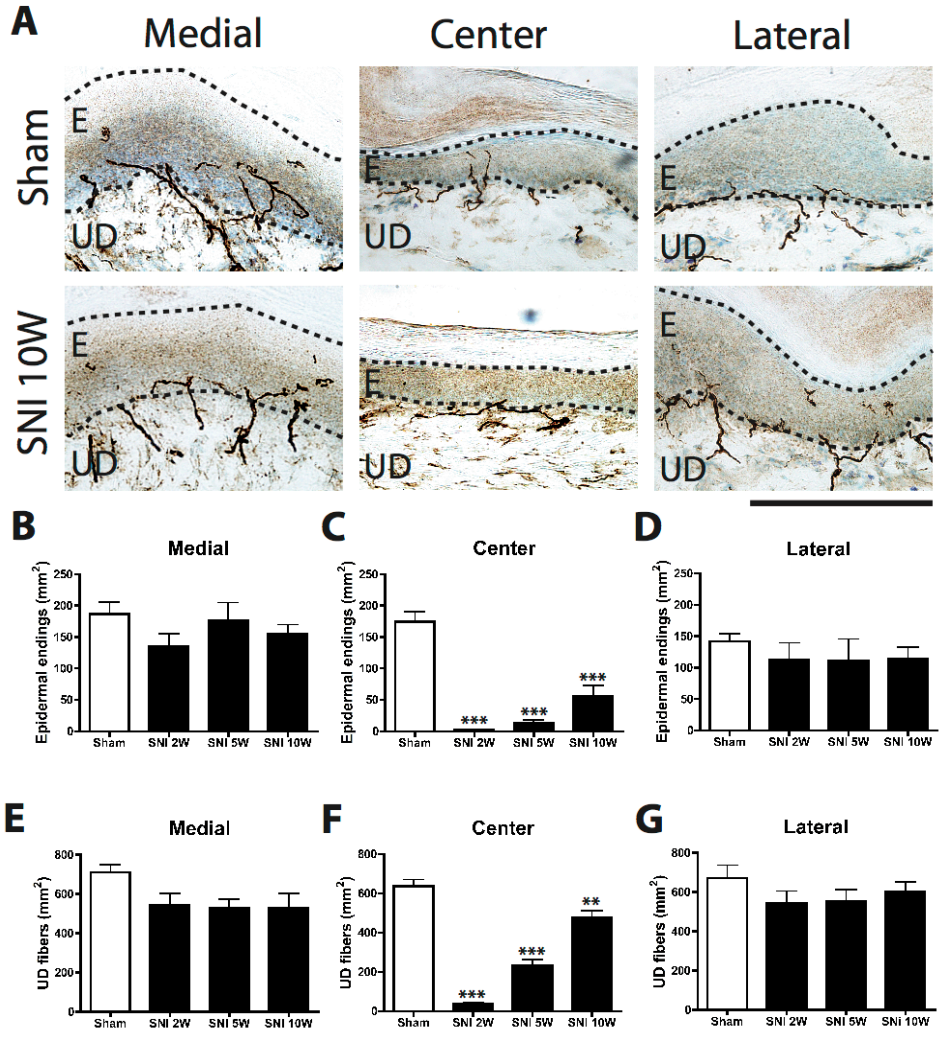

FIGURE 5 SUBSTANCE P IN THE SNI MODEL:

*Fig. 5A; Light microscopic micrographs showing nerve fibers labeled for Substance P (Sub P-IR) in the epidermis and upper dermis in the foot sole of SNI-treated (10 weeks postoperative) and sham-treated rats (2 weeks postoperative). The foot sole skin was divided in medial (innervated by saphenous nerve), center (tibial nerve) and lateral (sural nerve) areas. Fig. 5 B-G: histograms showing the number of epidermal (B-D) and upper dermal (E-G) Sub P-immunoreactive (IR) fibers per mm2 in the medial, center and lateral areas of the foot sole in SNI- and sham-treated rats at different time points. Note the significant decrease in Sub P-IR fibers in the foot sole center area of SNI-treated rats at all time points as compared to sham-treated rats (C and F). There were no significant differences in the medial and lateral areas between SNI- and sham-treated rats (B, D, E and G). . **: $p < 0.01$, ***: $p < 0.001$ (ANOVA). E = epidermis, UD = upper dermis. Scale bar: 250 µm.*

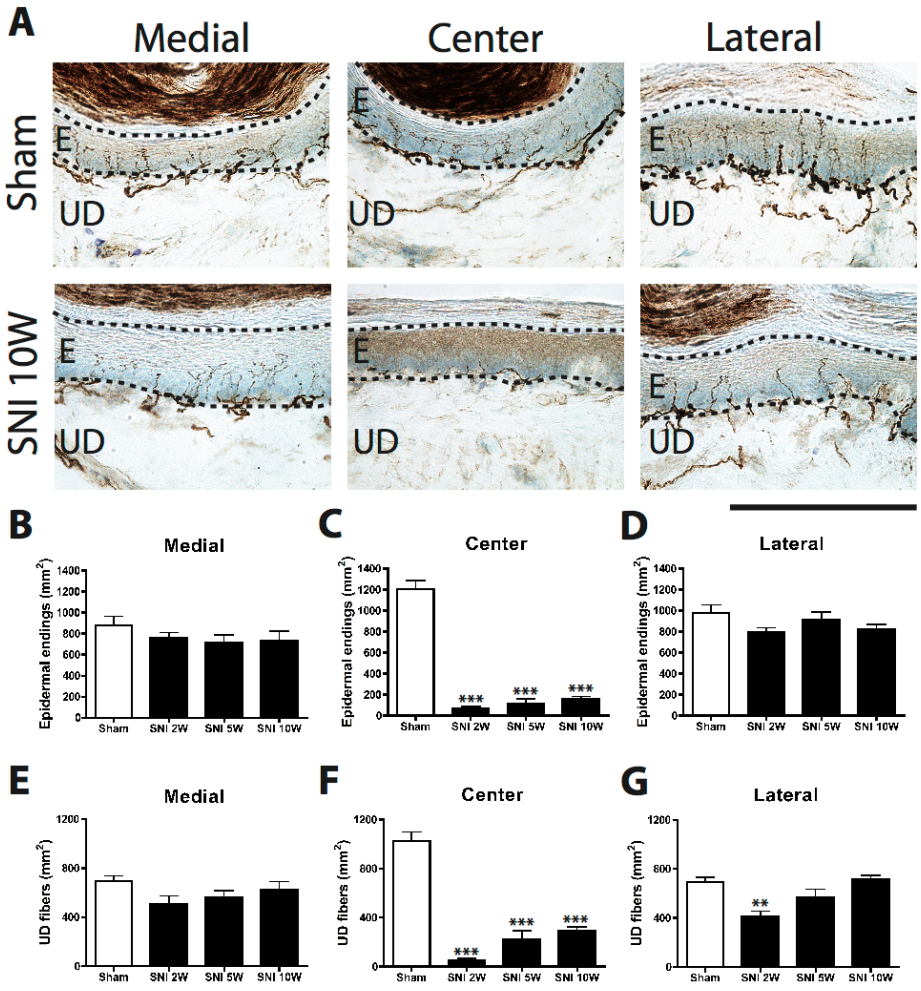

FIGURE 6 P2X3 IN THE SNI MODEL:

*Fig. 6A: Light microscopic micrographs showing nerve fibers labeled for P2X3 in the epidermis and upper dermis in the foot sole of SNI-treated (10 weeks postoperative) and sham-treated rats (10 weeks postoperative). The foot sole skin was divided in medial (innervated by saphenous nerve), center (tibial nerve) and lateral (sural nerve) areas. Fig. 6 B-G: histograms showing the number of epidermal (B-D) and upper dermal (E-G) P2X3-immunoreactive (IR) fibers per mm2 in the medial, center and lateral areas of the foot sole in SNI- and sham-treated rats at different time points. Note the significant decrease in P2X3-IR fibers in the foot sole center area of SNI-treated rats at all time points as compared to sham-treated rats (C and F). We found no significant differences in the medial and lateral areas between SNI- and sham-treated rats (B, D, E and G). **: $p < 0.01$, ***: $p < 0.001$ (ANOVA). E: epidermis, UD: upper dermis. Scale bar: 250 µm.*

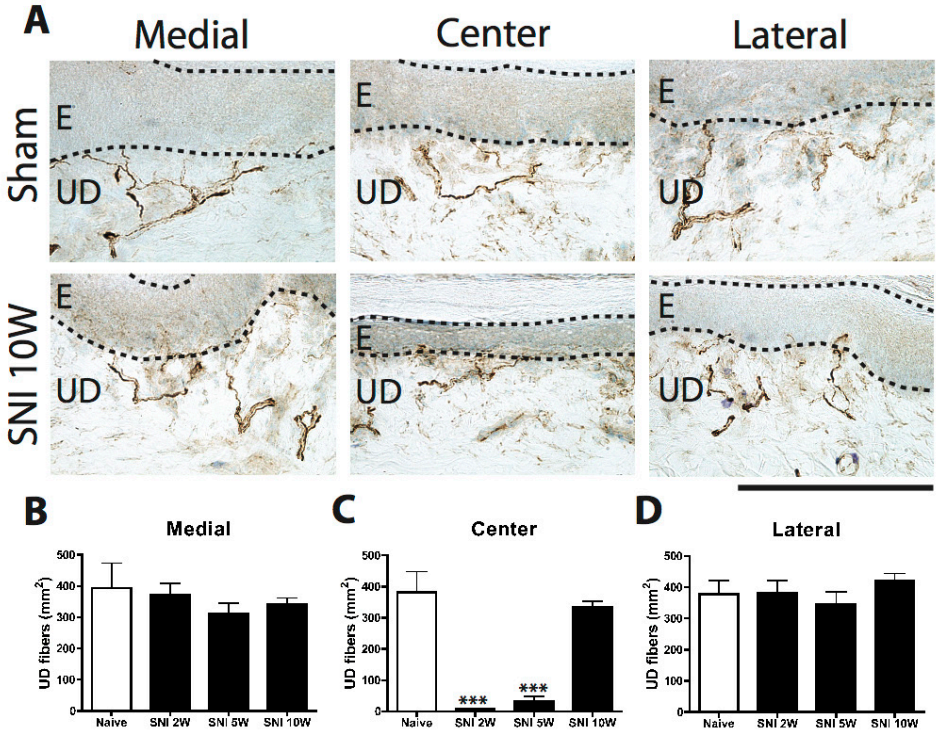

FIGURE 7 NF-200 IN THE SNI MODEL:

*Fig. 7A: Light microscopic micrographs showing nerve fibers labeled for NF-200 in the epidermis and upper dermis in the foot sole of SNI-treated (10 weeks postoperative) and sham-treated rats (10 weeks postoperative). The foot sole skin was divided in medial (innervated by saphenous nerve), center (tibial nerve) and lateral (sural nerve) areas. Note the absence of NF-200 immunoreactive (IR) fibers in the epidermis. Fig. 7 B-D: histograms showing the number of upper dermal P2X3-IR fibers per mm2 in the medial, center and lateral areas of the foot sole in SNI- and sham-treated rats at different time points. Note the significant decrease in P2X3-IR fibers in the foot sole center area of SNI-treated rats at 2 and 5 weeks postoperatively (PO) as compared to sham-treated rats, with a complete re-innervation at 10 weeks PO (C) We found no significant differences in the medial and lateral areas between SNI- and sham-treated rats (B and D). **: $p < 0.01$, ***: $p < 0.001$, (ANOVA). E: epidermis, UP: upper dermis. Scale bar: 250 µm.*

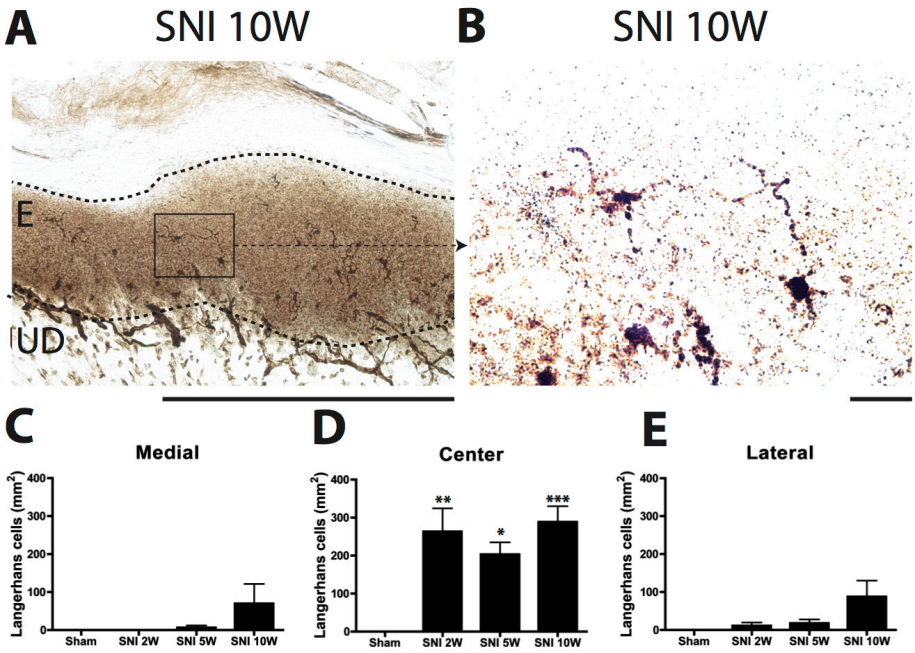

FIGURE 8 LANGERHANS CELLS IN THE SNI MODEL:

*Fig. A and B: Light microscopic micrographs showing labeling for PGP-9.5 in the foot sole (center area) of a SNI-treated rat 10 weeks after operation. Next to PGP-9.5 immunoreactive (IR) fibers, there are several PGP-9.5-IR Langerhans cells (LCs) located in the epidermis (arrowhead in B). C-E: histograms showing the number of PGP-9.5-IR LCs per mm2 in the epidermis of sham- and SNI-treated at different time points. The foot sole skin was divided in medial (innervated by saphenous nerve), center (tibial nerve) and lateral (sural nerve) areas. Note the significant increase in the number of LCs in the center area of the foot sole, whit no significant changes in the medial and lateral areas. *: p < 0.05, **: p < 0.01, ***: p < 0.001 (ANOVA), E: epidermis, UD: upper dermis. Scale bar: A; 250 µm, B; 25 µm.*

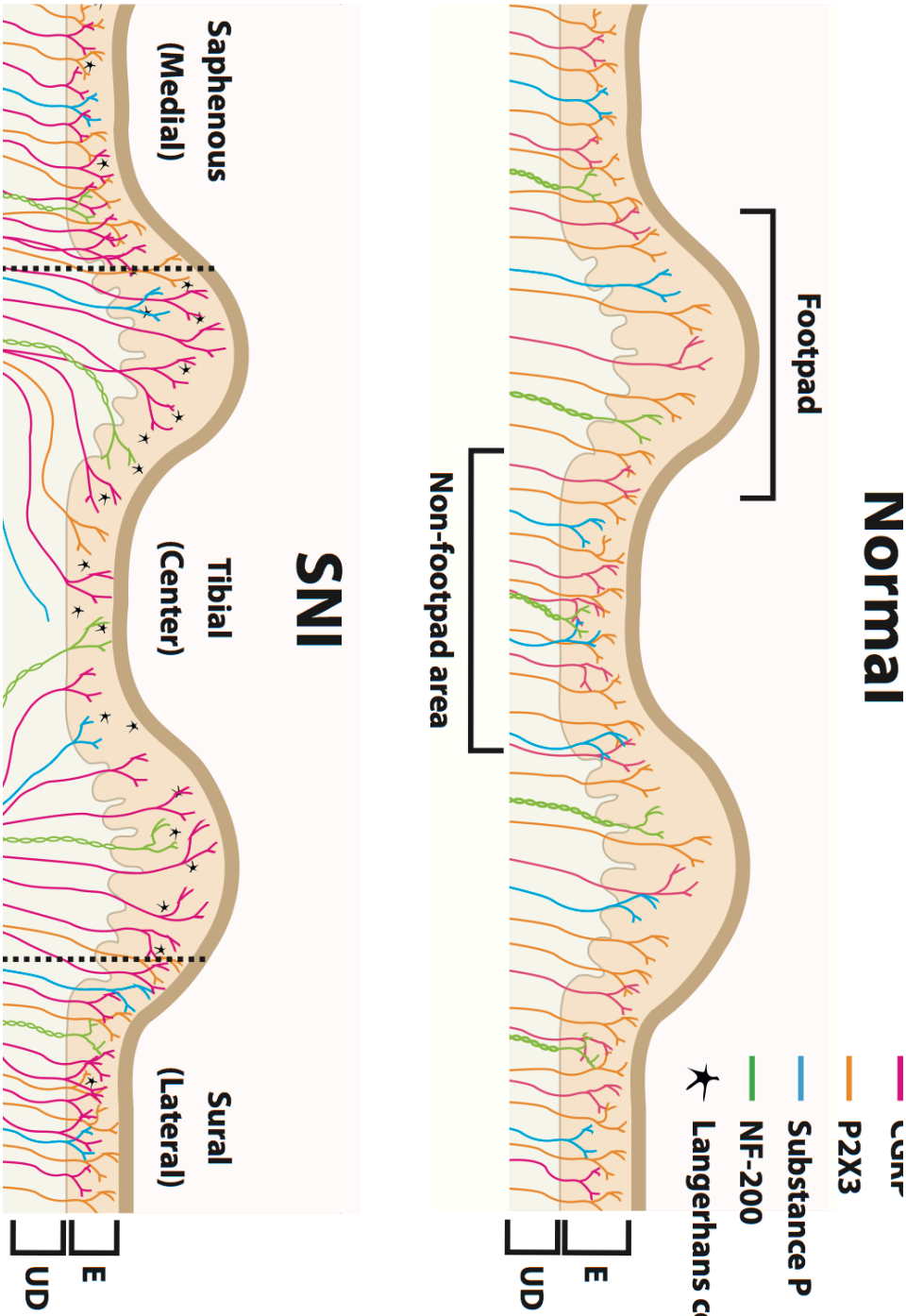
Normal
Footpad
Non-footpad area
CGRP
P2X3
Substance P
NF-200
Langerhans cell
E
UD
SNI
Saphenous
(Medial)
Tibial
(Center)
Sural
(Lateral)
E
UD

FIGURE 9 ILLUSTRATION OF THE SKIN INNERVATION IN NORMAL AND SNI SITUATION:

Illustration showing the innervation pattern of subgroups of sensory skin fibers in the normal situation and in the SNI model 10 weeks PO. In the naïve animals the peptidergic CGRP and non-peptidergic P2X3 fibers have a lower density in the footpads as compared to the non-footpad areas, while the Substance P and NF-200 fibers have an equal distribution over the complete foot sole. In the SNI model there is a significant increase of CGRP epidermal fibers in the medial and lateral area of the foot sole and there is a complete re-innervation of the center area. In addition the footpads in the SNI model are hyper-innervated with CGRP fibers. Substance P and P2X3 and NF-200 fibers show no increased density in the uninjured medial and lateral area after 10 weeks PO. In addition, Substance P and P2X3 fibers hardly re-innervate the center area, however the NF-200 fibers have the same density of fibers in the denervated area as in the normal situation. In the SNI model the medial, center and lateral area have all an increase in LC's, with the center area being the most prominent one. In addition the epidermis thickness of the SNI model has decreased significantly in all the three areas after 10 weeks PO.

6

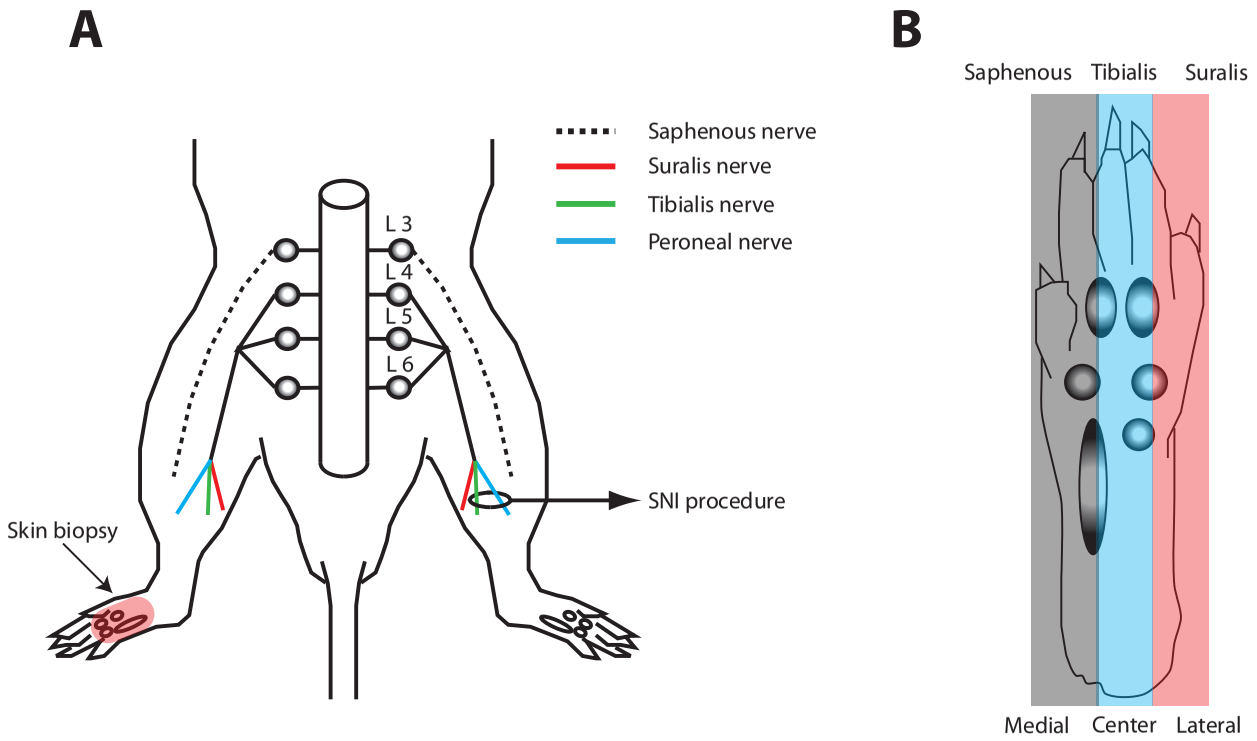

FIGURE 1:

Figure 1 A shows a drawing of the SNI procedure and the location where the skin biopsy is taken from the contralateral foot sole. Figure 1 B displays a drawing of the cutaneous innervation pattern of the saphenous, tibial and sural nerve in the hind foot sole of a rat.

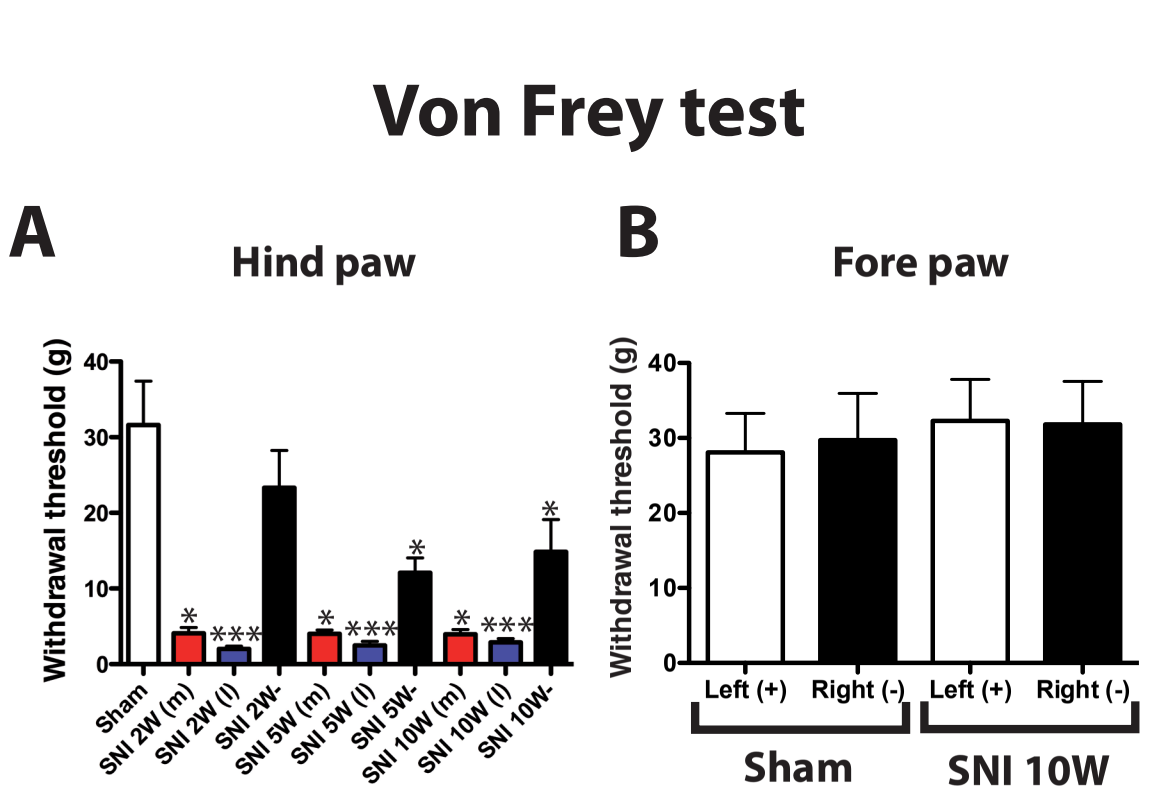

FIGURE 2:

*A histogram showing the mechanical withdrawal threshold in grams (g) of the ipsilateral medial (m) and lateral (l) part of the foot sole and the contralateral hind limb foot sole (-) of the sham and SNI-treated group after a unilateral nerve injury (Fig. 2 A) (n=13 per group). The significant differences depicted in Figure 2 A are the differences between the SNI-treated group and the shams. Figure 2 B shows the ipsi- (Left+) and contralateral (Right-) front paw mechanical sensitivity of sham and SNI-treated rats. Kruskal-Wallis test with Dunn's post-hoc test. *: p <0.05, ***: p <0.001.*

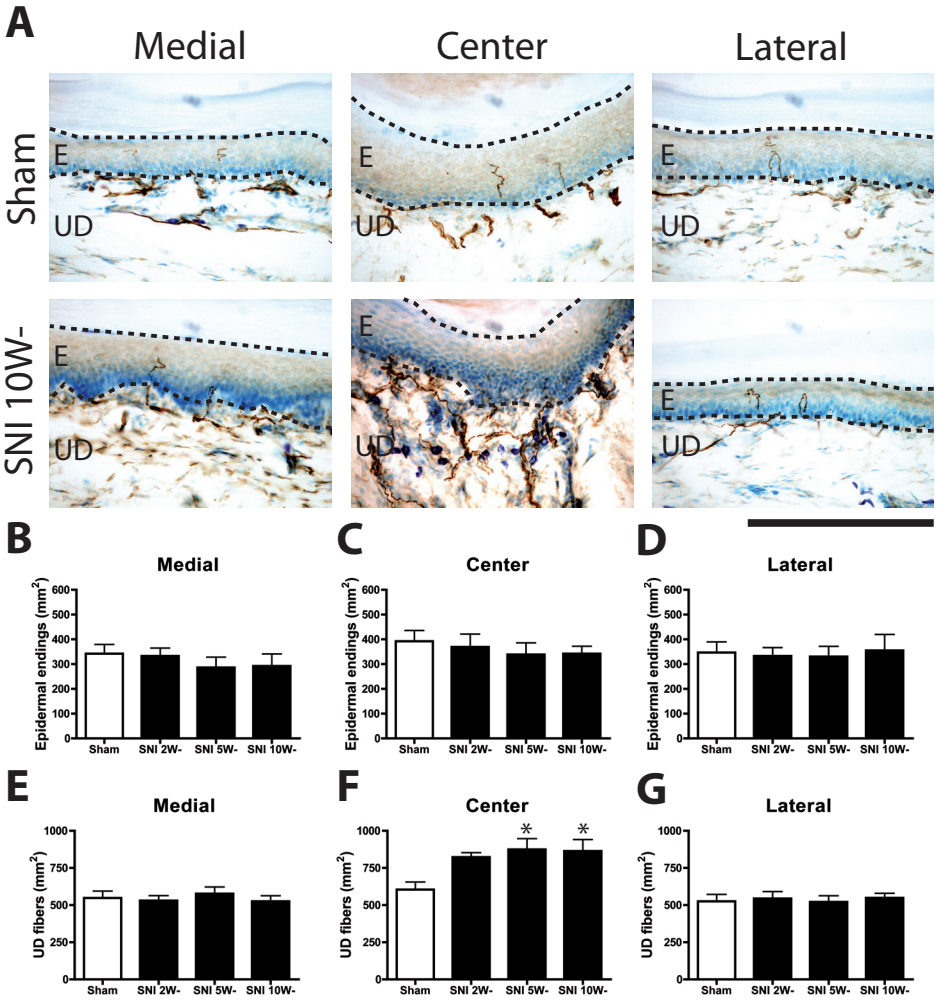

FIGURE 3:

*Microphotographs showing CGRP-IR fibers in skin biopsies taken from the medial (saphenous), center (tibial) and lateral (sural) part of the foot sole contralateral to the SNI or sham-operated side (Fig. 3 A). Fig. 3 B-D displays histograms of the number of CGRP-IR fibers (mm2) in the epidermis (E) and fig. 3 E-G shows the number of CGRP-IR fibers (mm2) in the upper dermis (UD). Note the significant increase ($p < 0.05$) of upper dermal CGRP-IR fibers in the center (tibial) area of the contralateral foot sole at 5 and 10 weeks PO (Fig. 3 A and F). One-way ANOVA with post-hoc Tukey test; *: $p < 0.05$, Scale bar: 250 µm.*

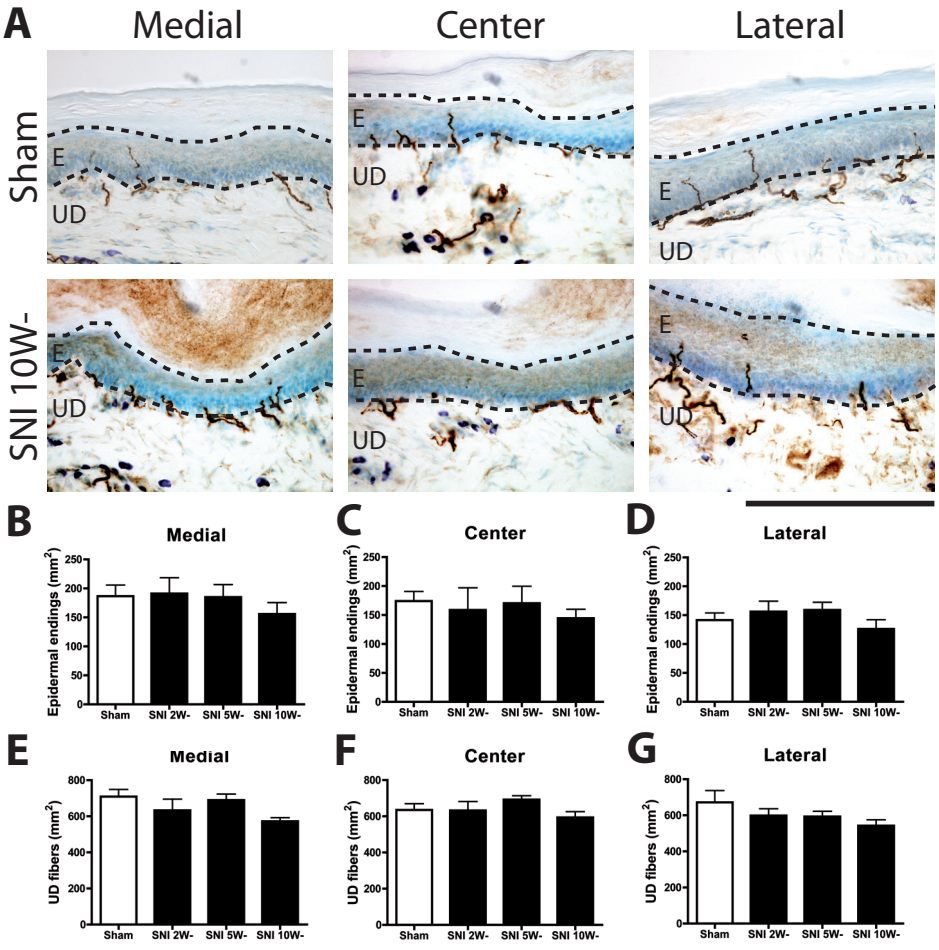

FIGURE 4:

Microphotographs showing staining for Substance P-IR fibers in skin biopsies taken from the medial (saphenous), center (tibial) and lateral (sural) part of the foot sole contralateral to the SNI or sham operated side (Fig. 4 A). Fig. 4 B-D displays histograms of the number of Substance P-IR fibers per mm2 in the epidermis (E) and fig. 4 E-G shows the number of Substance P-IR fibers (mm2) in the upper dermis (UD). Scale bar: 250 µm.

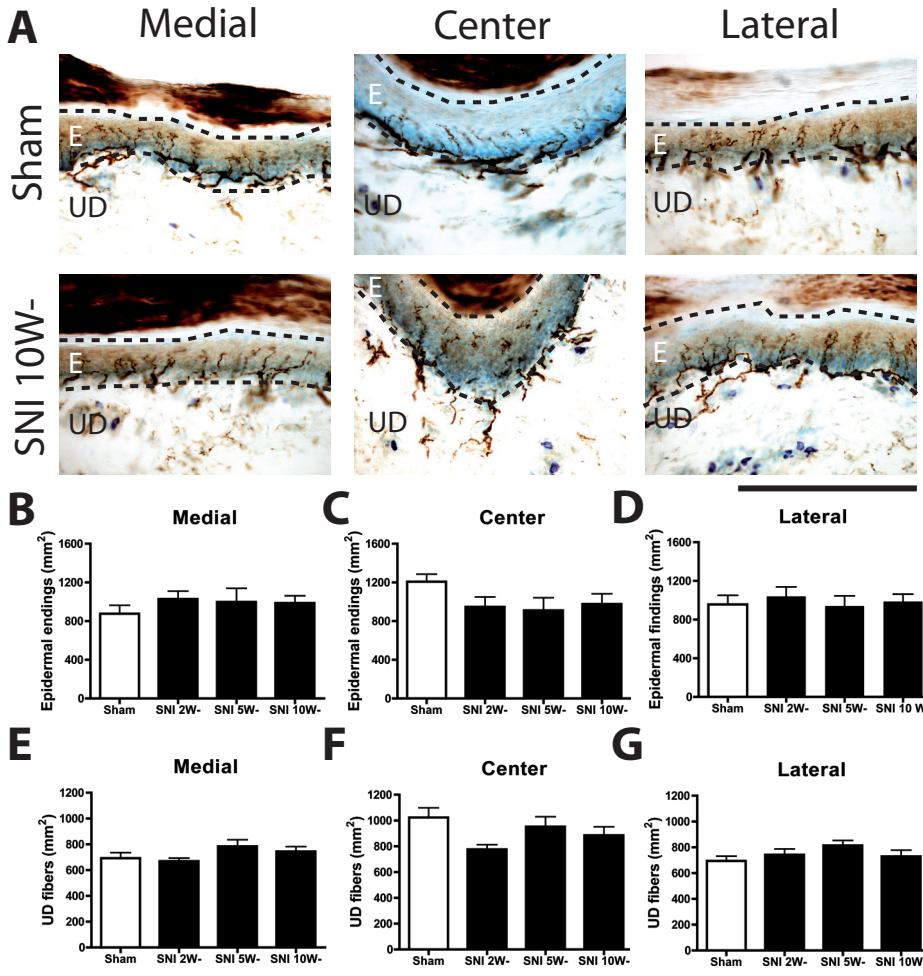

FIGURE 5:

Microphotographs showing staining for P2X3-IR fibers in skin biopsies taken from the medial (saphenous), center (tibial) and lateral (sural) part of the foot sole contralateral to the SNI or Sham operated side (Fig. 5 A). Fig. 5 B-G displays histograms of the number of P2X3-IR fibers per mm2 in the epidermis (E) and fig. 5 E-G shows the number of P2X3-IR fibers (mm2) in the upper dermis (UD). Scale bar: 250 µm.

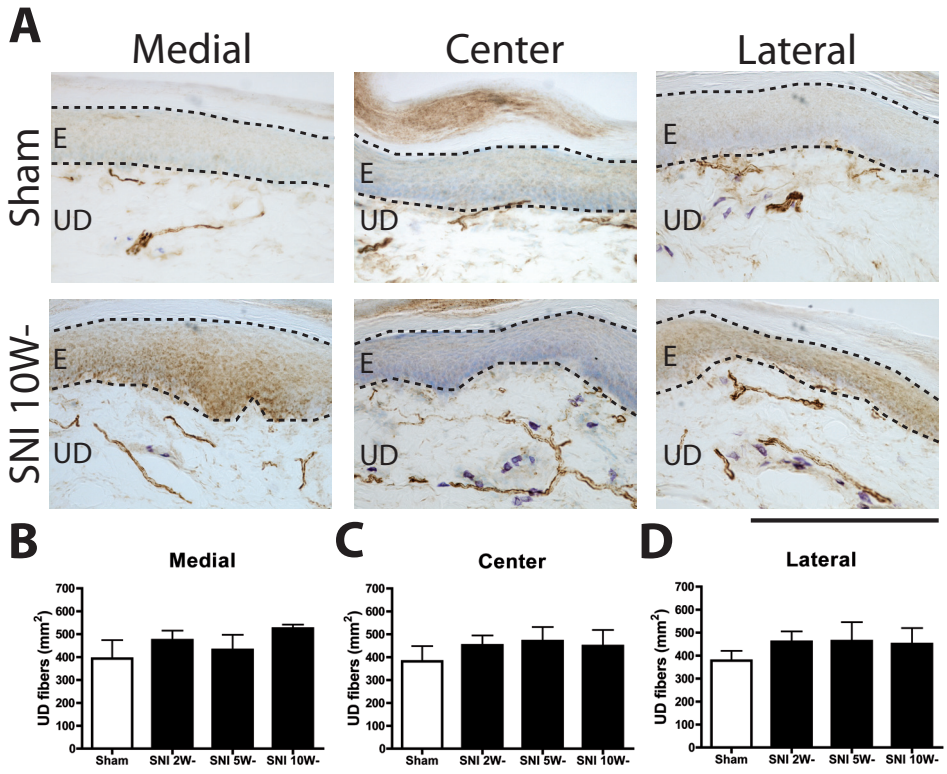

FIGURE 6:

Micrographs showing staining for NF-200-IR fibers in skin biopsies taken from the medial (saphenous), center (tibial) and lateral (sural) part of the foot sole (Fig. 6 A). Fig. 6 B-D displays histograms of the number of NF-200-IR fibers per mm2 in the upper dermis (UD). Scale bar: 250 µm.

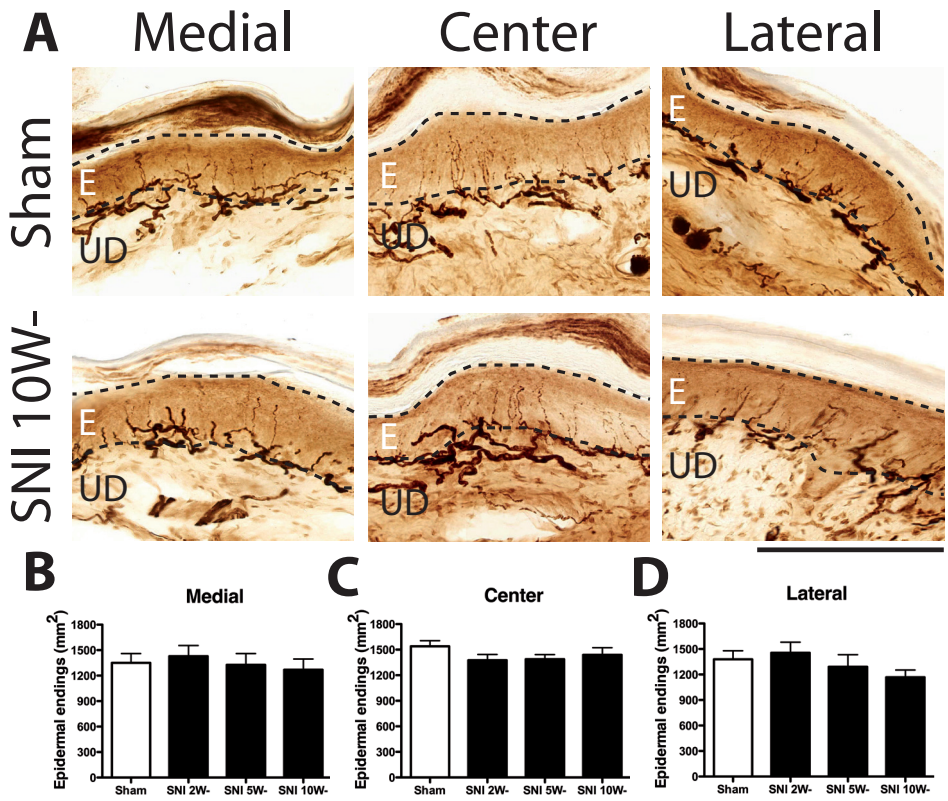

FIGURE 7:

Micrographs showing staining for PGP 9.5-IR fibers in skin biopsies taken from the medial (saphenous), center (tibial) and lateral (sural) part of the foot sole (Fig. 7 A). Fig. 7 B-D displays histograms of the number of PGP 9.5-IR fibers per mm2 in the epidermis (E). Scale bar: 250 µm.

7

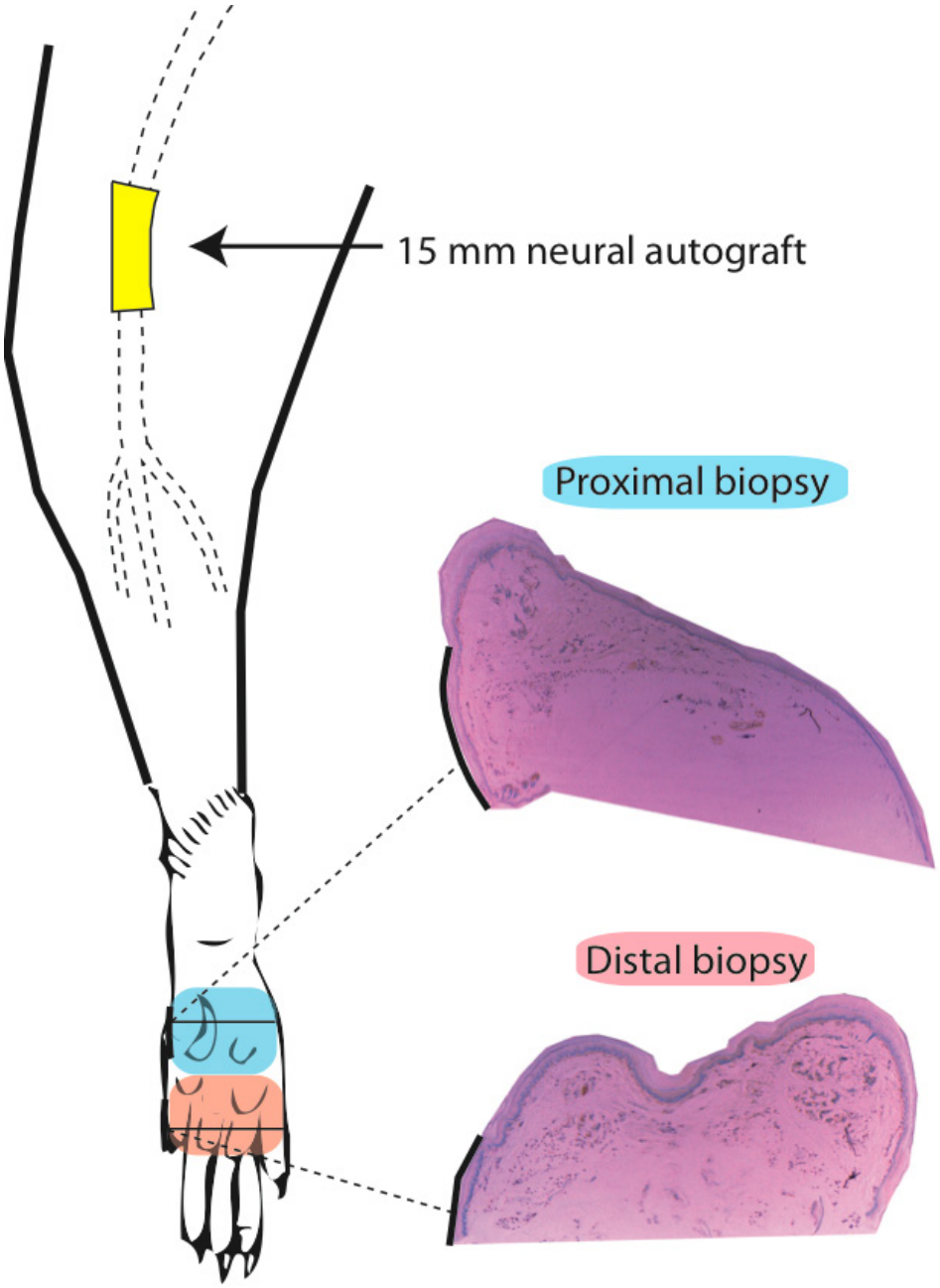

FIGURE 1:

Detailed image illustration of our model. Depicted are the 15 mm nerve autograft reconstruction and the biopsies taken at 12 weeks for both proximal and distal segments in the rat foot sole.

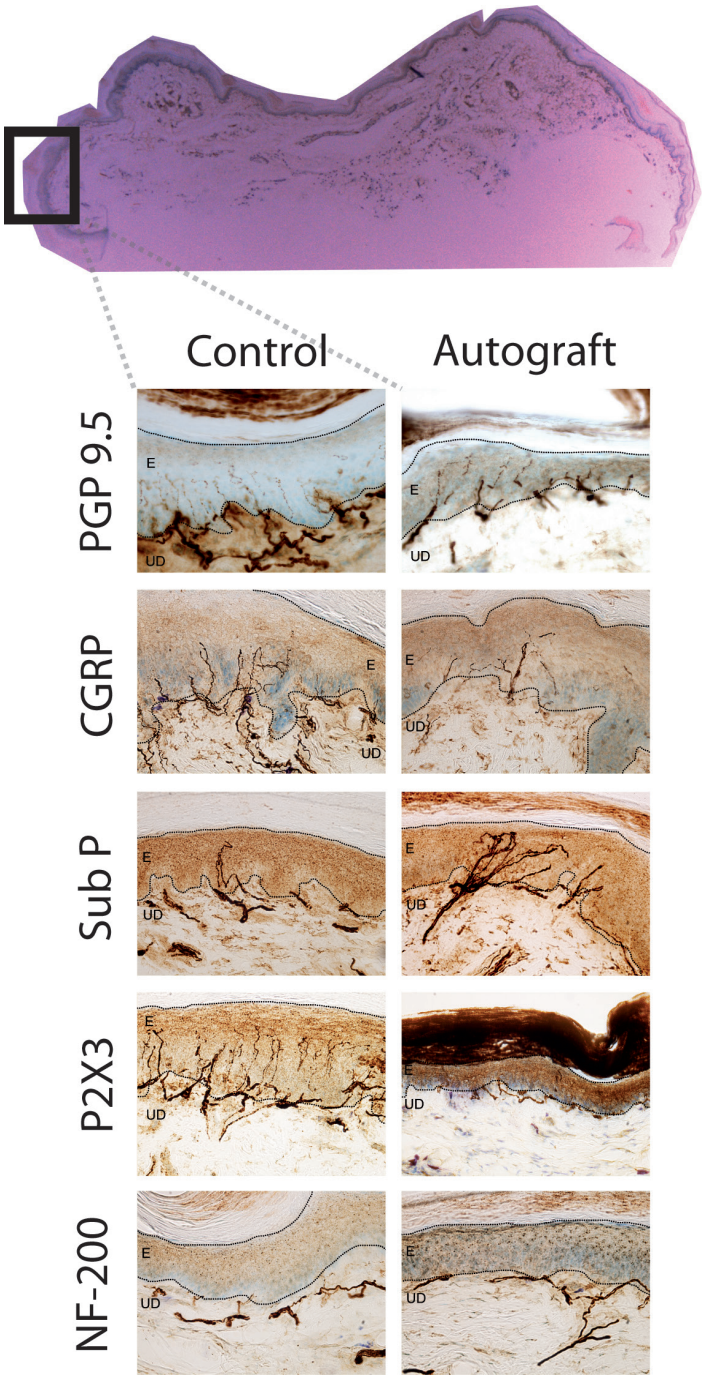

FIGURE 4:

An overview of the micrographs of the different markers used. Pictures are taken with a 20x10 objective.

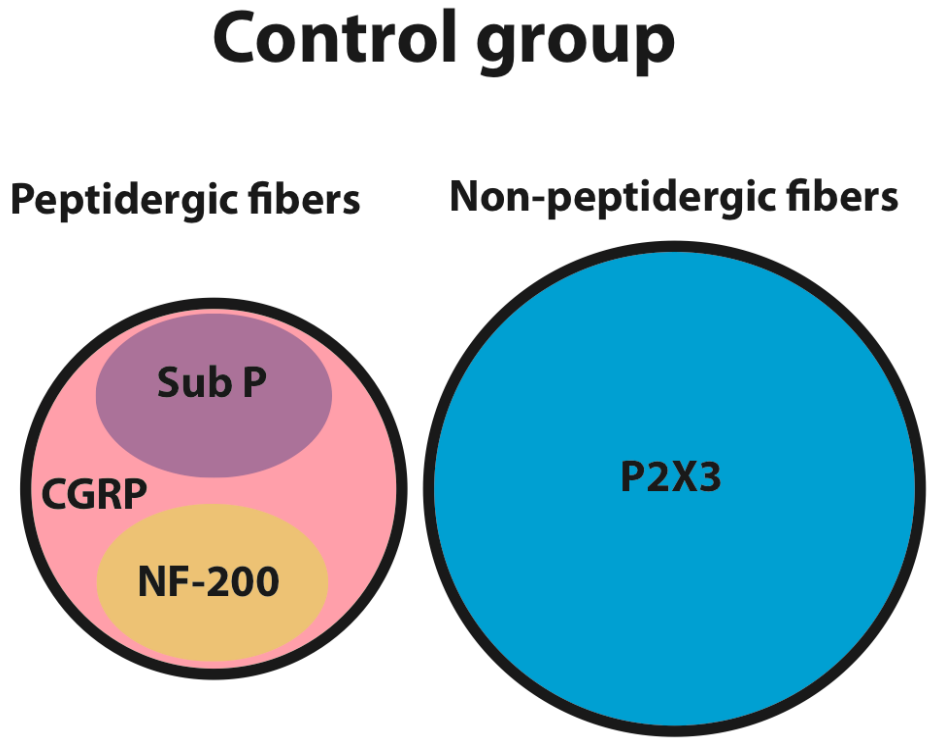

FIGURE 6:

Distribution of the five different subgroups of sensory nerve fibres in the rat foot sole 12 weeks after reconstructing the 15 mm nerve defect using an autograft. Distribution of the five different subgroups of sensory nerve fibres in the healthy rat foot sole.

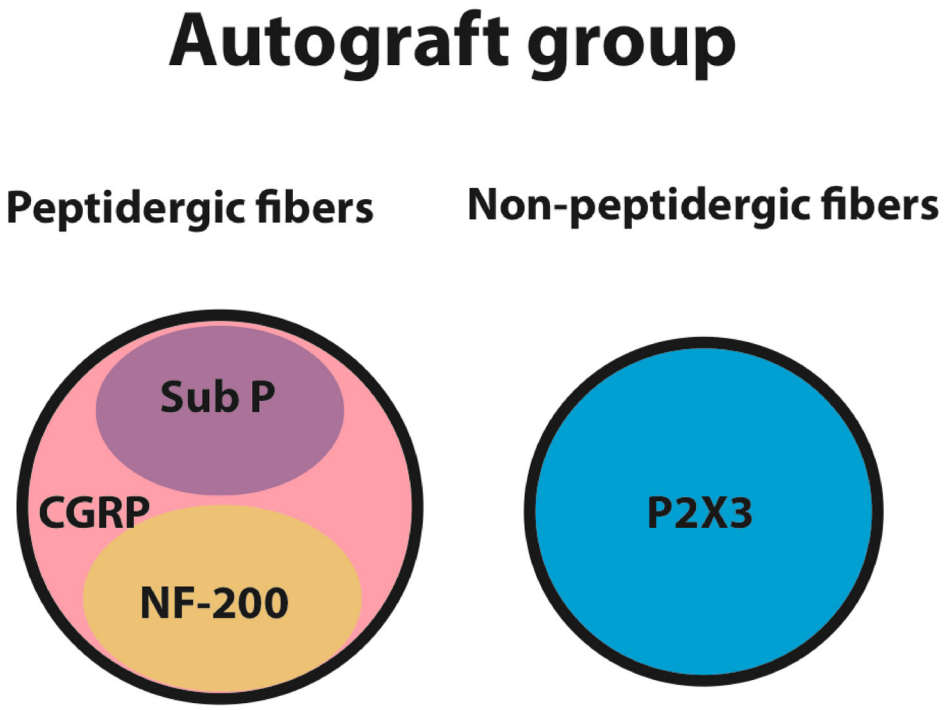

FIGURE 7:

Distribution of the five different subgroups of sensory nerve fibres in the rat foot sole 12 weeks after reconstructing the 15 mm nerve defect using an autograft. Distribution of the five different subgroups of sensory nerve fibres in the healthy rat foot sole.

8

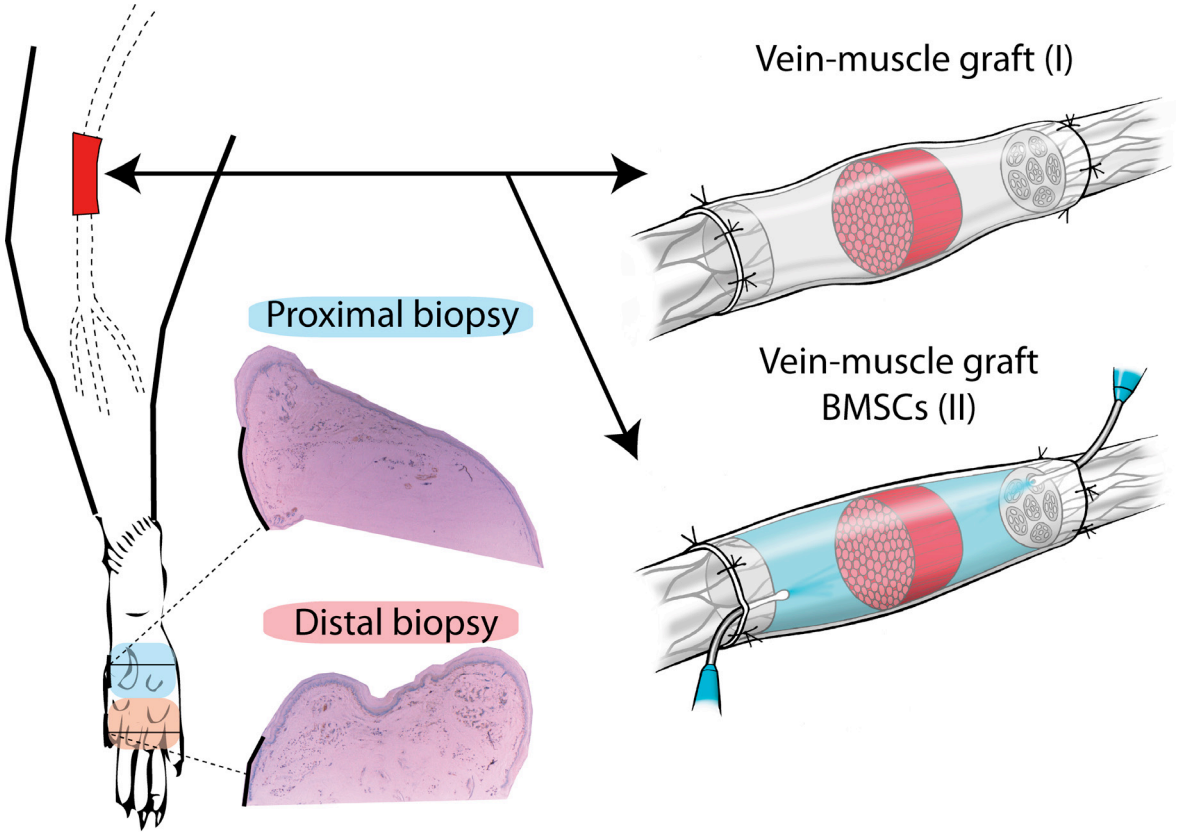

FIGURE 1:

Detailed illustration of the surgical model of the vein-muscle grafts used and the location of the skin biopsies.

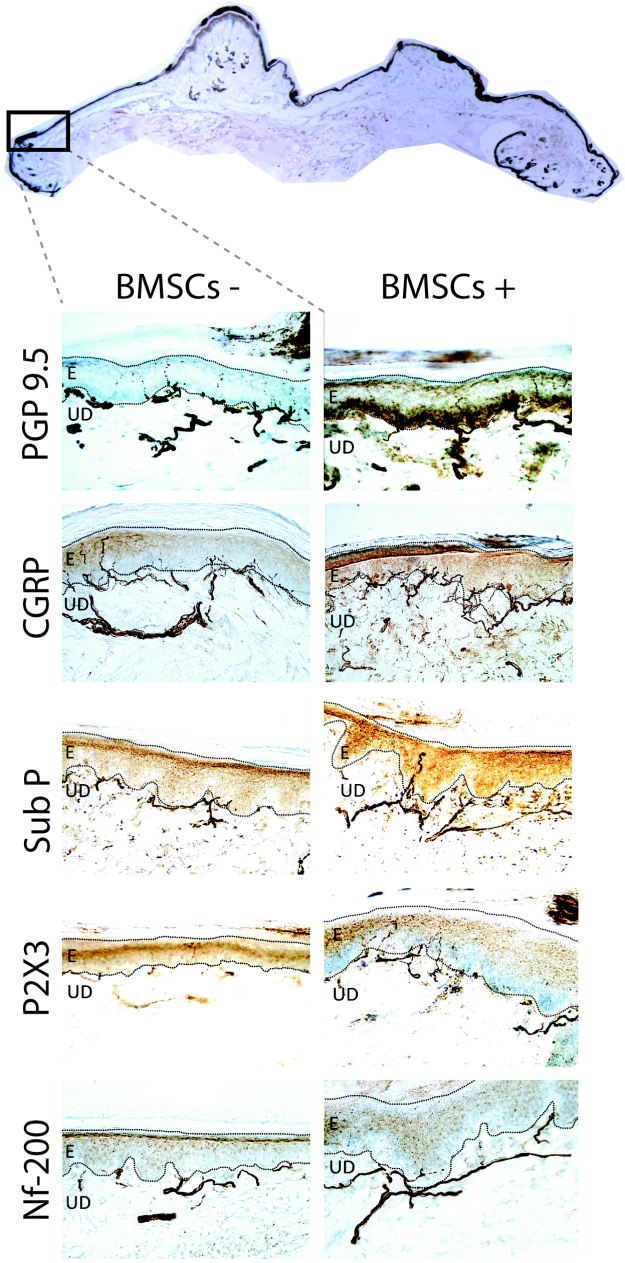

FIGURE 3:

An overview with example of the micrographs of the different markers used. Pictures are taken with a 20x10 objective for both the proximal and distal segment. PGP 9.5-IR is a pan neuronal marker. The calcitonin gene-related peptide (CGRP-IR) marker stains the peptidergic fibres. Substance P-IR (Sub P) also stains the peptidergic fibres. Neurofilament 200 (NF200-IR) stains the Aδ-fibres. The P2X purinoceptor 3 (P2X3-IR) staining visualizes all non-peptidergic fibres.

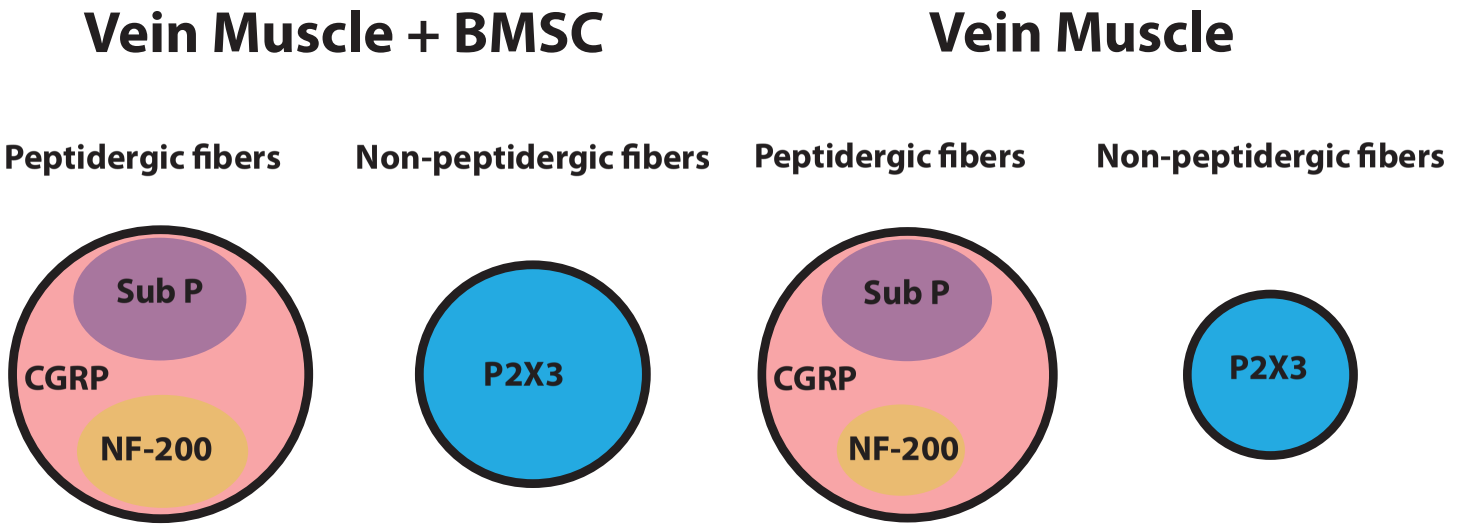

FIGURE 5:

A schematic illustration of the different stainings in proportion to each other. PgP 9.5-IR is a pan neuronal marker. The calcitonin gene-related peptide (CGRP-IR) marker stains the peptidergic fibres. Substance P-IR (Sub P) also stains the peptidergic fibres. Neurofilament 200 (NF200-IR) stains the Aδ-fibres. The P2X purinoceptor 3 (P2X3-IR) staining visualizes all non-peptidergic fibres

9

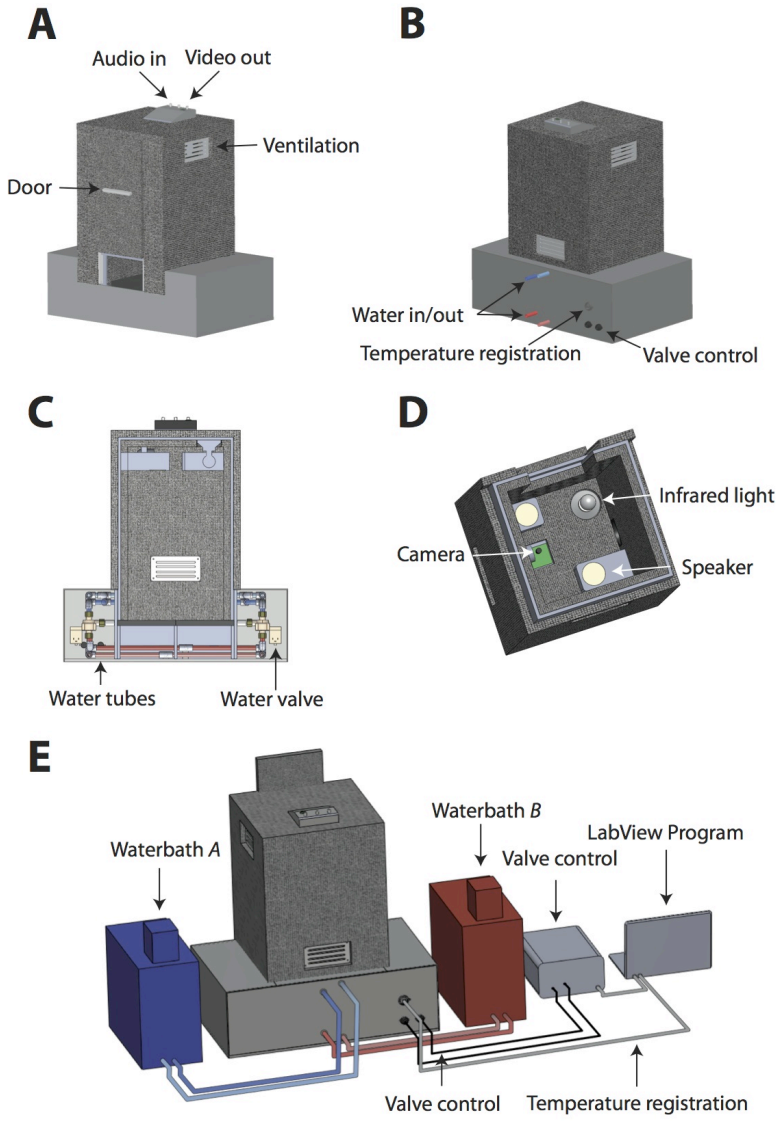

FIGURE 1:

The RAMP consists of two parts, the dark grey box and the four plates, which are connected by water tubes and are suited in a light grey Plexiglas case (Fig. 1A-C). On the roof of the RAMP, wiring is suited which enables plugging of the audio for the speakers and the video output for tracking the rat (Fig. 1A). The light grey base functions as the case for the plates and water tubes. Furthermore, the hardware for the valve control and temperature registration is located here (Fig. 1C). The main purpose of the dark grey box is that it is sound- and lightproof and the camera, which records the movement of the rat, is housed in the box (Fig. 1D). Next to the camera, an infrared light is placed to detect the animal in the dark. In addition, speakers are positioned to produce background noise for the rats during the experiment to minimize stress (Fig. 1D).

Fig. 1E shows a drawing of the complete set-up of the RAMP. Two water baths (A and B) are connected to the plates to provide circulated water, which is constantly on specific temperatures. Also a power box is suited to provide the water valves of power and to switch the valves between the two water baths by means of the LabView 8.5 program in the computer (Fig. 1E). Also the temperature sensors, which are suited under every plate, are linked to the computer to monitor if the plates have the right temperature (Fig. 1E).

FIGURE 2:

Fig. 2A displays a detailed drawing of the four plates, water valves and water tubes. Each of the eight-water valves is connected to the two water baths and a plate, which enables switching between the two water baths (Fig. 2A). Fig. 2B and C shows a schematic drawing of the internal structure of the plates in transversal and sagittal orientation. The four temperature sensors are placed under each of the four plates in the center point (Fig. 2B and C).

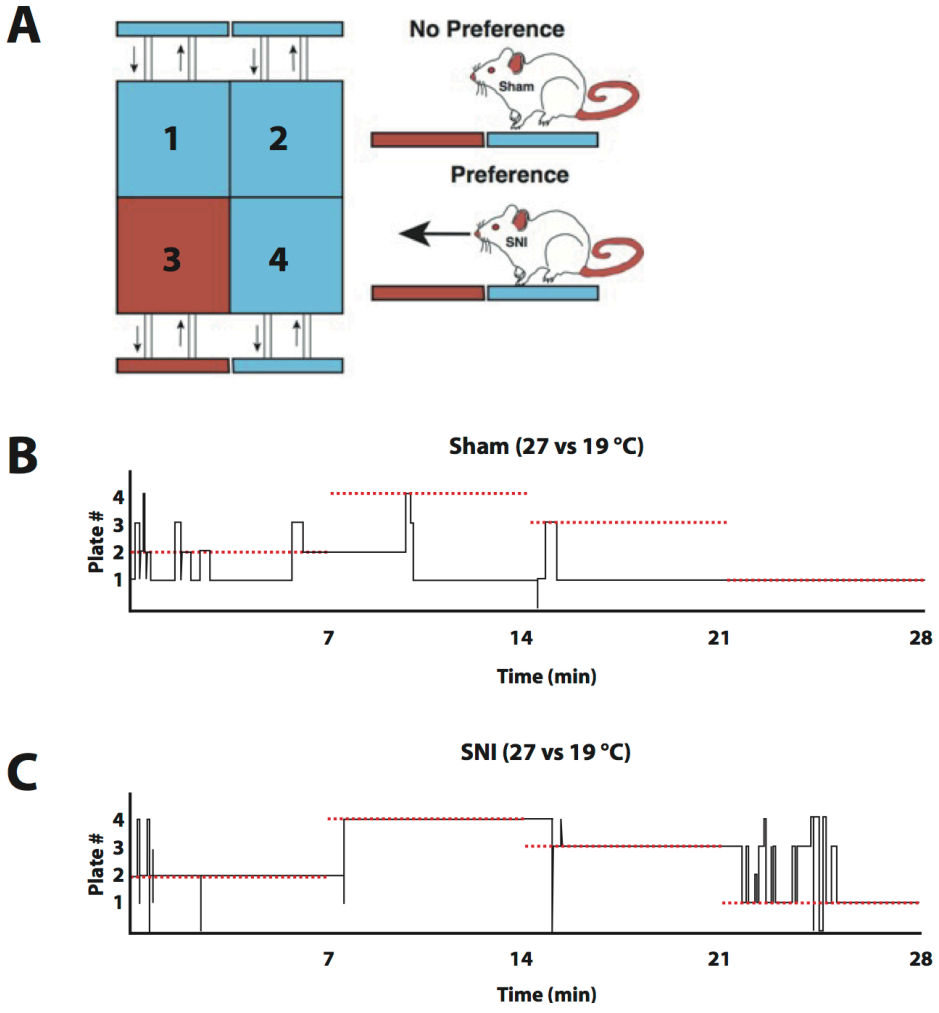

FIGURE 4:

Fig. 4A shows a schematic drawing of the RAMP. There is one comfortable plate (red) and three plates (blue) with a hot or cold temperature. The concept of the RAMP is that the SNI group shows a stronger preference for the comfortable plate. In Fig. 4B we display typical data of a sham and SNI rat (3 weeks postoperatively) during an experiment with the comfortable at 27 °C and the other three plates are 19 °C. The red dotted line displays which plate is at 27 °C and the black line exhibits the location of the SNI or sham rat. It is evident that the SNI rat displays a strong preference for the comfortable plate (27°C) while the sham-treated rat does not show a clear preference for the comfortable plate.

10

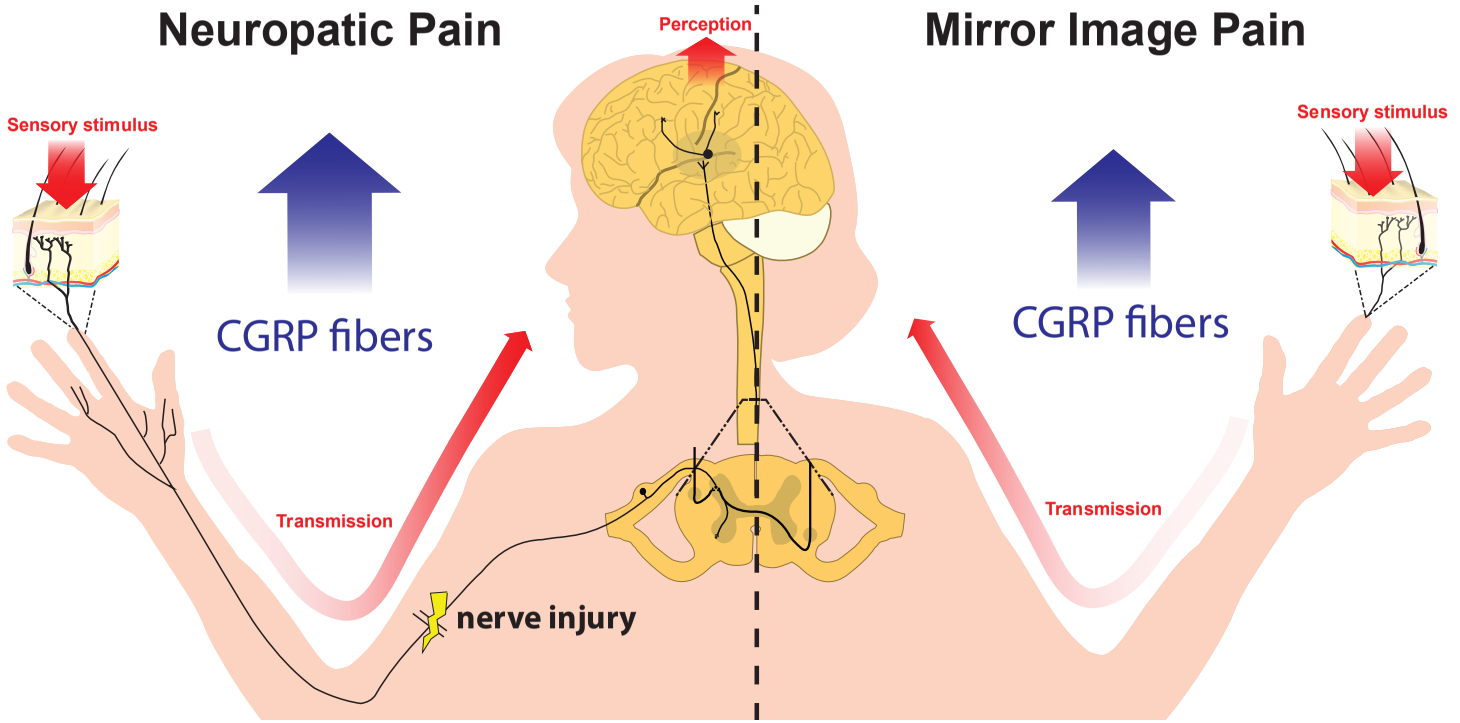

FIGURE 1:

Uninjured peptidergic CGRP fibers demonstrate the most profound alterations in their innervation pattern after ipsilateral induction of neuropathic pain, due to partial nerve injury, as compared to other subgroups of sensory fibers (Substance P, NF-200 and P2X3). Additionally, an increase in skin CGRP neuropeptide content on the contralateral side after ipsilateral induction of neuropathic pain might play a pivotal role in the pathophysiology of mirror image pain.

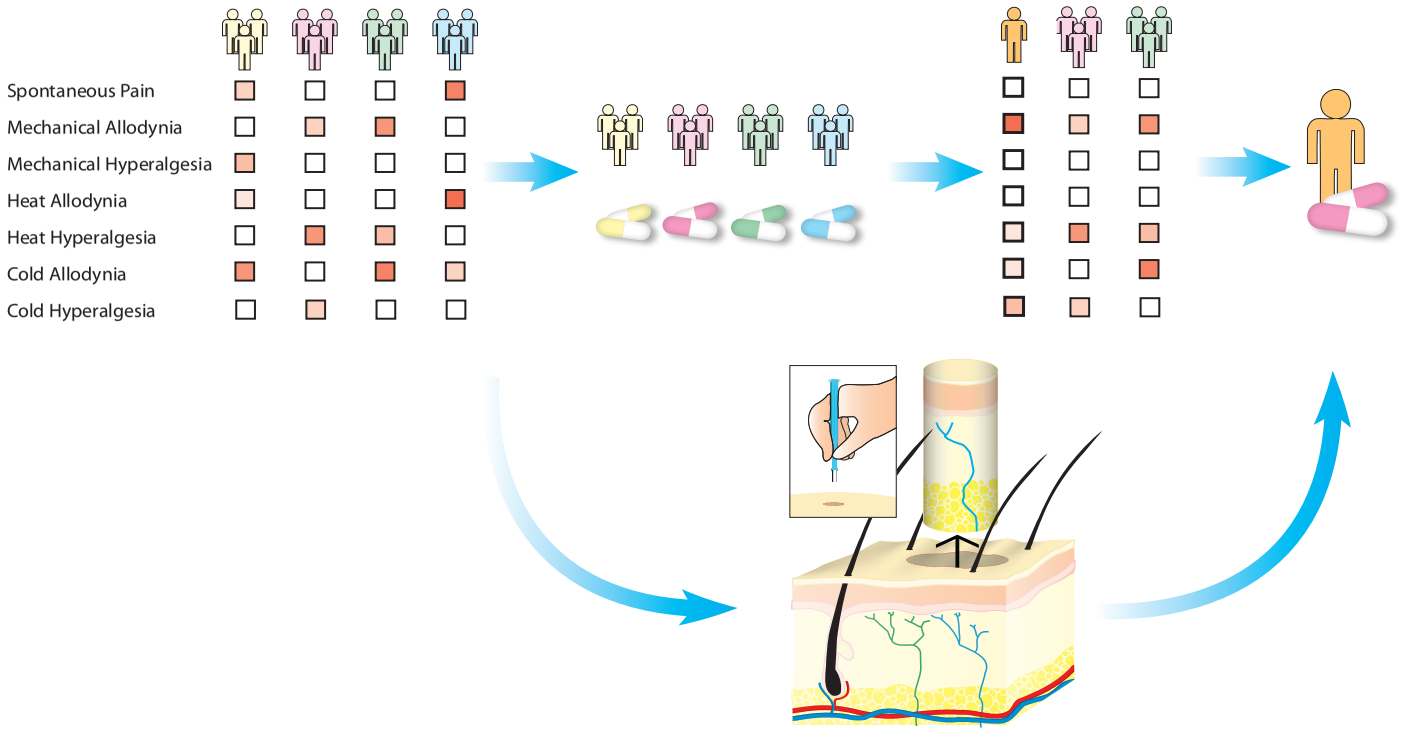

FIGURE 2:

Diagnosis of neuropathic pain is guided by the symptoms the patient is presenting with and the treatment of choice is based on a trial and error process. However, labeling of sensory skin fibers provides essential information for discriminating more efficiently nerve injury-induced neuropathic pain from other types of neuropathic pain.

“Missing a train is only painful if you run after it.”
Nassim Taleb